



Faculty of Health, Engineering and Sciences  
School of Mechanical and Electrical Engineering

**PHD DISSERTATION**

**Adaptive Relaying Protocol Multiple-Input  
Multiple-Output Orthogonal Frequency Division  
Multiplexing Systems**

Ibrahim Khalil Sileh

Student Number: 0050096562

**Principal Supervisor**

A/Prof. Wei Xiang

**Co-Supervisor**

Dr. Andrew Maxwell

May, 2014



# Abstract

In wireless broadband communications, orthogonal frequency division multiplexing (OFDM) has been adopted as a promising technique to mitigate multi-path fading and provide high spectral efficiency. In addition, cooperative communication can explore spatial diversity where several users or nodes share their resources and cooperate through distributed transmission. The concatenation of the OFDM technique with relaying systems can enhance the overall performance in terms of spectral efficiency and improve robustness against the detrimental effects of fading.

Hybrid relay selection is proposed to overcome the drawbacks of conventional forwarding schemes. However, exciting hybrid relay protocols may suffer some limitations when used for transmission over frequency-selective channels. The combination of cooperative protocols with OFDM systems has been extensively utilized in current wireless networks, and have become a promising solution for future high data rate broadband communication systems including 3D video transmission. This thesis covers two areas of high data rate networks. In the first part, several techniques using cooperative OFDM systems are presented including relay selection, space time block codes, resource allocation and adaptive bit and power allocation to introduce diversity.

Four (4) selective OFDM relaying schemes are studied over wireless networks; selective OFDM; selective OFDMA; selective block OFDM and selective unequal block OFDM. The closed-form expression of these schemes is derived. By exploiting the broadcast nature, it is demonstrated that spatial diversity can be improved. The upper bound of outage probability for the protocols is derived.

A new strategy for hybrid relay selection is proposed to improve the system

performance by removing the sub-carriers that experience deep fading. The per-subcarrier basis selection is considered with respect to the predefined threshold signal-to-noise ratio. The closed-form expressions of the proposed protocol in terms of bit error probability and outage probability are derived and compared with conventional hybrid relay selection. Adaptive bit and power allocation is also discussed to improve the system performance.

Distributed space frequency coding applied to hybrid relay selection to obtain full spatial and full data rate transmission is explored. Two strategies, single cluster and multiple clusters, are considered for the Alamouti code at the destination by using a hybrid relay protocol. The power allocation with and without sub-carrier pairing is also investigated to mitigate the effect of multipath error propagation in frequency-selective channels.

The second part of this thesis investigates the application of cooperative OFDM systems to high data rate transmission. Recently, there has been growing attention paid to 3D video transmission over broadband wireless channels. Two strategies for relay selection hybrid relay selection and first best second best are proposed to implement unequal error protection in the physical layer over error-prone channels. The closed-form expressions of bit error probability and outage probability for both strategies are examined. The peak signal-to-noise ratio is presented to show the quality of reconstruction of the left and right views.

# Certification of Dissertation

I certify that the ideas, designs and experimental work, results, analyses and conclusions set out in this dissertation are entirely my own effort, except where otherwise indicated and acknowledged.

I further certify that the work is original and has not been previously submitted for assessment in any other course or institution, except where specifically stated.

\_\_\_\_\_

/ /

Ibrahim Khalil Sileh, Candidate

\_\_\_\_\_

/ /

A/Prof. Wei Xiang, Principal supervisor

\_\_\_\_\_

/ /

Dr. Andrew Maxwell, Associate supervisor



# Acknowledgments

First and foremost, without the enlightenment of ALLAH, this thesis would not have been done successfully.

I would like to express my deep gratitude to my supervisor A/Prof. Wei Xi-ang. I would also like to thank my associate supervisor Dr. Andrew Maxwell for his insightful comments and for contributing his broad perspectives to this thesis. My thanks go to Prof. Youngi Li for his invaluable suggestions and recommendations throughout the project.

My special appreciation goes to my colleague Catherine Hills for her assistance with the proofreading. Thanks also go to A/Prof. John Leis for his brilliant advice.

I would like to gratefully thank the Staff of the Faculty of Health, Engineering and Sciences, School of Mechanical and Electrical Engineering at the University of Southern Queensland, Toowoomba, Australia, who have been supported me immensely during this research.

Finally, I am especially grateful to my family for all the love, concern, understanding, their everlasting moral support and encouragement when I felt frustrated during the research process. Without them none of this would have been possible and so it is to them I dedicate this work.

IBRAHIM KHALIL SILEH

*University of Southern Queensland*

*May 2014*



# List of publications

The following publications were produced during the period of candidature:

[1] I. K. Sileh, W. Xiang and K. M. Alajel, “Outage probability of unequal block-based OFDM amplify-and-forward relay protocol over wideband channels,” in *Proc. IEEE 12th International Symposium on Communications and Information Technologies (ISCIT 2012)*, Gold Coast, Australia, Oct. 2012, pp.1-5.

The work in the paper is presented in Chapter 3.

[2] I. K. Sileh , W. Xiang, and A. Maxwell “Joint Subcarrier Pairing and Resource Allocation for Adaptive Hybrid Relay Protocol in OFDM Systems,” in *Proc. IEEE 24th International Symposium on Personal, Indoor and Mobile Radio Communications (PIMRC13)*, London, UK, Sep. 2013, pp.2011-2015.

The work in the paper is presented in Chapter 4.

[3] I. K. Sileh , W. Xiang, and A. Maxwell “Error Probability of OFDM-based Hybrid Relay Protocols Over Wideband Fading Channels,” in *Proc. IEEE International Conference on Ultra-Wideband (ICUWB)*, Sydney, Australia, Sep. 2013, pp.255-260.

The work in the paper is presented in Chapter 4.

[4] I. K. Sileh and W. Xiang, “Distributed space-frequency coding for OFDM-based hybrid relay selection,” in *Proc. IEEE 12th International Symposium on Communications and Information Technologies (ISCIT 2012)*, Gold Coast, Australia, Oct. 2012, pp.1-5.

The work in the paper is presented in Chapter 5.

[5] I. K. Sileh , W. Xiang and A. Maxwell “Power allocation of distributed space-frequency coding for OFDM-based hybrid relay selection,” in *Proc. IEEE*

*7th International Conference on Signal Processing and Communication Systems*, Gold Coast, Australia, Dec. 2013.

The work in the paper is presented in Chapter 5.

[6] I. K. Sileh, K. M. Alajel, and W. Xiang, “Cooperative relay selection based UEP scheme for 3D video transmission over Rayleigh fading Channel,” in *Proc. IEEE International Conference on Digital Image Computing Techniques and Applications (DICTA)*, Noosa, Australia, Dec. 2011, pp.689-693.

The work in the paper is presented in Chapter 6.

[7] K. M. Alajel, W. Xiang, and I. K. Sileh, “Best relays selection method for error-resilient 3-D video transmission” in *Proc. IEEE 12th International Symposium on Communications and Information Technologies (ISCIT 2012)*, Gold Coast, Australia, Oct. 2012, pp.1-5.

The work in the paper is presented in Chapter 6.

# Contents

<b>Abstract</b>	<b>i</b>
<b>Acknowledgments</b>	<b>v</b>
<b>List of Publications</b>	<b>vii</b>
<b>List of Figures</b>	<b>xii</b>
<b>List of Tables</b>	<b>xvi</b>
<b>Acronyms &amp; Abbreviations</b>	<b>xvii</b>
<b>Chapter 1 Introduction</b>	<b>1</b>
1.1 Research Motivations . . . . .	2
1.1.1 Cooperative Systems . . . . .	3
1.1.2 Orthogonal Frequency Division Multiplexing . . . . .	4
1.1.3 High Data Rate Applications . . . . .	6
1.2 Research Problem . . . . .	7
1.3 Summary of Original Contributions . . . . .	8
1.4 Structure of the thesis . . . . .	9
<b>Chapter 2 Background</b>	<b>11</b>
2.1 Introduction . . . . .	11
2.2 Cooperative Relaying . . . . .	11
2.2.1 Amplify-and-Forward (AF) . . . . .	13
2.2.2 Decode-and-Forward (DF) . . . . .	14
2.2.3 Hybrid Relay Protocol (HRP) . . . . .	16
2.3 Adaptive Techniques for OFDM Relaying Systems . . . . .	20
2.3.1 Resource Allocation (RA) . . . . .	21
2.3.2 Adaptive Bit and Power Allocation . . . . .	23
2.3.3 Subcarrier Permutation (SP) . . . . .	25
2.3.4 Joint Subcarrier Permutation (SP) and Resource Allocation	27

2.4	Distributed Space-Frequency Coding (DSFC) for OFDM Technique	29
2.5	3D Video Transmission in Wireless Networks . . . . .	32
2.6	Conclusion . . . . .	33
<b>Chapter 3 Selective OFDM Relaying</b>		<b>35</b>
3.1	Introduction . . . . .	35
3.2	Motivation and Related Work . . . . .	36
3.3	System Model . . . . .	37
3.4	Outage Probability Analysis . . . . .	39
3.4.1	Outage Probability of End-to-end Single Sub-carrier . . . . .	40
3.4.2	Selective OFDM . . . . .	41
3.4.3	Selective OFDMA . . . . .	44
3.4.4	Selective Block-OFDM Relaying . . . . .	46
3.4.5	Selective Unequal Block-OFDM Relaying . . . . .	48
3.5	Results and discussions . . . . .	51
3.6	Conclusion . . . . .	56
<b>Chapter 4 Selective Per-subcarrier OFDM-based HRP</b>		<b>57</b>
4.1	Introduction . . . . .	57
4.2	Related Work . . . . .	59
4.3	System Model . . . . .	61
4.3.1	MC-HRP Strategy . . . . .	64
4.3.2	Proposed MC-AHRP Strategy . . . . .	65
4.4	Cumulative Density Function Derivation . . . . .	66
4.4.1	MC-HRP Scheme . . . . .	67
4.4.2	MC-AHRP Scheme . . . . .	68
4.5	Bit and Power Allocation at the Source . . . . .	71
4.6	Bit and Power Allocation at the Relay . . . . .	72
4.6.1	Without Subcarrier Permutation . . . . .	72
4.6.2	With Subcarrier Permutation . . . . .	73
4.7	Performance Analysis . . . . .	75
4.7.1	Bit Error Probability Performance . . . . .	75
4.7.2	Outage Probability . . . . .	81
4.7.3	System Capacity . . . . .	82
4.8	Simulation Results . . . . .	83
4.9	Conclusion . . . . .	93
<b>Chapter 5 Space-Frequency Coding with OFDM-HRP Systems</b>		<b>95</b>
5.1	Introduction . . . . .	95
5.2	Related Work . . . . .	97

5.3	System Model . . . . .	100
5.4	Power Allocation and Sub-carrier Pairing for DSFC-OFDM . . . . .	108
5.4.1	Power allocation . . . . .	108
5.4.2	Sub-carrier Pairing . . . . .	113
5.4.3	Joint Power Allocation and Sub-carrier Pairing . . . . .	114
5.5	Simulation Results . . . . .	116
5.6	Conclusion . . . . .	120
<b>Chapter 6 3D Video Transmission Over Cooperative OFDM Re-</b>		
<b>laying Systems</b>		<b>121</b>
6.1	Introduction . . . . .	121
6.2	Motivation and Related Work . . . . .	123
6.3	3D video coding and DIBR Representation . . . . .	126
6.3.1	H.264/AVC Coding . . . . .	126
6.3.2	Depth Image Based Rendering (DIBR) Representation . . . . .	127
6.4	System Model . . . . .	128
6.4.1	UEP Based on HRP . . . . .	131
6.4.2	UEP Based on First and Second Best AF relays (FBSB) . . . . .	133
6.5	PDF of proposed protocols . . . . .	134
6.5.1	UEP Based on HRP . . . . .	134
6.5.2	UEP Based on First and Second Best AF relays (FBSB) . . . . .	137
6.6	End-To-End Performance Analysis . . . . .	138
6.6.1	Bit Error Probability Performance . . . . .	138
6.6.2	Outage Probability Performance . . . . .	139
6.7	Simulation and Numerical Results . . . . .	140
6.8	Conclusion . . . . .	152
<b>Chapter 7 Conclusions and Future Work</b>		<b>153</b>
7.1	Introduction . . . . .	153
7.2	Conclusions . . . . .	154
7.3	Future Work . . . . .	157
7.4	Final Remarks . . . . .	159
<b>References</b>		<b>161</b>

# List of Figures

- 2.1 Cooperative communication with three terminals. . . . . 12
- 2.2 Spectral characteristic of OFDM transmission. . . . . 13
- 2.3 Block diagram of the AF-OFDM relaying with adaptive power loading. . . . . 14
- 2.4 Adaptive decode-and-forward relay protocol. . . . . 15
- 2.5 Block diagram of hybrid forwarding relay scheme a) Ideal mode b) Outage mode. . . . . 17
- 2.6 Block diagram of hybrid forwarding relay for OFDM system. . . . . 20
- 2.7 Block diagram of hybrid forwarding relay with different selection style a) Selection criterion I b) Selection criterion II. . . . . 20
- 2.8 Block diagram of the OFDM transceiver with adaptive resource allocation. . . . . 24
- 2.9 Bit and power allocation. . . . . 25
- 2.10 Channel coefficients for the first and second hops. . . . . 26
  
- 3.1 System model of selective OFDM relaying. . . . . 37
- 3.2 Frame structure of selective OFDM relaying where  $i \in \{1, \dots, M\}$  and the selected relay forwards the entire sub-carriers of the OFDM symbol. . . . . 42
- 3.3 Frame structure of selective OFDMA relaying where  $i \in \{1, \dots, M\}$ . 45
- 3.4 Frame structure of selective block OFDM relaying where  $i \in \{1, \dots, M\}$ . 47
- 3.5 Frame structure of selective Unequal block OFDM relaying where  $i \in \{1, \dots, M\}$ . . . . . 49

3.6	Outage probability versus SNR with $M=10$ and $N=16$ without direct transmission. . . . .	53
3.7	Outage probability versus SNR with $M=10$ and $N=16$ with direct transmission. The dash line represents the upper bound while the solid line denotes the simulation results. . . . .	53
3.8	Outage probability versus $M$ with $\text{SNR}=10$ dB and $N=16$ without direct transmission. . . . .	55
3.9	Outage probability versus $N$ with $M=10$ and $\text{SNR}=10$ dB. . . . .	55
4.1	Transceiver block diagram of the relay node a) MC-HRP b) MC-AHRP. . . . .	63
4.2	Transceiver block diagram of the relay node with sub-carrier pairing. . . . .	74
4.3	Numerical results of the error probability versus different values of SNR threshold of the MC-AHRP and the MC-HRP schemes (proposed by Li) for different values of $d_r = \frac{d_{sr}}{d_{sd}}$ and $\text{SNR}=15$ dB. . . . .	84
4.4	Numerical results of the error probability versus different values of SNR threshold of MC-AHRP for different values of $d_r$ and average SNR. . . . .	84
4.5	The bit error probability of the MC-AHRP and the MC-HRP schemes versus different values of SNR for $d_r = 0.5$ and $\gamma_{th} = 1$ , the theoretical results (solid line) and the simulation results (dashed line). . . . .	86
4.6	The bit error probability of the MC-AHRP scheme versus different values of SNR for different values of $d_r$ and $\gamma_{th} = 1$ , the theoretical results (solid line) and the simulation results (dashed line). . . . .	87
4.7	The bit error probability of the MC-AHRP (solid line) and the MC-HRP (dashed line) schemes versus different values of SNR for different values of $\gamma_{th}$ and $d_r = 0.5$ . . . . .	88
4.8	Numerical results of the error probability of MC-AHRP versus different values of SNR for different values of $d_r$ and $\gamma_{th} = 1$ dB. . . . .	89

4.9	Outage probability of the MC-AHRP (solid line) and the MC-HRP (dashed line) schemes versus SNR for both schemes for different values of $d_r$ with $\gamma_{th} = 2\text{dB}$ . . . . .	89
4.10	Outage probability of the MC-AHRP (solid line) and the MC-HRP (dashed line) schemes versus SNR for both schemes for different values of SNR threshold with $d_r = 0.5$ . . . . .	90
4.11	Capacity performance versus different values of SNR with and without RA and SP for $d_r=0.3$ . . . . .	91
4.12	Capacity performance versus relative distance $d_r = d_{sr}/d_{sd}$ for different values of $\gamma_{th}$ and SNR=15 dB. . . . .	91
4.13	Capacity performance of MC-AHRP protocol versus relative distance $d_r = d_{sr}/d_{sd}$ with and without RA and SP for SNR=15 dB. . . . .	92
5.1	Cooperative system architecture . . . . .	100
5.2	System model for the distributed Alamouti code with: a) 2 relay nodes and b) 4 relay nodes. . . . .	103
5.3	DSFC-OFDM transceiver architecture. . . . .	107
5.4	BEP performance of the DSFC-OFDM based on HRP for single cluster. . . . .	117
5.5	BEP performance of the DSFC-OFDM based on HRP for two clusters. . . . .	118
5.6	BEP performance of the DSFC-OFDM based on HRP versus SNR with and without adaptive techniques when M=6 and N=64. . . . .	118
5.7	System capacity of the proposed versus SNR for two clusters with 4 relay nodes. . . . .	119
5.8	System capacity of the proposed versus SNR with and without adaptive techniques. . . . .	119
6.1	Block diagram of color-plus-depth video representation. . . . .	127
6.2	Color-plus-depth representation in DIBR for Newspaper test sequence a) color image b) depth map. . . . .	128
6.3	Virtual left and right views generation in DIBR process. . . . .	129

---

6.4	System Model. . . . .	130
6.5	Hybrid relay selection system model. . . . .	132
6.6	First and second best relay selection system model. . . . .	133
6.7	Bit error probability performance of the UEP-based HRP and EEP versus SNR . . . . .	141
6.8	Outage probability performance of the UEP-based HRP and EEP versus SNR. . . . .	142
6.9	Average PSNR of video sequence. . . . .	143
6.10	Average PSNR of the Interview sequence versus SNR for EEP and UEP based HRP. . . . .	145
6.11	Average PSNR of the Interview sequence versus SNR for EEP and UEP based HRP. . . . .	146
6.12	Average PSNR of the Interview sequence versus SNR for EEP and UEP based HRP. . . . .	147
6.13	Original frames of <i>Interview</i> sequence. . . . .	148
6.14	Reconstructed frames of EEP at $SNR = 12$ dB for <i>Interview</i> se- quence. . . . .	149
6.15	Reconstructed frames of UEP based HRP at $SNR = 12$ dB for <i>Interview</i> sequence. . . . .	150
6.16	Reconstructed frames of UEP based FBSB at $SNR = 12$ dB for <i>Interview</i> sequence. . . . .	151

# List of Tables

- 3.1 Scenarios for Sub-carriers Distribution . . . . . 52
- 4.1 SNR threshold values of modulation scheme . . . . . 72
- 4.2 Optimum Threshold of the Given Range of Channel Simulation  
Parameters . . . . . 85
- 5.1 Transmission sequence for each relay node for single cluster . . . . 102
- 5.2 Transmission sequence for each relay node for two clusters . . . . 104
- 6.1 Average PSNR of different UEP Protocols for the *Interview* sequence 144



# Acronyms & Abbreviations

ABPA	Adaptive bit and power allocation
ADF	Adaptive decode-and-forward
AF	Amplify-and-forward
AVC	Advance video coding
AWGN	Additive white Gaussian noise
BEP	Bit error probability
BER	Bit error rate
BL	Bit loading
BPSK	Binary phase shift key
CD	Cooperative diversity
CDF	Cumulative density function
CRC	Cyclic redundancy check
CSI	Channel state information
DIBR	Depth image based rendering
DF	Decode-and-forward
DSFC	Distributed space frequency coding
EEP	Equal error protection
FBSB	First best second best
FEC	Forward error correction
HRP	Hybrid relay protocol
iid	Independent and identical distribution
ISI	Inter-symbol interference
MC-AHRP	Multi-carrier adaptive hybrid relay protocol
MC-HRP	Multi-carrier hybrid relay protocol
MGF	Moment generation function

MIMO	Multi-input-multi-output
OFDM	Orthogonal Frequency Division Multiplexing
OSP	Ordered subcarrier pairing
PA	Power allocation
PDF	Probability density function
PSNR	Peak signal-to-noise ratio
QAM	Quadrature amplitude modulation
RA	Resource allocation
RS	Relay selection
SNR	Signal-to-noise ratio
SP	Sub-carrier pairing
STBC	Space time block codes
STC	Space time codes
TDM	Time division multiplexing
UEP	Unequal error protection
VCL	Video coding layer



# Chapter 1

## Introduction

The growing demand for high data rate wireless communication systems over broadband channels necessitates a system re-design to increase compatibility with the wireless environment. System performance can be significantly limited by channel defects such as channel fading and inter-symbol interference (ISI). An important technique to mitigate the detrimental effects of fading in a wireless system is the use of diversity techniques including temporal, spatial, or frequency diversity or their hybrids. Diversity provides the destination with multiple copies of the source signal. Several techniques have been previously investigated in the literature to achieve diversity including multiple-input multiple-output systems (MIMO) [1], OFDM modulation, space time-frequency block codes [2, 3], relay selection [4] and adaptive bit and power allocation [5].

The evolution of wireless broadband networks, such as WiMax, Wi-Fi, LTE and 3GPP, has created an important need for research into video transmission. Video transmission over wireless networks is one of the most popular methods for future generations of wireless systems. Recently, three-dimensional (3D) video transmission has attracted much interest [6–8] and it is anticipated to grow significantly in wireless multimedia applications. However, transmitting 3D video over wireless networks is a challenging task due to the inherent high error probability and bandwidth constraints. Cooperative communications offer the potential to overcome these challenges by transforming the link between transmitter and receiver into multiple hops with shorter, more reliable links.

Conventional relaying amplify-and-forward (AF) and decode-and-forward (DF) schemes have suffered from noise amplification and error propagation [4,9,10]. The hybrid relay protocol (HRP) overcomes these drawbacks [11–13]. Many different forms of HRP approaches have been proposed although there is still potential for future improvement.

In order to achieve the benefits of the aforementioned techniques, there is considerable active research in cooperative networks over broadband wireless communication channels. The first part of this thesis contributes to this research through an investigation of the potential improvements in system performance by adopting diversity techniques. The second part investigates the advantages of cooperative communications and induced diversity to serve high data rate systems such as 3D video transmission.

## 1.1 Research Motivations

The main purpose of communication systems is to broadcast information from the source to the destination over a reliable channel with maximum throughput. Recently, cooperative communications have been developed to achieve this through the creation of multiple communication paths between the source and the destination. These links are mutually independent. As a result, the destination receives multiple versions of the source information, thus providing spatial diversity. In the past, multiple-input multiple-output (MIMO) systems have been proposed as an efficient technique to achieve transmission and reception diversity by using several antennas at the transmitter and/or receiver [1, 2]. It can obtain a potential high spectral efficiency to overcome the drawbacks caused by channel fading. The use of multiple antennae in small wireless terminals may, however, be impractical due to size, cost, or hardware restrictions. It has proven that the cooperative (relaying) communications can realize the benefits of conventional MIMO systems and provide cooperative diversity gains without any reliance on multiple antennae [4].

### 1.1.1 Cooperative Systems

The underlying concept of a cooperative system is that the client devices share resources and cooperate through distributed transmission to form virtual antenna arrays (VAA) that can reap the benefits of conventional MIMO systems without the additional hardware requirements. Moreover, it can enlarge the service footprint area covered by the system and enhance throughput by utilizing intermediate nodes and short links. This also enhances system reliability by exploiting spatial diversity.

In general, cooperative protocols are classified into two broad schemes named amplify-and-forward (AF) and decode-and-forward (DF). In the AF protocol, the relay amplifies and forwards the signals received from the source. However, it not only amplifies the signal received from the source, but also any noise received by the relay node. Alternatively, in the DF protocol, the relay attempts to decode the received signal, which may introduce error propagation, then re-encodes and forwards it to the destination. Various types of cooperative protocols have been proposed to overcome the shortcomings of the AF and DF schemes. The authors in [14–17] proposed an adaptive DF (ADF) scheme. An alternative protocol is proposed in [11], [18] known as hybrid relay protocol (HRP), and is designed to overcome the disadvantages of conventional relaying protocols. However, the signal may be corrupted when transmitted over sub-carriers that experience deep fading. In order to avoid this problem a new paradigm of HRP with multi-carrier technique is presented known as multi-carrier adaptive hybrid relay protocol (MC-AHRP).

Multiple cooperative communication systems can drastically increasing the cooperative diversity gains [4]. However, this can make degradation in the spectral efficiency due to the relays must transmit on orthogonal channels to avoid the interference. Relay selection is one of the most popular techniques has adopted to overcome this problem [14, 19–21]. In relay selection protocol, the relay that has best channel condition forwards the source signal toward the destination. Therefore, the communication protocol requires only two orthogonal channels. As a result, the bandwidth efficiency can be improved without any lost in cooperative

diversity.

### 1.1.2 Orthogonal Frequency Division Multiplexing

Orthogonal frequency division multiplexing (OFDM) is considered a physical layer technology in broadband wireless networks. It has been adopted as an effective technique to capture multi-path energy, mitigate ISI caused by multi-path propagation, and offer high spectral efficiency in broadband communications. In addition, OFDM is a transmission technique that transforms frequency-selective fading channels into several independent flat fading sub-channels. Therefore it is suitable for high data rate communication systems over frequency selective fading channels and has been widely accepted for commercial broadband wireless network standards such as IEEE 802.11 (WiFi) [22] and 802.16 (WiMax) [23]. It has also been proposed for the long-term-evolution (LTE) of universal mobile telecommunications systems (UMTS). Cooperative communication combined with OFDM is a promising technique to enhance the performance and enlarge the coverage area of high data rate communication systems.

Design and analysis of selective OFDM in cooperative communications have recently attracted considerable attention. OFDM-based relay systems have been adopted by the current wireless standard IEEE 802.16j. In general, there are two main strategies for selective OFDM relaying. The first strategy is to select an entire OFDM symbol by single relay, which is referred to as selective OFDM. The second way is to select a single relay for each subcarrier or group of sub-carriers and this is referred to as selective orthogonal frequency division multiple access (OFDMA) (per-subcarrier basis). Channel power gain suffers different attenuation according to the circumstance of the channel environments. An active area of research is using resource allocation [24] and adaptive bit and power allocation (ABPA) [25] for the OFDM-based relaying systems in an effort to overcome these drawbacks in channel environments.

Optimizing resource allocation or adaptive bit and power allocation (ABPA) are effective approaches to mitigating the detrimental effects of wireless channels in broadband communication systems. They offer multi-path diversity and there-

fore significant performance improvements can be achieved when implemented in a cooperative OFDM relay system. This can play a vital role in enhancing system performance by making full use of the channel parameters. A number of papers have discussed resource allocation in single hop OFDM systems to maximize the capacity or to minimize error performance [5, 26–34]. For OFDM relay protocols, the task of resource allocation is to allocate the amount of power per symbol not only for the source and the relay terminals but also for each sub-carrier on both hops. In addition, the ABPA consists of bit loading (BL) and power allocation (PA). The general idea of the BL algorithm is that the number of bits per symbol for each sub-carrier at source and relay will vary according to the channel state information (CSI) of the first and second hops. Therefore, it can reduce the transmission power from the source and relay as well as increasing data rates. In the PA algorithm, the amount of power assigned to each sub-carrier depends on the quality of the channel. As a result, sub-carriers that experience deep fading are assigned minimal or no power and vice versa for good sub-channel conditions.

Subcarrier permutation (pairing) (SP) can further improve the spectrum efficiency of OFDM-based relay systems by allowing the relay to reassign the sub-carriers in both hops. In the SP scheme, the  $n$ th subcarrier in the first hop joins with the  $m$ th subcarrier in the second hop based on the channel power quality of both links. The simplest method of employing SP is by arranging the sub-carriers in the first and second hops in descending or ascending order [35, 36]. However this technique might not provide an optimal solution especially when the relay is close to or far from the source. To cope with this, the sub-carriers in the relay are partitioned into two groups according to the forwarding scheme. Then an efficient SP can be implemented to achieve better capacity performance.

Space time coding (STC) schemes can provide spatial diversity by delivering the destination with a replica of the original signal via independent fading links. It has been proven that STC schemes can achieve full spatial diversity for MIMO [1], and for cooperative communications [14]. This is known as a distributed STC (DSTC) system due to the fact that the received signals arrive simultaneously at their destination from multiple users. As a result, it can achieve

the full transmission rate. This technique is efficient when used with flat fading channels. However, broadband communication systems suffer from severe multi-path fading and delay spread, which destroys their orthogonality when applied with STC. OFDM technique has ability to overcome this problem by dividing the wideband channel into numerous narrowband subchannels. Space frequency coding (SFC) combined with OFDM modulation has been investigated in order to explore multi-path and frequency diversities in MIMO systems [37] as well as cooperative diversity [38]. Moreover, it can reduce the harmful effects of fading in the frequency domains for OFDM systems.

### 1.1.3 High Data Rate Applications

Three dimensional video transmission has become one of the interesting areas of research in wireless communication systems. The video coding standard H.264/AVC (Advanced Video Coding) achieves high compression efficiency [39]. It has been widely accepted as a suitable video coding standard for wireless video transmission. H.264/AVC employs variable length coding, so the transmitted bit stream, which experiences unequal bit error sensitivity, may suffer severe degradation due to error-prone channels. To cope with this problem, unequal error protection (UEP) was proposed where the video bitstreams are partitioned into several layers of different levels of importance [40]. In UEP, the most important bits are protected with higher priority than less important bits. Several techniques of UEP have been studied for transmitting multimedia data over single-carrier MIMO systems [41–43] and over multi-carrier (OFDM) systems [8]. The extent to which performance of 3D video transmission can be further improved with depth image based rendering (DIBR) was investigated in [44]. To increase the robustness of transmitting 3D video scenes over wireless environments, cooperative communication, which exhibits high diversity gain can be used. A combination of OFDM relaying systems with DIBR technique can provide significant improvement in video transmission.

## 1.2 Research Problem

The previous discussion shows that diversity can take many forms according to the physical layer scheme used. The objective of this research is to design and analyse new techniques for diversity concatenated with OFDM relaying systems to overcome the drawbacks of conventional protocols. The approach is to modify the protocol by utilizing techniques such as relay selection, adaptive resource allocation, sub-carrier permutation and space time frequency coding in order to increase the robustness of channel variations. The research tasks in this thesis are:

### **Subproblem 1:**

To investigate the outage probability performance of selective OFDM relaying with, and then without direct transmission over frequency-selective Rayleigh fading channels. Unequal block-OFDM relaying is proposed to provide a unified scheme.

### **Subproblem 2:**

To investigate a new type of hybrid relay protocol concatenated with multi-carrier (OFDM) technique called a multi-carrier adaptive hybrid relay protocol, which avoids the sub-carriers that experience deep fading over frequency-selective channels. For comparison purposes a conventional hybrid relay selection will be extended from a single carrier system to multi-carrier system. An efficient algorithm of adaptive bit and power allocation with, and then without subcarrier pairing is proposed.

### **Subproblem 3:**

To investigate the use of a DSFC based hybrid relay protocol with relay selection to overcome the drawbacks of multi-path fading in frequency-selective channels. Full-rate and full diversity order can be achieved by exploiting the advantages of DSFC and relay selection. Power allocation optimization, with and without subcarrier permutation, is investigated to further improve system performance.

**Subproblem 4:**

To investigate unequal error protection (UEP) in the physical layer based on relay selection to deliver 3D video scenes to the end user with useful improvements in error resilience and reliability. Two strategies for UEP are proposed based on hybrid relay selection and first best second best relay selection. The proposed schemes take into account the protection level of the 3D video sequences.

### 1.3 Summary of Original Contributions

The main contribution of this thesis can be summarized as follows:

- **Selective OFDM(A) Relaying Scheme:** The selective OFDM(A) schemes, where the AF approach is used at the relay node is investigated in Chapter 3. It was shown that selective OFDM is less complex than selective OFDMA, whereas selective OFDMA has better outage probability performance. To achieve a flexible tradeoff between complexity and diversity gain, selective unequal block OFDM is proposed and developed. The closed-form expression of outage probability is analyzed when the direct link is assumed to be absent. The proposed protocol was published in [45].
- **Selective Per-sub-carriers OFDM-based HRP:** The conventional hybrid protocol is extended from a single carrier to a multi-carrier system. As a result of the selectivity of channels, some sub-carriers experience deep fading, which degrades system performance. To solve this problem an adaptive hybrid relay protocol based OFDM is proposed where an adaptive DF scheme is used to distinguish the corrupted sub-carriers as described in Chapter 4. The selection per-subcarrier for a single relay is considered. The closed-form expression of bit error probability and outage probability for both protocols are derived over frequency-selective Rayleigh fading channels. Adaptive bit and power allocation techniques with low computational complexity is adopted to achieve better performance. The proposed MC-AHRP and power allocation algorithm was published in [46] and [47].

- **Space-Frequency Coding in Conjunction with HRP Scheme:** The distributed space frequency code (DSFC) is implemented in the selected relay to obtain spatial diversity and full transmission rate in Chapter 5. The hybrid relay selection is utilized to overcome the inherent drawbacks of conventional relaying strategies. The selected relays are organized into clusters to reduce complexity without any loss in performance. Power allocation was applied optimally with and without sub-carrier pairing to further improve system performance. The simulation results demonstrated that the proposed scheme has better performance in terms of bit error probability and capacity than conventional schemes and the hybrid relay protocol using orthogonal channels. The proposed DSFC and power allocation algorithm over frequency selective channel was published in [48] and [49].

- **3D Video Transmission Over Cooperative OFDM Relaying Systems:** The proposed UEP of 3D video transmission based on relay selection is investigated in Chapter 6. Two schemes are proposed: hybrid relay protocol (HRP) and first-best second-best (FBSB) relay selection. Closed-form expression of both schemes is investigated in terms of bit error probability and outage probability based on moment generation function. The peak signal-to-noise ratio (PSNR) results show that the HRP outperforms the FBSB at low SNR due to its higher gain. Whereas, FBSB obtains better PSNR at high SNR than HRP due to it providing higher diversity. The proposed UEP based cooperative communication system was published in [50] and [51].

## 1.4 Structure of the thesis

This thesis is composed of two fundamental parts. The first part of this dissertation studies system performance of the OFDM relaying protocols and consists of Chapter 3, 4, and 5. The second part considers 3D video transmission protocols based on cooperative OFDM system and is addressed in Chapter 6.

**Chapter 2:** presents background on a cooperative communication, OFDM techniques and its application in multimedia transmission. Diverse techniques that

could be used to improve the performance of OFDM-relaying system are also addressed including resource allocation, relay selection, distributed space time coding, sub-carrier pairing as well as unequal error protection for 3D video transmission.

**Chapter 3:** selective OFDM performance in terms of outage probability is addressed and a new approach that can provide a unified scheme is proposed.

**Chapter 4:** demonstrates a new scheme of hybrid relay protocol is proposed and analyzed in order to decrease system complexity and overcome drawbacks in the conventional scheme. Adaptive bit and power allocation to maximize the system capacity under individual power constraint is proposed. Sub-carrier pairing is also investigated to further improve system performance.

**Chapter 5:** investigates distributed space frequency codes over selective OFDM relaying based on hybrid relay selection. Resource allocation and sub-carrier pairing techniques are addressed to provide a substantial improvement in system performance.

**Chapter 6:** presents cooperative communication based on OFDM techniques in multimedia applications. Taking advantage of cooperative diversity, a new technique is proposed using potentially unequal error protection to enhance 3D video transmission over error-prone channels. A closed-form expression of the bit error probability and outage probability are investigated for two particular relay selection schemes; hybrid relay selection and first best second best schemes.

**Chapter 7:** concludes the dissertation with a discussion of future directions in this area of research.

# Chapter 2

## Background

### 2.1 Introduction

This chapter is dedicated to presents a brief review of prior work for two related areas of communication. The first is the cooperative OFDM relaying systems involving resource allocation, subcarrier permutation, and distributed space-frequency coding. It begins in Section 2.2 by introducing cooperative relaying networks employed in single-carrier and multi-carriers transmissions. There are two notable relaying strategies and another secondary strategy created by modifying or combining these strategies. A brief background on these strategies is provided. Section 2.3 discusses prior work for selective OFDM-based relaying protocols including resource allocation, adaptive bit and power allocation and subcarrier pairing. Distribution space-frequency coding in broadband communication with and without resource allocation is discussed in Section 2.4. The later area is the 3D video transmission over OFDM relaying protocols is reviewed in Section 2.5. Section 2.6 concludes the chapter.

### 2.2 Cooperative Relaying

The main aim of communication systems are to broadcast information from the source to the destination via a reliable channel with maximum throughput. Cur-

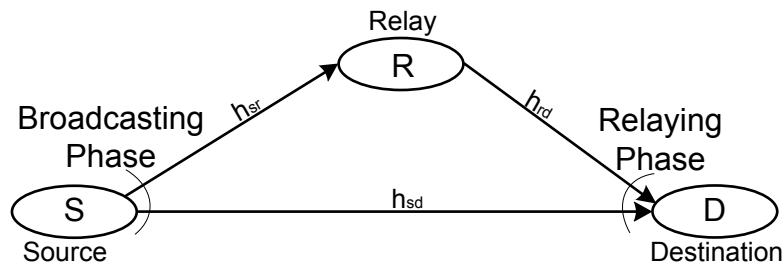


Figure 2.1: Cooperative communication with three terminals.

rently, cooperative relaying is emerging as an effective protocol for next generation of wireless networks. The classical relay channel model was examined by Van der Meulen [52, 53] and involves three nodes known as source, relay and destination as illustrated in Figure 2.1. Later, Cover and El Gamal [54] evaluated the channel capacity for discrete memoryless and Gaussian relay channels. Relaying or cooperative communications techniques can achieve a cooperative spatial diversity by allowing users to cooperate in their transmissions [4, 55, 56]. This enlarges the coverage area and further improves the system performance and reliability. In [4] and [14], Laneman et al. proposed several cooperative diversity schemes and analyzed outage behavior performance. The concepts of fixed relaying such as amplify-and-forward, decode-and-forward, selective relaying, and incremental relaying schemes have been investigated. User cooperation diversity was introduced by Sendonaris et al. in [55] and [57]. In this series of papers, the authors implemented a two-user code division multiple access (CDMA) cooperative system, where both users are active and use orthogonal codes to avoid multiple access interference. Another technique to achieve diversity that incorporates error-control-coding into cooperation was introduced by Hunter et al. in [58]. In [59], Boyer et al. introduced the concept of multihop diversity, in which each relay combines the signals received from all of the previous transmissions. This kind of spatial diversity is especially applicable in multihop ad hoc networks. In cooperative communication systems, relaying protocols are designated in accordance with their functions. Consequently in the next sub-sections type will be summarized.

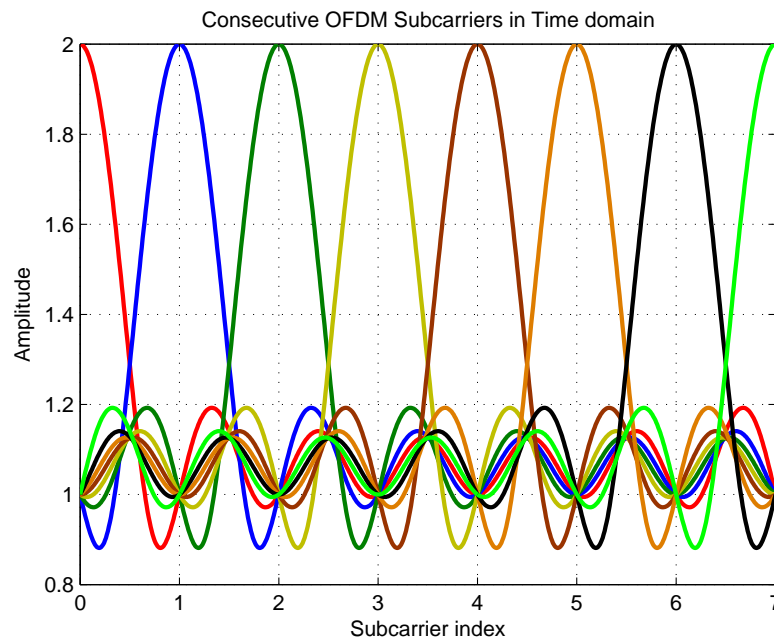


Figure 2.2: Spectral characteristic of OFDM transmission.

Most of research work in cooperative relaying has employed OFDM techniques to overcome inherent problems in frequency-selective channels by exploiting the advantage of converting frequency-selective channel into several frequency-flat sub-channels. In OFDM system, the total bandwidth of the wideband signal is divided into  $N$  narrowband sub-channels with bandwidth  $\frac{W}{N}$ . The bandwidth of each sub-channel should be less than the channel coherence bandwidth to ensure its experience flat fading. Figure 2.2 illustrated the the spectrum of OFDM symbol in frequency domain where the spectra of sub-carriers are overlapped for bandwidth efficiency due to orthogonality. Practically inverse discrete Fourier transform (IDFT) and discrete Fourier transform (DFT) can be used at the transmitter and receiver respectively to implement these orthogonal signal efficiently [60].

### 2.2.1 Amplify-and-Forward (AF)

Amplify-and-forward (non-regenerative) relaying is extremely attractive in cooperative communications due to its easy implementation at the relay terminal and does not utilize any form of decoding. As a result the hardware complexity can

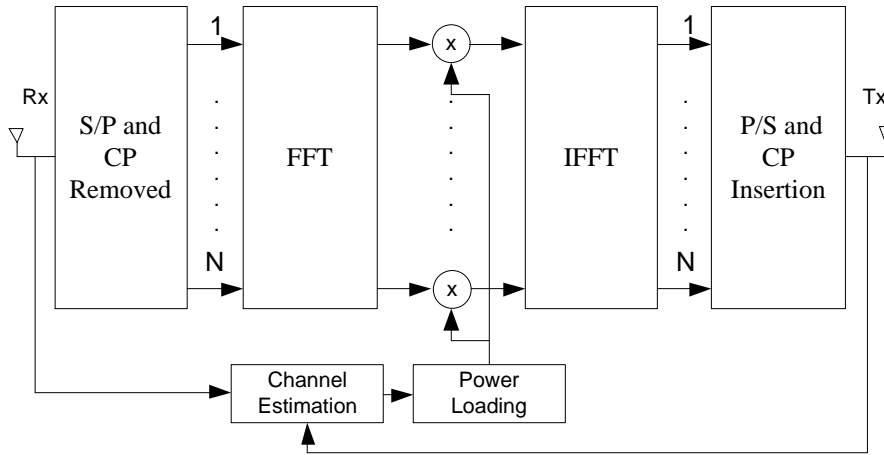


Figure 2.3: Block diagram of the AF-OFDM relaying with adaptive power loading.

be reduced at the relay. The block diagram of the AF relay node is illustrated in Figure 2.3. In the AF scheme, the relay node broadcasts a scale version of source signals under a power constraint to the destination node [4]. In general, there are two different ways to amplify the output of the relay signal according to the relay ability to estimate the first hop channel [4, 61].

The performance of AF-OFDM relaying schemes have attracted some attention in the literature regarding dual hops. Megumi et al. investigated the outage probability for several allocation schemes [62]. In [63–65], a multiple AF-OFDM relaying protocol was considered. The relays transmit in orthogonal channels in [65], while in [63,64], relay selection was considered. Two types of relay selection involving a “per-subcarrier basis” and an “all-subcarrier basis” were investigated to obtain diversity gain [63].

### 2.2.2 Decode-and-Forward (DF)

In a decode-and-forward scheme, the relay node fully decodes the received signal and then re-encodes and retransmits it to the destination. However if the channel quality is weak or in deep fade, the relay fails to decode the received signal successfully. Therefore it experiences error propagation which leads to deterioration of the received signal at the destination. Decode-and-forward may be classified into two schemes according to the decoding style: fixed and adaptive. The main

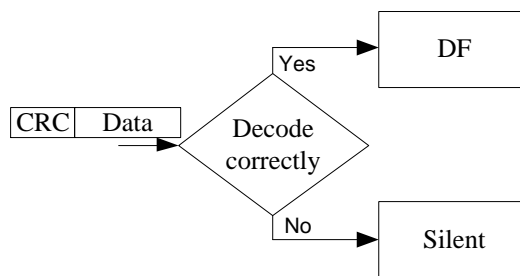


Figure 2.4: Adaptive decode-and-forward relay protocol.

difference between them is that fixed DF always decodes the received signal, while adaptive DF only decodes for sufficient received signal quality.

### 2.2.2.1 Fixed Decode-and-Forward (DF)

In fixed DF relay schemes, the relay always decodes what it receives from the source in the first time slot regardless whether it can decode the received signal correctly or not [4]. It then forwards the decoded signals to the destination in the second time slot. If however the relay fails to decode the received signal successfully, it induces errors at the destination because the relay retransmits the erroneous version of the original signals. This has been extensively studied in single carrier systems over frequency-flat fading channels [4, 58, 66–68].

DF forwarding schemes have been widely investigated in cooperative communications over frequency-selective channels by exploiting the advantages of OFDM modulation [69–74]. In these papers, the authors were considered the relay selection and studied the diversity order that can be achieved by the network in frequency selective fading channels.

### 2.2.2.2 Adaptive Decode-and-Forward (ADF)

The main advantage of the ADF scheme is to eliminate the error propagation induced by the forwarding relay [4, 15, 16, 75]. The underlying concept of ADF is that the relay forwards the received signal to the destination only when it fully decodes the source message successfully, as shown in Figure 2.4. There are two

modes to verify if the relay has successfully decoded the received signal: “ideal mode” and “outage mode”. In the ideal mode, the symbol is appended with cyclic redundancy check (CRC) code [76], while in outage mode the SNR threshold value is considered [15]. Without loss of generality, if the relay detects the check sum correctly in ideal mode or if the received SNR is greater than threshold value, the relay decodes the received signal. Otherwise it refrains from doing so. Ritesh et al. [77] proposed a relay selection scheme utilizing the Shannon’s capacity formula to evaluate the threshold value ( $\gamma_{th} = 2^r - 1$ ), where  $r$  is the rate (capacity). The basic idea of this protocol is that the relays estimate the instantaneous SNR of the first hop and compares it with the SNR threshold. The relays which have an instantaneous SNR larger than the threshold are included in the decoding set and all participate in the second phase (beamforming technique) or the destination selects the best relay (incremental relay selection). The authors in [16], investigated the outage probability of parallel DF relay system in Rayleigh fading channels with dissimilar fading parameters. They represented the end-to-end SNR of the indirect links ( $S - R_i - D$ ) by a random variable denoted  $\xi_i$ . Subsequently, the authors in [75,78] proposed an adaptive decode-and-forward in which the relay forwards the source signal only if decoded correctly. Therefore the probability density function (PDF) is given as

$$f_{\xi_i}(x) = f_{\xi_i|\text{decoded incorrectly}}(x)P_e[\text{decoded incorrectly}] + f_{\xi_i|\text{decoded correctly}}(x)P_e[\text{decoded correctly}] \quad (2.1)$$

To date, all mentioned work on ADF have assumed the channel is flat-fading. At the timing of writing there appears to have been no discovered work considering the OFDM technique incorporated with ADF over frequency-selective channel.

### 2.2.3 Hybrid Relay Protocol (HRP)

As mentioned in the previous subsections, the AF and DF protocols experience noise amplification and error propagation, respectively. In order to overcome the inherent problems in both protocols, a hybrid relay protocol has been recently proposed [11,18]. In general, the channels used in the single carrier systems are flat

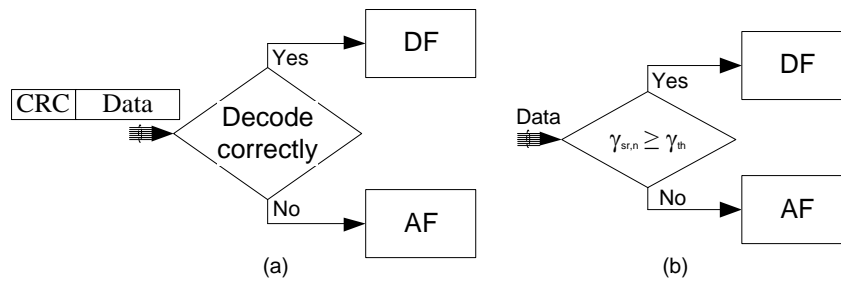


Figure 2.5: Block diagram of hybrid forwarding relay scheme a) Ideal mode b) Outage mode.

fading channels. The authors in [18] and [79] proposed a relay selection scheme based on hybrid relay protocol by adopting CRC codes to ensure whether the codeword is decoded correctly or not, as shown in Figure 2.5. The fundamental idea of the protocol is to classify all the relays into two groups, either the “AF”, or “DF” group according to the instantaneous received signal to noise ratio (SNR). The relays that are able to decode the received signal from the source successfully are included in the DF group, otherwise they are included in the AF group. In [18] the authors studied the frame error rate (FER) performance of hybrid relay selection (HRS) with adopted relay selection, while in [79] an all-participate scheme is considered. A dynamic optimal combination was proposed in [80] by discarding the relays which undergo the deep fading. Liu et. al. modified the relay selection by using SNR threshold value to improve the system performance [81–84]. The closed-form symbol error rate (SER) expression of HRS scheme was derived in [85], and the optimum power allocation under fixed total transmit power is considered. The authors of [86], introduced the hybrid forwarding protocol and derived a closed-form expression of analytical solution of the outage probability over Rayleigh fading channels. The system model is based on a single relay where it can choose a forwarding strategy between AF and DF. If the received SNR at the relay exceeds the predetermined threshold, then the AF protocol is used. Otherwise, the relay performs the DF protocol. Outage probability under optimal power allocation was investigated in [87] based upon opportunistic hybrid forward cooperation. In this protocol the transmitted power

is restricted. The authors assumed that the perfect CSI is available at both the source and the destination. The power assigned at the source and relay can be written as

$$\begin{aligned} P_s &= \varepsilon P_{total} \\ P_r &= (1 - \varepsilon) P_{total} \end{aligned} \tag{2.2}$$

where  $\varepsilon, (1 - \varepsilon)$  indicate the proportions of  $P_{total}$  allocated to the source and the selected relay. The authors of [88] proposed a static hybrid AF and DF relaying protocol. In this protocol, the AF relaying group is composed by the relays that are close to the source and the DF group contains of the remaining relays. The BER performance for both all-participating and opportunistic hybrid AF-DF relaying was considered. In [89], the authors proposed a hybrid decode-amplify-forward (HDAF) protocol in which the relay performs DF if the decoding process succeeds. If the relay cannot decode the received signal successfully, it performs the AF scheme instead of remaining silent. The main shortcoming of this protocol is that the relay has always to decode the received signal in order to decide which scheme to use. Therefore, the authors of [90] proposed SNR-HDAF that selected the protocol to be used at the relay based on the SNR of its received signal. The basic idea of this protocol is that if the received SNR is greater than the threshold SNR the relay performs DF scheme, while it performs the AF scheme in the other case. The authors derived the closed-form expression for the outage probability and error probability over independent non-identical flat Rayleigh fading channels. When the channel parameters between the source and relay are substantially good, the received signal at the relay not corrupted and in this case it is better to use the AF scheme. According to this concept the authors in [91] propose a new adaptive relaying protocol called threshold-based adaptive decode-amplify-forward relaying protocol (T-ADAF). In addition, outage probability and average channel capacity for incremental hybrid decode-amplify-forward were investigated in [12].

In this protocol, the relay compares the received SNR to the average SNR of the source relay link. If the SNR of the received signal is greater than the average SNR of the source-relay link, then the relay performs the AF scheme. On the

other hand, if the SNR of the received signal does not exceed the average SNR of the source-relay link, then the relay performs ADF. The closed-form expression of symbol error probability (SER) of single relay and multiple-relay scenarios was derived and compared with other protocols (e.g AF, ADF, and SNR-HDAF). The authors in [92] investigated the optimization of channel capacity by choosing an optimal relay depending on adaptive relay table (ART). In order to prolong the network lifetime, Heo proposed in [93], [94], an adaptive relay selection based on individual and total power constraint for hybrid relay system. In this protocol, the relays are divided into two groups and two relays are selected according to instantaneous channel conditions. In [93], the optimization problem to maximize the received SNR at the destination with total transmission power constraint of one communication and individual residual power of each relay was considered.

All of above researches on hybrid forwarding scheme have aimed at single-carrier systems. However, Hybrid relay protocol combined with OFDM has received less attention so far. The earlier work was done by Can et.al [11] where each sub-carrier in the relay chooses the forwarding scheme according to the quality of the channel gains. Subsequently system capacity under power allocation for OFDM based hybrid forward relay with two selection criterion was investigated in [95]. The schematic diagram of these protocols are shown in Figures 2.6 and 2.7. In Figure 2.6,  $P_{e,DF}$ ,  $P_{e,AF}$  and  $P_{e,DT}$  denote the probability of error for the DF, AF and DT protocols. While in Figure 2.7,  $\alpha_{sr,n}$ ,  $\mu_{rd,n}$  and  $\beta_{sd,n}$  represent the channel power gains of the source-relay, relay-destination and direct transmission links respectively.  $\gamma_{sr,n}$  and  $\gamma_{th}$  are the instantaneous SNR for the first hop and the threshold value respectively. In these protocols the relay should possess all the subcarrier parameters (direct and indirect) in the network in order to give a forwarding scheme for each sub-carrier. This leads to an increase the overhead signals which can be increased the complexity and reduced the channel capacity. The authors in [80] proposed a dynamic optimal combination strategy for the hybrid relay protocol and evaluated the system BER. The relays are reordered in descending order of the SNR between the source and relays. The first relay performs the DF protocol if the SNR of the S-R link is greater than threshold

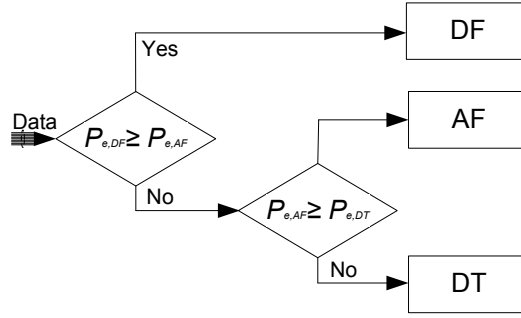


Figure 2.6: Block diagram of hybrid forwarding relay for OFDM system.

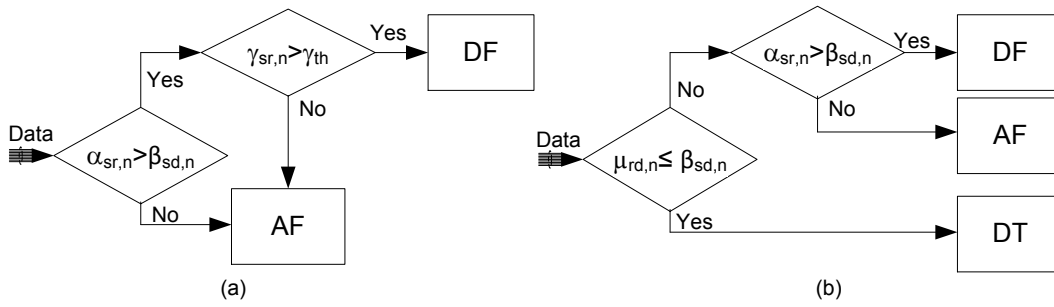


Figure 2.7: Block diagram of hybrid forwarding relay with different selection style  
 a) Selection criterion I b) Selection criterion II.

value. The rest of relays follow the AF protocol and discard the relays which satisfied the dynamic optimal combination strategy. This protocol has a high loss in spectral efficiency due to all relays participating in the communication phase.

## 2.3 Adaptive Techniques for OFDM Relaying Systems

The channel fading in broadband wireless communication systems is generally frequency-selective. The OFDM relaying systems can provide an additional degree of freedom due to the OFDM channel being composed of  $N$  sub-channels with the relay using a half-duplex transmission. The same subcarrier in the first and second slots experience different fading. Even if the subcarrier experiences high gain in the first hop, it is possible to experience deep fade in the second

hop, and vice versa. Under these circumstances resource allocation and subcarrier pairing may increase efficiency. It has been proven that these techniques provide substantial improvements to the OFDM relaying systems over frequency-selective channels. The most important result of this strategy is that the sub-carrier permutation achieves much better performance than adaptive resource allocation.

### 2.3.1 Resource Allocation (RA)

Power allocation for single-carrier relaying systems and multi-carrier systems have been intensively investigated to further increase system performance. Prior work has studied power allocation issues in single-carrier systems to yielded higher system transmission rates [96–98]. The authors in [96] considered optimal power allocation algorithms for both AF and DF schemes in order to minimize the outage probability under overall power constraints. Optimal power allocation to maximize the system capacity was investigated in [97] for DF protocol, while for AF relaying scheme in [98] and taking into account direct transmission. These pioneering works considered either maximizing system capacity, or minimizing outage probability under power constraint in single-carrier systems. However, for OFDM systems each subcarrier experiences independent channel fades and can carry different numbers of bits/symbols, therefore they should be allocated transmission power levels independently. These optimizations either maximize the channel capacity which refers to rate adaptive or minimizing the transmission power refers to margin adaptive. It has been proven that these techniques can enhance the performance of the communication networks [25,99–105]. The objective of the margin adaptive protocol is to minimize overall transmission power under fixed data rate and fixed target BER constraints [25, 99, 100]. Mathematically, can be formulated as

$$\begin{aligned}
 P_T &= \text{Min} \sum_{n=1}^N P_n \\
 \text{Subject to } &\sum_{n=1}^N C_n = C
 \end{aligned} \tag{2.3}$$

where  $P_T$  and  $P_n$  are the total transmit power and the power assigns to  $n$ th sub-carrier respectively.  $C$  and  $C_n$  denote the overall channel capacity and the individual throughput in each sub-carrier respectively. In rate adaptive, the objective is to maximize sum capacity under an aggregate transmit power constraint [101, 102, 106, 107].

$$\begin{aligned}
 C &= \text{Max} \sum_{n=1}^N C_n \\
 \text{Subject to } & \sum_{n=1}^N P_n = P_T
 \end{aligned} \tag{2.4}$$

The work in [99], and [101] considered a multiuser OFDM in single hop transmissions. The authors of [25, 100, 102, 106, 107] investigated OFDM cooperative systems. Their results shown that the system performance can be substantially enhanced when the overall power is distributed to the source and relay optimally.

For multi-hop systems, the optimum power allocation was calculated in [108–113] in order to maximize system capacity for DF-OFDM systems while in [24, 35, 114–116], the AF-OFDM systems were considered. Power allocation based on RA for DF-OFDM relaying system was discussed under individual and global power constraint in [110]. The quality of the channel parameters of the direct and indirect links were taken into account and a modified water-filling algorithm was proposed. However, sub-optimal power allocation may converse to an optimal solution with some improvements to the system complexity [117]. The closed-form expression of symbol error rate (SER) expression was derived in [118] for HRS and the optimum power allocation (OPA) is presented. In order to reduce the overhead signals in a multi-relay AF-OFDM system, suboptimal power allocation with and without sub-channel selection were proposed in [119], which are known as cooperative channel equalization (CCE) and CCE-S, respectively. The substance of CCE algorithm is to distribute the source power uniformly for the sub-carriers and the total relay power is set to be equal to all sub-carriers as

$$\begin{aligned}
 P_{s,n} &= \frac{P_s}{N} \\
 P_n &= \frac{P_T}{N}
 \end{aligned} \tag{2.5}$$

where  $P_{s,n}$  and  $P_s$  are the transmit power of the  $n$ th sub-carrier and the overall power at the source.  $P_n$  and  $P_T$  are the transmit power at the  $n$ th sub-carrier in all relays and the total power budget for relays, while  $N$  is the number of sub-carriers in the OFDM symbol. Eventually the power assigned to each individual sub-carrier is distributed optimally between the relays.

### 2.3.2 Adaptive Bit and Power Allocation

Adaptive bit and power allocation (power allocation (PA) with bit loading (BL)) has been regarded as an efficient way to enhance the system capacity in a cooperative wireless network. The main task of the BL algorithm is to assign an appropriate number of bits in each subcarrier taking into account the channel qualities. Adaptive BL utilizes prior knowledge of channel state information (CSI) to improve the system performance by allocating more bits to sub-carriers that have higher SNR. Without any loss of generality, each subcarrier has a variable number of bits which can be achieved by using different modulation schemes. Therefore, sub-carriers with high channel gains are assigned more bits and employ higher order modulation schemes, whereas sub-carriers experience deep fade or lower channel quality may carry less or zero bits. However, in equal bit loading (EBL), the modulation scheme is constant over all the sub-carriers in the OFDM symbol.

In single-link OFDM communication systems, ABPA techniques have been intensively investigated by utilizing a feedback channel. The block diagram of the OFDM transceiver is illustrated in Figure 2.8. The most important approaches were water-filling [5, 27–29] and greedy [26, 31] algorithms which have proven to be the optimal solution for resource allocation. The main objective of these algorithms is to either maximize system capacity or to minimize system errors (error and outage probability).

The basic structure of the greedy (successive bit allocation) algorithm is to initialize the number of bits allocated to all sub-carriers with a zero. Then the additional transmit power of each sub-carrier is computed and one bit is added to the subcarrier with the least additional transmit power. The process continues until the total capacity has satisfied the information rate constraint.

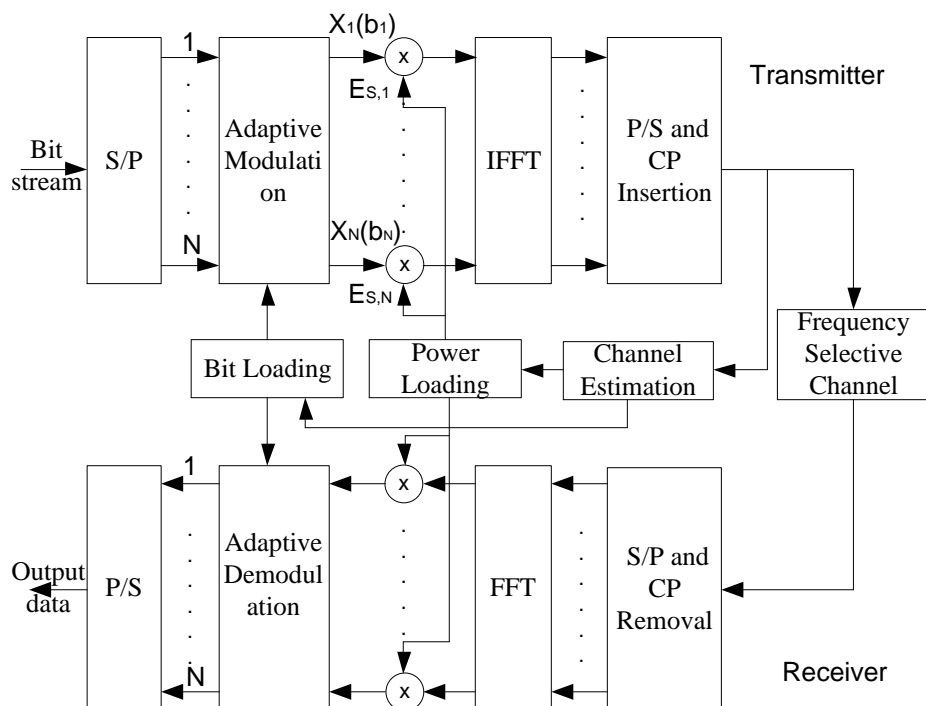


Figure 2.8: Block diagram of the OFDM transceiver with adaptive resource allocation.

As the result, optimization of resource allocation can enhance the system performance substantially. Another method of bit loading algorithm is based on mode switching level. This approach selects a suitable modulation scheme for each subcarrier based on the predetermined SNR threshold for fixed target (BER). This can reduce the computational complexity of BL implementation at the source and decrease the overhead signals. The simply selects the number of bits assigned to each subcarrier (e.g, 0, 1, 2, 4, 6 and 8). These being no transmission, BPSK and M-QAM, where  $M = 2^{b_i}$  as shown in Figure 2.9. However, for relaying transmission the main question is how to allocate the limited power among the source and relay and further among all sub-carriers efficiently. Several papers have demonstrated that combined adaptive modulation with OFDM system can provide a substantial improvement in the system performance [106,107]. Integrated design of resource allocation and OFDM relaying gained extensive interest recently. Since square QAM with gray mapping is an efficient modulation technique and easy to implements [120].

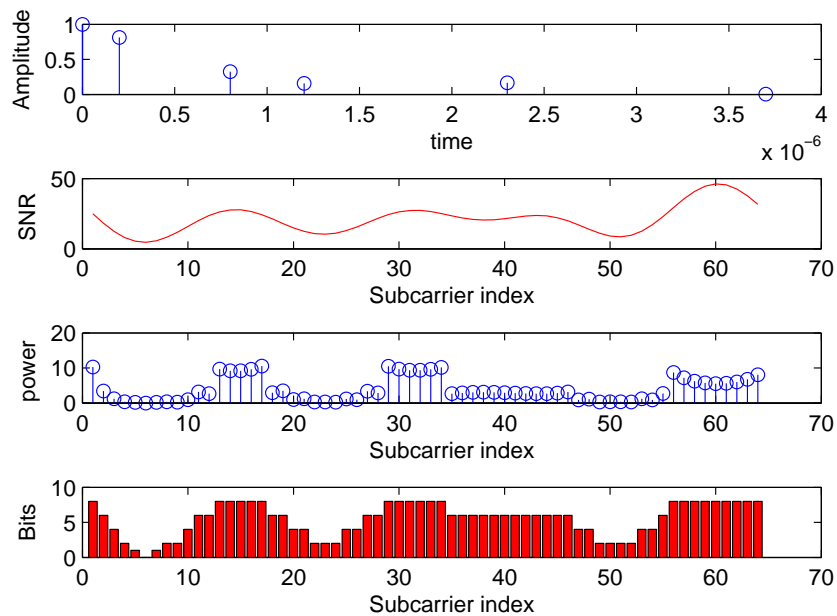


Figure 2.9: Bit and power allocation.

### 2.3.3 Subcarrier Permutation (SP)

In OFDM relaying systems, each time slot is composed of several parallel channels. Since these channels experience frequency-selective fading, the end-to-end subcarrier capacity is limited by the worst one. Figure 2.10 illustrates the channel power gain of the first and second time slot. Thus, the subcarrier capacity decreases when the source information is retransmitted on the same subcarrier in the second hop. The issue is resolved by using an additional degree of freedom provided by OFDM relaying systems that is subcarrier permutation as proposed in [117]. The underlying concept of subcarrier permutation is that the information bearing symbol on the  $i$ th sub-carrier in the first hop may be retransmitted on the same or different sub-carrier in the second hop depending on the CSI. In this work, the authors studied the subcarrier permutation technique for a regenerative

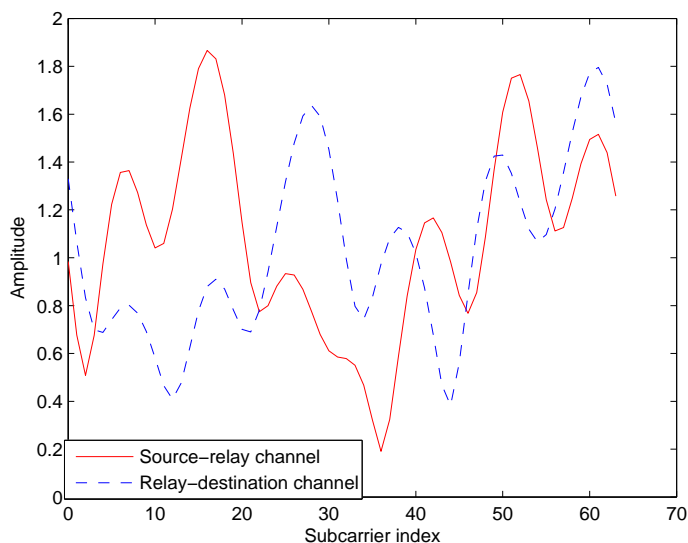


Figure 2.10: Channel coefficients for the first and second hops.

relay system based on OFDM modulation. The Hungarian algorithm was used for subcarrier permutation and the water-filling algorithm was used over selected subcarrier pair for optimal power allocation. The authors in [36, 60, 108] proposed a sorted subcarrier pairing algorithm by matching the subcarrier with highest channel gain at the first slot with the highest one in the second slot which is known as best to best algorithm (BTB) [121] or ordered subcarrier pairing (OSP). The results proved that the system capacity is maximized. However, it does not provide an optimal solution when the direct transmission is available. Therefore, [122] modified the sorted pairing algorithm by selecting the pairing either ascending-sorted or descending-sorted depending on the channel conditions of the S-D and S-R links.

The system capacity of the OFDM based AF multi-relay system with joint relay selection and subcarrier coupling was investigated in [123–125]. The brute force search was investigated in [123] while an opportunistic relay protocol with limited overhead signals was adopted in [125]. Authors in [126] investigated the symbol error probability of an AF-OFDM relaying network with SP and variable-gain of the relay over Rayleigh fading channels. They proved that the system performance can be significantly improved when discarding the worst sub-

carriers. In [127,128], the authors derived the closed-form expressions of average end-to-end SNR and throughput for multi-user downlink OFDMA systems using sub-carrier pairing. In [127] the AF protocol was considered while in [128] performed the DF protocol. The opposite subcarrier pairing scheme is presented in [129] by matching the sub-carrier possesses highest SNR in the first hop with the sub-carrier possesses lowest SNR in the second hop. Following this the closed-form expressions of BER for BTB and best-to-worse (BTW) subcarrier mapping were derived in [121] for the uncoded dual-hop OFDM AF relaying system.

Subcarrier pairing performance appears to has only been investigated either for AF or DF schemes in the literature.

#### 2.3.4 Joint Subcarrier Permutation (SP) and Resource Allocation

Since resource allocation and subcarrier permutation have been proven to improve the system performance when employed independently, it is no surprise that a joint power allocation and sub-carrier pairing scheme proposed in [117] can further improve the system performance. The objective of this paper was to maximize the transmission rate under an aggregate power constraint of the source and relay terminals. The authors of [117] studied sub-optimal power allocation algorithm of an AF-OFDM scheme by evaluating an equivalent channel gain to perform SP and then using water-filling approach for power allocation. In [35], the authors investigated the optimal power allocation of an OFDM-based AF relay system under individual power constraints by dividing the optimization problem in to two sub-optimal problems at the source and relay nodes. The power optimization at the source assumed uniform power allocation at the relay and the power optimization at the relay assumed uniform power allocation at the source. Then ordered subcarrier pairing was considered to perform the subcarrier matching. Optimal power allocation with OSP approach for two-hop regenerative relay system based on OFDM was proposed in [108] with and without diversity (the destination combines signals from the source and the relay). The authors

in [130, 131] were proposed joint SP and PA with total system power constraint while in [132] under individual power constraint by formulating the optimization problem into a mixed binary integer programming problem. The OSP scheme was adopted for sub-carrier matching and the water-filling algorithm was considered for power allocation. The authors in [60] derived an equivalent channel gain model for each sub-carrier pair and employed water-filling algorithm to optimize the total power in the first step. Then in the second step, the allocated power over each sub-carrier pair was partitioned between the source and the relay optimally. The multi-hop OFDM system was considered using a DF scheme in [104, 133] and AF and DF protocols with and without diversity were adopted in [60]. In [134] combined adaptive bit and power allocation (ABPA) with the sub-carrier pairing were investigated in AF-OFDM relaying system. The greedy algorithm and discrete-rate adaptation were adopted for bit loading technique. The performance of BER and system throughput were discussed and the authors concluded that the proposed algorithm obtained an evident improvement compared to conventional fixed modulation. In [135], resource allocation was investigated with and without sub-carrier pairing for a multi-relay DF-OFDM cooperative network to minimizing the total transmit power under a target rate constraint. Several bit loading algorithms were devised by utilizing an equivalent channel gain. The authors in [136] studied multiple relay OFDMA based DF cooperative networks and decomposed the optimization problem into sub-optimal solutions by using uniform PA and an equivalent channel gain for SP approach. The objective was to maximize the aggregate throughput under joint overall transmission power and sub-channels occupation constraints, whereas maintaining the maximum fairness among all relay terminals. They have proven that the maximum capacity of any sub-carrier when the product of power allocation and channel power gain for both hops are equal and mathematically can be expressed as,

$$P_{s,k}(n)G_{s,k}(n) = P_{r,k}(n)G_{r,k}(n), \quad (2.6)$$

where  $P_{s,k}(n)$ ,  $G_{s,k}(n)$  are the power allocation and channel power gain in  $n$ th sub-carrier for  $k$ th relay in the first hop and  $P_{r,k}(n)$ ,  $G_{r,k}(n)$  are the power allocation

and channel power gain in  $n$ th sub-carrier for  $k$ th relay in the second hop.

In [24], sub-carrier pairing and resource allocation for downlink transmission using multi-relay AF-OFDM systems were investigated jointly under separate power constraints. The authors proposed a suboptimal algorithm by employing equal power allocation to assist in sub-carrier assignment and then an iterative water-filling algorithm was executed for power allocation at the source and for all relays. The authors in [131,137] investigated a joint optimal subcarrier assignment and power-allocation policy for the multiuser cooperative OFDM AF Multi-Relay Networks. While single user single DF relay is considered in [138].

To date, most identified research has focussed on resource allocation and sub-carrier pairing in OFDM cooperative systems by exploiting either AF or DF approaches. However, there are still several unresolved problems of sub-carrier permutation and resource allocation in hybrid cooperative relay systems. Most of the algorithms mentioned above are based on an exhaustive sorting scheme.

## **2.4 Distributed Space-Frequency Coding (DSFC) for OFDM Technique**

During the last decade, the combination of space time coding (STC) with MIMO systems has been proposed to provide full spatial diversity and increase the system capacity. The spatial diversity can be achieved by providing the receiver with multiple versions of the transmitted signal through independent fading links [1, 2]. In a MIMO system, the transmitter and the receiver are deployed with multiple antennae to provide different paths. Therefore, the probability of all the links suffering deep fades is reduced significantly. The space between antennae should be few wavelengths in order to avoid the interference. However, it should be noted that a requirement of multiple antennae on small size devices such as ad hoc or sensor is difficult, if not impossible. To cope with this problem, cooperative diversity (CD) was proposed.

Cooperative communication can provide cooperative diversity by the collaboration of multiple single antenna relays. The authors in [4] proposed an efficient

strategy to achieve CD known as repetition-based when the relays contribute on orthogonal channels. However, this can reduce the spectral efficiency to a great extent with high number of relays. Diverse strategies have been investigated to improve the spectral efficiency, such as cooperative beamforming [139], relay selection and distributed space time codes [14]. Among these strategies DSTCs is powerful technique due to it being able to provide full rate transmission in addition to high throughput. The main conclusion of [14] was that the spatial diversity is equal to the available relays in the system not just the number of decoding relays. The outage capacity in a high-SNR regime was analyzed. The authors in [140] derived the pairwise error probability (PEP) for DSTC using a single relay AF mode, while in [141] a large number of relays were considered. The construction of DSTC in [142] has been done by exploiting the broadcast nature of the wireless communication and the optimal maximum likelihood (ML) decoder was proposed. The authors in [143] considered a time-reversal STC for multi-hop cooperative AF and DF relaying communications to achieve spatial diversity over flat and frequency-selective fading channels. In order to exploit DSTC, each AF relay node in the system encodes the received signal from the previous hop and then forwards it to the next hop. Jing and Hassibi [144] derived diversity and coding gains for multiple DF relay utilizing linear dispersion (LD) space-time code. In [145], the STC has been done at the source by dividing the encoded data into two consecutive vectors, each of them  $N$  symbols in length. Then at each relay node, the received vector is multiplied by a unique signature vector. The symbol error rate (SER) was derived for a non-orthogonal AF (NAF) scheme. The authors in [146] investigated opportunistic DSTC (O-DSTC) with full and half duplex mode. The system cooperative diversity considered that consisted of two users using DF scheme, collaborating with each other in transmitting their data to the same receiver. An incremental relaying strategy based on DF scheme in conjunction with DSTC was investigated in [147] and the closed-form of PEP was derived. All the aforementioned techniques were considered narrowband applications (systems) where the channels experience flat-fading.

In broadband systems, combined STC trellis with MIMO-OFDM systems were

first explored in [148] over quasi-static broadband channels while [149] takes into consideration the high doppler spread and interleaving across the OFDM sub-carriers. Then STBC based Alamoti was considered into MIMO-OFDM system in [150–153]. The prior work all used coding in time domain so an alternatives the coding being done in frequency domain. The so-called space-frequency code (SFC) investigated in [154–156]. The authors in [157] improved the STF-OFDM system by dividing the OFDM sub-carriers into groups, then employed linear constellation precoding. In [3], the authors considered a STF code to achieved higher diversity gain over MIMO frequency-selective block-fading channels. This was extended in [158] by applying space-time, space-frequency and space-time-frequency (STF) coding. They showed that the ST-coded OFDM cannot achieve multi-path diversity while SF and STF-coded OFDM can achieve the maximum diversity and full rate over multipath fading channels, at the expense of a high decoding complexity. The previous works have deployed co-located antennas in the terminals to construct MIMO systems over frequency-selective channels, which are difficult to place in the design of small mobile nodes.

Recently, cooperative OFDM systems have received considerable attention for high data rates systems. Distributed OFDM-STBC based on DF mode has been first introduced in [142] by utilizing a single relay and two consecutive OFDM symbols. The source broadcasts the data to the source and destination in the first time slot, then both nodes (source and relay) use a precoded matrix and forward their information to the destination simultaneously. Later, Hakam and Mural [159] investigated the PEP performance of D-OFDM-STBC using an AF single relay which ignored the broadcast nature of wireless transmissions in the first time slot.

Combinations of DSTC with OFDM have been proposed as a way to combat timing errors, [160] assuming multiple perfect DF schemes. Whereas in [161], the authors considered the same scheme to combat both timing errors and frequency offsets for asynchronous communications with a dual fixed DF protocol. The authors in [162] proposed space time code by employing OFDM at the source node and the relay composed of time reversal and complex conjugate. The authors

in [163, 164], demonstrated that full frequency and cooperative diversity as well as full rate transmission can be achieved using DSFC approach. In [163] both erroneous DF and AF protocols are considered for synchronous systems. For the DF scheme, each relay in decoding set forwards the coded symbol to the destination. In the AF protocol, the source data is divided into subblocks, each of which is transmitted by individual relay with a different encoder. Then the relays normalized the received signal on each sub-carrier and assigned null to the rest of sub-carriers. In [164], the multiple AF relay protocol was applied and a circular shift was employed at the relays to form SF codes. They showed that the proposed scheme can achieve a diversity gain of  $\min(ML_1, ML_2)$ , where  $M$  is the number of relay terminals, and  $L_1$  and  $L_2$  are the number of taps of the S-R and R-D multipath channels, respectively. The authors in [165, 166] propose a DSFC scheme to achieve both spatial and multi-path diversity based on erroneous DF relay protocols.

## 2.5 3D Video Transmission in Wireless Networks

Recently, the communication technologies have received a great development in hardware and software which result in substantial enhancements of bandwidth and reliability. The end user can deliver a high data rate applications with reasonable quality of service. Three dimensional video transmission has been gaining attention in wireless systems over different types of channels due to its emergence in new communication technologies. 3D transmission over wireless channels has been suffered from several issues such as the appropriate coding technique, error resilience, display factors etc [167]. The quality of the received signal at the display side can be severely degraded when transmitted over broadband channel. This requires efficient techniques in both application and physical layers to make 3D video transmission reliable in inherently noisy error-prone environments.

Error-resilience is one of the most popular technology to overcome the short-falls of 3D video transmission. In addition, 3D video sequence can be partitioned into different fractions according to the relative importance of the data and visa

verse. Unequal error protection (UEP) is one of the most popular kind of error-resilience uses in 3D video transmission where assign high protection level for a high-priority sequence and low-priority. It takes an important consideration in high data rate application systems due to provides different level of protection for data according to the system requirements.

Various strategies to realize the UEP have been investigated that implemented at the transmitter such as Forward Error Correction (FEC) [44,167], Hierarchical Modulation (HM) [6,168] and MIMO Systems [6,7,41,42]. There has been a considerable research activity for multimedia transmission over MIMO system due to provides spatial diversity. The systems in [41–43,169] treated frequency-flat fading channels while in [6–8], frequency-selective channels were considered. However, this techniques introduce more overhead signals to the encoded bit-stream result in the loss in bandwidth efficiency or increase the system complexity especially for small terminals. Recently, a new kind of UEP knows as cooperative communication systems exhibits the spatial diversity [50,51,170–173]. In this technique, the relay with good channel power gain retransmits the most important coded data and low protection data retransmits with low channel gain. In the following, briefly addressed this techniques. However the single-carrier system is considered. It is clearly notice from the literature that the UEP has received much less attention in cooperative networks in broadband wireless channels. As a result, the 3D video transmission over OFDM-based relay system is an open issues.

## 2.6 Conclusion

This chapter is dedicated to reviewing the existing works on the cooperative-OFDM systems and its application in multimedia transmission. Various types of relaying protocols were reviewed. The important techniques that can implemented efficiently in the OFDM systems including: resource allocation and adaptive bit and bower allocation. These techniques also can be used in OFDM-based cooperative network to further enhance the system performance. Some specific techniques where only employed in OFDM relaying system including: sub-carrier

pairing and distributed space time block code were addressed. Finally, the major 3D video coding techniques and standards in the literature were discussed.

# Chapter 3

## Selective OFDM Relaying

### 3.1 Introduction

Recently, the use of high data rate applications has increased rapidly in ad hoc and infrastructure-based wireless networks. The main obstacles in these networks are interference, channel attenuation and fading caused by negative impacts of multi-path signals on the received signal. OFDM-based cooperative systems can provide higher data rates and mitigate the effect of fading as well as achieve spatial diversity. Moreover, spectral efficiency can be improved by exploiting relay selection algorithms which have been widely studied in the literature [4, 10, 62]. In this chapter selective OFDM, selective OFDMA, and selective block-OFDM relaying protocols are presented and discussed. As a tradeoff between complexity and diversity gain a new relaying protocol, unequal block OFDM using amplify-and-forward (AF) relay is proposed.

The contributions of this chapter are two-fold:

- Propose the unequal block-OFDM relaying protocol that can represent the unique solution of the selective OFDM relaying.
- The closed-form and upper bound expressions of outage probability for selective unequal block-OFDM relaying over frequency selective Rayleigh fading channels is tackled and the comparison results with the other protocols are summarized, taking into consideration the broadcast nature.

Two cases are studied in this chapter. First of all, when the destination not able to receive the source signal directly due to the obstacles or distance between both terminals. Finally, the direct transmission is existing to exhibit the broadcast nature advantages.

The rest of this chapter is organized as follows. Motivation and related works are discussed in Section 3.2. In section 3.3, the system model is discussed. Section 3.4 reviews the outage probability analysis of existing protocols and proposed protocol. Numerical and simulation results are presented in section 3.5. Section 3.6 concludes the chapter.

## 3.2 Motivation and Related Work

The design and analysis of selective OFDM in cooperative communications have recently attracted considerable attention in broadband transmission. In general, there are two main strategies for selective OFDM relaying. The first strategy is to select the single best relay for all OFDM sub-carriers, referred to as selective OFDM relaying “all-subcarrier basis” [69,174]. The second strategy is to select a single relay for each sub-carrier, which is well known as selective OFDMA relaying “per-subcarrier basis” [70]. In [69] and [70], the authors studied these protocols for dual-hop and multi-hop systems respectively, based on the DF relaying protocol. It is shown that selective OFDMA yields much better performance than the selective OFDM at the cost of system complexity. The outage probability performance of these two OFDM relaying strategies using the AF protocol was analyzed in [62]. The authors in [175] investigated the outage probability performance of joint optimal power allocation and relay selection for AF and DF relay protocols using equal bit allocation at source and relay nodes. In frequency-selective channels, different sub-carriers may experience different level of fading. Data transmitted on the sub-carriers which experience deep fade will have a high probability of being lost at the destination. The main shortcoming of selective OFDM is the difficulty in finding the relay which has an uncorrupted signal over all of the sub-carriers. Selective OFDMA offers high performance. However,

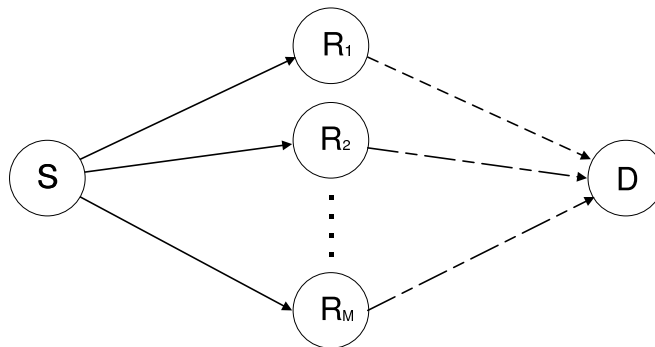


Figure 3.1: System model of selective OFDM relaying.

because it uses a single relay per sub-carrier, it become practically impossible to locate a relay for each of the sub-carriers when the OFDM symbol consists of a large number of sub-carriers. The authors in [176, 177] proposed a block-based OFDM over DF relay system to overcome this problem. The underlying concept of this protocol is that an OFDM symbol is divided into blocks and each block is transmitted independently over a single relay. Each relay uses the same number of sub-carriers. In practice, due to load balancing, the available sub-carriers with high channel condition at each relay might be unequal. In this case, each relay selects a block which has different number of sub-carriers.

### 3.3 System Model

The system considered here is illustrated in Figure 3.1. It consists of a single source (S), single destination (D), and  $M$  relay terminals  $R_i, i = 1, 2, \dots, M$ . Each node in the system is assumed to be equipped with a single antenna, and use half-duplex transmission. Perfect time and frequency synchronization are considered at each node. The source broadcasts an OFDM symbol with  $N$  sub-carriers to destination through  $M$  relay nodes. The channel is assumed to be slow fading frequency-selective between any two nodes in the network. Therefore, acquiring the channel parameters at the destination are relatively simple. The relay selection process and subcarrier allocation are conducted at the beginning of each

transmitted block by sending a preamble symbol to the relay nodes and destination from the source as proposed in [19, 178]. The relay nodes convey the received signal from the source to the destination. The destination can compute the individual end-to-end SNR for all links of relay nodes in the network. Then it selects the sub-carriers that has the maximum SNR among  $\{\gamma_{1,n}, \dots, \gamma_{M,n}\}$ , where  $n \in \{N\}$ . The destination sends a feedback signal in the safety channel that instructs the selected relays with its corresponding block of sub-carriers to participate in the communication protocol.

The channel fading gains between the source-relays and relays-destination for each subcarrier are denoted as  $h_{sr_i,n}$  and  $h_{r_i,d,n}$  respectively, where  $i = 1, 2, \dots, M, n = 1, 2, \dots, N$ . These channels are independent and the power gains follow exponential random variables. The communications time is divided equally between the source and the relay according to half-duplex transmission, thus there are two time slots. In the first time slot, the source broadcasts the information-bearing symbols to the relay nodes. The received signals of the  $i$ th relay on the  $n$ th subcarrier can be written as

$$y_{sr_i,n} = \sqrt{P_{s,n}} h_{sr_i,n} x(n) + w_{r_i}, \quad (i = 1, 2, \dots, M) \quad (3.1)$$

where  $P_{s,n}$  is the amount of power allocated to subcarrier  $n$  and the total source power is  $P_s = \sum_{n=1}^N P_{s,n}$ , and  $x(n)$  and  $w_{r_i}$  are a unit energy symbol to be transmitted from the source and additive white Gaussian noise (AWGN). In the second time slot, the relay simply amplifies the received noisy signal by an amplification factor  $\beta_{i,n}$  and forwards it to the destination [179]. The amplification factor for each sub-carrier that satisfies the power constraints is  $E(|x_{r_i}(n)|^2) \leq P_{r_i}$  and it can be expressed as

$$\beta_{i,n} = \sqrt{\frac{P_{r_i,n}}{|h_{sr_i,n}|^2 P_{s,n} + \sigma_r^2}}, \quad (3.2)$$

where  $P_{r_i,n}$  is the transmitted power of the  $n$ th subcarrier for the  $i$ th relay node and  $\sigma_r^2$  denotes the variance of AWGN at the relay node. The received signal at the destination from the  $i$ th relay node for  $n$ th subcarrier can be denoted as

$$\begin{aligned} y_{r_i,d,n} &= \beta_{i,n} h_{r_i,d,n} y_{sr_i,n} + w_d \\ &= \beta_{i,n} h_{r_i,d,n} (\sqrt{P_{s,n}} h_{sr_i,n} x(n) + w_{r_i}) + w_d \end{aligned} \quad (3.3)$$

where  $w_d$  is the AWGN at the destination. The instantaneous SNR at the destination of the  $i$ th relay on the  $n$ th subcarrier can be evaluated as

$$\begin{aligned}\gamma_{i,n} &= \frac{|\beta_{i,n}\sqrt{P_{s,n}}h_{sri,n}h_{rdi,n}|^2}{|\beta_{i,n}h_{rdi,n}w_r + w_d|^2} \\ &= \frac{\frac{P_{s,n}|h_{sri,n}|^2}{\sigma_r^2} \frac{P_{ri,n}|h_{rdi,n}|^2}{\sigma_d^2}}{\frac{P_{s,n}|h_{sri,n}|^2}{\sigma_r^2} + \frac{P_{ri,n}|h_{rdi,n}|^2}{\sigma_d^2} + 1} \\ &= \frac{\gamma_{sri,n}\gamma_{rdi,n}}{\gamma_{sri,n} + \gamma_{rdi,n} + 1},\end{aligned}\tag{3.4}$$

where  $\gamma_{sri,n}$  and  $\gamma_{rdi,n}$  are the instantaneous SNR for S-R, R-D links for the  $n$ th subcarrier respectively and can be defined by

$$\begin{aligned}\gamma_{sri,n} &= \frac{P_{s,n} |h_{sri,n}|^2}{\sigma_r^2} = \bar{\gamma} |h_{sri,n}|^2 \\ \gamma_{rdi,n} &= \frac{P_{ri,n} |h_{rdi,n}|^2}{\sigma_d^2} = \bar{\gamma} |h_{rdi,n}|^2,\end{aligned}\tag{3.5}$$

where  $\bar{\gamma}$  is the average SNR. From all the relays located between the source and destination, the destination selects the best relay(s) with suitable sub-carriers according to the selective protocol.

### 3.4 Outage Probability Analysis

In wireless communication systems an essential performance measure is the outage probability. Before evaluating the outage probability of the proposed scheme, the end-to-end outage performance of selective OFDM, selective OFDMA and selective block-OFDM schemes are analyzed. Each OFDM symbol consists of  $N$  sub-carriers which can represent  $N$  independent source to destination links. In order to simplify the following analysis, the end-to-end analysis of single sub-carrier will be studied. Then the system performance is analyzed when the direct link is assumed to be absent due to either the long distance between the source and the destination or high shadowing caused by obstacles. In equal bit loading, the data is divided uniformly across all sub-carriers so that each sub-carrier has the same number of bits. Therefore, the relay is in outage if any of sub-carriers has a rate below the target rate ( $r$ ) where  $r = \text{total data}/N$ . Thereafter, the direct

link is taken into account in order to improve the diversity gain by exploiting the broadcast nature of communication networks.

### 3.4.1 Outage Probability of End-to-end Single Sub-carrier

The outage probability is defined as the probability that the channel mutual information (I) between the source and destination for the  $n$ th sub-carrier in the  $i$ th relay falls below a predefined threshold value  $\gamma_{out}$ . The mutual information depends on the amount of the channel state information available at the destination and as a result of the end-to-end signal to noise ratio (SNR). The mutual information of any subcarrier in  $i$ th relay between the source and destination can be expressed as

$$I_{i,n} = \frac{1}{2} \log_2(1 + \gamma_{i,n}), \quad (3.6)$$

where  $\frac{1}{2}$  factor indicates that the data transmitting requires two time slots (or orthogonal channels).  $I_{i,n}$  denotes the maximum mutual information in a particular information transmission procedure for  $n$ th sub-carrier in  $i$  relay. The outage probability can be represented mathematically as

$$P_{out} = Pr(I < r) = Pr\left(\frac{1}{2} \log_2(1 + \gamma_{i,n}) < r\right) = Pr(\gamma_{i,n} < 2^{2r} - 1), \quad (3.7)$$

where  $\gamma_{out} = 2^{2r} - 1$ ,  $r$  is the target rate of each subcarrier.

The outage probability formula in (3.7) is actually corresponding to the cumulative density function of  $\gamma_{i,n}$  evaluated at  $2^{2r} - 1$ . The CDF  $F_{\gamma_{i,n}}$  of  $\gamma_{i,n}$  can be derived as [180]

$$\begin{aligned} F_{\gamma_{i,n}}(\gamma) &= Pr(\gamma_{i,n} \leq \gamma) = Pr\left(\frac{\gamma_{sr_i,n} \gamma_{r_i,d,n}}{\gamma_{sr_i,n} + \gamma_{r_i,d,n} + 1} \leq \gamma\right) \\ &= \int_0^\infty Pr\left(\frac{\gamma_{sr_i,n} y}{\gamma_{sr_i,n} + y + 1} \leq \gamma\right) f_{\gamma_{r_i,d,n}}(y) dy \\ &= \int_0^\gamma Pr(\gamma_{sr_i,n} > \frac{\gamma y + \gamma}{y - \gamma}) f_{\gamma_{r_i,d,n}}(y) dy \\ &\quad + \int_\gamma^\infty Pr(\gamma_{sr_i,n} \leq \frac{\gamma y + \gamma}{y - \gamma}) f_{\gamma_{r_i,d,n}}(y) dy \end{aligned} \quad (3.8)$$

The value of  $Pr(\gamma_{sr_i,n} > \frac{\gamma y + \gamma}{y - \gamma}) = 1$ ,  $Pr(\gamma_{sr_i,n} \leq \frac{\gamma y + \gamma}{y - \gamma}) = 1 - e^{-\frac{\gamma y + \gamma}{\gamma_{sr_i,n}(y - \gamma)}}$  and  $f_{\gamma_{r_i,d,n}}(y) = \frac{1}{\gamma_{r_i,d,n}} e^{-\frac{y}{\gamma_{r_i,d,n}}}$ . Then substituting in (3.7), the  $F_{\gamma_{i,n}}(\gamma)$  can be rewritten

as

$$\begin{aligned}
F_{\gamma_{i,n}}(\gamma) &= \int_0^\gamma \frac{1}{\tilde{\gamma}_{r_i d,n}} e^{-\frac{y}{\tilde{\gamma}_{r_i d,n}}} dy + \int_\gamma^\infty (1 - e^{-\frac{\gamma y + \gamma}{\tilde{\gamma}_{sr_i,n}(y-\gamma)}}) \frac{1}{\tilde{\gamma}_{r_i d,n}} e^{-\frac{y}{\tilde{\gamma}_{r_i d,n}}} dy \\
&= \int_0^\gamma \frac{1}{\tilde{\gamma}_{r_i d,n}} e^{-\frac{y}{\tilde{\gamma}_{r_i d,n}}} dy + \int_\gamma^\infty \frac{1}{\tilde{\gamma}_{r_i d,n}} e^{-\frac{y}{\tilde{\gamma}_{r_i d,n}}} dy \\
&\quad - \frac{1}{\tilde{\gamma}_{r_i d,n}} \int_\gamma^\infty (e^{-\frac{\gamma y + \gamma}{\tilde{\gamma}_{sr_i,n}(y-\gamma)}}) e^{-\frac{y}{\tilde{\gamma}_{r_i d,n}}} dy \\
&= 1 - \frac{1}{\tilde{\gamma}_{r_i d,n}} \int_\gamma^\infty (e^{-\frac{\gamma y + \gamma}{\tilde{\gamma}_{sr_i,n}(y-\gamma)}}) e^{-\frac{y}{\tilde{\gamma}_{r_i d,n}}} dy
\end{aligned} \tag{3.9}$$

letting  $z = y - \gamma$ , the CDF of  $\gamma_i$  can be rewritten as

$$\begin{aligned}
F_{\gamma_{i,n}}(\gamma) &= 1 - \frac{1}{\tilde{\gamma}_{r_i d,n}} \int_0^\infty e^{-\frac{\gamma(z+\gamma+1)}{\tilde{\gamma}_{sr_i,n}z}} e^{-\frac{1}{\tilde{\gamma}_{r_i d,n}}(z+\gamma)} dz \\
&= 1 - \frac{1}{\tilde{\gamma}_{r_i d,n}} e^{-\gamma\left(\frac{1}{\tilde{\gamma}_{sr_i,n}} + \frac{1}{\tilde{\gamma}_{r_i d,n}}\right)} \int_0^\infty e^{-\left(\frac{\gamma^2 + \gamma}{\tilde{\gamma}_{sr_i,n}z} + \frac{1}{\tilde{\gamma}_{r_i d,n}}z\right)} dz \\
&= 1 - 2\sqrt{\frac{(\gamma^2 + \gamma)}{\tilde{\gamma}_{sr_i,n}\tilde{\gamma}_{r_i d,n}}} e^{-\gamma\left(\frac{1}{\tilde{\gamma}_{sr_i,n}} + \frac{1}{\tilde{\gamma}_{r_i d,n}}\right)} \times K_1\left(2\sqrt{\frac{(\gamma^2 + \gamma)}{\tilde{\gamma}_{sr_i,n}\tilde{\gamma}_{r_i d,n}}}\right)
\end{aligned} \tag{3.10}$$

where  $K_1$  is the first order modified bessel function of the second kind. The approximation value of  $F_{\gamma_{i,n}}(\gamma)$  represents the upper bound and can be expressed by using the approximation  $K_1(x) \approx \frac{1}{x}$  [181] Eq. [9.6.9] as

$$\begin{aligned}
F_{\gamma_{i,n}}(\gamma) &= 1 - e^{-\gamma\left(\frac{1}{\tilde{\gamma}_{sr_i,n}} + \frac{1}{\tilde{\gamma}_{r_i d,n}}\right)} \\
&= 1 - e^{-\frac{\gamma}{\tilde{\gamma}_{i,eq}}}
\end{aligned} \tag{3.11}$$

where  $\frac{1}{\tilde{\gamma}_{i,eq}} = \frac{1}{\tilde{\gamma}_{sr_i,n}} + \frac{1}{\tilde{\gamma}_{r_i d,n}}$ . Therefore, the approximate of the PDF which is the derivative of the CDF with respect to  $\gamma$  and can be evaluated as

$$f_{\gamma_{i,n}}(\gamma) = \frac{1}{\tilde{\gamma}_{i,eq}} e^{-\frac{\gamma}{\tilde{\gamma}_{i,eq}}}. \tag{3.12}$$

This approximate form can be used to calculate the protocol performance and it is further assumed that all the channel coefficients of the sub-carriers are independent. In the rest of this chapter, two transmission schemes are considered : without diversity (absent direct link) and with diversity (the direct link is available).

### 3.4.2 Selective OFDM

In this scheme the destination selects the relay that has maximum end-to-end SNR and broadcasts the index of the selected relay to all the relays by a feedback

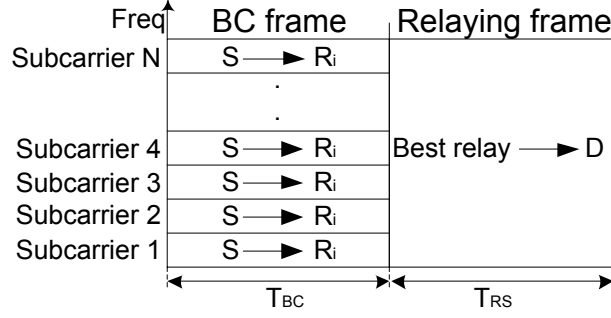


Figure 3.2: Frame structure of selective OFDM relaying where  $i \in \{1, \dots, M\}$  and the selected relay forwards the entire sub-carriers of the OFDM symbol.

channel. Then, the selected relay retransmits the entire OFDM symbol received from the source to the destination in the second time interval. The frame structure of selective OFDM is illustrated in Figure 3.2. The received SNR at the destination node can be expressed as

$$\gamma^S = \max_{i=1, \dots, M} \{\gamma_{r_i, n}\}_{n=1}^N. \quad (3.13)$$

The end-to-end outage probability of selective OFDM relaying is given by

$$P_{\text{out}}^{\text{OFDM}}(\gamma_{\text{out}}) = \prod_{i=1}^M P_{\text{out}, r_i}^{\text{OFDM}}(\gamma_{\text{out}}), \quad (3.14)$$

where  $P_{\text{out}, r_i}^{\text{OFDM}}$  is the outage probability of the  $i$ th relay.

Since the relay conveys the entire OFDM symbol to the destination, it is in a state of outage if any subcarrier is in outage. Therefore, the outage probability of the  $i$ th relay can be written as [69]

$$\begin{aligned} P_{\text{out}, r_i}^{\text{OFDM}}(\gamma_{\text{out}}) &= 1 - Pr(\gamma_{r_i, 1} > \gamma_{r_i, 2} > \dots > \gamma_{r_i, N} > \gamma_{\text{out}}) \\ &= 1 - \prod_{n=1}^N (1 - P_{r_i, n}(\gamma_{\text{out}})). \end{aligned} \quad (3.15)$$

where  $P_{r_i, n}$  is the outage probability of the  $n$ th sub-carrier in the  $i$ th relay, which is equivalent to the CDF evaluated in (3.11) after substituting  $\gamma = \gamma_{\text{out}}$ .

By substituting (3.11) into (3.15), the outage probability of the  $i$ th relay can be rewritten as

$$P_{\text{out}, r_i}^{\text{OFDM}}(\gamma_{\text{out}}) = 1 - \prod_{n=1}^N \left( 1 - \left( 1 - e^{-\frac{\gamma_{\text{out}}}{\bar{\gamma}_{i, n, eq}}} \right) \right) = 1 - e^{-N \frac{\gamma_{\text{out}}}{\bar{\gamma}_{i, n, eq}}}, \quad (3.16)$$

The overall system outage probability can be expressed by substituting (3.16) into (3.14) as

$$P_{out}^{OFDM}(\gamma_{out}) = \left(1 - e^{-N \frac{\gamma_{out}}{\bar{\gamma}_{i,n,eq}}}\right)^M. \quad (3.17)$$

From (3.17), the full diversity order (M-fold) can be achieved, which is represented by the number of relays in the network. However, the gain is drastically affected by the number of sub-carriers  $N$ .

When the direct link is available, the destination combines the SNRs from the direct link and the best relay for each sub-carrier by using MRC. Therefore, the relay is in outage if the received signal from the relay and source after combining of any sub-carrier is in outage. The end-to-end SNR at the destination can be written as

$$\gamma^S = \max_{i=1,\dots,M} \{\gamma_{sd,n} + \gamma_{r_i,n}\}_{n=1}^N \quad (3.18)$$

The probability of two random variables with convolution formula of probability density function can be evaluated as

$$\begin{aligned} Pr(x + y < u) &= \int_0^u \left[ \int_0^{u-x} f_y(y) dy \right] f_x(x) dx \\ &= \int_0^u F_y(u-x) f_x(x) dx = \int_0^u Pr(y < u-x) f_x(x) dx \end{aligned} \quad (3.19)$$

Since the sub-carriers are independent, the end-to-end outage probability can be given as

$$\begin{aligned} P_{out}^{OFDM1}(\gamma_{out}) &= 1 - \prod_{n=1}^N \left( 1 - Pr \left( \max_{i=1,\dots,M} (\gamma_{sd,n} + \gamma_{r_i,n}) < \gamma_{out} \right) \right) \\ &= 1 - \prod_{n=1}^N \left( 1 - Pr \left( \alpha_0 + \max_{i=1,\dots,M} \frac{\gamma \alpha_i \beta_i}{\gamma \alpha_i + \gamma \beta_i + 1} < \frac{2^{2r} - 1}{\gamma} \right) \right) \\ &= 1 - \prod_{n=1}^N \left( 1 - \int_0^{\gamma_{out}} Pr \left( \max_{i=1,\dots,M} \frac{\gamma \alpha_i \beta_i}{\gamma \alpha_i + \gamma \beta_i + 1} < \gamma_{out} - \alpha_0 \right) \frac{1}{\bar{\gamma}_{sd,n}} e^{-\frac{x}{\bar{\gamma}_{sd,n}}} d\alpha_0 \right) \end{aligned} \quad (3.20)$$

Let  $\gamma_{out}z = \gamma_{out} - \alpha_0 \implies \alpha_0 = \gamma_{out}(1 - z)$ ,  $d\alpha_0 = -\gamma_{out}dz$

$$\begin{aligned}
P_{out}^{OFDM1}(\gamma_{out}) &= 1 - \prod_{n=1}^N \left( 1 - \int_0^1 \prod_{i=1}^M Pr \left( \frac{\gamma\alpha_i\beta_i}{\gamma\alpha_i + \gamma\beta_i + 1} < \gamma_{out}z \right) \frac{\gamma_{th}}{\tilde{\gamma}_{sd,n}} e^{-\frac{\gamma_{out}(1-z)}{\tilde{\gamma}_{sd,n}}} dz \right) \\
&= 1 - \prod_{n=1}^N \left( 1 - \int_0^1 \prod_{i=1}^M \left( \frac{Pr \left( \frac{\gamma\alpha_i\beta_i}{\gamma\alpha_i + \gamma\beta_i + 1} < \gamma_{out}z \right)}{\gamma_{out}z} \right) \frac{(\gamma_{out})^{(M+1)}}{\tilde{\gamma}_{sd,n}} z^M e^{-\frac{\gamma_{out}(1-z)}{\tilde{\gamma}_{sd,n}}} dz \right)
\end{aligned} \tag{3.21}$$

For high SNR values,  $\lim_{\gamma \rightarrow \infty} e^{-\frac{\gamma_{out}(1-z)}{\tilde{\gamma}_{sd,n}}} = 1$  and  $\int_0^1 z^M dz = \frac{1}{M+1}$ . By using Lemma 1 of [4], The upper bound can be evaluated as

$$\limsup_{\gamma_{out} \rightarrow 0} \frac{Pr \left( \frac{\gamma\alpha_i\beta_i}{\gamma\alpha_i + \gamma\beta_i + 1} < \gamma_{out}z \right)}{(\gamma_{out}z)^M} \leq \prod_{i=1}^M \left( \frac{1}{\tilde{\gamma}_{sr_i,n}} + \frac{1}{\tilde{\gamma}_{r_i,d,n}} \right) \tag{3.22}$$

The upper bound can be obtained as

$$P_{UBout}^{OFDM1}(\gamma_{out}) = 1 - \prod_{n=1}^N \left( 1 - \frac{(\gamma_{out})^{(M+1)}}{\tilde{\gamma}_{sd,n}(M+1)} \prod_{i=1}^M \left( \frac{1}{\tilde{\gamma}_{sr_i,n}} + \frac{1}{\tilde{\gamma}_{r_i,d,n}} \right) \right) \tag{3.23}$$

It can be seen from (3.23) that the diversity order is  $(M+1)$ -fold and outperforms the diversity obtained in (3.17) because the system exhibits direct transmission that enhances the diversity order.

### 3.4.3 Selective OFDMA

In this scheme, each relay in the system selects a single subcarrier, which has the maximum SNR as illustrated in Figure 3.3. The received SNR at the destination is given by

$$\gamma^S = \left\{ \left( \max_{n=1, \dots, N} \gamma_{r_i,n} \right) \right\}_{i=1}^M. \tag{3.24}$$

The relay is in outage when all sub-carriers are in outage. Therefore, the average outage probability can be written as

$$P_{out}^{OFDMA}(\gamma_{out}) = 1 - \prod_{n=1}^N (1 - P_n^{OFDMA}(\gamma_{out})), \tag{3.25}$$

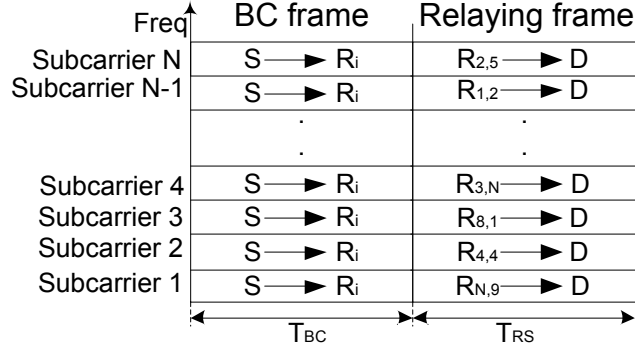


Figure 3.3: Frame structure of selective OFDMA relaying where  $i \in \{1, \dots, M\}$ .

where  $P_n^{\text{OFDMA}}(\gamma_{out})$  is the outage probability of the  $n$ th subcarrier, which is equivalent to the CDF of a selective relay in  $M$  multiple nodes and can be given as

$$\begin{aligned}
 P_{out}^{\text{OFDMA}}(n) &= Pr \left( \max_{i=1, \dots, M} (\gamma_{i,1}, \dots, \gamma_{i,N}) < \gamma_{out} \right) \\
 &= \prod_{i=1}^M (F_{\gamma_{i,n}}(\gamma_{out})) \\
 &= \prod_{i=1}^M \left( 1 - e^{-\frac{\gamma_{out}}{\bar{\gamma}_{i,n,eq}}} \right).
 \end{aligned} \tag{3.26}$$

Finally, by substituting (3.26) into (3.25), the overall outage probability can be obtained as

$$\begin{aligned}
 P_{out}^{\text{OFDMA}}(\gamma_{out}) &= 1 - \prod_{n=1}^N \left( 1 - \prod_{i=1}^M \left( 1 - e^{-\frac{\gamma_{out}}{\bar{\gamma}_{i,n,eq}}} \right) \right) \\
 &= 1 - \left( 1 - \prod_{i=1}^M \left( 1 - e^{-\frac{\gamma_{out}}{\bar{\gamma}_{i,n,eq}}} \right) \right)^N \\
 &= 1 - \left( 1 - \left( 1 - e^{-\frac{\gamma_{out}}{\bar{\gamma}_{i,n,eq}}} \right)^M \right)^N.
 \end{aligned} \tag{3.27}$$

It can also be seen from (3.27) that the diversity gain depends on the number of sub-carriers in the OFDM symbol and the relay nodes.

When the direct link is exists, the destination combines the SNRs from the direct link and the best sub-carrier in each relay by using MRC. Therefore the relay is in outage if the received signal from the relay and source after the combining of any sub-carrier is in outage. The end-to-end SNR at the destination can

be written as

$$\gamma^S = \left\{ \left( \gamma_{sd,n} + \max_{n=1,\dots,N} \gamma_{r_i,n} \right) \right\}_{i=1}^M. \quad (3.28)$$

Similarly as in selective OFDM relaying, the end-to-end outage probability can be given as

$$\begin{aligned} P_{\text{out}}^{\text{OFDMA1}}(\gamma_{\text{out}}) &= 1 - \prod_{i=1}^M \left( 1 - Pr \left( \gamma_{sd,n} + \max_{n=1,\dots,N} \gamma_{r_i,n} < \gamma_{\text{out}} \right) \right) \\ &= 1 - \prod_{i=1}^M \left( 1 - Pr \left( \alpha_0 + \max_{n=1,\dots,N} \frac{\gamma \alpha_i \beta_i}{\gamma \alpha_i + \gamma \beta_i + 1} < \frac{2^{2r} - 1}{\gamma} \right) \right) \\ &= 1 - \prod_{i=1}^M \left( 1 - \int_0^{\gamma_{\text{out}}} Pr \left( \max_{n=1,\dots,N} \frac{\gamma \alpha_i \beta_i}{\gamma \alpha_i + \gamma \beta_i + 1} < \gamma_{\text{out}} - \alpha_0 \right) \frac{1}{\bar{\gamma}_{sd,n}} e^{-\frac{x}{\bar{\gamma}_{sd,n}}} d\alpha_0 \right) \end{aligned} \quad (3.29)$$

and the upper bound can be obtained as

$$P_{\text{UBout}}^{\text{OFDMA1}}(\gamma_{\text{out}}) = 1 - \prod_{i=1}^M \left( 1 - \frac{(\gamma_{\text{out}})^{(N+1)}}{\bar{\gamma}_{sd,n}(N+1)} \prod_{n=1}^N \left( \frac{1}{\bar{\gamma}_{sr_i,n}} + \frac{1}{\bar{\gamma}_{r_i,d,n}} \right) \right) \quad (3.30)$$

It is also observed that the diversity order presented in (3.30) equal to (M+1) due to the number of relays  $M$  in the selective OFDMA is the same as the number of sub-carriers  $N$ .

### 3.4.4 Selective Block-OFDM Relaying

In this scheme, each relay selects a single block of sub-carriers as shown in Figure 3.4 and is performed independently for each block, Therefore, the overall system is in outage if any block is in outage. The overall received SNR at the destination can be given as

$$\gamma^S = \max_{b=1,\dots,B} \left\{ \left\{ \gamma_{r_i,n} \right\}_{n=1,\dots,N_b} \right\}_{b=1}^B. \quad (3.31)$$

The outage probability of selective block-OFDM can be given as in [176]

$$P_{\text{out}}^{\text{Block}}(\gamma_{\text{out}}) = 1 - \prod_{b=1}^B \left( 1 - P_{\text{out},b}^{\text{Block}}(\gamma_{\text{out}}) \right), \quad (3.32)$$

where  $B$  is the number of blocks and  $P_{\text{out},b}^{\text{Block}}(\gamma_{\text{out}})$  is the end-to-end outage probability of block  $b$ , since each relay independently selects the single block which

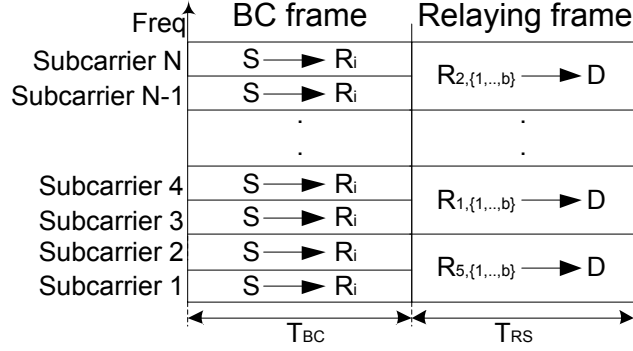


Figure 3.4: Frame structure of selective block OFDM relaying where  $i \in \{1, \dots, M\}$ .

has the maximum SNR. Thus,  $P_{out,b}^{\text{Block}}(\gamma_{out})$  can be expressed as

$$P_{out,b}^{\text{Block}}(\gamma_{out}) = \prod_{i=1}^M P_{out}^{\text{Block},b}(\gamma_{out}), \quad (3.33)$$

where  $P_{out}^{\text{Block},b}(\gamma_{out})$  is the outage probability of block b. Each block consists of  $N_b$  of sub-carriers ( $N_b = \frac{N}{B}$ ) and the relay retransmits the information to the destination in the second time interval. Therefore the block (relay) is in outage if any subcarrier in block b is in outage. The outage probability of block b can be evaluated as

$$\begin{aligned} P_{out}^{\text{Block},b}(\gamma_{out}) &= 1 - \prod_{n=1}^{N_b} (1 - Pr(\gamma_{i,n} < \gamma_{out})) \\ &= 1 - \prod_{n=1}^{N_b} (1 - F_{\gamma_{i,n}}(\gamma_{out})) \\ &= 1 - \prod_{n=1}^{N_b} \left( 1 - \left( 1 - e^{-\frac{\gamma_{out}}{\bar{\gamma}_{i,n,eq}}} \right) \right) \\ &= 1 - e^{-N_b \frac{\gamma_{out}}{\bar{\gamma}_{i,n,eq}}}. \end{aligned} \quad (3.34)$$

Substituting (3.34) into (3.33) the probability of  $P_{out,b}^{\text{Block}}(\gamma_{out})$  can be rewritten as

$$P_{out,b}^{\text{Block}}(\gamma_{out}) = \prod_{i=1}^M \left( 1 - e^{-N_b \frac{\gamma_{out}}{\bar{\gamma}_{i,n,eq}}} \right). \quad (3.35)$$

Substituting (3.35) into (3.32), the expression for  $P_{out}^{\text{Block}}(\gamma_{out})$  can be obtained as

$$\begin{aligned}
P_{out}^{\text{Block}}(\gamma_{out}) &= 1 - \prod_{b=1}^B \left( 1 - \prod_{i=1}^M \left( 1 - e^{-N_b \frac{\gamma_{out}}{\gamma_{eq}}} \right) \right) \\
&= 1 - \left( 1 - \prod_{i=1}^M \left( 1 - \left( e^{-N_b \frac{\gamma_{out}}{\bar{\gamma}_{i,n,eq}}} \right) \right) \right)^B.
\end{aligned} \tag{3.36}$$

It can also be seen from (3.36) that the diversity gain depends on the number of blocks and relay nodes.

Following the same procedure in the previous subsections, in the case of the direct transmission being available, the end-to-end SNR at the destination can be written as

$$\gamma^S = \max_{b=1,..,B} \left\{ \{(\gamma_{sd,n} + \gamma_{r_i,n})\}_{n=1,..,N_b} \right\}_{b=1}^B. \tag{3.37}$$

The destination selects the best group of sub-carriers from each relay in the network, then combines with the direct link. Therefore, the system is in outage when any sub-carrier in the network is in outage. Mathematically this can be expressed as

$$\begin{aligned}
P_{out}^{\text{BOFDM1}}(\gamma_{out}) &= 1 - \prod_{b=1}^B \left[ 1 - \prod_{n=1}^{N_b} \left( 1 - Pr \left( \gamma_{sd,n} + \max_{i=1,..,M} \gamma_{r_i,n} < \gamma_{out} \right) \right) \right] \\
&= 1 - \prod_{b=1}^B \left[ 1 - \prod_{n=1}^{N_b} \left( 1 - Pr \left( \alpha_0 + \max_{i=1,..,M} \frac{\gamma \alpha_i \beta_i}{\gamma \alpha_i + \gamma \beta_i + 1} < \frac{2^{2r} - 1}{\gamma} \right) \right) \right] \\
&= 1 - \prod_{b=1}^B \\
&\quad \times \left[ 1 - \prod_{n=1}^{N_b} \left( 1 - \int_0^{\gamma_{th}} Pr \left( \max_{i=1,..,M} \frac{\gamma \alpha_i \beta_i}{\gamma \alpha_i + \gamma \beta_i + 1} < \gamma_{out} - \alpha_0 \right) \frac{e^{-\frac{x}{\bar{\gamma}_{sd,n}}}}{\bar{\gamma}_{sd,n}} d\alpha_0 \right) \right].
\end{aligned} \tag{3.38}$$

The upper bound can be obtained as

$$P_{UBout}^{\text{OFDM2}}(\gamma_{out}) = 1 - \prod_{b=1}^B \left[ 1 - \prod_{n=1}^{N_b} \left( 1 - \frac{(\gamma_{th})^{(M+1)}}{\bar{\gamma}_{sd,n} (M+1)} \prod_{i=1}^M \left( \frac{1}{\bar{\gamma}_{sr_i,n}} + \frac{1}{\bar{\gamma}_{r_i,d,n}} \right) \right) \right]. \tag{3.39}$$

### 3.4.5 Selective Unequal Block-OFDM Relaying

In this scheme, the overall number of sub-carriers are divided into several groups (B) where each group has a different number of sub-carriers as shown in Figure

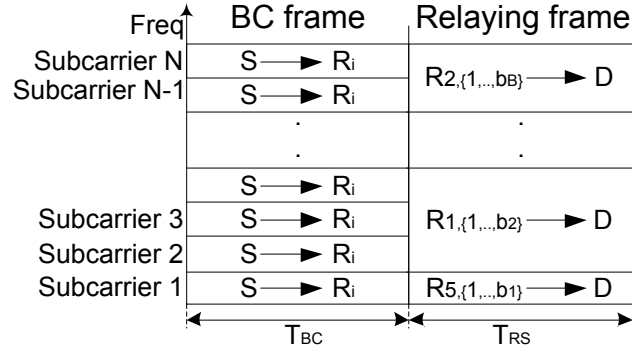


Figure 3.5: Frame structure of selective Unequal block OFDM relaying where  $i \in \{1, \dots, M\}$ .

3.5. Thus, the overall system is in outage if any sub-carrier in any block is in outage. The end-to-end SNR at the destination can be expressed as

$$\gamma^S = \max_{j=1, \dots, B} \left\{ \left\{ \gamma_{r_i, n} \right\}_{n=1, \dots, N_{b_j}} \right\}_{j=1}^B. \quad (3.40)$$

The outage probability of this protocol can be evaluated as

$$P_{out}^{Ublock}(\gamma_{out}) = 1 - (1 - P_{out, b_1}^{Ublock}(\gamma_{out})) (1 - P_{out, b_2}^{Ublock}(\gamma_{out})) \times \dots \times (1 - P_{out, b_B}^{Ublock}(\gamma_{out})), \quad (3.41)$$

where  $B$  is the number of blocks and  $P_{out, b_j}^{Ublock}(\gamma_{out})$   $j = 1, \dots, B$  is the end-to-end outage probability of each block  $b_j$ . Since each relay selects the individual block which has maximum SNR, the  $P_{out, b_j}^{Ublock}(\gamma_{out})$  can be written as

$$P_{out, b_j}^{Ublock}(\gamma_{out}) = \prod_{j=1}^M P_{out}^{Ublock, b_j}(\gamma_{out}) \quad j = 1, \dots, B. \quad (3.42)$$

where  $P_{out}^{Ublock, b_j}(\gamma_{out})$  is the outage probability of  $j$ th block. Each block consist of a different number of sub-carriers  $N_{block_j}$   $j = 1, \dots, B$ , where  $(N_{b_1} + N_{b_2} + \dots + N_{b_B} = N)$ . Therefore, the  $j$ th block is in outage if any subcarrier in  $j$ th block is in outage. The outage probability of  $j$ th block can be evaluated

as

$$\begin{aligned}
P_{out}^{Ublock,b_j}(\gamma_{out}) &= 1 - \prod_{n=1}^{N_{b_j}} (1 - Pr(\gamma_{i,n} < \gamma_{out})) \quad j = 1, \dots, B \\
&= 1 - \prod_{n=1}^{N_{b_j}} (1 - F_{\gamma_{i,n}}(\gamma_{out})) \\
&= 1 - \prod_{n=1}^{N_{b_j}} \left( 1 - \left( 1 - e^{-\frac{\gamma_{out}}{\bar{\gamma}_{i,n,eq}}} \right) \right) \\
&= 1 - e^{-N_{b_j} \frac{\gamma_{out}}{\bar{\gamma}_{i,n,eq}}}.
\end{aligned} \tag{3.43}$$

Substituting (3.43) into (3.42) gives

$$P_{out}^{Ublock}(b_j) = \prod_{i=1}^M \left( 1 - e^{-N_{b_j} \frac{\gamma_{th}}{\bar{\gamma}_{i,n,eq}}} \right) \quad j = 1, \dots, B. \tag{3.44}$$

Finally by substituting (3.44) into (3.41), the outage probability can be expressed

as

$$\begin{aligned}
P_{out}^{Ublock}(\gamma_{out}) &= 1 - \left( 1 - \prod_{i=1}^M \left( 1 - e^{-N_{b_1} \frac{\gamma_{out}}{\bar{\gamma}_{i,n,eq}}} \right) \right) \left( 1 - \prod_{i=1}^M \left( 1 - e^{-N_{b_2} \frac{\gamma_{out}}{\bar{\gamma}_{i,n,eq}}} \right) \right) \dots \\
&\quad \times \left( 1 - \prod_{i=1}^M \left( 1 - e^{-N_{b_B} \frac{\gamma_{out}}{\bar{\gamma}_{i,n,eq}}} \right) \right),
\end{aligned} \tag{3.45}$$

when  $b_1 = b_2 = \dots = b_B$  and  $N_{b_1} = N_{b_2} = \dots = N_{b_B} = N_b$  and substituting into (3.45) results in:

$$\begin{aligned}
P_{out}^{Ublock}(\gamma_{out}) &= 1 - \left( 1 - \prod_{i=1}^M \left( 1 - e^{-N_b \frac{\gamma_{out}}{\bar{\gamma}_{i,n,eq}}} \right) \right) \left( 1 - \prod_{i=1}^M \left( 1 - e^{-N_b \frac{\gamma_{out}}{\bar{\gamma}_{i,n,eq}}} \right) \right) \dots \\
&\quad \times \left( 1 - \prod_{i=1}^M \left( 1 - e^{-N_b \frac{\gamma_{out}}{\bar{\gamma}_{i,n,eq}}} \right) \right) \\
&= 1 - \left( 1 - \prod_{i=1}^M \left( 1 - e^{-N_b \frac{\gamma_{out}}{\bar{\gamma}_{i,n,eq}}} \right) \right)^B.
\end{aligned} \tag{3.46}$$

It is observed that (3.46) is completely identical to (3.17), (3.27) and (3.36), which means that selective block-OFDM is a special case from selective unequal block-OFDM.

Following the same analysis for selective block OFDM relaying with direct transmission, the overall outage probability of unequal block OFDM relaying can be evaluated. The end-to-end SNR at the destination when the direct link presents between the source and the destination can be written as

$$\gamma^S = \max_{j=1,\dots,B} \left\{ \{(\gamma_{sd,n} + \gamma_{r_i,n})\}_{n=1,\dots,N_{b_j}}^N \right\}_{j=1}^B. \quad (3.47)$$

Similarly as in Selective Block-OFDM Relaying, the system is in outage when any sub-carrier in the network is in outage and can be written as

$$\begin{aligned} P_{\text{out}}^{\text{UBOFDM1}}(\gamma_{\text{out}}) &= 1 - \left[ 1 - \prod_{n=1}^{N_{b_1}} \left( 1 - Pr \left( \gamma_{sd,n} + \max_{i=1,\dots,M} \gamma_{r_i,n} < \gamma_{\text{out}} \right) \right) \right] \\ &\times \left[ 1 - \prod_{n=1}^{N_{b_2}} \left( 1 - Pr \left( \gamma_{sd,n} + \max_{i=1,\dots,M} \gamma_{r_i,n} < \gamma_{\text{out}} \right) \right) \right] \\ &\times \dots \\ &\times \left[ 1 - \prod_{n=1}^{N_{b_B}} \left( 1 - Pr \left( \gamma_{sd,n} + \max_{i=1,\dots,M} \gamma_{r_i,n} < \gamma_{\text{out}} \right) \right) \right], \end{aligned} \quad (3.48)$$

The upper bound can be obtained as

$$\begin{aligned} P_{\text{UBout}}^{\text{OFDM2}}(\gamma) &= 1 - \left[ 1 - \prod_{n=1}^{N_{b_1}} \left( 1 - \frac{(\gamma_{th})^{(M+1)}}{\bar{\gamma}_{sd,n}(M+1)} \prod_{i=1}^M \left( \frac{1}{\bar{\gamma}_{sr_i,n}} + \frac{1}{\bar{\gamma}_{r_i,d,n}} \right) \right) \right] \\ &\times \dots \\ &\times \left[ 1 - \prod_{n=1}^{N_{b_B}} \left( 1 - \frac{(\gamma_{\text{out}})^{(M+1)}}{\bar{\gamma}_{sd,n}(M+1)} \prod_{i=1}^M \left( \frac{1}{\bar{\gamma}_{sr_i,n}} + \frac{1}{\bar{\gamma}_{r_i,d,n}} \right) \right) \right]. \end{aligned} \quad (3.49)$$

It can be seen that the diversity order obtained from selective OFDMA as depicted in (3.36) is much higher than that obtained from other protocols due to its dependence on the number of relays and sub-carriers in OFDM symbol. In addition, (3.49) represents a unified equation of outage probability for all protocols.

### 3.5 Results and discussions

In this section, the numerical and simulation results of the outage probability for the proposed selective-OFDM system is presented and compared with conventional systems. The number of sub-carriers in each OFDM symbol is 16 and

Table 3.1: Scenarios for Sub-carriers Distribution

	Number of sub-carriers			
	block 1	block 2	block 3	block 4
Scenario 1	1	1	1	rest of sub-carriers
Scenario 2	3	3	5	5
Scenario 4	4	4	4	4

the target rate transmitted by each subcarrier is configured to 1 bps/Hz. The path-loss exponent is assumed to be set to 4. The channel is assumed to be block fading channel (slow fading). The Monte Carlo simulation results are validated with analytical results. In order to understand the behavior of system performance against the distribution of the sub-carriers in each block of  $i$ th relay. The number of blocks are assumed to be four and three scenarios for sub-carrier distribution considered as shown in table Table 3.1.

Figures 3.6 and 3.7 show the outage performance of present protocols for different values of the system SNR with  $M=10$ ,  $B=4$  and  $N=16$  without and with direct transmission. The analytical results of the outage probability are achieved using (3.17), (3.27), (3.36) and (3.46) for the direct transmission and (3.23), (3.30), (3.39) and (3.49) for absence of the direct transmission. The results demonstrate that scenario 1 performs very poorly compared to scenarios 2 and 3 and it is close to being a selective-OFDM protocol because most sub-carriers are allocated in one relay. In addition, the performance of scenario 1 and scenario 2 are located between the performance of selective OFDM relaying and selective block relaying. However, the selective equal block relaying is a special case of unequal block relaying, being the optimal case. Without loss of generality, the performance of selective block using either equal or unequal blocks will be measured as between selective OFDM and selective OFDMA. It can also be seen from both Figures that the system with direct transmission outperforms the one without direct transmission for all protocols due to exploiting the diversity of broadcast nature. The results demonstrates that employing direct transmis-

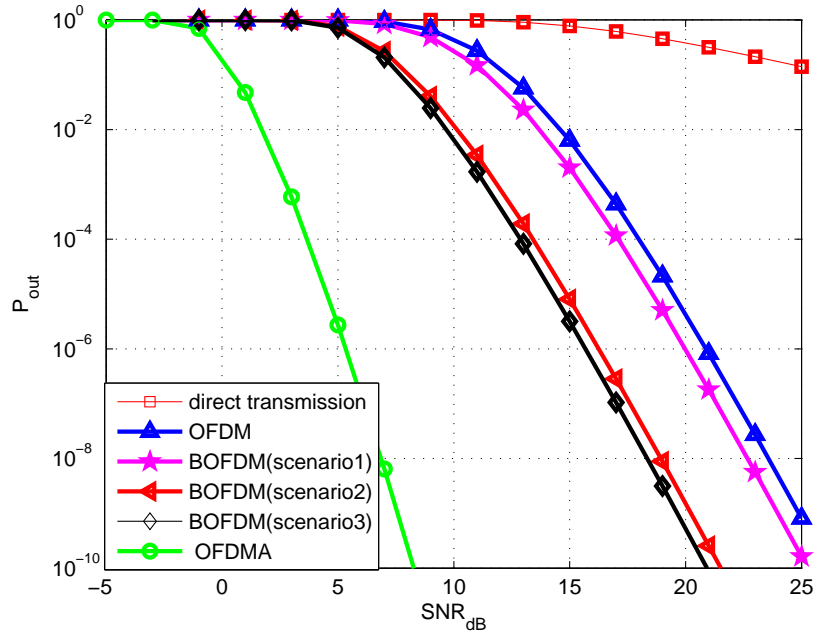


Figure 3.6: Outage probability versus SNR with  $M=10$  and  $N=16$  without direct transmission.

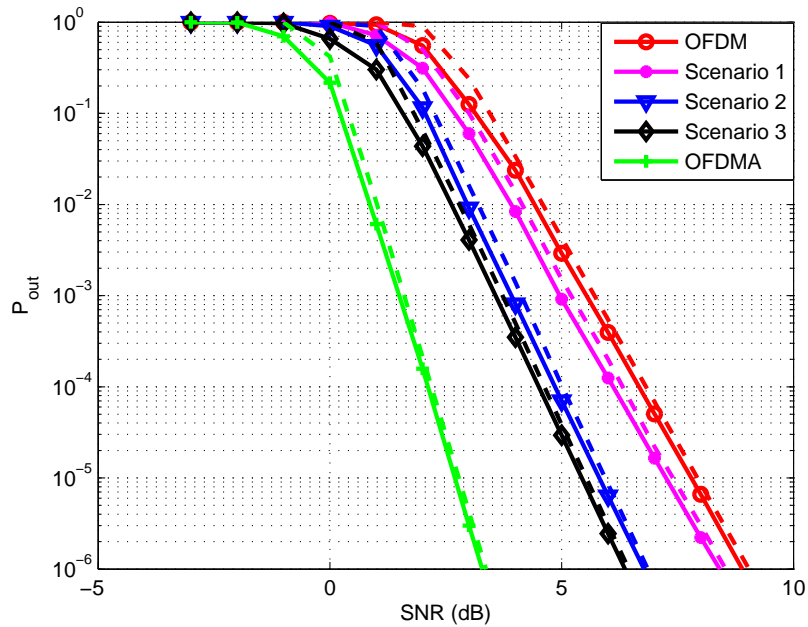


Figure 3.7: Outage probability versus SNR with  $M=10$  and  $N=16$  with direct transmission. The dash line represents the upper bound while the solid line denotes the simulation results.

sion can provide substantial improvement in the diversity order and gain for all considered protocols except selective OFDMA.

It is worth pointing out that the diversity order is defined as the slope of the outage probability in log-scale in the high SNR regime [14]. It can be seen from Figure 3.6 that the diversity order of selective OFDM, selective block-OFDM and selective unequal block-OFDM have the same diversity order which approximately equal to 10 that equivalent to the number of relays. While in Figure 3.7 the diversity order is slightly higher due to exploiting the broadcast nature. For both figures the diversity order of selective OFDMA is higher than other protocols due to the number of relays should be equal to the number of sub-carriers and each sub-carrier using single relay. The selective OFDMA relaying already provides high performance due to taking advantage of the full diversity order available in the system as illustrated in Figure 3.6.

Figure 3.8 demonstrates the outage performance of present protocols versus the number of relays with SNR=8 dB, B=4 and N=16. The results demonstrate that the performance of all protocols is directly proportional to the number of relays and that selective OFDM exhibits the worst performance. Selective OFDMA shows the best performance compared with other protocols, with selective block relaying performance located between selective OFDMA relaying and selective OFDM relaying. Selective unequal block relaying performance ranges between selective block relaying and selective OFDM relaying.

Figure 3.9 illustrates the performance of protocols versus the number of sub-carriers allocated in each relay with SNR=10, B=4, and M=8. In general, the results demonstrate that the outage probability degrades slowly for selective OFDMA but it deteriorates rapidly for the other protocols when the number of sub-carriers increases. Furthermore, the performance of all scenarios is located between selective OFDM and selective OFDMA. Scenario 3 obtains better performance than scenarios 1 and 2.

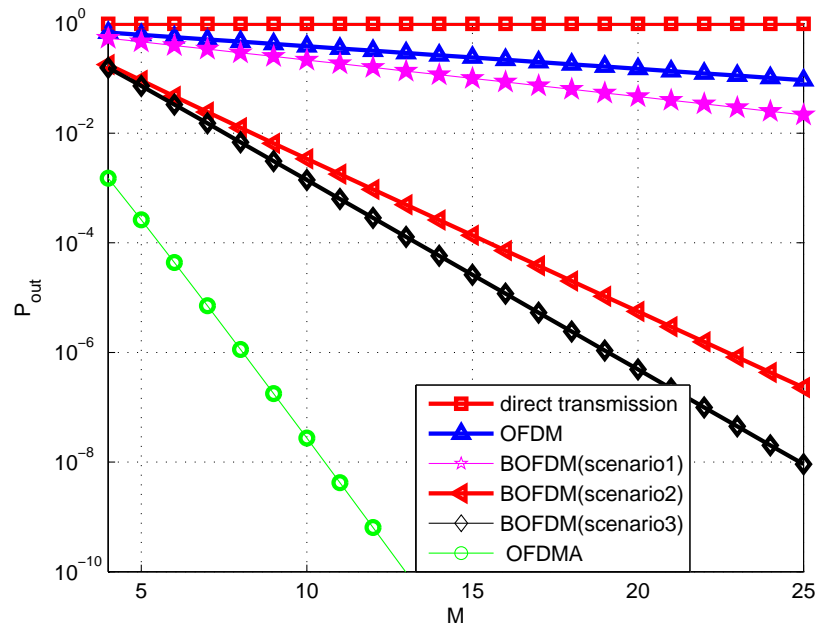


Figure 3.8: Outage probability versus  $M$  with SNR=10 dB and  $N=16$  without direct transmission.

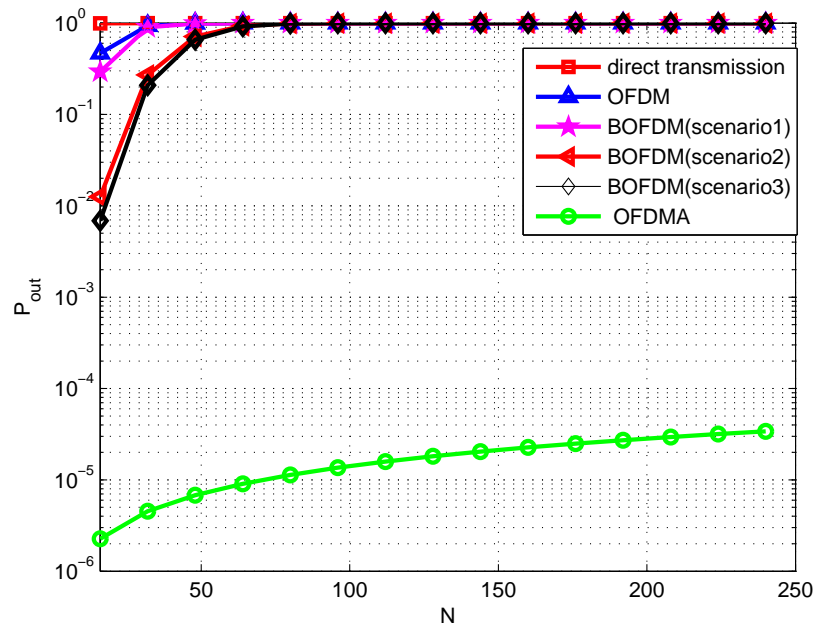


Figure 3.9: Outage probability versus  $N$  with  $M=10$  and SNR=10 dB.

## 3.6 Conclusion

In this chapter, the selective OFDM relaying protocol that consists of several scenarios is analyzed and the outage probability performance is presented. To overcome the load balancing, selective unequal block has been proposed. Selective block OFDM relaying is a special case of selective unequal block-OFDM relaying when the number of sub-carriers are equal in each block. Selective block-OFDM achieved better performance than selective unequal block-OFDM with versus SNR, M, and N. By applying direct transmission, the performance of selective OFDMA is slightly improved because its originally performs best performance. All of the other protocols achieved a significant improvement in both diversity and gain.

# Chapter 4

## Selective Per-subcarrier OFDM-based HRP

### 4.1 Introduction

As mentioned in previous chapters, high data rate applications require an efficient technique to combat the variations of the channel parameters when transmitting over broadband wireless environments. Several techniques have been proposed in literature such as MIMO, OFDM and relaying, which exploit the diversity gain of these systems to overcome performance deterioration. Undoubtedly, the most prominent technique is a combination of OFDM and relaying, especially in small size mobile nodes. However, the proposed schemes are based on “all-subcarrier basis” relay selection which require CRC codes to ensure correct decoding. This requires that the relay always decodes the received signal. SNR threshold metrics have been investigated recently to modify the “per-subcarrier” relay selection scheme [90]. This work uses the SNR threshold on a “per-subcarrier” relay selection to select the best forwarding protocol without unnecessary calculations.

Adaptive bit and power allocation (ABPA) has been investigated as one of the most attractive techniques to provide high system capacity in OFDM relay networks. There are two popular strategies used to allocate power and bits to each subcarrier in the OFDM relay systems, these being uniform and adaptive bit and power allocation [25, 134]. In uniform bit and power allocation, the same

number of bits and the same amount of power assigned to each subcarrier in the OFDM symbol. On the other hand, different rates and powers are allocated to each sub-carrier in adaptive BPA to maximize the system capacity.

In this chapter, two schemes based on hybrid relay protocol and the OFDM technique will be investigated. These are multi-carrier hybrid relay protocol (MC-HRP) and multi-carrier adaptive hybrid relay protocol (MC-AHRP).

The MC-HRP is an extension of the conventional single-carrier hybrid relay protocol [81–83,89,90] to a multi-carrier system. In MC-HRP scheme, the  $n$ th sub-carrier performs the DF scheme when the received SNR is greater than threshold SNR value. Otherwise, the  $n$ th sub-carrier performs the AF scheme. Transmitted signals over the low SNR sub-carriers may be corrupted the received signal at the destination due to selectivity in the frequency-selective channels. By exploiting the fact that when the source-relay channel power gain is sufficiently high enough, AF and DF schemes can offer the same performance and by avoiding sub-carriers that suffer deep fading, MC-AHRP deal with this aspects. In the MC-AHRP the  $n$ th subcarrier utilizes AF when the instantaneous SNR is larger than threshold value. Otherwise, it performs adaptive decode-and-forward (ADF) scheme. For any subcarrier of the ADF scheme that fails to be decoded, the destination selects the subcarrier from the direct transmission path instead. Performance results show that MC-AHRP outperforms all the relaying protocols including MC-HRP.

The main contribution of this chapter can be summarized as follows:

- A conventional HRP scheme is extended from the single carrier system to multi-carrier system, which is termed MC-HRP.
- A new scheme termed MC-AHRP, based on the combination of OFDM technique with AF-ADF relaying schemes that aims to reduce the problems associated with amplifying low SNR sub-carriers, is proposed.
- The theoretical error probability, outage probability and capacity are analyzed and evaluated for both proposed protocols.

- Suboptimal joint ABPA and SP with OFDM based AHRP are proposed with low computational complexity to further improve the system capacity.

The remainder of this chapter is organized as follows. In Section 4.2, related works are discussed. A system model is presented in Section 4.3. In Section 4.4, a cumulative density function is investigated. In Section 4.5, the bit and power allocation at the source is presented and at the relay in Section 4.6. The performance analysis of the proposed protocols in terms of bit error probability and outage probability is derived in Section 4.7. Numerical and simulation results are given and discussed in Section 4.8. Finally, concluding remarks are drawn in Section 4.9.

## 4.2 Related Work

It should be noted that significant effort has been placed to study of the performance hybrid relay protocol over single carrier systems (ie. flat fading) [81–83]. The authors in [90], [91] and [182] investigated threshold metrics to modify the relay selection scheme, thus improving the system performance. The authors of [90] proposed signal-to-noise ratio hybrid relay selection (SNR-HDAF), where the forwarding scheme of each sub-carrier is based on the quality of the received signal. The basic idea of this protocol is that if the received SNR is greater than the threshold SNR, the relay performs the DF scheme and utilizes the AF scheme in the other case. The closed-form expressions for the outage probability and error probability were derived over independent non-identical Rayleigh flat-fading channels.

The authors in [14–17], investigated an adaptive DF (ADF) scheme to overcome the drawbacks of the conventional DF protocol. The relay in this protocol utilizes the DF protocol if the decoded received signal is correct, otherwise it remains silent. The closed-form expression of outage probability was derived in [14] for all participate (repetition-based) protocol while the relay selection is introduced in [15] and [16].

There appears to have been less work considering the OFDM technique incorporated with HRP. For example, in the protocol proposed in [11], the forwarding scheme is based on per-subcarrier basis, that each subcarrier in the relay node will use either AF or the DF forwarding schemes or direct transmission according to analytical bit error rate (BER). However, the relay requires full knowledge of the CSI of the both direct and indirect links, which imposes high computational complexity and requires a large signalling overhead. The BER performance for all-participate hybrid DF-AF relaying is presented in [80] with a selective OFDM scheme adopted by retransmitting the entire OFDM symbol. Since the OFDM technique is active over frequency-selective channels, some sub-carriers will experience deep fading. Thus the received signal at the destination may be corrupted by using the AF scheme where it is difficult for the relay to decode all sub-carriers correctly. To avoid sub-carriers that experience deep fading, a new scheme of hybrid relay protocol based on a combined OFDM technique with AF-ADF relaying schemes is proposed and introduced here as MC-AHRP.

Adaptive bit and power allocation (ABPA) has been regarded as an efficient way to enhance system capacity in cooperative wireless networks [183]. ABPA for OFDM techniques, with and without relaying protocols, has been addressed in several recent papers [25, 184]. Subcarrier permutation (SP) has also been proposed as an efficient way to improve system performance [117]. In the SP scheme, the  $n$ th subcarrier in the first hop joins with the  $m$ th subcarrier in the second hop based on the channel state information (CSI) of both links. ABPA and SP conjunction with OFDM modulation have been well documented in the literature for conventional protocols [35, 104, 108, 185, 186]. The existing strategies for adaptive bit and power allocation mentioned before are considered either AF or DF relaying schemes. However, the computational requirement for searching for the best sub-carrier in the second time slot to matched with the best sub-carrier in the first time slot is high. ABPA has received much less attention for conventional hybrid relay protocols [187] which outperforms the conventional AF and DF schemes in terms of normalized capacity. To further improve the throughput of the proposed protocol, adaptive bit and power allocation is considered.

### 4.3 System Model

The system model is composed of a single source/destination (S, D) pair and a single relay (R). The transceiver block diagram of the relay node is depicted in Figure 4.1. All nodes in the system are equipped with a single antenna, and time division multiplexing (TDM) is applied, so that the source and relay cannot transmit simultaneously. All system terminals are composed of OFDM transceivers with  $N$  sub-carriers and perfect time and frequency synchronization assumed. The channel is assumed to be slow frequency-selective where the channel coefficients remain unchanged throughout one block but change independently from one block to the next.

The channels between each pair of nodes are independent and identical (i.i.d) with  $L$  independent delay paths. The impulse response and frequency response of the channel between any pair of nodes are given by

$$h_{ij}(\tau) = \sum_{l=0}^{L-1} \alpha_{ij}(l) \delta(\tau - \tau_l), \quad i \in \{S, R\} \text{ and } j \in \{R, D\}, \quad (4.1)$$

and

$$H_{ij}(f) = \sum_{l=0}^{L-1} \alpha_{ij}(l) e^{-j2\pi\tau_l f}, \quad (4.2)$$

where  $\alpha_{ij}(l)$  is the  $l$ th path complex amplitude of the source to the  $i$ th relay and  $i$ th relay to the destination channels and modeled as zero-mean complex Gaussian random variables with variance  $\sigma^2(l)$  and normalized power such that  $\sum_{l=0}^{L-1} \sigma_{l,ij}^2 = 1$ .  $\tau_l$  and  $\delta(\cdot)$  denote the delay of the  $l$ th path and the Dirac delta function respectively.

The complete channel state information are known at the relay. The relay computes the instantaneous SNR of each sub-carrier in the network. The SNR of the  $n$ th subcarrier can be expressed as

$$\begin{aligned} SNR(n) &= \frac{E\{|H_{sr,n}|^2 |X(n)|^2\}}{E\{|W(n)|^2\}}, \\ &= E_s \frac{E\{|H_{sr,n}|^2\}}{\sigma_{r,n}^2}, \end{aligned} \quad (4.3)$$

where  $E\{|X(n)|^2\}$  and  $E\{|W(n)|^2\}$  denote the average symbol energy and

the additive white Gaussian noise (AWGN) variance respectively. In practice, the variance of AWGN at the relay can be replaced by  $\sigma_{r,n}^2$  for each sub-carrier.

In general there are two methods for relay selection, either CRC or SNR threshold. The authors in [82, 83] reported that the SNR threshold provided smarter forwarding decisions than the CRC strategy due to its depending only on the channel state information of the first hop. However, the CRC method requires the relay always decodes the received signal to ensure correct decoding, which imposes a calculation overhead and introduces a delay. In the current study the SNR threshold method is used based on a “per-subcarrier” relay selection to select the best forwarding protocol for each subcarrier without unnecessary calculations. This illustrated in Figures 4.1(a) and 4.1(b). After the relay has calculated the instantaneous SNR for all sub-carriers of the first hop, it then compares them with a threshold SNR value. Then, the relay selects the forward scheme for each sub-carrier according to the quality of the received signal and the type of protocol. On one hand, using the CRC method, all sub-carriers are used by the relay. However, if the worst sub-carriers are utilized the fade may result in deterioration of the received signal at the relay and subsequently at the destination. On the other hand, the SNR threshold method can provide more flexibility by identifying which sub-carriers are experiencing deep fade. As a result, while SNR threshold method may not be the optimal choice, it may be the most practical choice because the optimum choice will take longer to calculate, which adds a delay to the time taken to make a decision. The forwarding scheme used by any sub-carrier feeds to the destination only in case without adaptive bit and power allocation. However, when the system performs ABPA the complete CSI and forwarding scheme for all sub-carriers should be known at the transmitter and the receiver.

In order to capture the path-loss effects on the system performance by taking into consideration the location of relay nodes, the channel model can be represented by:  $E(h_{ij}^2) \propto d_{ij}^{-\alpha}$  where  $d_{ij}$   $i \in \{S, R\}$ ,  $j \in \{R, D\}$  is the distance between terminals  $i$  and  $j$ ,  $\alpha$  is the power exponent, and  $E(\cdot)$  is the statistical average operation. Without loss of generality, the relative distance between  $S - R$  and

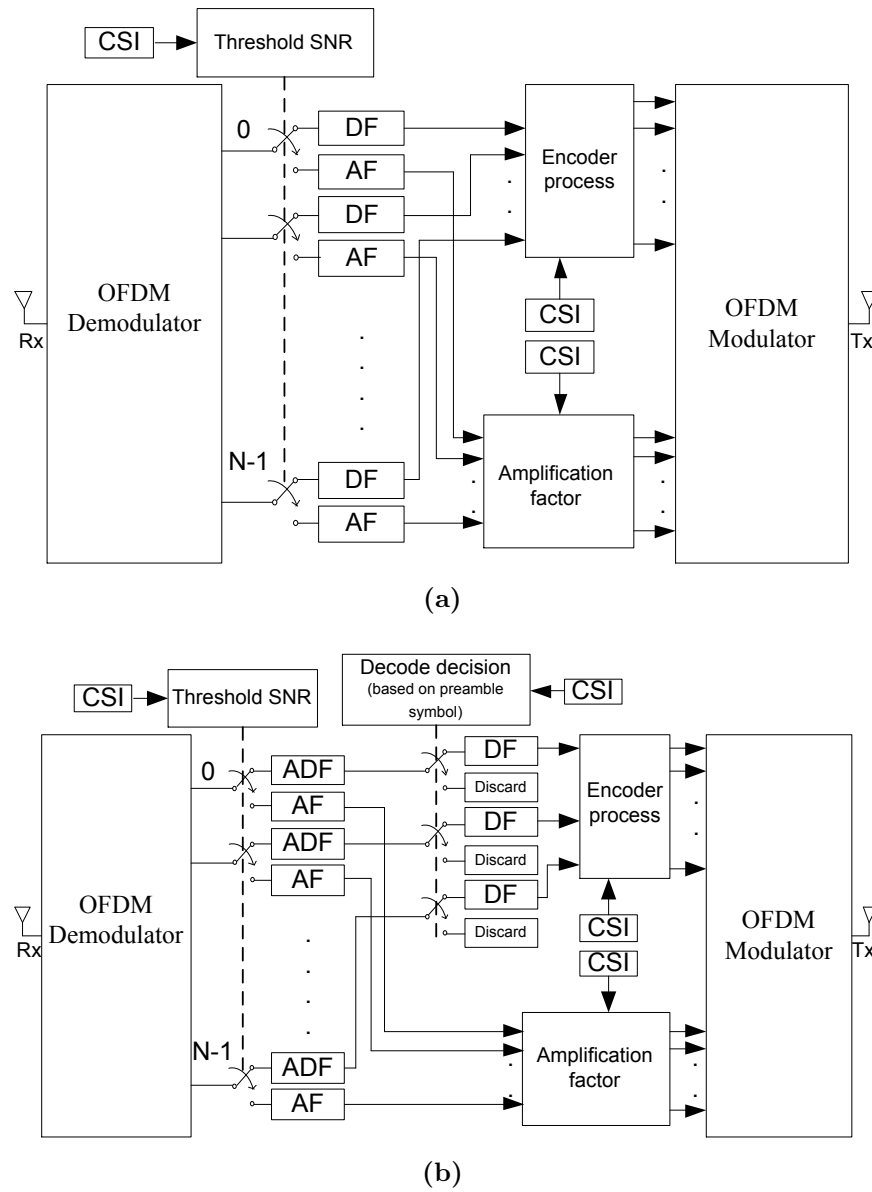


Figure 4.1: Transceiver block diagram of the relay node a) MC-HRP b) MC-AHRP.

$R - D$  links can be calculated by normalizing the distance between the source and relay ( $d_{sr}$ ) and the relay and destination ( $d_{rd}$ ) to the distance between the source and destination ( $d_{sd}$ ). It can be donated as  $d_r = \frac{d_{sr}}{d_{rd}}$ . For both schemes, the communications time is divided equally between the source and the relay according to half-duplex transmission, thus there are two time slots.

### 4.3.1 MC-HRP Strategy

In the MC-HRP scheme illustrated in Figure 4.1(a), the direct link is assumed to be absent due to either the long distance between the source and the destination or high shadowing caused by obstacles [126, 185]. After the relay has calculated the instantaneous SNRs for all sub-carriers of the first hop, it then compares them with a threshold SNR value  $\gamma_{th}$ . The  $\gamma_{th}$  is the average value of the instantaneous received SNR at the relay which is defined as  $\gamma_{th} = \frac{\sum_{n=1}^N \gamma_{sr,n}}{N}$ . If the instantaneous SNR of any subcarrier exceeds the threshold value, the DF scheme is used, otherwise the subcarrier utilizes the AF scheme. The communication process of this protocol can be described as follows: the source broadcasts an OFDM symbol to the relay node in the first time slot. Therefore, the received signals at the relay for the  $n$ th subcarrier, can be written as

$$y_{r,n} = \sqrt{P_{s,n}} h_{sr,n} x(n) + w_r. \quad (4.4)$$

Depending on the amplitude of the received signal relative to the threshold value, the relay either scales the version of the received noisy signal by an amplification factor  $\beta_n$  as in equation (3.2) or detects and re-encodes the receive signal and forwards it to the destination. The instantaneous SNR at the relay node is expressed as

$$\gamma_{sr,n} = \frac{P_{s,n} |h_{sr,n}|^2}{N_0} = \bar{\gamma} |h_{sr,n}|^2, \quad (4.5)$$

where  $\bar{\gamma}$  is the average SNR and is defined by

$$\bar{\gamma} = \frac{P_{s,n}}{N_0}. \quad (4.6)$$

In the second time slot, the relay node broadcasts the received signal from the source to the destination. It uses either the AF or DF scheme corresponding to the quality of the received signal. Therefore, the received signal at the destination from the  $n$ th subcarrier can be denoted as

$$y_{d,n} = \begin{cases} \beta_n h_{rd,n} (\sqrt{P_{sr,n}} h_{sr,n} x(n) + w_r) + w_d, & \text{if } n \in \text{AF} \\ h_{rd,n} x(n) + w_d, & \text{if } n \in \text{DF}. \end{cases} \quad (4.7)$$

Then the overall instantaneous SNR between the source and the destination for  $n$ th subcarrier can be written as

$$\gamma_n = \begin{cases} \frac{\gamma_{sr,n}\gamma_{rd,n}}{\gamma_{sr,n}+\gamma_{rd,n}+1}, & \text{if } \gamma_{sr,n} \leq \gamma_{th} \\ \min\{\gamma_{sr,n}, \gamma_{rd,n}\}, & \text{if } \gamma_{sr,n} > \gamma_{th}, \end{cases} \quad (4.8)$$

where  $\gamma_{rd,n}$  is the instantaneous SNR of the  $n$ th subcarrier between the relay and the destination nodes defined by

$$\gamma_{rd,n} = \frac{P_{r,n} |h_{rd,n}|^2}{N_0} = \bar{\gamma} |h_{rd,n}|^2. \quad (4.9)$$

### 4.3.2 Proposed MC-AHRP Strategy

In the following, the proposed MC-AHRP scheme is described. The block diagram of the MC-AHRP transceiver at the relay is illustrated in Figure 4.1(b). The frequency-selective channel in an OFDM system consists of  $N$  parallel sub-channels, each of which experience flat-fading. Therefore, whilst the power channel gain of some sub-channels is sufficient, it is still possible there are other sub-carriers experiencing deep fade. If the worst sub-carriers are utilized, the fade may result in deterioration of the received signal at the relay, and subsequently at the destination. Thus the MC-HRP is inefficient because it always amplifies the sub-carriers with a very low SNR. To overcome this dilemma and to identify which sub-carriers are experiencing deep fade, the existing ADF scheme can be improved upon.

In contrast to MC-HRP presented in page 58, MC-AHRP reduces the problems associated with amplifying low SNR sub-carriers, by discarding the sub-carriers that have low SNR. If the instantaneous SNR of any subcarrier is greater than the predetermined threshold, then the AF forwarding scheme is used. This ensures that only uncorrupted sub-carrier signals are amplified by the AF scheme, particularly when the specified threshold value is high enough. Alternatively, when the instantaneous SNR of any subcarrier is less than the threshold value, the subcarrier implements the ADF scheme [17]. In the ADF scheme, any subcarrier which correctly decodes the received signal uses the DF scheme, otherwise the subcarrier is discarded. The channel power gains for both direct and indirect links are mutually independent. The sub-carriers experiencing deep fading in the

source-relay link may not be in deep fade in direct transmission. Therefore, the destination selects the sub-carriers that have been discarded by the relay from the direct transmission instead.

In MC-AHRP the source broadcasts an OFDM symbol to the relay and the destination nodes in the first time slot. The received signal of the  $n$ th sub-carrier at the relay and the destination during the broadcasting phase can be expressed as

$$\begin{aligned} y_{r,n} &= \sqrt{P_{s,n}} h_{sr,n} x(n) + w_r \\ y_{d,n} &= \sqrt{P_{s,n}} h_{sd,n} x(n) + w_d. \end{aligned} \quad (4.10)$$

In the second time slot, the received signal at the destination from the  $n$ th sub-carrier can be denoted as

$$y_{d,n} = \begin{cases} \beta_n h_{rd,n} (\sqrt{P_{sr,n}} h_{sr,n} x(n) + w_r) + w_d, & \text{if } n \in \text{AF} \\ h_{rd,n} x(n) + w_d, & \text{if } n \in \text{DF} \\ h_{sd,n} x(n) + w_d, & \text{if } n \in \text{DT}. \end{cases} \quad (4.11)$$

Then, the end-to-end instantaneous SNR received at the destination can be expressed as

$$\gamma_n = \begin{cases} \frac{\gamma_{sr,n} \gamma_{rd,n}}{\gamma_{sr,n} + \gamma_{rd,n} + 1}, & \text{if } \gamma_{sr,n} > \gamma_{th} \\ \gamma_{rd,n}, & \text{if subcarrier decoded correctly} \\ \gamma_{sd,n}, & \text{if subcarrier fail to decode.} \end{cases} \quad (4.12)$$

where  $\gamma_{sd,n}$  is the instantaneous SNR of the  $n$ th subcarrier between the source and the destination defined by

$$\gamma_{sd,n} = \frac{P_{s,n} |h_{sd,n}|^2}{N_0} = \bar{\gamma} |h_{sd,n}|^2. \quad (4.13)$$

## 4.4 Cumulative Density Function Derivation

The aim of this section is to calculate the cumulative density function (CDF) of the end-to-end instantaneous SNR at the destination for both schemes. Since the channel coefficient for the  $n$ th subcarrier between any two nodes follows Rayleigh

fading distribution and the instantaneous SNRs  $h_{sr,n}$ ,  $h_{rd,n}$ , and  $h_{rd,n}$  follow exponential distributions, the CDF and PDF can be written as

$$\begin{aligned} F_{\gamma_{ij,n}}(\gamma) &= 1 - e^{-\frac{\gamma}{\bar{\gamma}_{ij,n}}}, i \in \{S, R\}, j \in \{R, D\} \\ f_{\gamma_{ij,n}}(\gamma) &= \frac{1}{\bar{\gamma}_{ij,n}} e^{-\frac{\gamma}{\bar{\gamma}_{ij,n}}}, i \in \{S, R\}, j \in \{R, D\}. \end{aligned} \quad (4.14)$$

The conditional PDF and CDF of  $\gamma_n = \frac{\gamma_{sr,n}\gamma_{rd,n}}{\gamma_{sr,n} + \gamma_{rd,n} + 1}$  is very complicated to derive. Therefore, a tight upper bound (as in [188]) can be used, which is more mathematically tractable and in a form suitable for analysis. Moreover, it is shown to be quite accurate at medium and high SNR values [19]. An upper bound equivalent to approximate value of the end-to-end instantaneous SNR at the destination is given by

$$\gamma_n \leq \frac{\gamma_{sr,n}\gamma_{rd,n}}{\gamma_{sr,n} + \gamma_{rd,n}} \leq \min\{\gamma_{sr,n}, \gamma_{rd,n}\}. \quad (4.15)$$

#### 4.4.1 MC-HRP Scheme

The destination has the ability to distinguish whether the  $n$ th subcarrier is part of the AF or DF group by receiving a single bit from the relay. The CDF of  $\gamma_n$  at the destination can be expressed as [12, 84, 90, 189]

$$F_{\gamma_n} = Pr(\gamma_{sr,n} \leq \gamma_{th})Pr(n \in \mathcal{G}AF) + Pr(\gamma_{sr,n} > \gamma_{th})Pr(n \in \mathcal{G}DF), \quad (4.16)$$

where  $Pr(\gamma_{sr,n} > \gamma_{th})$  is the probability of the instantaneous SNR at the  $n$ th subcarrier being greater than a specified threshold value.  $Pr(n \in \mathcal{G}AF)$ , and  $Pr(n \in \mathcal{G}DF)$  are the probability of the  $n$ th subcarrier related to AF or DF groups. Since the instantaneous SNR for the sub-carriers between the source and relay follow the exponential distribution, it is straightforward to get that

$$\begin{aligned} Pr(\gamma_{sr,n} > \gamma_{th}) &= e^{-\frac{\gamma_{th}}{\bar{\gamma}_{sr,n}}} \\ Pr(\gamma_{sr,n} \leq \gamma_{th}) &= 1 - e^{-\frac{\gamma_{th}}{\bar{\gamma}_{sr,n}}}. \end{aligned} \quad (4.17)$$

The corresponding conditional CDF of  $\gamma_n$  given  $\gamma_{sr,n} \leq \gamma_{th}$  (or  $n \in \mathcal{G}AF$ ) is expressed as

$$\begin{aligned} F_{\gamma_n}(\gamma \mid \gamma_{sr,n} \leq \gamma_{th}) &\approx Pr(\min\{\gamma_{sr,n}, \gamma_{rd,n}\} < \gamma \mid \gamma_{sr,n} \leq \gamma_{th}) \\ &= 1 - Pr(\gamma \mid \gamma_{sr,n} \leq \gamma_{th})Pr(\gamma_{rd,n} > \gamma) \\ &= 1 - (1 - F_{\gamma_{sr,n}}(\gamma \mid \gamma_{sr,n} \leq \gamma_{th}))(1 - F_{\gamma_{rd,n}}(\gamma)). \end{aligned} \quad (4.18)$$

The conditional CDF of  $F_{\gamma_{sr,n}}(\gamma \mid \gamma_{sr,n} \leq \gamma_{th})$  can be calculated by using the method presented in [190] as

$$F_{\gamma_{sr,n}}(\gamma \mid \gamma_{sr,n} \leq \gamma_{th}) = \begin{cases} \frac{Pr(\gamma_{sr,n} \leq \gamma, \gamma_{sr,n} \leq \gamma_{th})}{Pr(\gamma_{sr,n} \leq \gamma_{th})}, & \text{if } \gamma \leq \gamma_{th} \\ 1, & \text{if } \gamma > \gamma_{th} \end{cases} \quad (4.19)$$

$$= \begin{cases} \frac{1 - e^{-\frac{\gamma}{\bar{\gamma}_{sr,n}}}}{1 - e^{-\frac{\gamma_{th}}{\bar{\gamma}_{sr,n}}}}, & \text{if } \gamma \leq \gamma_{th} \\ 1. & \text{if } \gamma > \gamma_{th} \end{cases}$$

To evaluate the corresponding conditional CDF of  $\gamma_n$  by substituting (4.19) into (4.18) and noting that  $F_{\gamma_{rd,n}}(\gamma) = 1 - e^{-\frac{\gamma}{\bar{\gamma}_{rd,n}}}$ , it may be shown that

$$F_{\gamma_n}(\gamma \mid \gamma_{sr,n} \leq \gamma_{th}) = \begin{cases} 1 - \frac{e^{-\frac{\gamma}{\bar{\gamma}_{sr,n}}} - e^{-\frac{\gamma_{th}}{\bar{\gamma}_{sr,n}}}}{1 - e^{-\frac{\gamma_{th}}{\bar{\gamma}_{sr,n}}}} e^{-\frac{\gamma}{\bar{\gamma}_{rd,n}}}, & \text{if } \gamma \leq \gamma_{th} \\ 1. & \text{if } \gamma > \gamma_{th} \end{cases} \quad (4.20)$$

and the PDF is obtained by differentiating (4.20) with respect to  $\gamma$  as

$$f_{\gamma_n}(\gamma \mid \gamma_{sr,n} \leq \gamma_{th}) = \begin{cases} \frac{\frac{1}{\bar{\gamma}_{eq,n}} e^{-\frac{\gamma}{\bar{\gamma}_{eq,n}}} - \frac{1}{\bar{\gamma}_{rd,n}} e^{-\frac{\gamma_{th}}{\bar{\gamma}_{sr,n}}} e^{-\frac{\gamma}{\bar{\gamma}_{rd,n}}}}{1 - e^{-\frac{\gamma_{th}}{\bar{\gamma}_{sr,n}}}}, & \text{if } \gamma \leq \gamma_{th} \\ 0. & \text{if } \gamma > \gamma_{th} \end{cases} \quad (4.21)$$

The corresponding conditional CDF of  $\gamma_n$  given  $\gamma_{sr,n} > \gamma_{th}$  (or  $n \in \mathcal{GDF}$ ) can be expressed as

$$F_{\gamma_n}(\gamma \mid \gamma_{sr,n} \geq \gamma_{th}) = 1 - e^{-\frac{\gamma}{\bar{\gamma}_{rd,n}}} \quad (4.22)$$

$$f_{\gamma_n}(\gamma \mid \gamma_{sr,n} \geq \gamma_{th}) = \frac{1}{\bar{\gamma}_{rd,n}} e^{-\frac{\gamma}{\bar{\gamma}_{rd,n}}}.$$

By substituting (4.17), (4.20), and (4.22) into (4.16), the CDF of  $\gamma_n$  can be rewritten as

$$F_{\gamma_n} = (1 - e^{-\frac{\gamma_{th}}{\bar{\gamma}_{sr,n}}}) \left( 1 - \frac{e^{-\frac{\gamma}{\bar{\gamma}_{sr,n}}} - e^{-\frac{\gamma_{th}}{\bar{\gamma}_{sr,n}}}}{1 - e^{-\frac{\gamma_{th}}{\bar{\gamma}_{sr,n}}}} e^{-\frac{\gamma}{\bar{\gamma}_{rd,n}}} \right) + e^{-\frac{\gamma_{th}}{\bar{\gamma}_{sr,n}}} \left( 1 - e^{-\frac{\gamma}{\bar{\gamma}_{rd,n}}} \right). \quad (4.23)$$

#### 4.4.2 MC-AHRP Scheme

In this section, the CDF of the MC-AHRP scheme for independent identical Rayleigh fading channels is derived. Previously it was mentioned that the  $n$ th sub-carrier used the AF scheme when the received SNR at the relay was larger

than the threshold value. Therefore, the CDF of the end-to-end instantaneous SNR  $\gamma_n$  at the destination is given by [78, 191]

$$F_{\gamma_n}^{\text{MC-AHRP}}(\gamma) = \Pr(\gamma_{sr,n} > \gamma_{th})\Pr(n \in \mathcal{GAF}) + \Pr(\gamma_{sr,n} \leq \gamma_{th})\Pr(n \in \mathcal{GADF}), \quad (4.24)$$

where  $\Pr(n \in \mathcal{GADF})$  is the probability of  $n$ th sub-carrier being related to the ADF scheme. It can be evaluated by following the method presented in [16]. Let the random variable  $\zeta_n$  represent the received instantaneous SNR on the  $n$ th sub-carrier at the destination. The unconditional CDF of  $\zeta_n$  can be given as [16, 192]

$$F_{\zeta_n}(\gamma) = F_{\zeta_n|nth-err}(\gamma)\Pr(nth - err)F_{\zeta_n|nth-corr}(\gamma)\Pr(nth - corr), \quad (4.25)$$

where  $\Pr(nth - err)$  denotes the probability that the  $n$ th sub-carrier will not be in the decoding set.  $\Pr(nth - corr)$  represents the probability that the  $n$ th sub-carrier can decode the received signal correctly. The  $F_{\zeta_n|nth-err}(\gamma)$  represents the conditional CDF of the instantaneous SNR between the source and relay and can be expressed as [190]

$$F_{\gamma_{sr,n}}(\gamma | \gamma_{sr,n} \leq \gamma_{th}) = \begin{cases} \frac{1 - e^{-(\gamma/\bar{\gamma}_{sr,n})}}{(1 - e^{-(\gamma_{th}/\bar{\gamma}_{sr,n})})}, & \text{if } \gamma \leq \gamma_{th} \\ 1, & \text{if } \gamma > \gamma_{th}. \end{cases} \quad (4.26)$$

Furthermore,  $\Pr(nth - err)$  and  $\Pr(nth - corr)$  can be expressed as

$$\begin{aligned} \Pr(nth - err) &= 1 - e^{-\frac{\gamma}{\bar{\gamma}_{sd,n}}} \\ \Pr(nth - corr) &= 1 - e^{-\frac{\gamma}{\bar{\gamma}_{rd,n}}} \end{aligned} \quad (4.27)$$

The CDF of  $\zeta_i$  can be evaluated by substituting (4.26) and (4.27) into (4.25) as

$$F_{\zeta_n}(\gamma) = \frac{1 - e^{-(\gamma/\bar{\gamma}_{sr,n})}}{(1 - e^{-(\gamma_{th}/\bar{\gamma}_{sr,n})})} (1 - e^{-\frac{\gamma}{\bar{\gamma}_{sd,n}}}) + (1 - \frac{1 - e^{-(\gamma/\bar{\gamma}_{sr,n})}}{(1 - e^{-(\gamma_{th}/\bar{\gamma}_{sr,n})})}) (1 - e^{-\frac{\gamma}{\bar{\gamma}_{rd,n}}}), \quad (4.28)$$

and the PDF of  $\zeta_i$  can be obtained by differentiating (4.28) with respect to  $\gamma$  as

$$\begin{aligned} f_{\zeta_n}(\gamma) &= \frac{1}{(1 - e^{-(\gamma_{th}/\bar{\gamma}_{sr,n})})} \left[ \frac{1}{\bar{\gamma}_{sd,n}} e^{-\frac{\gamma}{\bar{\gamma}_{sd,n}}} - \frac{\bar{\gamma}_{sr,n}\bar{\gamma}_{sd,n}}{\bar{\gamma}_{sr,n} + \bar{\gamma}_{sd,n}} e^{-\gamma(\frac{1}{\bar{\gamma}_{sr,n}} + \frac{1}{\bar{\gamma}_{sd,n}})} \right] \\ &+ \frac{1}{(1 - e^{-(\gamma_{th}/\bar{\gamma}_{sr,n})})} \left[ \frac{1}{\bar{\gamma}_{eq,n}} e^{-\frac{\gamma}{\bar{\gamma}_{eq,n}}} - \frac{1}{\bar{\gamma}_{rd,n}} e^{-\frac{\gamma}{\bar{\gamma}_{rd,n}}} e^{-\frac{\gamma_{th}}{\bar{\gamma}_{sr,n}}} \right]. \end{aligned} \quad (4.29)$$

The corresponding conditional CDF of  $\gamma_n$  given  $\gamma_{sr,n} > \gamma_{th}$  can be expressed as

$$\begin{aligned} F_{\gamma_n}(\gamma \mid \gamma_{sr,n} > \gamma_{th}) &\approx Pr(\min\{\gamma_{sr,n}, \gamma_{rd,n}\} < \gamma \mid \gamma_{sr,n} > \gamma_{th}) \\ &= 1 - Pr(\gamma \mid \gamma_{sr,n} > \gamma_{th})Pr(\gamma_{rd,n} > \gamma) \\ &= 1 - (1 - F_{\gamma_{sr,n}}(\gamma \mid \gamma_{sr,n} > \gamma_{th}))(1 - F_{\gamma_{rd,n}}(\gamma)). \end{aligned} \quad (4.30)$$

Using the same method as in (4.19), the conditional CDF of  $F_{\gamma_{sr,n}}(\gamma \mid \gamma_{sr,n} > \gamma_{th})$  can be written as

$$\begin{aligned} F_{\gamma_{sr,n}}(\gamma \mid \gamma_{sr,n} > \gamma_{th}) &= \begin{cases} \frac{Pr(\gamma_{sr,n} < \gamma, \gamma_{sr,n} > \gamma_{th})}{Pr(\gamma_{sr,n} > \gamma_{th})}, & \text{if } \gamma > \gamma_{th} \\ 1, & \text{if } \gamma \leq \gamma_{th} \end{cases} \\ &= \begin{cases} \frac{1 - e^{-\frac{\gamma}{\bar{\gamma}_{sr,n}}}}{e^{-\frac{\gamma_{th}}{\bar{\gamma}_{sr,n}}}}, & \text{if } \gamma > \gamma_{th} \\ 1, & \text{if } \gamma \leq \gamma_{th}. \end{cases} \end{aligned} \quad (4.31)$$

Substituting (4.31) into (4.30) gives

$$F_{\gamma_n}(\gamma \mid \gamma_{sr,n} > \gamma_{th}) = \begin{cases} 1 - (1 - \frac{1 - e^{-\frac{\gamma}{\bar{\gamma}_{sr,n}}}}{e^{-\frac{\gamma_{th}}{\bar{\gamma}_{sr,n}}}})e^{-\frac{\gamma}{\bar{\gamma}_{rd,n}}}, & \text{if } \gamma > \gamma_{th} \\ 1, & \text{if } \gamma \leq \gamma_{th} \end{cases} \quad (4.32)$$

and the PDF of  $\gamma_n$  can be obtained by differentiating (4.32) with respect to  $\gamma$  to give

$$f_{\gamma_{sr,n}}(\gamma \mid \gamma_{sr,n} > \gamma_{th}) = \begin{cases} \frac{1}{\bar{\gamma}_{rd,n}} \left( e^{-\frac{\gamma}{\bar{\gamma}_{rd,n}}} - \frac{e^{-\frac{\gamma}{\bar{\gamma}_{rd,n}}} - \frac{1}{\bar{\gamma}_{sr,n}} e^{-\frac{\gamma}{\bar{\gamma}_{eq,n}}}}{e^{-\frac{\gamma_{th}}{\bar{\gamma}_{sr,n}}}} \right), & \text{if } \gamma > \gamma_{th} \\ 0, & \text{if } \gamma \leq \gamma_{th}. \end{cases} \quad (4.33)$$

Finally the CDF of the scheme can be evaluated by substituting (4.17), (4.28) and (4.32) into (4.24) as

$$\begin{aligned} F_{\gamma_n}^{\text{AHRP}}(\gamma) &= e^{-\frac{\gamma_{th}}{\bar{\gamma}_{sr,n}}} \left[ 1 - \left( 1 - \frac{1 - e^{-\frac{\gamma}{\bar{\gamma}_{sr,n}}}}{e^{-\frac{\gamma_{th}}{\bar{\gamma}_{sr,n}}}} \right) e^{-\frac{\gamma}{\bar{\gamma}_{rd,n}}} \right] + \left( 1 - e^{-\frac{\gamma}{\bar{\gamma}_{sr,n}}} \right) \left( 1 - e^{-\frac{\gamma}{\bar{\gamma}_{sd,n}}} \right) \\ &\quad + \left( 1 - e^{-\frac{\gamma_{th}}{\bar{\gamma}_{sr,n}}} \right) \left( 1 - \frac{1 - e^{-\frac{\gamma}{\bar{\gamma}_{sr,n}}}}{1 - e^{-\frac{\gamma_{th}}{\bar{\gamma}_{sr,n}}}} \right) \left( 1 - e^{-\frac{\gamma}{\bar{\gamma}_{rd,n}}} \right). \end{aligned} \quad (4.34)$$

## 4.5 Bit and Power Allocation at the Source

The objective in this section is to maximize the aggregate system capacity under given individual power constraints at the source and the relay. The instantaneous capacity for each subcarrier at the destination can be expressed as

$$C_n = \frac{1}{2} \log_2(1 + \gamma_n), \quad (4.35)$$

where  $\gamma_n$  is the end-to-end instantaneous SNR and can be expressed as

$$\gamma_n = \begin{cases} \frac{\frac{G_{sr,n} P_{s,n} G_{rd,n} P_{r,n}}{\sigma_r^2 \sigma_d^2}}{\frac{G_{sr,n} P_{s,n}}{\sigma_r^2} + \frac{G_{rd,n} P_{r,n}}{\sigma_d^2} + 1} & \text{if } n \in \mathcal{G}AF \\ \frac{G_{rd,n} P_{r,n}}{\sigma_d^2}, & \text{if } n \in \mathcal{G}ADF \end{cases} \quad (4.36)$$

where  $P_s$  and  $P_r$  are the total power at the source and the relay respectively.  $G_{sr,n}$  and  $G_{rd,n}$  are the channel power gain coefficients for  $n$  sub-carrier links, source-relay and relay-destination respectively. In this protocol the optimization problem will be split into two sub-optimal problems at the relay by dividing the sub-carriers into two groups. Then each group will be optimized independently.

For the first hop, the source knows the channel power gains. In the uniform bit and power allocation algorithm, the number of bits assigned to each sub-carrier is fixed (for example, BPSK modulation). Furthermore, the transmission power allocated to different sub-carriers are distributed uniformly and can be written as

$$P_n = \frac{P_s}{N}. \quad (4.37)$$

To implement adaptive BPA at the source. The transmit power is assumed to be known. In this scheme, the main task is how to distribute the total power over sub-carriers optimally. Firstly, the selection of a suitable modulation scheme for each sub-carrier is carried out based on the predetermined SNR threshold when the bit error rate (BER) is equal to  $10^{-3}$  as shown in Table 4.1 [193]. This can reduce the computational complexity of bit loading implementation at the source. Accordingly the source can restrict the number of bits assigned to each subcarrier to either 0, 1, 2, 4, 6, or 8 for no-transmission, BPSK, and MQAM,

Table 4.1: SNR threshold values of modulation scheme

Modulation Scheme	SNR Threshold (dB)
No-Modulation	<5
BPSK	5
QPSK	8
16QAM	12
64QAM	18
256QAM	24

respectively. Finally a water-filling algorithm is employed to evaluate the power allocated to each subcarrier established in [194]

$$P_n = \frac{(P_S + \sum_{n=1}^N \frac{\Gamma \sigma_r^2}{G_{sr,n}})}{N} - \frac{\Gamma \sigma_n^2}{G_{sr,n}}, \quad (4.38)$$

where  $\Gamma$  is the SNR gap, which is a function of the target BER and a channel coding scheme and can be expressed as [102]

$$\Gamma = -\frac{\ln(5\text{BER})}{1.5}. \quad (4.39)$$

## 4.6 Bit and Power Allocation at the Relay

In this section, the proposed adaptive bit and power allocation for OFDM-based HRP relaying with and without sub-carrier permutation at the relay node is introduced.

### 4.6.1 Without Subcarrier Permutation

In this protocol, fixed pairing is considered where the sub-carrier on the second hop retransmits the data on the same sub-carrier index used in the first hop. Because there are two sub-carrier groups (AF and DF), the resource allocation can be implemented independently. Due to the fact that the sub-carriers in the AF group does not require demodulation, decoding and re-encoding processes, the

number of bits carried by the  $n$ th sub-carrier is the same at both hops. In addition, the amplification factor already relies on the channel power gain in the first hop. The amount of power allocated to each sub-carrier in the AF group at the relay can be written as

$$P_n = \frac{\Gamma \sigma^2}{G_{rd,n}} (2^{b_n} - 1), \quad n \in \mathcal{G}_{AF}. \quad (4.40)$$

The overall power consumption of the AF group is the sum of the individual power allocations of each sub-carrier. The residual power at the relay can be expressed as

$$P_{DF} = P_r - \sum_{n \in \mathcal{G}_{AF}} P_n. \quad (4.41)$$

In the same context, the power allocation for each subcarrier in the DF group depends heavily on the channel power gain in the second hop. Therefore, the residual power is allocated to the sub-carriers in the DF group according to the water-filling algorithm as a single in-single out (SISO) system.

### 4.6.2 With Subcarrier Permutation

Subcarrier permutation is considered to further improve the system performance by exploiting the independence of the channel power gains in both hops. Therefore, the relay can use the same or different sub-carriers to retransmit the information bearing symbol from the source to the destination. The block diagram of the MC-AHRP scheme is illustrated in Figure 4.2

This scheme can be implemented in two parts. In the first, resource allocation and sub-carrier permutation are done on the sub-carriers in the AF group. The overall subcarrier capacity is limited by the worst subcarrier of the first and second hop. Therefore, maximum capacity can only be achieved when the channel power gains are the same at both hops [108, 130]. The residual power is equal to the overall power for the AF group subtracted from the total power available at the relay. The residual power is optimally distributed to the sub-carriers in the DF group in the second part. The proposed algorithm can be summarized as:

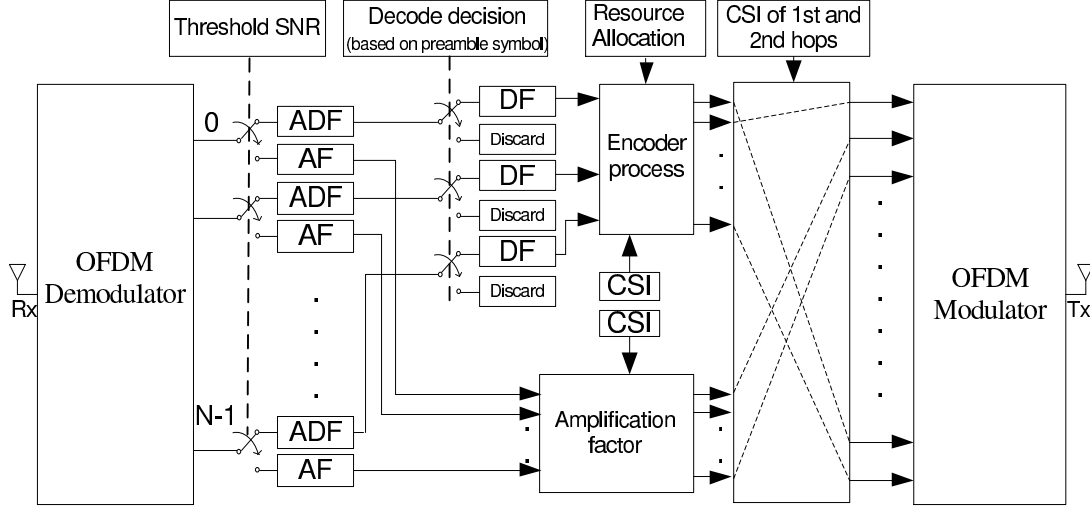


Figure 4.2: Transceiver block diagram of the relay node with sub-carrier pairing.

Part 1) For all using sub-carriers, calculate the channel power gains at both hops.

$$S = \{1, \dots, N\}$$

**for**  $n \in \mathcal{G}_{AF}$  **do**

**for**  $j \in S$  **do**

$$\Delta_{n,j} = G_{sr,n} - G_{rd,j}$$

**end for**

$$\hat{n}, \hat{j} = \arg \min \Delta_{n,j}$$

$$P_j = \frac{\Gamma \sigma^2}{G_{rd,\hat{j}}} (2^{b_{\hat{n}}} - 1)$$

$$S = S - \{j\}$$

**end for**

Part 2)

1. Calculate the residual power

$$P_{DF} = P_r - \sum_{n \in \mathcal{G}_{AF}} P_n,$$

2. The channel power gains for the remaining sub-carriers  $S$  for the second hop are arranged in descending order, i.e.  $G_{rd,j} \geq G_{rd,j+1} \dots \geq G_{rd,N-K}$ , where  $K$

is the number of sub-carriers in the AF group. The relay chooses the best sub-carriers corresponding to the number of sub-carriers in the DF group and discards the rest of the sub-carriers.

3. The sub-optimal water-filling algorithm is performed on the selected sub-carriers to allocate the power and assign a corresponding number of bits over the residual power constraint.

This technique reduces the computational complexity and increases the throughput of the DF group. The sub-carriers at the relay are divided into two groups. Each group has different number of sub-carrier where  $N_{AF}$  is the number of subcarrier in AF group, while  $N_{DF}$  is the number of sub-carrier in the DF group. The AF implements sub-carrier pairing independently by seeking the sub-carriers in the second hop have the same number of bits in the first hop. Then the rest of sub-carriers are sorted in descending order. Then the DF group chooses the best  $N_{DF}$  sub-carriers. Therefore the complexity of doing a sub-carrier match is equal to  $N_{AF}N + 1$ . It can be seen that the complexity in this protocol is quite low.

## 4.7 Performance Analysis

In this section the performance analysis in terms of bit error probability, outage probability and throughput are discussed for MC-HRP and MC-AHRP schemes.

### 4.7.1 Bit Error Probability Performance

In this section, the closed-form expression of BEP performance is derived over independent identical Rayleigh fading channels. For both MC-HRP and MC-AHRP schemes the relay retransmits the entire OFDM symbols received from the source to the destination in the second time interval. Each OFDM symbol consists of  $N$  independent links (sub-carriers). Therefore the total average BEP of the OFDM relaying system can be expressed as in [195]

$$P_e = \frac{1}{N} \sum_1^N P_e(n), \quad (4.42)$$

where  $P_e(n)$  is the average error probability of the  $n$ th sub-carrier at the destination. The average BEP of the  $n$ th sub-carrier can be computed by averaging the conditional error probability in AWGN over the PDF as presented in [196]

$$P_e(n) = \int_0^{\infty} Q(\sqrt{c\gamma})f_{\gamma}(n)d\gamma, \quad (4.43)$$

where  $c$  is a modulation constant and  $Q(x) = a \operatorname{erfc}(bx)$  is the Gaussian Q-function given by  $(1/\sqrt{2\pi}) \int_x^{\infty} \exp(-t^2/2)dt$ .  $a$  and  $b$  are constants that depend on the type of modulation scheme (e.g. for BPSK  $a = 0.5$  and  $b = 1$ , QPSK  $a = 1$  and  $b = 0.5$ ). In order to evaluate the average BEP of each protocol, it should first calculate the instantaneous probability density function  $f_{\gamma}(n)$  of the system under consideration as illustrated in (4.43).

#### 4.7.1.1 MC-HRP Scheme

The average error probability on each sub-carrier of the *MC – HRP* can be formulated by

$$\begin{aligned} P_e^{\text{HRP}}(n) &= \Pr(\gamma_{sr,n} \leq \gamma_{th})P_e^{\text{AF}}(n) + \Pr(\gamma_{sr,n} > \gamma_{th})P_e^{\text{DF}}(n) \\ &= \Pr(\gamma_{sr,n} \leq \gamma_{th}) \int_0^{\gamma_{th}} Q(\sqrt{2\gamma})f_{\gamma_n}(\gamma | \gamma_{sr,n} \leq \gamma_{th})d\gamma \\ &\quad + \Pr(\gamma_{sr,n} > \gamma_{th}) \int_{\gamma_{th}}^{\infty} Q(\sqrt{2\gamma})f_{\gamma_n}(\gamma | \gamma_{sr,n} > \gamma_{th})d\gamma \end{aligned} \quad (4.44)$$

Substituting (4.17), along with (4.21) and (4.22) into (4.44) yields

$$\begin{aligned} P_e^{\text{HRP}}(n) &= (1 - e^{-\frac{\gamma_{th}}{\bar{\gamma}_{sr,n}}}) \int_0^{\gamma_{th}} Q(\sqrt{2\gamma}) \left( \frac{\frac{1}{\bar{\gamma}_{eq,n}} e^{-\frac{\gamma}{\bar{\gamma}_{eq,n}}} - \frac{1}{\bar{\gamma}_{rd,n}} e^{-\frac{\gamma_{th}}{\bar{\gamma}_{sr,n}} e^{-\frac{\gamma}{\bar{\gamma}_{rd,n}}}}}{1 - e^{-\frac{\gamma_{th}}{\bar{\gamma}_{sr,n}}}} \right) d\gamma \\ &\quad + e^{-\frac{\gamma_{th}}{\bar{\gamma}_{sr,n}}} \int_{\gamma_{th}}^{\infty} Q(\sqrt{2\gamma}) \left( \frac{1}{\bar{\gamma}_{rd,n}} e^{-\frac{\gamma}{\bar{\gamma}_{rd,n}}} \right) d\gamma \\ &= \int_0^{\infty} Q(\sqrt{2\gamma}) \left( \frac{1}{\bar{\gamma}_{eq,n}} e^{-\frac{\gamma}{\bar{\gamma}_{eq,n}}} - \frac{1}{\bar{\gamma}_{rd,n}} e^{-\frac{\gamma_{th}}{\bar{\gamma}_{sr,n}} e^{-\frac{\gamma}{\bar{\gamma}_{rd,n}}}} \right) d\gamma \\ &\quad - \int_{\gamma_{th}}^{\infty} Q(\sqrt{2\gamma}) \left( \frac{1}{\bar{\gamma}_{eq,n}} e^{-\frac{\gamma}{\bar{\gamma}_{eq,n}}} - \frac{1}{\bar{\gamma}_{rd,n}} e^{-\frac{\gamma_{th}}{\bar{\gamma}_{sr,n}} e^{-\frac{\gamma}{\bar{\gamma}_{rd,n}}}} \right) d\gamma \\ &\quad + e^{-\frac{\gamma_{th}}{\bar{\gamma}_{sr,n}}} \int_{\gamma_{th}}^{\infty} Q(\sqrt{2\gamma}) \left( \frac{1}{\bar{\gamma}_{rd,n}} e^{-\frac{\gamma}{\bar{\gamma}_{rd,n}}} \right) d\gamma \end{aligned} \quad (4.45)$$

By applying the integration by part gives

$$\begin{aligned}
& \int_{\gamma_{th}}^{\infty} Q(\sqrt{2\gamma}) \left( \frac{1}{\bar{\gamma}_{rd,n}} e^{-\frac{\gamma}{\bar{\gamma}_{rd,n}}} \right) d\gamma \\
& \int u(x)v'(x)dx = u(x)v(x) - \int u'(x)v(x)dx \\
& u = Q(\sqrt{2\gamma}) \quad dv = \frac{1}{\bar{\gamma}_{rd,n}} e^{-\frac{\gamma}{\bar{\gamma}_{rd,n}}} \\
& du = \frac{1}{\sqrt{2\pi}} e^{-\gamma} d\gamma \quad v = e^{-\frac{\gamma_{th}}{\bar{\gamma}_{rd,n}}} \\
& = Q(\sqrt{2\gamma}) e^{-\frac{\gamma_{th}}{\bar{\gamma}_{rd,n}}} - \int_{\gamma_{th}}^{\infty} \frac{1}{\sqrt{2\pi}} e^{-\gamma} e^{-\frac{\gamma_{th}}{\bar{\gamma}_{rd,n}}} d\gamma \\
& = Q(\sqrt{2\gamma}) e^{-\frac{\gamma_{th}}{\bar{\gamma}_{rd,n}}} - \sqrt{\frac{\bar{\gamma}_{rd,n}}{1+\bar{\gamma}_{rd,n}}} Q\left(\sqrt{\frac{2\gamma_{th}(1+\bar{\gamma}_{rd,n})}{\bar{\gamma}_{rd,n}}}\right) \\
& = Q(\sqrt{2\gamma}) e^{-\frac{\gamma_{th}}{\bar{\gamma}_{rd,n}}} - \sqrt{\lambda_{rd,n}} Q\left(\sqrt{\frac{2\gamma_{th}}{\lambda_{rd,n}}}\right)
\end{aligned} \tag{4.46}$$

where  $\lambda_{rd,n} = \frac{\bar{\gamma}_{rd,n}}{1+\bar{\gamma}_{rd,n}}$ . It is shown in [196] that the integration of Q-function over PDF represents the average error probability. Therefore

$$\int_0^{\infty} Q(\sqrt{2\gamma}) \frac{1}{\bar{\gamma}_{rd,n}} e^{-\frac{\gamma}{\bar{\gamma}_{rd,n}}} d\gamma = 0.5 \left( 1 - \sqrt{\frac{\bar{\gamma}_{rd,n}}{1+\bar{\gamma}_{rd,n}}} \right) \tag{4.47}$$

Substituting the results of (4.46) and (4.47) into (4.45), the result would be

$$\begin{aligned}
P_e^{\text{MC-HRP}}(n) &= 0.5 \left[ 1 - \sqrt{\frac{\bar{\gamma}_{eq,n}}{1+\bar{\gamma}_{eq,n}}} \right] - 0.5 e^{-\frac{\gamma_{th}}{\bar{\gamma}_{sr,n}}} \left[ 1 - \sqrt{\frac{\bar{\gamma}_{rd,n}}{1+\bar{\gamma}_{rd,n}}} \right] \\
&\quad - \left[ Q\left(\sqrt{2\gamma_{th}}\right) e^{-\frac{\gamma_{th}}{\bar{\gamma}_{eq,n}}} - \sqrt{\frac{\bar{\gamma}_{eq,n}}{1+\bar{\gamma}_{eq,n}}} Q\left(\sqrt{\frac{2\gamma_{th}(1+\bar{\gamma}_{eq,n})}{\bar{\gamma}_{eq,n}}}\right) \right] \\
&\quad + e^{-\frac{\gamma_{th}}{\bar{\gamma}_{sr,n}}} \left[ Q\left(\sqrt{2\gamma_{th}}\right) e^{-\frac{\gamma_{th}}{\bar{\gamma}_{rd,n}}} - \sqrt{\frac{\bar{\gamma}_{rd,n}}{1+\bar{\gamma}_{rd,n}}} Q\left(\sqrt{\frac{2\gamma_{th}(1+\bar{\gamma}_{rd,n})}{\bar{\gamma}_{rd,n}}}\right) \right] \\
&\quad + e^{-\frac{\gamma_{th}}{\bar{\gamma}_{sr,n}}} \left[ Q\left(\sqrt{2\gamma_{th}}\right) e^{-\frac{\gamma_{th}}{\bar{\gamma}_{rd,n}}} - \sqrt{\frac{\bar{\gamma}_{rd,n}}{1+\bar{\gamma}_{rd,n}}} Q\left(\sqrt{\frac{2\gamma_{th}(1+\bar{\gamma}_{rd,n})}{\bar{\gamma}_{rd,n}}}\right) \right] \\
&= 0.5 \left[ 1 - \sqrt{\lambda_{eq,n}} \right] - 0.5 e^{-\frac{\gamma_{th}}{\bar{\gamma}_{sr,n}}} \left[ 1 - \sqrt{\lambda_{rd,n}} \right] \\
&\quad - \left[ Q\left(\sqrt{2\gamma_{th}}\right) e^{-\frac{\gamma_{th}}{\bar{\gamma}_{eq,n}}} - \sqrt{\lambda_{eq,n}} Q\left(\sqrt{\frac{2\gamma_{th}}{\lambda_{eq,n}}}\right) \right] \\
&\quad + 2e^{-\frac{\gamma_{th}}{\bar{\gamma}_{sr,n}}} \left[ Q\left(\sqrt{2\gamma_{th}}\right) e^{-\frac{\gamma_{th}}{\bar{\gamma}_{rd,n}}} - \sqrt{\lambda_{rd,n}} Q\left(\sqrt{\frac{2\gamma_{th}}{\lambda_{rd,n}}}\right) \right]
\end{aligned} \tag{4.48}$$

where  $\lambda_{eq,n} = \frac{\bar{\gamma}_{eq,n}}{1+\bar{\gamma}_{eq,n}}$ . Finally, the closed form expression of the error probability of the MC-HRP can be calculated by substituting (4.48) into (4.42).

#### 4.7.1.2 MC-AHRP Scheme

The average error probability on each subcarrier at the destination can be expressed as [17]

$$P_e^{\text{AHRP}}(n) = Pr(\gamma_{sr,n} > \gamma_{th})P_e^{\text{AF}} + Pr(\gamma_{sr,n} \leq \gamma_{th})P_e^{\text{ADF}}, \quad (4.49)$$

where  $P_e^{\text{AF}}$  is the error probability of the received signal at the destination when the  $n$ th subcarrier uses an ADF protocol and can be formulated as [75, 78]

$$P_e^{\text{ADF}} = P_e(\text{nth} - \text{err})P_{\text{error}}^{\text{ADF}} + (1 - P_e(\text{nth} - \text{err}))P_{\text{succ}}^{\text{ADF}}. \quad (4.50)$$

When the sub-carrier at the relay cannot decode the received signal successfully, the destination selects the same sub-carrier from the direct link. Therefore, the probability of error and the subcarrier incorrectly detects the received signal at the relay can be given as

$$\begin{aligned} P_{\text{error}}^{\text{ADF}} &= \int_0^{\gamma_{th}} Q(\sqrt{2\gamma})f_{\gamma_n^{sd}}(\gamma | \gamma_{sr,n} \leq \gamma_{th})d\gamma \\ &= \int_0^{\infty} Q(\sqrt{2\gamma})f_{\gamma_n^{sd}}(\gamma | \gamma_{sr,n} \leq \gamma_{th})d\gamma - \int_{\gamma_{th}}^{\infty} Q(\sqrt{2\gamma})f_{\gamma_n^{sd}}(\gamma | \gamma_{sr,n} \leq \gamma_{th})d\gamma \end{aligned} \quad (4.51)$$

where  $f_{\gamma_n^{sd}}(\gamma | \gamma_{sr,n} \leq \gamma_{th})$  represents the instantaneous SNR between the source and the destination given as  $f_{\gamma_n^{sd}}(\gamma | \gamma_{sr,n} \leq \gamma_{th}) = \frac{1}{\bar{\gamma}_{sd,n}}e^{-\frac{\gamma}{\bar{\gamma}_{sd,n}}}$ . Therefore the  $P_{\text{error}}^{\text{ADF}}$  can be rewritten as

$$\begin{aligned} P_{\text{error}}^{\text{ADF}} &= \int_0^{\infty} Q(\sqrt{2\gamma})\frac{1}{\bar{\gamma}_{sd,n}}e^{-\frac{\gamma}{\bar{\gamma}_{sd,n}}}d\gamma - \int_{\gamma_{th}}^{\infty} Q(\sqrt{2\gamma})\frac{1}{\bar{\gamma}_{sd,n}}e^{-\frac{\gamma}{\bar{\gamma}_{sd,n}}}d\gamma \\ &= 0.5 \left[ 1 - \sqrt{\frac{\bar{\gamma}_{sd,n}}{1 + \bar{\gamma}_{sd,n}}} \right] - Q(\sqrt{2\gamma_{th}})e^{-\frac{\gamma_{th}}{\bar{\gamma}_{sd,n}}} \\ &\quad + \sqrt{\frac{\bar{\gamma}_{sd,n}}{1 + \bar{\gamma}_{sd,n}}} Q \left( \sqrt{\frac{2\gamma_{th}(1 + \bar{\gamma}_{sd,n})}{\bar{\gamma}_{sd,n}}} \right) \\ &= 0.5 \left[ 1 - \sqrt{\lambda_{sd,n}} \right] - Q(\sqrt{2\gamma_{th}})e^{-\frac{\gamma_{th}}{\bar{\gamma}_{sd,n}}} + \sqrt{\lambda_{sd,n}} Q \left( \sqrt{\frac{2\gamma_{th}}{\lambda_{sd,n}}} \right). \end{aligned} \quad (4.52)$$

where  $\lambda_{sd,n} = \frac{\bar{\gamma}_{sd,n}}{1+\bar{\gamma}_{sd,n}}$ . Similarly the error probability  $P_{\text{succ}}^{\text{ADF}}$  can be evaluated as

$$\begin{aligned}
P_{\text{succ}}^{\text{ADF}} &= \int_0^\infty Q(\sqrt{2\gamma}) f_{\gamma_n^{rd}}(\gamma \mid \gamma_{sr,n} \leq \gamma_{th}) d\gamma \\
&= \int_0^\infty Q(\sqrt{2\gamma}) f_{\gamma_n^{rd}}(\gamma \mid \gamma_{sr,n} \leq \gamma_{th}) d\gamma - \int_{\gamma_{th}}^\infty Q(\sqrt{2\gamma}) f_{\gamma_n^{rd}}(\gamma \mid \gamma_{sr,n} \leq \gamma_{th}) d\gamma \\
&= \int_0^\infty Q(\sqrt{2\gamma}) \frac{1}{\bar{\gamma}_{rd,n}} e^{-\frac{\gamma}{\bar{\gamma}_{rd,n}}} d\gamma - \int_{\gamma_{th}}^\infty Q(\sqrt{2\gamma}) \frac{1}{\bar{\gamma}_{rd,n}} e^{-\frac{\gamma}{\bar{\gamma}_{rd,n}}} d\gamma \\
&= 0.5 \left[ 1 - \sqrt{\frac{\bar{\gamma}_{rd,n}}{1 + \bar{\gamma}_{rd,n}}} \right] - Q(\sqrt{2\gamma_{th}}) e^{-\frac{\gamma_{th}}{\bar{\gamma}_{rd,n}}} \\
&\quad + \sqrt{\frac{\bar{\gamma}_{rd,n}}{1 + \bar{\gamma}_{rd,n}}} Q \left( \sqrt{\frac{2\gamma_{th}(1 + \bar{\gamma}_{rd,n})}{\bar{\gamma}_{rd,n}}} \right) \\
&= 0.5 \left[ 1 - \sqrt{\lambda_{rd,n}} \right] - Q(\sqrt{2\gamma_{th}}) e^{-\frac{\gamma_{th}}{\bar{\gamma}_{rd,n}}} + \sqrt{\lambda_{rd,n}} Q \left( \sqrt{\frac{2\gamma_{th}}{\lambda_{rd,n}}} \right).
\end{aligned} \tag{4.53}$$

By substituting (4.26) into (4.43) and doing the integration by part, the  $P_e(nth - err)$  can be rewritten as

$$\begin{aligned}
P_e(nth - err) &= \int_0^{\gamma_{th}} Q(\sqrt{2\gamma}) \frac{e^{-(\gamma/\bar{\gamma}_{sr,n})}}{\bar{\gamma}_{sr,n} (1 - e^{-(\gamma_{th}/\bar{\gamma}_{sr,n})})} d\gamma \\
&= \frac{1}{1 - e^{-(\gamma_{th}/\bar{\gamma}_{sr,n})}} \left( \int_0^\infty Q(\sqrt{2\gamma}) \frac{e^{-(\gamma_{th}/\bar{\gamma}_{sr,n})}}{\bar{\gamma}_{sr,n}} d\gamma - \int_{\gamma_{th}}^\infty Q(\sqrt{2\gamma}) \frac{e^{-(\gamma/\bar{\gamma}_{sr,n})}}{\bar{\gamma}_{sr,n}} d\gamma \right) \\
&= \frac{1}{1 - e^{-\frac{\gamma_{th}}{\bar{\gamma}_{sr,n}}}} \left[ 0.5 \left( 1 - \sqrt{\frac{\bar{\gamma}_{sr,n}}{1 + \bar{\gamma}_{sr,n}}} \right) - Q(\sqrt{2\gamma_{th}}) e^{-\frac{\gamma_{th}}{\bar{\gamma}_{sr,n}}} \right] \\
&\quad + \frac{1}{1 - e^{-\frac{\gamma_{th}}{\bar{\gamma}_{sr,n}}}} \left[ \sqrt{\frac{\bar{\gamma}_{sr,n}}{1 + \bar{\gamma}_{sr,n}}} Q \left( \sqrt{\frac{2\gamma_{th}(1 + \bar{\gamma}_{sr,n})}{\bar{\gamma}_{sr,n}}} \right) \right] \\
&= \frac{1}{1 - e^{-\frac{\gamma_{th}}{\bar{\gamma}_{sr,n}}}} \left[ 0.5 \left( 1 - \sqrt{\lambda_{sr,n}} \right) - Q(\sqrt{2\gamma_{th}}) e^{-\frac{\gamma_{th}}{\bar{\gamma}_{sr,n}}} + \sqrt{\lambda_{sr,n}} Q \left( \sqrt{\frac{2\gamma_{th}}{\lambda_{rd,n}}} \right) \right].
\end{aligned} \tag{4.54}$$

where  $\lambda_{sr,n} = \frac{\bar{\gamma}_{sr,n}}{1+\bar{\gamma}_{sr,n}}$ . The closed-form expression of the error probability of the  $P_e^{\text{ADF}}$  can be calculated by substituting (4.52), (4.53), and (4.54) into (4.50), and

the result is presented following.

$$\begin{aligned}
P_e^{\text{ADF}} &= \frac{1}{1 - e^{-\frac{\gamma_{th}}{\bar{\gamma}_{sr,n}}}} \left[ 0.5 \left( 1 - \sqrt{\lambda_{sr,n}} \right) - Q(\sqrt{2\gamma_{th}}) e^{-\frac{\gamma_{th}}{\bar{\gamma}_{sr,n}}} + \sqrt{\lambda_{sr,n}} Q \left( \sqrt{\frac{2\gamma_{th}}{\lambda_{rd,n}}} \right) \right] \\
&\times \left[ 0.5 \left( 1 - \sqrt{\lambda_{sd,n}} \right) - Q(\sqrt{2\gamma_{th}}) e^{-\frac{\gamma_{th}}{\bar{\gamma}_{sd,n}}} + \sqrt{\lambda_{sd,n}} Q \left( \sqrt{\frac{2\gamma_{th}}{\lambda_{sd,n}}} \right) \right] \\
&+ \left[ 1 - \frac{1}{1 - e^{-\frac{\gamma_{th}}{\bar{\gamma}_{sr,n}}}} \left( 0.5 \left( 1 - \sqrt{\lambda_{sr,n}} \right) - \frac{Q(\sqrt{2\gamma_{th}})}{e^{\frac{\gamma_{th}}{\bar{\gamma}_{sr,n}}}} + \sqrt{\lambda_{sr,n}} Q \left( \sqrt{\frac{2\gamma_{th}}{\lambda_{rd,n}}} \right) \right) \right] \\
&\times \left[ 0.5 \left[ 1 - \sqrt{\lambda_{rd,n}} \right] - Q(\sqrt{2\gamma_{th}}) e^{-\frac{\gamma_{th}}{\bar{\gamma}_{rd,n}}} + \sqrt{\lambda_{rd,n}} Q \left( \sqrt{\frac{2\gamma_{th}}{\lambda_{rd,n}}} \right) \right].
\end{aligned} \tag{4.55}$$

The PDF of the  $n$ th subcarrier consists of AF group can be expressed as

$$f_{\gamma_n^{\text{AF}}}(n \in \mathcal{GAF}) = \frac{1}{\bar{\gamma}_{eq,n}} e^{-\frac{\gamma}{\bar{\gamma}_{eq,n}}}. \tag{4.56}$$

The error probability when the  $n$ th subcarrier uses the AF scheme can be calculated after substituting (4.56) into (4.43) and doing the integration by part as

$$\begin{aligned}
P_e^{\text{AF}} &= \int_{\gamma_{th}}^{\infty} Q(\sqrt{2\gamma}) f_{\gamma_n^{\text{AF}}}(n \in \mathcal{GAF}) d\gamma \\
&= \int_{\gamma_{th}}^{\infty} Q(\sqrt{2\gamma}) \frac{1}{\bar{\gamma}_{eq,n}} e^{-\frac{\gamma}{\bar{\gamma}_{eq,n}}} d\gamma \\
&= Q(\sqrt{2\gamma_{th}}) e^{-\frac{\gamma_{th}}{\bar{\gamma}_{eq,n}}} - \sqrt{\frac{\bar{\gamma}_{eq,n}}{1 + \bar{\gamma}_{eq,n}}} Q \left( \sqrt{\frac{2\gamma_{th}(1 + \bar{\gamma}_{eq,n})}{\bar{\gamma}_{eq,n}}} \right) \\
&= Q(\sqrt{2\gamma_{th}}) e^{-\frac{\gamma_{th}}{\bar{\gamma}_{eq,n}}} - \sqrt{\lambda_{eq,n}} Q \left( \sqrt{\frac{2\gamma_{th}}{\lambda_{eq,n}}} \right).
\end{aligned} \tag{4.57}$$

Similarly procedure presented in the previous subsection can be used to solve

(4.49), the  $P_e^{\text{MC-AHRP}}(n)$  is given by

$$\begin{aligned}
& P_e^{\text{MC-AHRP}}(n) \\
&= e^{\frac{-\gamma_{th}}{\bar{\gamma}_{sr,n}}} \left[ Q(\sqrt{2\gamma_{th}}) e^{-\frac{\gamma_{th}}{\bar{\gamma}_{eq,n}}} - \sqrt{\lambda_{eq,n}} Q\left(\sqrt{\frac{2\gamma_{th}}{\lambda_{eq,n}}}\right) \right] \\
&+ \left[ 0.5 \left( 1 - \sqrt{\lambda_{sr,n}} \right) - Q(\sqrt{2\gamma_{th}}) e^{-\frac{\gamma_{th}}{\bar{\gamma}_{sr,n}}} + \sqrt{\lambda_{sr,n}} Q\left(\sqrt{\frac{2\gamma_{th}}{\lambda_{rd,n}}}\right) \right] \\
&\times \left[ 0.5 \left( 1 - \sqrt{\lambda_{sd,n}} \right) - Q(\sqrt{2\gamma_{th}}) e^{-\frac{\gamma_{th}}{\bar{\gamma}_{sd,n}}} + \sqrt{\lambda_{sd,n}} Q\left(\sqrt{\frac{2\gamma_{th}}{\lambda_{sd,n}}}\right) \right] \\
&+ \left[ 1 - e^{-\frac{\gamma_{th}}{\bar{\gamma}_{sr,n}}} - \left( 0.5 \left( 1 - \sqrt{\lambda_{sr,n}} \right) - \frac{Q(\sqrt{2\gamma_{th}})}{e^{\frac{\gamma_{th}}{\bar{\gamma}_{sr,n}}}} + \sqrt{\lambda_{sr,n}} Q\left(\sqrt{\frac{2\gamma_{th}}{\lambda_{rd,n}}}\right) \right) \right] \\
&\times \left[ 0.5 \left[ 1 - \sqrt{\lambda_{rd,n}} \right] - Q(\sqrt{2\gamma_{th}}) e^{-\frac{\gamma_{th}}{\bar{\gamma}_{rd,n}}} + \sqrt{\lambda_{rd,n}} Q\left(\sqrt{\frac{2\gamma_{th}}{\lambda_{rd,n}}}\right) \right].
\end{aligned} \tag{4.58}$$

Substituting (4.58) into (4.42), the aggregate error probability of the proposed protocol can be evaluated.

### 4.7.2 Outage Probability

In wireless communication systems an essential performance measure is outage probability. This is defined as the probability that the mutual information between the source and destination falls below a predefined threshold value  $\gamma_{th}$ .

$$P_{\text{out}} = F_{\gamma_{i,n}}(\gamma_{\text{out}}) \tag{4.59}$$

where  $F_{\gamma_{i,n}}$  is the CDF of the received SNR,  $\gamma_{\text{out}} = 2^{2r} - 1$  and  $r$  is the number of bits in each subcarrier. Since the relay retransmits the entire OFDM symbol from the source, it is in a state of outage if any subcarrier has an outage. The overall system outage probability can be expressed as in [196]

$$P_{\text{out}}^{\text{OFDM}} = 1 - \prod_{n=1}^N (1 - F_{\gamma_n}(\gamma_{\text{out}})). \tag{4.60}$$

The CDF for  $\gamma_n$  of MC-HRP scheme can be expressed as

$$P_{\text{out}}(\gamma_{\text{out}}) = \left(1 - e^{-\frac{\gamma_{\text{th}}}{\bar{\gamma}_{sr,n}}}\right) \left(1 - \frac{e^{-\frac{\gamma_{\text{out}}}{\bar{\gamma}_{sr,n}}} - e^{-\frac{\gamma_{\text{th}}}{\bar{\gamma}_{\text{out}sr,n}}}}{1 - e^{-\frac{\gamma_{\text{th}}}{\bar{\gamma}_{sr,n}}}} e^{-\frac{\gamma_{\text{out}}}{\bar{\gamma}_{rd,n}}}\right) + e^{-\frac{\gamma_{\text{th}}}{\bar{\gamma}_{sr,n}}} \left(1 - e^{-\frac{\gamma_{\text{out}}}{\bar{\gamma}_{rd,n}}}\right). \quad (4.61)$$

Similarly, the CDF of the MC-AHRP scheme can be calculated by substituting  $\gamma$  by  $\gamma_{\text{out}}$  into (4.38)

$$P_{\text{out}}(\gamma_{\text{out}}) = e^{-\frac{\gamma_{\text{th}}}{\bar{\gamma}_{sr,n}}} \left[1 - \left(1 - \frac{1 - e^{-\frac{\gamma_{\text{out}}}{\bar{\gamma}_{sr,n}}}}{e^{-\frac{\gamma_{\text{th}}}{\bar{\gamma}_{sr,n}}}}\right) e^{-\frac{\gamma_{\text{out}}}{\bar{\gamma}_{rd,n}}}\right] + \left(1 - e^{-\frac{\gamma_{\text{out}}}{\bar{\gamma}_{sr,n}}}\right) \left(1 - e^{-\frac{\gamma_{\text{out}}}{\bar{\gamma}_{sd,n}}}\right) + \left(1 - e^{-\frac{\gamma_{\text{th}}}{\bar{\gamma}_{sr,n}}}\right) \left(1 - \frac{1 - e^{-(\gamma_{\text{out}}/\bar{\gamma}_{sr,n})}}{1 - e^{-(\gamma_{\text{th}}/\bar{\gamma}_{sr,n})}}\right) \left(1 - e^{-\frac{\gamma_{\text{out}}}{\bar{\gamma}_{rd,n}}}\right). \quad (4.62)$$

By substituting (4.61) and (4.62) into (4.60), the overall outage probability for both protocols can be evaluated.

### 4.7.3 System Capacity

As mentioned in the previous section, the relay is capable of choosing different forwarding schemes for each subcarrier based on the instantaneous SNR. For the MC-HRP scheme, the  $N$  sub-carriers are divided into two groups (AF and DF) whereas for the MC-AHRP scheme, they are divided into three groups (AF, DF, and direct transmission). According to the instantaneous SNRs calculated in (4.36) and (4.12), the instantaneous capacity for each subcarrier in both schemes can be described as in [35, 108]. For the MC-HRP this gives:

$$C_n = \begin{cases} \frac{1}{2} \log\left(1 + \frac{\gamma_{sr,n} \gamma_{rd,n}}{\gamma_{sr,n} + \gamma_{rd,n} + 1}\right), & \text{if } n \in \mathcal{G}AF \\ \frac{1}{2} \log(1 + \min\{\gamma_{sr,n}, \gamma_{rd,n}\}), & \text{if } n \in \mathcal{G}DF. \end{cases} \quad (4.63)$$

and for the MC-AHRP scheme:

$$C_n = \begin{cases} \frac{1}{2} \log\left(1 + \frac{\gamma_{sr,n} \gamma_{rd,n}}{\gamma_{sr,n} + \gamma_{rd,n} + 1}\right), & \text{if } n \in \mathcal{G}AF \\ \frac{1}{2} \log(1 + \gamma_{rd,n}), & \text{if } n \in \mathcal{G}DF \\ \frac{1}{2} \log(1 + \gamma_{sd,n}), & \text{Otherwise.} \end{cases} \quad (4.64)$$

Therefore the throughput of the system using MC-HRP scheme can be written as:

$$\begin{aligned}
C_{\text{MC-HRP}} &= \sum_{n \in \mathcal{G}_{AF}} C_n + \sum_{n \in \mathcal{G}_{DF}} C_n \\
&= \frac{1}{2N} \sum_{n \in \mathcal{G}_{AF}} \log\left(1 + \frac{\gamma_{sr,n} \gamma_{rd,n}}{\gamma_{sr,n} + \gamma_{rd,n} + 1}\right) \\
&\quad + \frac{1}{2N} \sum_{n \in \mathcal{G}_{DF}} \log(1 + \min\{\gamma_{sr,n}, \gamma_{rd,n}\}),
\end{aligned} \tag{4.65}$$

and for the MC-AHRP scheme:

$$\begin{aligned}
C_{\text{MC-AHRP}} &= \sum_{n \in \mathcal{G}_{AF}} C_n + \sum_{n \in \mathcal{G}_{DF}} C_n + \sum_{n \in \mathcal{DT}} C_n \\
&= \frac{1}{2N} \sum_{n \in \mathcal{G}_{AF}} \log\left(1 + \frac{\gamma_{sr,n} \gamma_{rd,n}}{\gamma_{sr,n} + \gamma_{rd,n} + 1}\right) \\
&\quad + \frac{1}{2N} \left[ \sum_{n \in \mathcal{G}_{DF}} \log(1 + \gamma_{rd,n}) + \sum_{n \in \mathcal{DT}} \log(1 + \gamma_{sd,n}) \right].
\end{aligned} \tag{4.66}$$

Comparing (4.65) and (4.66), it can be seen that the capacity of the MC-AHRP scheme is higher than the MC-HRP due to its avoidance of the weak sub-carriers at the relay.

## 4.8 Simulation Results

In this section, the simulation and numerical results are presented to demonstrate the BEP performance of the proposed protocol and make comparisons to the conventional protocols. BPSK modulation is performed for all simulations and the path-loss exponent is assumed to be equal to 3. The channel between any two nodes in the system is modeled as quasi-static frequency-selective fading channels (pedestrian ITU-R model). A frame size of 100 symbols is used. It is assumed that the OFDM system combined with  $N = 64$  Sub-carriers and a CP length of 16. It is also assumed that perfect CSI is available at the relay and the destination.

Figures 4.3 and 4.4 show the effect of threshold value on the system performance with the performance of both schemes compared using different relay locations. From Figure 4.3, it can be observed that the MC-HRP scheme outperforms the MC-AHRP scheme when the relay is located closer to the source

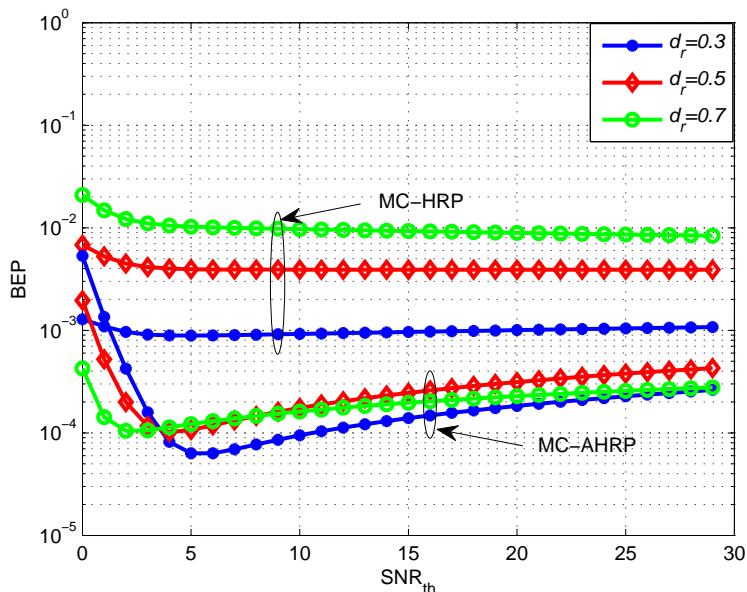


Figure 4.3: Numerical results of the error probability versus different values of SNR threshold of the MC-AHRP and the MC-HRP schemes (proposed by Li) for different values of  $d_r = \frac{d_{sr}}{d_{sd}}$  and SNR=15 dB.

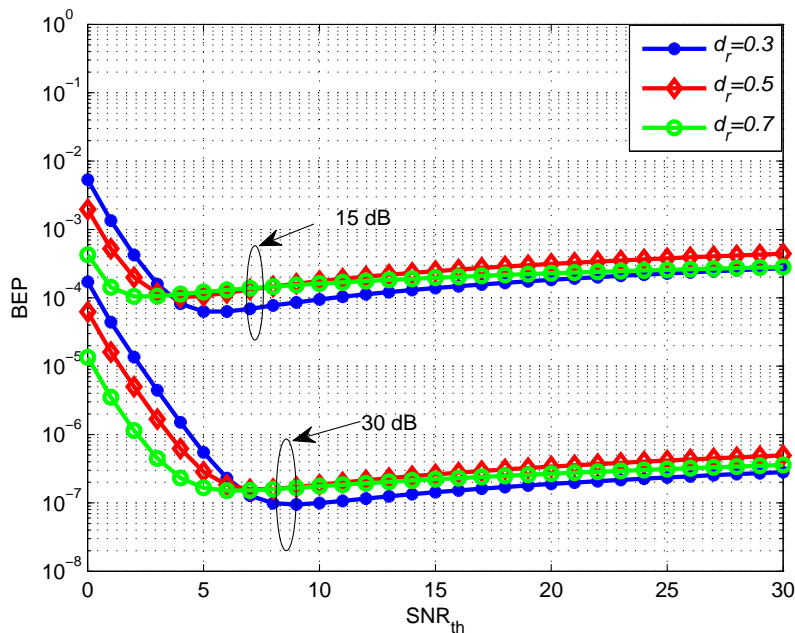


Figure 4.4: Numerical results of the error probability versus different values of SNR threshold of MC-AHRP for different values of  $d_r$  and average SNR.

Table 4.2: Optimum Threshold of the Given Range of Channel Simulation Parameters

SNR	Optimal Threshold Value		
	$d_r = 0.3$	$d_r = 0.5$	$d_r = 0.7$
10	4.3	3	1
15	5.5	4.1	2.9
20	6.6	5.2	4.2
25	7.7	6.3	5.3
30	8.8	7.4	6.4
35	9.9	8.4	7.5

for very low values of SNR threshold because most of sub-carriers in MC-AHRP perform the AF scheme. On the other hand, the MC-AHRP provides better performance than the MC-HRP scheme at medium-to-high values of SNR threshold irrespective of relay location because a high threshold value leads to an increase the sub-carriers using the ADF scheme. Figure 4.4 shows that the MC-AHRP scheme performance improves when the SNR increases regardless of the SNR threshold values. The optimal threshold is the value which can achieve the best performance (minimum bit error probability) and it depends on the received SNRs at the relay. It can be calculated by taking the first derivative of the bit error probability formula and then setting this to zero [197]. Due to difficulties to calculate the first derivative of BEP in Equation (4.58), the optimal threshold value with the chosen range of simulation parameters can be done by drawing the BEP as a function of SNR threshold with different values of SNR and calculate the minimum value of BEP. Table 4.2 shows the optimal threshold values for different relay locations. It can be seen that the threshold value increases with increasing of SNR.

For the validation, the simulation results have been evaluated and compared with the mathematical results. The simulation and mathematical results are presented to demonstrate the bit error probability (BEP) performance of the

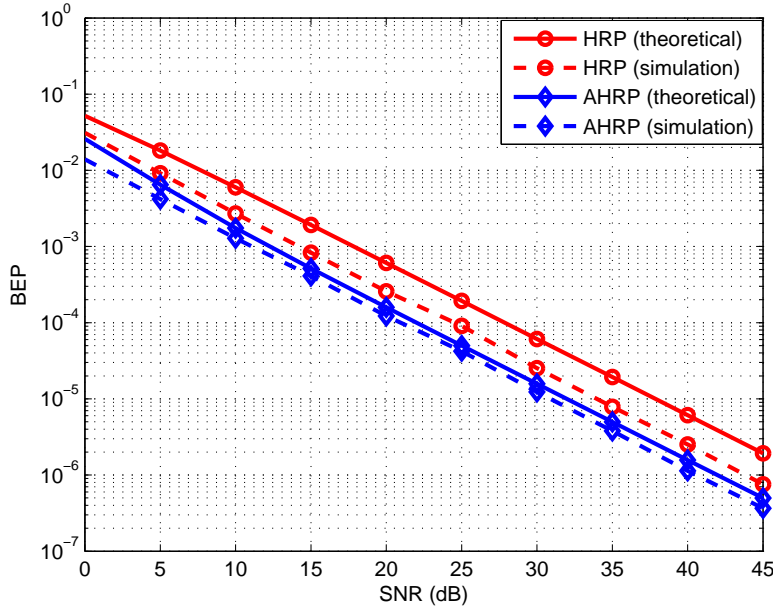


Figure 4.5: The bit error probability of the MC-AHRP and the MC-HRP schemes versus different values of SNR for  $d_r = 0.5$  and  $\gamma_{th} = 1$ , the theoretical results (solid line) and the simulation results (dashed line).

proposed protocol and make comparisons to the conventional protocols. Figure 4.5 compares the BEP performance of the MC-AHRP and MC-HRP schemes versus SNR for  $d_r = 0.5$  and  $\gamma_{th} = 1$  dB. It is observed that the MC-AHRP outperforms the MC-HRP scheme over the range of SNRs. As can be seen from the figure, MC-AHRP can achieve an approximately 4 dB gain in comparison with MC-HRP at the bit error probability of  $10^{-4}$ . It also can be seen that the performance of both protocols improves as SNR increases. One can see there is a high agreement between the mathematical modeling results and the simulation results, e.g. at the 25 SNR, the mathematical value (MC-HRP) of the BEP is  $0.5 \times 10^{-4}$  and the simulation value is  $10^{-4}$ . At the same SNR value of 25, the BEP value is  $5 \times 10^{-5}$  using MC-AHRP and the mathematical value is  $6 \times 10^{-5}$ . These differences in the values are considered to be small and can be accepted.

Figure 4.6 shows the BEP performance of the MC-AHRP protocol for various SNRs when the threshold  $\gamma_{th}$  value is set to 1 dB. The analysis considers three normalized relay locations at  $d_r = 0.3, 0.5,$  and  $0.7$ . The results demon-

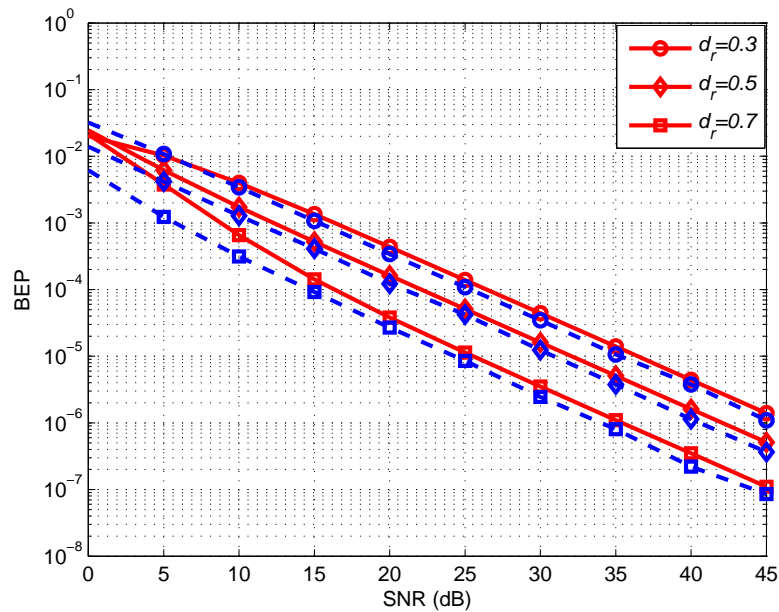


Figure 4.6: The bit error probability of the MC-AHRP scheme versus different values of SNR for different values of  $d_r$  and  $\gamma_{th} = 1$ , the theoretical results (solid line) and the simulation results (dashed line).

strate that when the relay is closer to the destination, the scheme gives a better performance. In this figure, the results of the mathematical models and the simulation are almost matched since there are no remarkable differences in the results especially at high values of SNR. This can validate the developed mathematical model. It can also be observed for both figures that there are difference in simulation results when compared with the numerical results for low to moderate SNR values. This is due to the approximation of the numerical results.

Figure 4.7 compares the average BEP performance of both schemes. It presents the performance results for  $\gamma_{th} = 1, 2$ , and 3 dB when the relay is located centrally between the source and the destination. The results demonstrate that the MC-AHRP scheme outperforms the MC-HRP scheme irrespective of the SNR threshold value. The MC-HRP performance is relatively unchanged for different threshold values over the range of SNRs. On the other hand, the MC-AHRP performance decreased at lower SNRs when the threshold value increased while giving better performance at medium-to-high SNR values. The reason behind this

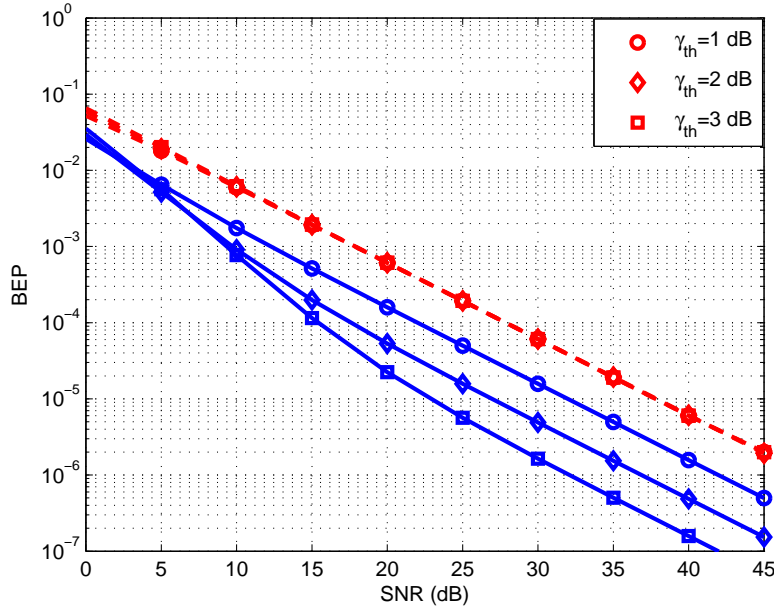


Figure 4.7: The bit error probability of the MC-AHRP (solid line) and the MC-HRP (dashed line) schemes versus different values of SNR for different values of  $\gamma_{th}$  and  $d_r = 0.5$ .

is that when the threshold value increases, it leads to an increased probability of sub-carriers performing perfect DF (decoding the received signal correctly) at high SNR, while at low SNR, most of sub-carriers perform direct transmission.

Figure 4.8 compares the BEP performance for different values of SNR and various  $d_r$ . The performance was significantly improved when the SNR value increased across the range of distance. The results demonstrate that the best location for the relay changed according to the SNR value with optimal placement being near the destination for high SNR values. The main reasons for this are a reduction in the corrupted signal at the AF sub-carriers, and an increase in the perfect DF sub-carriers leading to reduction in the direct sub-carriers.

Figures 4.9 and 4.10 show that the numerical results of outage probability of the MC-AHRP scheme outperform the MC-HRP scheme regardless of relay location or SNR threshold value. The results also demonstrate that the performance of the MC-AHRP scheme improves when the relay location is closer to the destination and when the threshold SNR is increased. The diversity gain of both

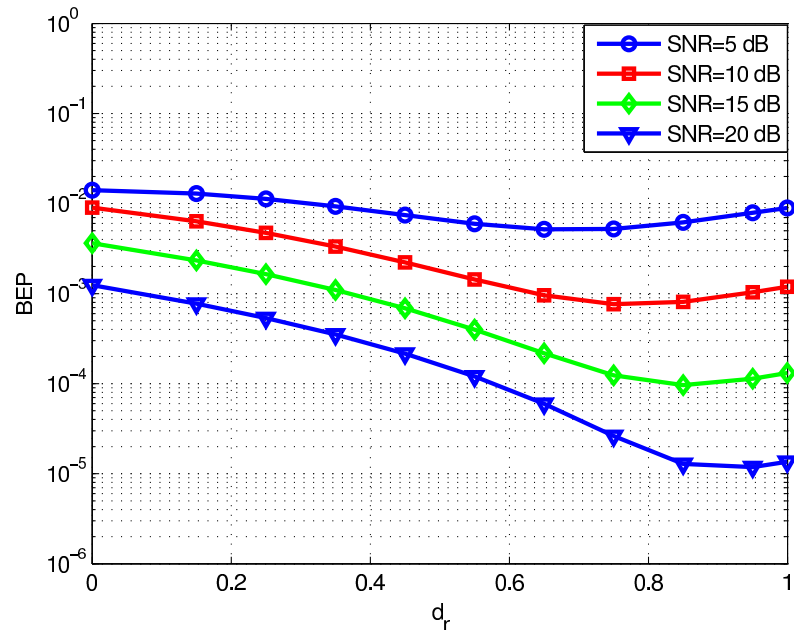


Figure 4.8: Numerical results of the error probability of MC-AHRP versus different values of SNR for different values of  $d_r$  and  $\gamma_{th} = 1$ dB.

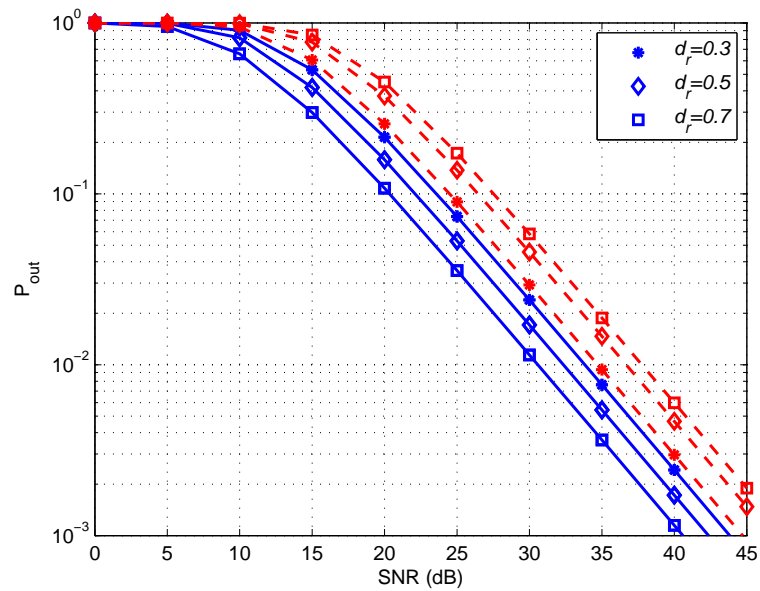


Figure 4.9: Outage probability of the MC-AHRP (solid line) and the MC-HRP (dashed line) schemes versus SNR for both schemes for different values of  $d_r$  with  $\gamma_{th} = 2$ dB.

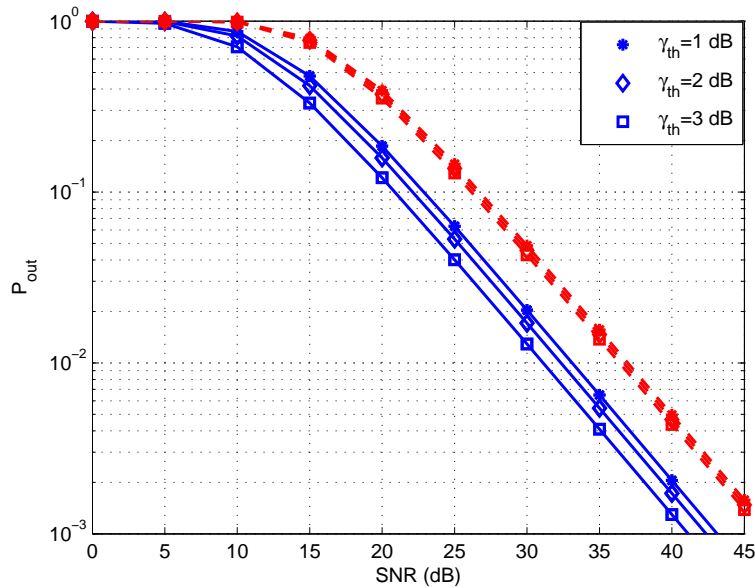


Figure 4.10: Outage probability of the MC-AHRP (solid line) and the MC-HRP (dashed line) schemes versus SNR for both schemes for different values of SNR threshold with  $d_r = 0.5$ .

schemes is equal to one due to the single relay being used in the system.

Figure 4.11 plots the capacity performance (in bps/Hz) of various protocols over a range of SNRs when the relay position is close to the source (relative distance  $d_r = 0.3$ ). In this instance, the power is chosen to be  $P_t = 5$  dB and is uniformly distributed between the source and relay nodes ( $P_s = P_r$ ). Additionally, the distance between the source and relay nodes is normalized by the source to destination distance (i.e.,  $d_r = d_{sr}/d_{rd}$ ). Figure 4.11 shows that adaptive bit and power allocation results in a capacity gain of approximately 0.2 bps/Hz compared with uniform rate and power allocation. After performing the sub-carrier permutation the capacity gain is again improved and it can be observed that ABPA with SP yields the best capacity performance.

In order to evaluate the effects of relay location on the system capacity performance, comparisons can be made of the proposed protocol at various relative distances  $d_r$  for different values of  $\gamma_{th}$  as shown in Figure 4.12, and for different protocols as shown in in Figure 4.13.

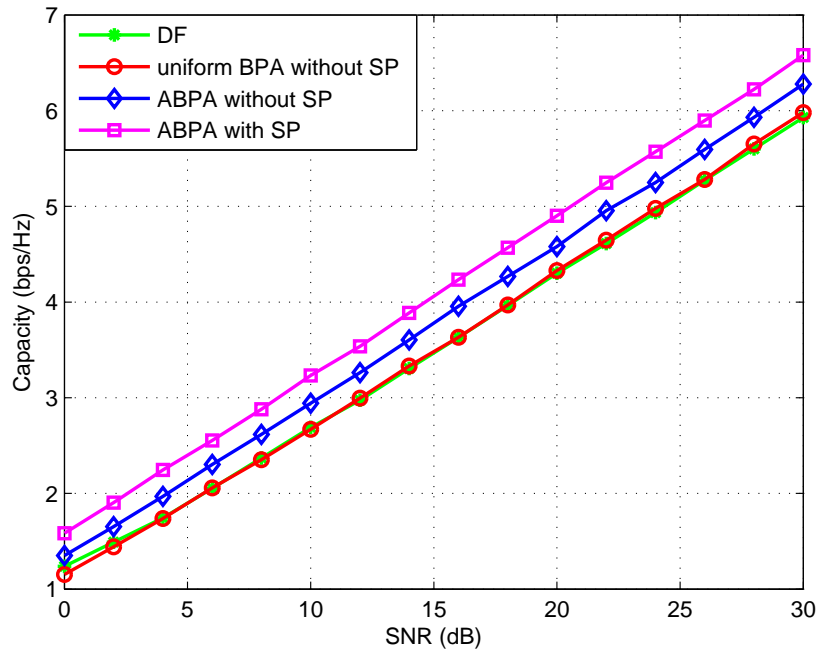


Figure 4.11: Capacity performance versus different values of SNR with and without RA and SP for  $d_r=0.3$ .

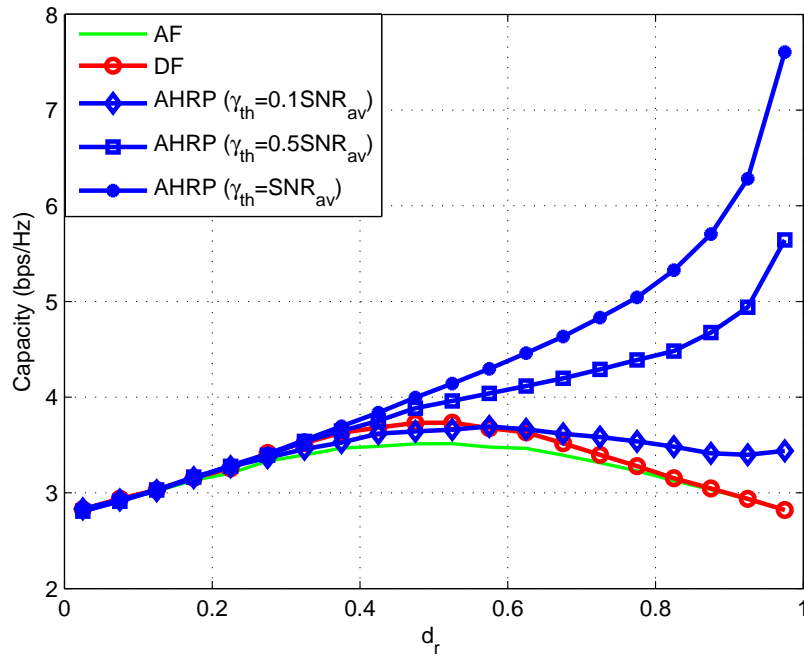


Figure 4.12: Capacity performance versus relative distance  $d_r = d_{sr}/d_{sd}$  for different values of  $\gamma_{th}$  and SNR=15 dB.

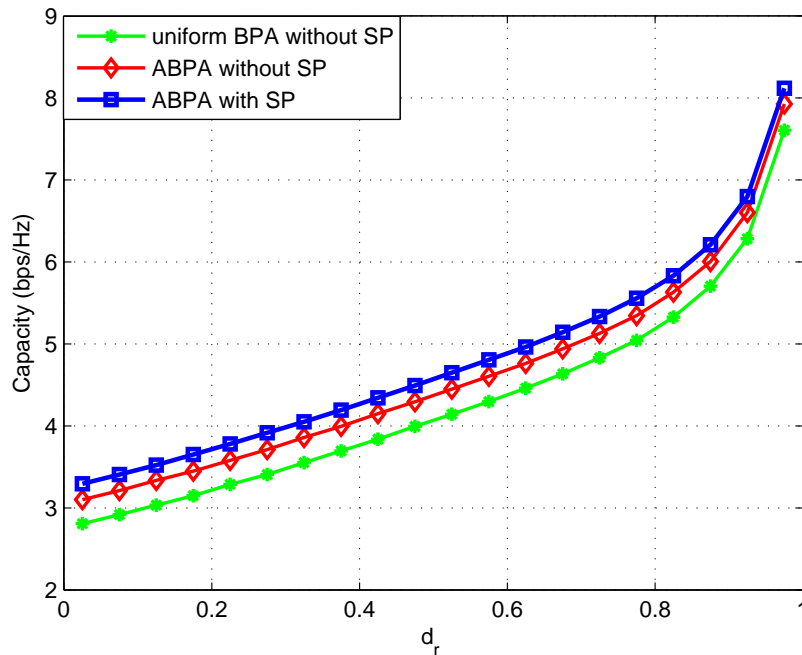


Figure 4.13: Capacity performance of MC-AHRP protocol versus relative distance  $d_r = d_{sr}/d_{sd}$  with and without RA and SP for SNR=15 dB.

In Figure 4.12, the results show that the proposed scheme with uniform bit and power allocation provides better performance than the DF scheme at middle and high SNR range while it exhibits worse performance at low SNR values. Of note is that when the threshold value is increased, the capacity also increases again rapidly, especially when the relay is close to the destination.

From Figure 4.13, it can be seen that there is an increased system throughput with respect to relay locations when performing ABPA and SP, and that the capacity of each protocol increases significantly with  $d_r$ . This is because the sub-carriers in the AF group retransmit the received signal with the same number of bits as assigned by the source and should consequently be allocated the appropriate amount of power corresponding to the number of bits. In the same context, the channel power gain for the second hop when the relay is close to the destination is satisfied. This then reduces the power allocation required for each sub-carrier in the AF group. As a result, the amount of power that can be assigned to the DF group is increased, hence improving system capacity.

Subcarrier permutation attempts to match each sub-carrier in the first hop with a sub-carrier in the second hop which has a similar channel power gain. Since the AF group is composed of sub-carriers with the highest channel power gain, low power can be correspondingly assigned to the AF group, and the power assigned to the DF group will be increased. As a result the system performance achieves significant capacity improvement as demonstrated in Figures 4.11, 4.12 and 4.13, due to appropriate power assigned increasingly to the DF group with lower optimized power gain distributed to the AF group.

## 4.9 Conclusion

This chapter proposed a new scheme of HRP in conjunction with the OFDM technique based on per-subcarrier selection over frequency-selective channels. The performance of MC-HRP was established by extending the conventional HRP protocols from a single carrier to a multi-carrier system. Bit error probability, outage probability, and capacity performances have been analyzed and compared for both schemes considering multiple relay locations. It has been shown that the MC-AHRP scheme yields a significant improvement in performance compared with MC-HRP over the range of SNR values, particularly when the relay is located closer to the destination and at high SNR values. The results show that the proposed protocol can achieve performance very close to the perfect DF scheme (error-free delivery) with a reasonable computational complexity. Results demonstrate that the system performance can be further improved by applying adaptive bit and power allocation and sub-carrier pairing.



# Chapter 5

## Space-Frequency Coding with OFDM-HRP Systems

### 5.1 Introduction

Multipath fading is one of the major limitations in a wireless communication systems. Diversity is an efficient technique to overcome the detrimental effects of multipath fading at the receiver [1]. Diversity is achieved by providing the receiver with several copies of the original signal through independent links. By doing so, the probability that all the replicas arriving at the receiver have experienced severe fading simultaneously is reduced significantly [4]. There are several kinds of diversity includes; spatial, temporal and frequency. Spatial diversity has received great attention due to it being simplest to implement in multiple antennae devices. However, in small devices (e.g. mobile, ad hoc and sensor) it is difficult to implement multiple antennae due to cost and hardware limitations.

Cooperative diversity has been proposed recently to exploit the benefits of spatial diversity by collaborating and sharing resources of multiple single antenna terminals (relays) [4, 55]. This can drastically increase the cooperative diversity gains but at the expense of a decrease in the spectral efficiency as in an orthogonal channel implementation only one relay is allowed to transmit in each time slot. It is well-known as “repetition-based” [4]. Relay selection [14, 19], and DSFC [159] techniques have emerged as promising solutions to overcome this problem. Re-

lay selection can reap the potential benefits of multiple-relay systems with less complexity. In a relay selection scheme only a single relay forwards the source signal while in a DSFC protocol all relay nodes broadcast the source signal to the destination simultaneously. In addition, OFDM technique has been proven to provide multipath and frequency diversity and can enhance the system performance when the power allocation employing optimally. For OFDM cooperative systems, sub-carrier permutation can be maximized the system capacity if the sub-carriers of the two hops are coupled according to their channel gain.

Meanwhile, cooperative OFDM systems have received considerable attention due to their ability to mitigate the impairment of multipath fading in frequency-selective channels. DSFC combined with OFDM modulation was investigated in [198] to explore multipath diversity and cooperative diversity for perfect DF protocol whereas in [163], both erroneous DF and AF protocols were considered. There have been some recent efforts on implementations of DSFC with AF or DF schemes. In the course of the literature review, published work on the implementation of DSFC in HRP over frequency-selective channels was not discovered. The concept seems worthy and could offer further improvement in system performance with low complexity because the DSFC implements at the source and the DF relay.

This chapter focuses on distributed space frequency codes with HRP over frequency-selective channels. In the context of the HRP, the relays are classified into two groups based on how the relays process the received signal from the source. The relays that have the ability to decode the received signal correctly are included in the DF group and the rest are included in the AF group. Thereafter, the destination selects the best relay with maximum SNR from each group independently. Then each couple of relays are combined in one cluster to reduce the implementation complexity of DSFC. Power allocation can be optimized with and then without sub-carrier permutation between the source and relay nodes to further improve system capacity. The optimum problem is divided into two sub-optimal problems. The first one is to optimize the power allocation between the source and relay nodes under a sum power constraint. Then the relay power is

optimized for the selected relay nodes according to the channel power gain of the second time slot.

To summarize the contributions of this chapter:

- Propose an OFDM and DSFC based cooperative system using hybrid relay protocols over frequency-selective fading channels, where full rate transmission and full spatial diversity are achieved.
- Power allocation and sub-carrier pairing are investigated under global power constraint in order to further improve system performance.
- The system performance for the different schemes concatenated with the proposed protocol are evaluated, and the comparison results are summarized.

The rest of this chapter is organized as follows. Motivation and related works are discussed in Section 5.2. The system model is discussed in section 5.3. Section 5.4 is addressed the power allocation and sub-carrier pairing algorithms. Simulation results are presented in section 5.5. Section 5.6 concludes the chapter.

## 5.2 Related Work

The growing popularity of both cooperative communication and OFDM systems have created the requirement for an efficient technique to reap the benefits of temporal, spatial and frequency components together. Space-time coding schemes can achieve full spatial diversity for MIMO systems [1], [2] and for cooperative communications [199]. This is known as distributed STC [14], due to the fact that the received signals simultaneously arrive at the destination. This technique is efficient when used over flat fading channels. However, as mentioned before, broadband communication systems suffer from severe multi-path fading and delay spread, which destroy the orthogonality when its applied with STC. Therefore, the OFDM technique has been adopted as an effective technique to overcome this

issue by transforming frequency-selective fading channel into multiple flat fading sub-channels [148].

There has been extensive research efforts on STC combined with OFDM system to realize the benefits of coding and modulation [148, 150–153]. In these schemes, the coding has been done in the time domain while in [150, 156] the frequency domain was considered which refers to space-frequency code. The authors showed that the space-frequency code can provide full spatial and frequency diversity.

Hakam et al. [159] proposed DSTC concatenated with OFDM and then derived the symbol error probability for an AF single relay protocol. They considered two consecutive blocks. The source broadcasts the first block to the relay only in the first time slot. Then the source sends the second block and the relay retransmits the first block to the destination simultaneously in the second time slot. The same procedure was repeated for the third and fourth time slots but the source transmits the complex conjugate of the first and second blocks respectively. As a result the Alamouti code can be performed at the destination, resulting in full cooperative diversity. However, when there are obstacles between the transmitter and receiver nodes, the receiver is not necessarily able to receive the source signal. The authors in [198] considered perfect DF protocol with multi-relay nodes system where all nodes participate in second time slot. They performed SFC at the relay nodes by dividing the OFDM block into several sub-blocks. Then each sub-block was encoded independently.

In wireless fading channels, however it is difficult to have multiple relay nodes decode the received signal correctly due to selectivity in the channel. Therefore, Karim et al. in [163] designed a distributed space frequency code for both DF and AF protocols for synchronous systems. In the DF scheme, the relays that have correctly decoded the received information will collaborate to design DSFC and the rest of relays remain silent. The AF protocol divides the source data into sub-blocks, each of which is transmitted by individual relay with different encoder. The results show that full diversity can be achieved, but comes at the expense of high complexity.

In [200], the AF protocol is applied in a multiple relays system and a circular shift is employed at the relays. The symbol error rate was derived over frequency-selective channels. The authors in [165] propose a DSFC scheme to achieve both spatial and multi-path diversity based on erroneous DF relay protocols. Most of the previous work on cooperative SFC-OFDM systems has considered either AF or DF protocols. Implementation of DSFC at the AF relay node adds complexity to the relay while a perfect DF relay may not always be possible in the network.

In frequency-selective channels, the frequency response of the channel can drastically affect the bit error probability due to some sub-carriers experiencing deep fade. Power allocation algorithms has been investigated as an potential approach to overcome shortcoming in the system performance where more bits with less power are allocated in sub-carriers with a larger channel gain, and vice versa. It was initially investigated in single-hop OFDM systems [27, 201], however it has recently received much attention in cooperative OFDM systems [36, 107, 110, 183, 202] due to its ability to provide multi-path diversity, offering substantial gains to system performance. The optimal power allocation for AF single relay scheme was investigated in [117] where an aggregate power constraint was imposed. The water-filling algorithm was adopted as an optimal solution for power allocation which can result in a fractional number of bits/symbol. As a result, the encoder and decoder complexity will be increased. To reduce the complexity while maintaining the same performance, the number of bits can be forced to 0, 1, 2, 4 or 8 depending on the SNR and target BER [184]. In addition, it can reduce the overhead signals during the channel estimation stage.

In OFDM relaying systems, the fading gains for different channels are mutually independent, so a sub-carrier experiencing deep fading during the first time interval may not be in deep fade in the second time interval. By exploiting this context the sub-carrier permutation can further enhance the system performance [117, 136, 185]. The efficient and simplest method to implement SP is by ordering the sub-carriers in both hops in descending order [121, 203] or ascending order [204]. Then the strongest sub-carrier in the first hop matched with best sub-carrier in the second hop and so and so for the rest of sub-carriers. In addition,

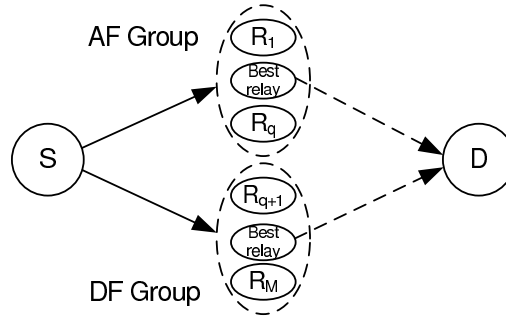


Figure 5.1: Cooperative system architecture

joint power allocation and sub-carrier permutation can reap the benefits of both techniques and then obtain a substantial improvement in system performance.

### 5.3 System Model

The DSF-coded cooperative OFDM system shown in Figure 5.1, consists of one source, one destination and  $M$  relay nodes  $R_i (i = 1, 2, \dots, M)$ . All the nodes are equipped with a single antenna and operate in half-duplex mode. Therefore, two time slots are required to transmit the information from the source to the destination. It is assumed that a direct link between the source and destination is not available. This configuration has been reported previously in [185, 205] where the destination is unable to receive the original signal directly from the source due to substantial obstacles or the sizeable distance between both terminal nodes. The relays are divided into two groups such that any relay which can correctly decode the received signal are included in the DF group and the rest are included in the AF group. In practical, the source appended the transmitted information with cyclic redundancy check code to ensure the code word is able to decoded at the relay or not. The relay selection is done at the destination when it takes into consideration the instantaneous SNR over all sub-carriers for all relay nodes. Then it chooses the relay with highest SNR from each group.

The channel is assumed to be quasi-static frequency-selective fading with  $L$  independent delay paths. The time domain impulse response of the channel between any pair of nodes was given in (4.1). The space-frequency code is implemented

at the source and the selected relays as:

- **Implementation at the source**

A stream of information bits is first mapped where any linear modulation can be implemented (e.g binary phase shift keying (BPSK) modulation), and divided into  $K$  blocks, where each block has  $N$  symbols. Then each block is divided into sub-blocks where each sub-block consists of  $b$  sub-carriers where  $b$  is the number of selected relay nodes. The  $k$ th block of data can be denoted by  $\mathbf{X}_k(n) = [X_k(0), X_k(1), \dots, X_k(N-1)]$ , where  $N$  is the number of OFDM sub-carriers. The information sequence of the  $k$ th block is encoded at the source by  $\mathbf{S}_k(n) = [S_k(bn), \dots, S_k(bn+b-1)]^T$   $n = 0, \dots, \frac{N}{b}$ , where  $(\cdot)^T$  denotes the transpose operation. For a single cluster ( $b = 2$ ), the encoded vector can be represented as  $S_k(n) = X_k(n)$ , if  $n$  is even,  $S_k(n) = -X_k^*(n)$  if  $n$  is odd,  $n = 0, \dots, N-1$ ,  $k = 1, \dots, K$ , where  $(\cdot)^*$  denotes complex conjugate. Then each block is fed through the serial to parallel convertor and into the  $N$ -point inverse fast Fourier transform (IFFT) and appended with a cyclic prefix (CP). The length of the CP must be longer than the channel delay spread to eliminate inter-symbol interference (ISI).

- **Implementation at the Relay Nodes**

The OFDM symbols are transmitted to the relay nodes in the first time slot. Therefore, the received signal in the frequency domain at the  $i$ th relay node can be written as

$$Y_{s,r_i,n} = \sqrt{P_{s,n}} H_{s,r_i,n} S_n + W_{r_i,n} \quad (5.1)$$

where  $P_{s,n}$  and  $S_n$  are the source transmission power, which is distributed uniformly over the sub-carriers, and the data symbol for the  $n$ th subcarrier in frequency domain, respectively.  $W_{r_i,n}$  represents the additive white Gaussian noise for the  $n$ th subcarrier of  $i$ th relay with zero-mean and unit variance. The variance of noise is assumed to be identical for all sub-carriers and relay nodes in the system. The channel coefficients are supposed to be constant for two consecutive OFDM symbol intervals. The relays are classified into two groups, referred to as the AF and DF relay groups. The relays that can decode the received signal correctly are included in the DF group and the rest are included in the AF group.

Table 5.1: Transmission sequence for each relay node for single cluster

Time	AF Relay	DF Relay
t	$\beta_n Y_{1,k}(n)$	$-S_{1,k}^*(n+1)$
t+T	$\beta_n Y_{1,k}(n+1)$	$S_{1,k}^*(n)$

- **AF Group**

The AF group consists of all the relays which are unable to decode the received signal correctly. The AF relays will simply amplify the received noisy signal from the source by a factor of  $\beta_i$  is defined in (3.2) and forward it to the destination. Since the variance of  $w_{r_i}(n)$  between the source and relay nodes is unity, the mean power of the received signal at the relay nodes is  $P_s + 1$ . The transmitted signal from the AF relay in the second time slot can be written as

$$S_{r_i,n}(k) = \sqrt{P_{r_i,n}} \beta_{i,n} Y_{s,r_i,n}(k), i \in 1, \dots, q \quad (5.2)$$

where  $q$  is the number of relay nodes in the AF group and  $P_{r_i,n}$  is the transmitted power from the  $i$ th relay for the  $n$ th sub-carrier.

- **DF Group**

The DF group consists of all the relays with error-free decoding. A selected relay will process a few simple steps of the received signal before forwarding it to the destination. First of all, the CP is discarded from the received OFDM symbol to eliminate the ISI. After conversion to the frequency domain by the  $N$ -point FFT, the signal is decoded to obtain the original data and the  $N$  data symbols are coded as follows

$$\begin{aligned} S_{2,k}(n) &= -S_{1,k}^*(n+1) = X_{1,k}(n+1) \\ S_{2,k}(n+1) &= S_{1,k}^*(n) = X_{1,k}^*(n) \quad n = 0, \dots, N-1 \end{aligned} \quad (5.3)$$

where the subscripts 1 and 2 denote the first and second hop respectively. Next, the coded vector,  $S^{DF}(k) = [S_{2,bn}(k), \dots, S_{2,bn+b-1}(k)]^T$   $n = 0, \dots, \frac{N}{b} - 1$  is modulated by the  $N$ -point IFFT and preceded with proper CP.

The destination has perfect knowledge of all parameters of links in the system and this can be estimated by sending training sequences. Then, the relay that

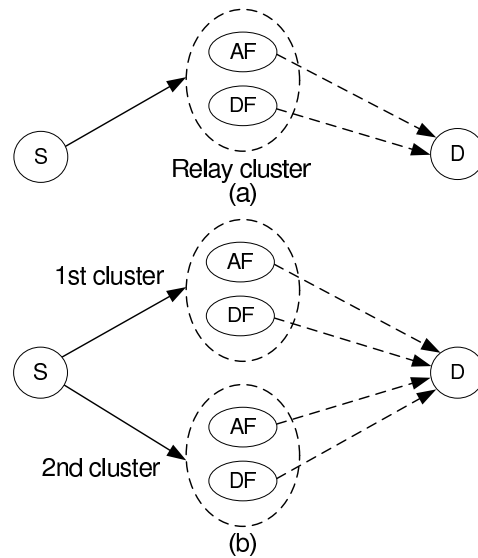


Figure 5.2: System model for the distributed Alamouti code with: a) 2 relay nodes and b) 4 relay nodes.

maximizes the destination SNR will be selected from the relays for each of the AF and DF groups as proposed in [94]. Then the selected relay nodes are divided into clusters with each one having a pair of relay nodes as presented in [206].

- **DSFC with Single Cluster**

As mentioned above, a single cluster consists of AF and DF relays as shown in Figure 5.2 a. Then the relays rearrange the received signal from the source according to the Alamouti code. The AF relay amplifies the received signal as in (4.2) and the DF relay retransmits the signal as in (5.1). The transmitted signals from both relays in relaying phase are illustrated in Table (5.1). The equivalent channel matrix for the two successive symbols duration can be written as [207,208]

$$H = H_{12} = \begin{bmatrix} h_1 & h_2 \\ -h_2^* & h_1^* \end{bmatrix}$$

where  $h_1$  and  $h_2$  represent the the equivalent channel of the AF and DF relay nodes respectively.

- **DSFC with Multiple Cluster**

In this scheme, all the selected relays are broken up into clusters where each cluster has two relays as described for DSFC with a single cluster. The system

Table 5.2: Transmission sequence for each relay node for two clusters

Time	Relay Cluster 1		Relay Cluster 2	
	AF Relay	DF Relay	AF Relay	DF Relay
t	$\beta_n Y_{1,k}(n)$	$-S_{1,k}^*(n+1)$	-	-
t+T	$\beta_n Y_{1,k}(n+1)$	$S_{1,k}^*(n)$	-	-
t+2T	-	-	$\beta_n Y_{1,k}(n+2)$	$-S_{1,k}^*(n+3)$
t+3T	-	-	$\beta_n Y_{1,k}(n+3)$	$S_{1,k}^*(n+2)$

model is shown in Figure 5.2 b where two clusters are considered. In this case  $b$  is set to be 4 and the encoded sequence at the source can be represented as

$$S_{1,k}(n) = \begin{cases} X_k(n), & \text{for } n = 0, 4, \dots, N-4 \\ -X_k^*(n), & \text{for } n = 1, 5, \dots, N-3 \\ X_k(n), & \text{for } n = 2, 6, \dots, N-2 \\ -X_k^*(n), & \text{for } n = 3, 7, \dots, N-1 \end{cases} \quad (5.4)$$

As for the single cluster, Table (5.2) illustrates the transmitted signals for all relay in the relaying phase.

In the second time slot, both relay nodes broadcast their information to the destination simultaneously. Therefore, the destination receives the combined signals from the relays. The equivalent channel matrix for the four successive symbols duration can be expressed as [207, 208]

$$H = \begin{bmatrix} H_{12} & 0 \\ 0 & H_{34} \end{bmatrix}$$

where  $H_{12}$  is the equivalent channel of the first cluster given above and  $H_{23}$  is the equivalent channel of the second cluster which consists of second AF and DF relay nodes.

#### • Implementation at the Destination Node

At the destination, perfect time and frequency synchronization for each hop are assumed, and perfect channel state information (CSI) is known. Since the adaptation process is based on a subband-by-subband basis, the power channel

gain of the  $b$  adjacent sub-carriers are the same. The destination evaluates the instantaneous SNR of all sub-carriers in the system. The instantaneous SNR received from both groups can be given as

$$\gamma_n = \begin{cases} \frac{\gamma_{sr_i,n}\gamma_{r_i,d,n}}{\gamma_{sr_i,n}+\gamma_{r_i,d,n}+1} = \frac{P_{s,n}P_{r_i,n}^{AF}\alpha_{i,n}\mu_{i,n}}{P_{s,n}\alpha_{i,n}+P_{r_i,n}^{AF}\mu_{i,n}+1}, & \text{if } i \in AF \\ \gamma_{r_j,d,n} = P_{r_j,n}^{DF}\nu_{j,n}, & \text{if } j \in DF \end{cases} \quad (5.5)$$

where  $\alpha_{i,n} = \frac{|h_{sr_i,n}|^2}{\Gamma\sigma^2}$ ,  $\mu_{i,n} = \frac{|h_{r_i,d,n}|^2}{\Gamma\sigma^2}$  and  $\nu_{j,n} = \frac{|h_{r_j,d,n}|^2}{\Gamma\sigma^2}$ .  $\Gamma$  is the SNR gap which is defined in (4.39).

Thereafter, the destination selects the relay from each group which has the highest SNR. This process is completed before the communication phase. The destination employs the MRC technique to enhance the overall received SNR. The received signal from the selected relays is taken and the CP discarding then the received signal is fed into the DFT modulator. The received signal of the  $(bn, \dots, bn+b-1)$  sub-carriers in the frequency domain at the destination can be expressed as

$$\begin{aligned} Y_{d,2n} &= H_{r_i,d,2n}^{AF}\beta_{2n}Y_{1,2n} + H_{r_i,d,2n}^{DF}S_{2n}^{DF} + W_{d,2n} \\ &= H_{r_i,d,2n}^{AF}(\sqrt{P_{s,r_i}}\beta_{2n}H_{s,r_i}^{AF}S_{2n}^{AF} + W_{r_i,2n}) + H_{r_i,d,2n}^{DF}S_{2n}^{DF} + W_{d,2n} \\ &= \sqrt{\frac{P_{s,r_i,2n}P_{r_i,d,2n}}{P_{s,r_i,2n}+1}}H_{2n}^{AF}S_{2n}^{AF} + H_{2n}^{DF}S_{2n}^{DF} + W_{2n} \end{aligned} \quad (5.6)$$

$$\begin{aligned} Y_{d,2n+1} &= H_{r_i,d,2n+1}^{AF}\beta_{2n+1}Y_{1,2n+1} + H_{r_i,d,2n+1}^{DF}S_{2n+1}^{DF} + W_{d,2n+1} \\ &= H_{r_i,d,2n+1}^{AF}(\sqrt{P_{s,r_i}}\beta_{2n+1}H_{s,r_i}^{AF}S_{2n+1}^{AF} + W_{r_i,2n+1}) + H_{r_i,d,2n+1}^{DF}S_{2n+1}^{DF} + W_{d,2n+1} \\ &= \sqrt{\frac{P_{s,r_i,2n+1}P_{r_i,d,2n+1}}{P_{s,r_i,2n+1}+1}}H_{2n+1}^{AF}S_{2n+1}^{AF} + H_{2n+1}^{DF}S_{2n+1}^{DF} + W_{2n+1} \end{aligned} \quad (5.7)$$

where  $W_{2n} = \sqrt{\frac{P_{r_i,d,2n}}{P_{s,r_i,2n+1}}}W_{r_i,2n} + W_{d,2n}$  and  $W_{2n+1} = \sqrt{\frac{P_{r_i,d,2n+1}}{P_{s,r_i,2n+1+1}}}W_{r_i,2n+1} + W_{d,2n+1}$ ,  $H_n^{AF} = H_{s,r_i,n}^{AF}H_{r_i,d,n}^{AF}$  and  $H_{DF} = H_{r_i,d,n}^{DF}$ .

By substituting the values of  $S_{2n}^{AF}$ ,  $S_{2n+1}^{AF}$ ,  $S_{2n}^{DF}$  and  $S_{2n+1}^{DF}$  into (5.6) and (5.7), then (5.6) and (5.7) can be rewritten in the following Alamouti code form on each

two adjacent sub-carriers in  $k$  block.

$$\begin{bmatrix} Y_{d,2n} \\ Y_{d,2n+1} \end{bmatrix} = \begin{bmatrix} \lambda X_{2n} & X_{2n+1} \\ -\lambda X_{2n+1}^* & X_{2n}^* \end{bmatrix} \begin{bmatrix} H_{2n}^{AF} & H_{2n+1}^{AF} \\ H_{2n}^{DF} & H_{2n+1}^{DF} \end{bmatrix} + \begin{bmatrix} W_{2n} \\ W_{2n+1} \end{bmatrix}$$

where  $\lambda = \sqrt{\frac{P_{s,r_i,2n+1}P_{r_i,d,2n+1}}{P_{s,r_i,2n+1}+1}}$ .

Similarly for two clusters shown in Figure 5.3a. The received signal at the destination for four consecutive sub-carriers can be expressed as

$$\begin{aligned} Y_{d,2n} &= \lambda H_{2n}^{AF} S_{2n}^{AF} + H_{2n}^{DF} S_{2n}^{DF} + W_{2n} \\ Y_{d,2n+1} &= \lambda H_{2n+1}^{AF} S_{2n+1}^{AF} + H_{2n+1}^{DF} S_{2n+1}^{DF} + W_{2n+1} \\ Y_{d,2n+2} &= \lambda H_{2n+2}^{AF} S_{2n+2}^{AF} + H_{2n+2}^{DF} S_{2n+2}^{DF} + W_{2n+2} \\ Y_{d,2n+3} &= \lambda H_{2n+3}^{AF} S_{2n+3}^{AF} + H_{2n+3}^{DF} S_{2n+3}^{DF} + W_{2n+3} \end{aligned} \quad (5.8)$$

$$\begin{bmatrix} Y_{d,1} \\ Y_{d,2} \\ Y_{d,3} \\ Y_{d,4} \end{bmatrix} = \begin{bmatrix} \lambda X_1 & X_2 & 0 & 0 \\ -\lambda X_2^* & X_1^* & 0 & 0 \\ 0 & 0 & \lambda X_3 & X_4 \\ 0 & 0 & -\lambda X_4^* & X_3^* \end{bmatrix} \begin{bmatrix} H_1^{AF} & H_2^{AF} & 0 & 0 \\ H_1^{DF} & H_2^{DF} & 0 & 0 \\ 0 & 0 & H_3^{AF} & H_4^{AF} \\ 0 & 0 & H_3^{DF} & H_4^{DF} \end{bmatrix} + \begin{bmatrix} W_1 \\ W_2 \\ W_3 \\ W_4 \end{bmatrix}$$

The channel coefficients for any adjacent sub-carriers are assumed to be approximately constant. The estimate vector at the SF decoder can be written as [1]

$$\begin{aligned} \hat{X}_{2n} &= (H_{2n}^{AF})^* Y_{r_i,d,2n} + H_{2n}^{DF} Y_{r_i,d,2n+1} \\ \hat{X}_{2n+1} &= (H_{2n}^{DF})^* Y_{r_i,d,2n} - H_{2n}^{AF} Y_{r_i,d,2n+1}. \end{aligned} \quad (5.9)$$

Substituting (5.6) and (5.7) into (5.9), then the estimate vector can be rewritten

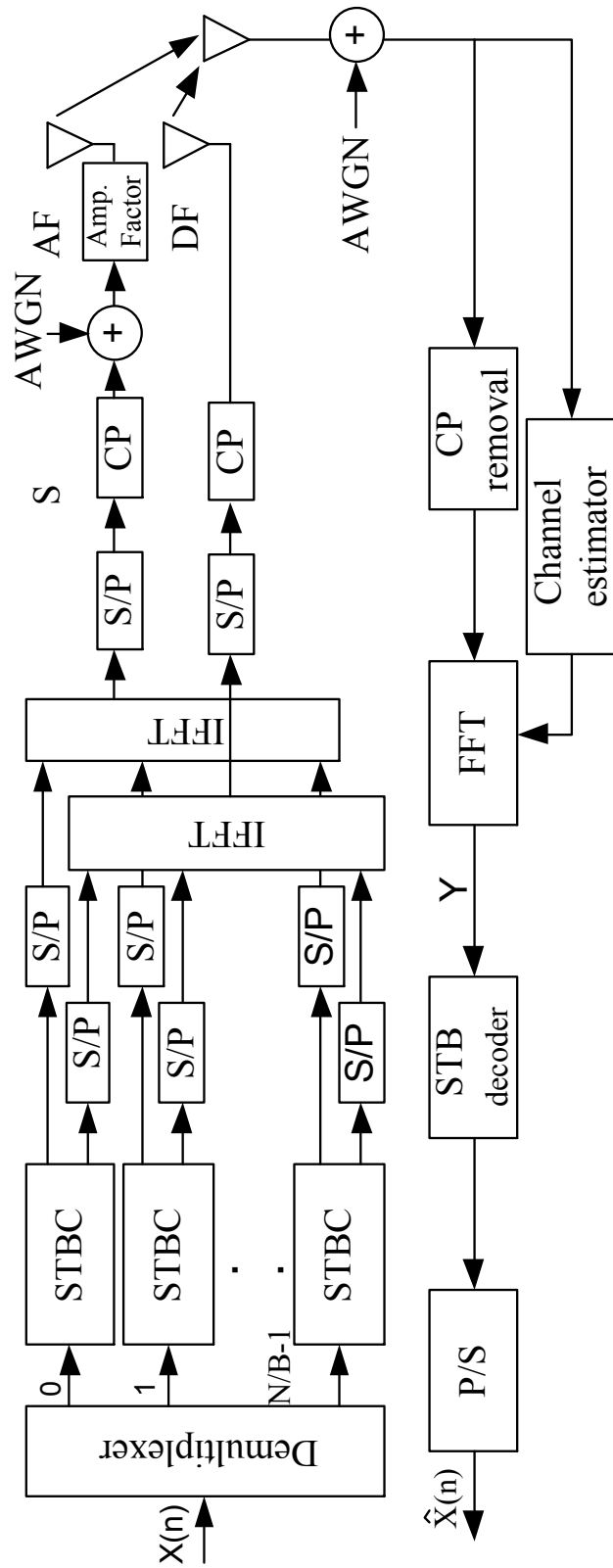


Figure 5.3: DSFC-OFDM transceiver architecture.

ten as

$$\begin{aligned}
\hat{X}_{2n} &= \left( \sqrt{\frac{P_{s,r_i} P_{r_i,d}}{P_{s,r_i} + 1}} |H^{AF}|^2 + |H^{DF}|^2 \right) X_{2n} \\
&\quad + Z(2n) \\
\hat{X}_{2n+1} &= \left( \sqrt{\frac{P_{s,r_i} P_{r_i,d}}{P_{s,r_i} + 1}} |H^{AF}|^2 + |H^{DF}|^2 \right) X_{2n+1} \\
&\quad + Z(2n+1)
\end{aligned} \tag{5.10}$$

where  $Z(2n) = H_{AF}^* W(2n) + H_{DF} W^*(2n+1)$ ,  $Z(2n+1) = H_{DF}^* W(2n) - H_{AF} W^*(2n+1)$ .

Finally, the OFDM symbols are forward to the destination. The block diagram of the proposed SFBC-OFDM system is illustrated in Fig. 5.3.

## 5.4 Power Allocation and Sub-carrier Pairing for DSFC-OFDM

In this section, power allocation, sub-carrier permutation and joint power allocation and sub-carrier permutation are studied to improve the throughput of the system. The optimization of power allocation with and without sub-carrier pairing is investigated under global power constraints.

### 5.4.1 Power allocation

In this section, the sub-carriers pairing technique is not used where the same sub-carrier in the second hop retransmits the information received from the source. It has been proven that adaptive power allocation can provide a significant improvement in data rates over non-adaptive by exploiting the complete knowledge of the CSI at the transmitter [107, 111, 209, 210]. The main reason behind this improvement is that the algorithm excludes the sub-carriers experiencing deep fading by assigning these sub-carriers zero while allocates high power level for good sub-carriers. It is assumed that the power channel parameters are perfectly estimated at the receiver and fed back to the source node. Subsequently the source

## 5.4 Power Allocation and Sub-carrier Pairing for DSFC-OFDM 109

evaluates the SNRs and assigns each sub-carrier a modulation constellation correspondingly.

A power loading algorithm determines the power assigned to each node as well as the required power of each sub-carrier in the network. This has been intensively investigated either to provide high capacity which is referred to as rate adaptive or to improve BER performance which is denoted as margin adaptive. The rate adaptive approach is considered where the objective is to maximize the data rate under a total power constraint. Since the end-to-end SNR for each sub-carrier in both relays are known at the destination, the overall data rate can be expressed as

$$\begin{aligned} C_n &= \frac{1}{2} \log_2 (1 + \gamma_n^{AF} + \gamma_n^{DF}) \\ &= \frac{1}{2} \log_2 \left( 1 + \frac{P_{s,n} P_{r_i,n}^{AF} \alpha_{i,n} \mu_{i,n}}{P_{s,n} \alpha_{i,n} + P_{r_i,n}^{AF} \mu_{i,n} + 1} + P_{r_j,n}^{DF} \nu_{j,n} \right) \end{aligned} \quad (5.11)$$

Since the best relay in both AF and DF groups forward the same data to the destination. It is very easy to combine the SNRs from both relays at the destination using MRC. The use of this formula is widely accepted in the literature, e.g., [35, 95, 110]. A tight upper bound of (5.11) can be used, which is more mathematically tractable and in a suitable form for analysis and can be rewritten as

$$C_n = \frac{1}{2} \log_2 \left( 1 + \frac{P_{s,n} P_{r_i,n}^{AF} \alpha_{i,n} \mu_{i,n}}{P_{s,n} \alpha_{i,n} + P_{r_i,n}^{AF} \mu_{i,n}} + P_{r_j,n}^{DF} \nu_{j,n} \right) \quad (5.12)$$

The factor  $\frac{1}{2}$  denotes that the system considered half-duplex and there are two time slots to complete the transmission of one symbol. The rate of an DSFC measures how many symbols per time slot (T) it transmits on average over the course of one block. In single-input single-output (SISO) system, the code rate equal to  $\frac{\text{symbols}}{T}$ , however in relaying systems it is equal to  $\frac{\text{symbols}}{2T}$ . The rate of the DSFC is equal to 0.5 due to the protocol has two time slots regardless how many relays in the system. Since OFDM symbols consist of  $N$  sub-carriers and the relay nodes retransmit the data over entire sub-carriers, the instantaneous information rate from source to destination can be expressed as

$$C = \sum_{n=1}^N C_n \quad (5.13)$$

The optimal power allocation can be achieved by maximizing the overall system capacity  $C$  under aggregate power constraint. Thus the problem of maximizing throughput can be formulated as

$$\arg \max \sum_{n=1}^N C_n \quad (5.14)$$

$$\begin{aligned} \text{subject to } & \sum_{n=1}^N P_{s,n} + \sum_{n=1}^N P_{r,n}^{AF} + \sum_{n=1}^N P_{r,n}^{DF} = P_T \\ & P_{s,n}, P_{r,n}^{AF}, P_{r,n}^{DF} \geq 0 \end{aligned} \quad (5.15)$$

where  $P_T$  is the total power budget.

As reported in the previous section, the DF relay was error free. In order to realize with this context and also to minimize the noise induced at the AF relay. The source should be allocated sufficient amounts of power. Therefore the optimization problem can be divided into two suboptimal problems. The first one is to divide the total power optimally between the source and the relay nodes taking into account the complete CSI in the system. Then the relays power allocation of the the relay nodes can be optimized to maximize the channel capacity of the second hop under relay power constraint. Let the total relay power be equal to the algebraic sum of the AF and DF relay nodes

$$P_R = \sum_{n=1}^N P_{R,n} = \sum_{n=1}^N P_{r,n}^{AF} + \sum_{n=1}^N P_{r,n}^{DF}. \quad (5.16)$$

The maximum throughput can be obtained when the power  $P_R$  is distributes optimally between both relays according to the power channel gains of the second hop subject to the constraint in (5.16). Therefore the capacity of the second hop in the  $n$ th sub-carrier can be expressed as

$$\bar{C}_n = \min\{\log_2(P_{r,n}^{AF}\mu_{i,n}), \log_2(P_{r,n}^{DF}\nu_{j,n})\}, \quad (5.17)$$

It should also meet the condition of [108, 136] to achieve the maximum capacity

$$P_{r,n}^{AF} \mu_{i,n} = P_{r,n}^{DF} \nu_{j,n}, \quad (5.18)$$

## 5.4 Power Allocation and Sub-carrier Pairing for DSFC-OFDM 11

The suboptimal problem can be written as

$$\begin{aligned} \max \bar{C} &= \sum_{n=1}^N \log_2 \left( 1 + \frac{\mu_{i,n} \nu_{j,n}}{\mu_{i,n} + \nu_{j,n}} \right) \\ \text{s.t.} \quad &\sum_{n=1}^N \frac{P_{R,n}}{2} = P_R \\ &P_{R,n} \geq 0, \end{aligned} \quad (5.19)$$

It is worth to point out that the solution of (5.19) can be obtained by using water-filing algorithm, the transmit power assigned to each sub-carrier in the second hop gives as

$$P_{R,n} = \left[ \eta - \frac{\mu_{i,n} \nu_{j,n}}{\mu_{i,n} + \nu_{j,n}} P_R \right]^+, \quad (5.20)$$

where  $[a]^+ = \max(a, 0)$  and  $\eta$  is the Lagrange multiplier that satisfies the power constraints in (5.16). The transmit power of each sub-carrier in AF and DF relay nodes is given by

$$\begin{aligned} P_{R,n}^{AF} &= \frac{\nu_{i,n}}{\mu_{i,n} + \nu_{i,n}} P_{R,n} = \psi_n P_{R,n} \\ P_{R,n}^{DF} &= \frac{\mu_{i,n}}{\mu_{i,n} + \nu_{i,n}} P_{R,n} = (1 - \psi_n) P_{R,n}. \end{aligned} \quad (5.21)$$

By substituting 5.21 into 5.12, the system capacity can be expressed as

$$C = \frac{1}{2} \sum_{n=1}^N \log_2 \left( 1 + \frac{P_{s,n} \psi_n P_{R,n} \alpha_{i,n} \mu_{i,n}}{P_{s,n} \alpha_{i,n} + \psi_n P_{R,n} \mu_{i,n}} + (1 - \psi_n) P_{R,n} \nu_{j,n} \right) \quad (5.22)$$

and substituting 5.16 into 5.15, the optimization problem can be rewritten as

$$\begin{aligned} &\arg \max C \\ \text{subject to} \quad &\sum_{n=1}^N P_{s,n} + \sum_{n=1}^N P_{R,n} = P_T \\ &P_{s,n}, P_{R,n} \geq 0 \end{aligned} \quad (5.23)$$

The suboptimal power allocation at the source and relay nodes can be obtained by applying Lagrange multiplier method and considering Karush-Kuhn-Tucker (KKT) conditions [211]. The Lagrangian function of the problem expressed in 5.23 can be formulated as

$$\begin{aligned} L &= \frac{1}{2} \sum_{n=1}^N \log_2 \left( 1 + \frac{P_{s,n} \psi_n P_{R,n} \alpha_{i,n} \mu_{i,n}}{P_{s,n} \alpha_{i,n} + \psi_n P_{R,n} \mu_{i,n}} + (1 - \psi_n) P_{R,n} \nu_{j,n} \right) \\ &\quad - \eta \left( \sum_{n=1}^N P_{s,n} + \sum_{n=1}^N P_{R,n} - P_T \right) \end{aligned} \quad (5.24)$$

calculating the partial derivative of 5.24 with respect to the variables  $P_{s,n}$ ,  $P_{R,n}$  and  $\eta$ , results

$$\begin{aligned}
\frac{\partial L[P_{s,n}, P_{R,n}, \eta]}{\partial P_{s,n}} &= \frac{1}{\left(1 + \frac{P_{s,n}\psi_n P_{R,n}\alpha_{i,n}\mu_{i,n}}{P_{s,n}\alpha_{i,n} + \psi_n P_{R,n}\mu_{i,n}} + (1 - \psi_n)P_{R,n}\nu_{j,n}\right)} \\
&\times \frac{(P_{s,n}\alpha_{i,n} + \psi_n P_{R,n}\mu_{i,n})(\psi_n P_{R,n}\alpha_{i,n}\mu_{i,n}) - P_{s,n}\psi_n P_{R,n}(\alpha_{i,n})^2\mu_{i,n}}{(P_{s,n}\alpha_{i,n} + \psi_n P_{R,n}\mu_{i,n})^2} - \eta = 0 \\
\frac{\partial L[P_{s,n}, P_{R,n}, \eta]}{\partial P_{R,n}} &= \frac{1}{\left(1 + \frac{P_{s,n}\psi_n P_{R,n}\alpha_{i,n}\mu_{i,n}}{P_{s,n}\alpha_{i,n} + \psi_n P_{R,n}\mu_{i,n}} + (1 - \psi_n)P_{R,n}\nu_{j,n}\right)} \\
&\times \frac{(P_{s,n}\alpha_{i,n} + \psi_n P_{R,n}\mu_{i,n})(P_{s,n}\psi_n\alpha_{i,n}\mu_{i,n}) - P_{s,n}\alpha_{i,n}P_{R,n}(\psi_n\mu_{i,n})^2}{(P_{s,n}\alpha_{i,n} + \psi_n P_{R,n}\mu_{i,n})^2} \\
&+ \frac{(1 - \psi_n)\nu_{j,n}}{\left(1 + \frac{P_{s,n}\psi_n P_{R,n}\alpha_{i,n}\mu_{i,n}}{P_{s,n}\alpha_{i,n} + \psi_n P_{R,n}\mu_{i,n}} + (1 - \psi_n)P_{R,n}\nu_{j,n}\right)} - \eta = 0 \\
\frac{\partial L[P_{s,n}, P_{R,n}, \eta]}{\partial \eta} &= P_{s,n} + P_{R,n} - P_T = 0
\end{aligned} \tag{5.25}$$

From 5.25, it can be determined that

$$\begin{aligned}
&(\psi_n P_{R,n}\mu_{i,n})^2\alpha_{i,n} - \eta \left( (P_{s,n}\alpha_{i,n} + \psi_n P_{R,n}\mu_{i,n})^2 (1 + (1 - \psi_n)P_{R,n}\nu_{j,n}) \right) \\
&- \eta \left( (P_{s,n}\psi_n P_{R,n}\alpha_{i,n}\mu_{i,n})(P_{s,n}\alpha_{i,n} + \psi_n P_{R,n}\mu_{i,n}) \right) = 0 \\
&(P_{R,n}\alpha_{i,n})^2\psi_n\mu_{i,n} + (1 - \psi_n)\nu_{j,n}(P_{s,n}\alpha_{i,n} + \psi_n P_{R,n}\mu_{i,n})^2 \\
&- \eta \left( (P_{s,n}\alpha_{i,n} + \psi_n P_{R,n}\mu_{i,n})^2 (1 + (1 - \psi_n)P_{R,n}\nu_{j,n}) \right) \\
&- \eta \left( (P_{s,n}\psi_n P_{R,n}\alpha_{i,n}\mu_{i,n})(P_{s,n}\alpha_{i,n} + \psi_n P_{R,n}\mu_{i,n}) \right) = 0 \\
&P_{s,n} + P_{R,n} - P_T = 0
\end{aligned} \tag{5.26}$$

Further manipulation of 5.26 yields

$$P_{s,n} = \begin{cases} \kappa P_{R,n} & \text{when } \mu_{i,n} \neq \nu_{j,n} \\ P_{R,n}, & \text{when } \mu_{i,n} = \nu_{j,n} \end{cases} \tag{5.27}$$

where  $\kappa = \frac{(1 - \psi_n)\psi_n\mu_{i,n}\nu_{j,n} + (1 - \psi_n)\nu_{j,n}\sqrt{(1 - \psi_n)\psi_n\mu_{i,n}\nu_{j,n} + \alpha_{i,n}(|\psi_n\mu_{i,n} - (1 - \psi_n)\nu_{j,n}|)}}{\alpha_{i,n}(|\psi_n\mu_{i,n} - (1 - \psi_n)\nu_{j,n}|)}$ .

The solution of the optimization problem as shown in 5.28 and 5.29

$$P_{s,n} = \begin{cases} \frac{\kappa}{1 + \kappa} P_T, & \text{when } \mu_{i,n} \neq \nu_{j,n} \\ \frac{P_T}{2}, & \text{when } \mu_{i,n} = \nu_{j,n} \end{cases} \tag{5.28}$$

## 5.4 Power Allocation and Sub-carrier Pairing for DSFC-OFDM 13

$$P_{R,n} = \begin{cases} \frac{1}{1+\kappa} P_T, & \text{when } \mu_{i,n} \neq \nu_{j,n} \\ \frac{P_T}{2}, & \text{when } \mu_{i,n} = \nu_{j,n} \end{cases} \quad (5.29)$$

By substituting 5.28 and 5.29 into 5.21, the following results can be achieved

$$P_{R,n}^{AF} = \begin{cases} \frac{\nu_{i,n}}{(1+\kappa)(\mu_{i,n}+\nu_{i,n})} P_T, & \text{when } \mu_{i,n} \neq \nu_{j,n} \\ \frac{P_T}{4}, & \text{when } \mu_{i,n} = \nu_{j,n} \end{cases} \quad (5.30)$$

$$P_{R,n}^{DF} = \begin{cases} \frac{\mu_{i,n}}{(1+\kappa)(\mu_{i,n}+\nu_{i,n})} P_T, & \text{when } \mu_{i,n} \neq \nu_{j,n} \\ \frac{P_T}{4}, & \text{when } \mu_{i,n} = \nu_{j,n} \end{cases} \quad (5.31)$$

It can be seen from 5.30 and 5.31 that the power assigned to each sub-carrier in both relays depends directly to the power channel gains of the second hop. The algorithm allocates more power to the sub-carrier experiencing high attenuation at one relay and the rest of the  $n$ th sub-carrier transmit power assigns to the second relay and Vice versa. It also can be seen that if the channel power gain for the sub-carrier in the DF group is high, the assigned power will be low and vice versa. As a result by allocating power appropriately in this manner, the issues of very close relays is overcome. The practicality of the proposed scheme was examined against the available protocols and the results are illustrated in Figure 5.7 on page 118. The results demonstrate that the proposed protocol outperform the available protocols for different range of SNR.

### 5.4.2 Sub-carrier Pairing

In this section the power allocation for all sub-carriers are assumed to be uniformly distributed in the transmitter and both relay nodes, thus each sub-carrier allocates  $P_n = \frac{P_T}{3N}$ . The power channel gains for the same sub-carrier in the multi-hop protocols are independent and the end to end system performance depends on the weakest channel gain. However the system throughput may be greatly degraded when the  $n$ th sub-carrier retransmits the received data from the source with the same sub-carrier in the second hop to the destination.

On the other hand, sub-carrier permutation can be implemented in multi-hop OFDM relaying systems to further enhance system performance. In a sub-carrier permutation algorithm, the  $n$ th sub-carrier in the first hop is matched with another sub-carrier in the second hop based on quality of the channel power gain. Practically this can be done by ordering the sub-carriers in both hops in descending order according to the CSI [108, 121]. Then the sub-carrier with the maximum channel power gain in the first hop is matched with the sub-carrier has maximum channel gain in the second hop. This process is repeated for the second best and so on until the worst sub-carrier in the first hop is allocated with the worst sub-carrier in the second hop.

### 5.4.3 Joint Power Allocation and Sub-carrier Pairing

In this subsection, the joint sub-carrier pairing and resource allocation will be analyzed for HRP. In this scheme, the sub-carrier pairing is considered at the beginning by using the best to best algorithm as presented in the previous subsection. Since the system consists of two relays participating in communication time interval. Therefore the sub-carrier pairing should be implemented in both relays independently. In the AF relay, the sub-carriers in both hops are ordered in descending according to the quality of the power channel gains. Whereas the DF relay uses error-free decoding, the sub-carriers in the second hop will be organised in descending order. The end-to-end SNR of each sub-carrier in both relays can be expressed as

$$\gamma_n = \begin{cases} \frac{\gamma_{sr_i,n}\gamma_{r_id,\hat{n}}}{\gamma_{sr_i,\hat{n}}+\gamma_{r_id,n}+1} = \frac{P_{s,n}P_{r_i,\hat{n}}^{AF}\alpha_{i,n}\mu_{i,\hat{n}}}{P_{s,n}\alpha_{i,n}+P_{r_i,\hat{n}}^{AF}\mu_{i,\hat{n}}+1}, & \text{if } i \in AF \\ \gamma_{r_jd,\hat{n}} = P_{r_j,\hat{n}}^{DF}\nu_{j,\hat{n}}, & \text{if } j \in DF \end{cases} \quad (5.32)$$

where  $\hat{n}$  and  $\check{n}$  denote the sub-carrier used by AF and DF relays in the second time slot respectively. Then the optimal power allocation will be adopted as presented in Section 5.4.1. Therefore the optimization problem can be expressed as

$$C = \frac{1}{2} \sum_{n=1}^N \log_2 \left( 1 + \rho_{n,\hat{n}} \frac{P_{s,n}\psi_n P_{R,\hat{n}}\alpha_{i,n}\mu_{i,\hat{n}}}{P_{s,n}\alpha_{i,n} + \psi_n P_{R,\hat{n}}\mu_{i,\hat{n}}} + \rho_{n,\check{n}}(1 - \psi_n)P_{R,n}\nu_{j,\check{n}} \right) \quad (5.33)$$

## 5.4 Power Allocation and Sub-carrier Pairing for DSFC-OFDM 15

$$\begin{aligned}
\text{subject to } & \sum_{n=1}^N P_{s,n} + \sum_{n=1}^N P_{R,n} = P_T \\
& P_{s,n}, P_{R,n} \geq 0 \\
& \rho_{n,\acute{n}}, \rho_{n,\grave{n}} = 0, 1 \\
& \sum_{n=1}^N \rho_{n,\acute{n}} = 1 \\
& \sum_{n=1}^N \rho_{n,\grave{n}} = 1
\end{aligned} \tag{5.34}$$

where  $\rho_{n,\acute{n}}$  and  $\rho_{n,\grave{n}}$  represent the indicator that the  $n$ th sub-carrier in the first hop retransmits the received data on the  $\acute{n}$ th sub-carrier by AF and  $\grave{n}$ th by DF relays and can takes 0 or 1 values.

The same procedure follows as in Section 5.4.1 to solve the optimization problem which is given as

$$P_{s,n} = \begin{cases} \frac{\kappa_{n,n}}{1+\kappa_{n,n}} P_T, & \text{when } \mu_{i,\acute{n}} \neq \nu_{j,\grave{n}} \\ \frac{P_T}{2}, & \text{when } \mu_{i,n} = \nu_{j,\grave{n}} \end{cases} \tag{5.35}$$

$$P_{R,\acute{n}}^{AF} = \begin{cases} \frac{\nu_{i,\grave{n}}}{(1+\kappa_{n,n})(\mu_{i,\acute{n}}+\nu_{i,\grave{n}})} P_T, & \text{when } \mu_{i,\acute{n}} \neq \nu_{j,\grave{n}} \\ \frac{P_T}{4}, & \text{when } \mu_{i,n} = \nu_{j,\grave{n}} \end{cases} \tag{5.36}$$

$$P_{R,\grave{n}}^{DF} = \begin{cases} \frac{\mu_{i,\acute{n}}}{(1+\kappa_{n,n})(\mu_{i,n}+\nu_{i,\acute{n}})} P_T, & \text{when } \mu_{i,\acute{n}} \neq \nu_{j,\grave{n}} \\ \frac{P_T}{4}, & \text{when } \mu_{i,\acute{n}} = \nu_{j,\grave{n}} \end{cases} \tag{5.37}$$

where  $\kappa_{n,n} = \frac{(1-\psi_n)\psi_n\mu_{i,\acute{n}}\nu_{j,\grave{n}}+(1-\psi_n)\nu_{j,\acute{n}}\sqrt{(1-\psi_n)\psi_n\mu_{i,\acute{n}}\nu_{j,\grave{n}}+\alpha_{i,n}(|\psi_n\mu_{i,\acute{n}}-(1-\psi_n)\nu_{j,\grave{n}}|)}} and  $\psi_n = \frac{\nu_{i,\grave{n}}}{\mu_{i,\acute{n}}+\nu_{i,\grave{n}}}$ .$

It is worth remarking that the half of the aggregate transmit power is assigned to the source and the rest is distributed between the selected relay nodes. The power allocation on each subcarrier at the source and selected relays is strongly depends on the sub-carrier pairing as shown in equations (5.35), (5.36) and (5.37). As a result the system capacity can gradely improve when the sub-carrier matched in both hops as illustrated in Figure 5.8.

## 5.5 Simulation Results

In this section, simulation results to demonstrate the BER and system capacity performance of the proposed protocol is presented with a varying number of relay nodes, and compare it to the conventional protocol. The BPSK modulation are performed for all simulations for fixed resource allocation and a frame size of 100 symbols. The channel between any two nodes in the system is modeled as a quasi-static frequency-selective fading channels (Pedestrian ITU-R model). The subcarriers is assumed to be set to  $N = 64$  and CP length of 16. The total power is set to 15 W. It is also assumed that perfect CSI is available at the nodes in the system. In order to simplify the SFC implementation and achieve full diversity and transmission rate, the distributed transmission pattern as proposed in [208] is considered. Two schemes: single cluster and dual clusters is simulated as illustrated in Figure 5.2. Each cluster has a pair of relay nodes (AF and DF).

Figure 5.4 plots the bit error probability performance of the protocols for various SNRs with a single cluster. The results demonstrate that the HRP scheme outperforms the AF scheme irrespective of the number of relay nodes in the network. This is due to noise amplification at the AF relay nodes. As can be seen from the figure, in the case of 2 relay nodes, the HRP performs better than the AF protocol at medium to high SNRs and both achieve a diversity order of 2. It can also be seen that the performance is substantially improved and the diversity order increases linearly with the number of the relays (2, 3, and 4). It is thus concluded that selective HRP has a diversity order equal to the number of the available relay nodes in the network instead of the number of the selected relays.

Figure 5.5 depicts the BEP performance with two clusters for different values of SNR. It can be seen that the diversity order of 2, when the relay selection is not taken into consideration (without relay selection WoRS), is similar to the performance of the single cluster. It can also notice that the diversity order of 4 in both schemes when relay selection (with relay selection WRS) is taken into account. It is again shown that the diversity order increases linearly with the number of the relays.

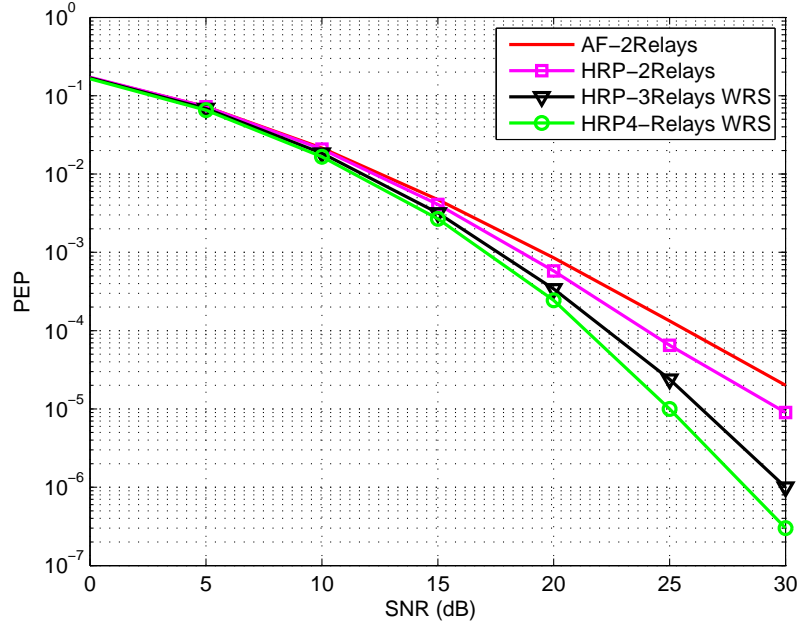


Figure 5.4: BEP performance of the DSFC-OFDM based on HRP for single cluster.

Figure 5.6 shows the bit error probability versus SNR under different adaptive algorithms. The system consists of 4 relay nodes organized into two clusters. It can be seen that the joint resource allocation and sub-carrier pairing outperforms the uniform resource allocation, uniform resource allocation with sub-carrier pairing and power allocation without SP. It also can be seen that the resource allocation provides better performance than the sub-carrier permutation at high SNR values.

Figure 5.7 illustrates the capacity of several protocols for various SNR values. The throughput of the proposed protocol is better than the convention protocols. Figure 5.7 also compares the proposed scheme with the hybrid relay protocol repetition based proposed (e.g., three orthogonal time slot). It can be observed that the proposed scheme outperforms the hybrid relay protocol over the entire SNR range. The improvement in the system capacity is linearly proportional with the SNR which provides a gain over the DF scheme about 0.5 bps/Hz at 30 dB and about 0.15 bps/Hz at 5dB.

The effect of the adaptive resource allocation and sub-carrier pairing on the

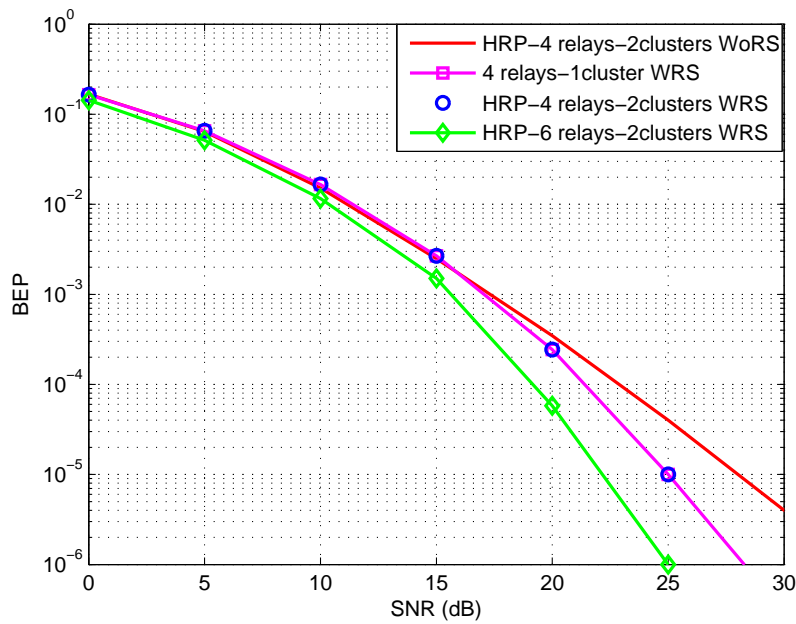


Figure 5.5: BEP performance of the DSFC-OFDM based on HRP for two clusters.

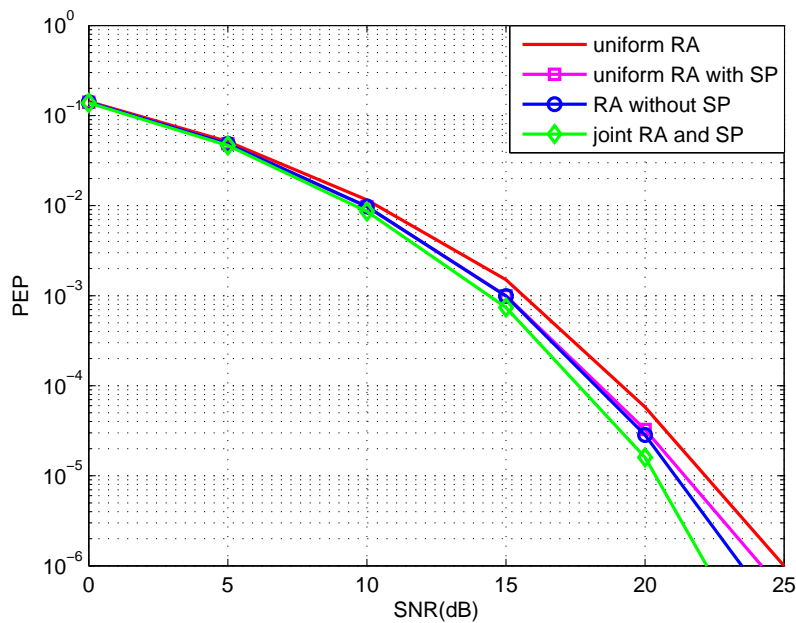


Figure 5.6: BEP performance of the DSFC-OFDM based on HRP versus SNR with and without adaptive techniques when  $M=6$  and  $N=64$ .

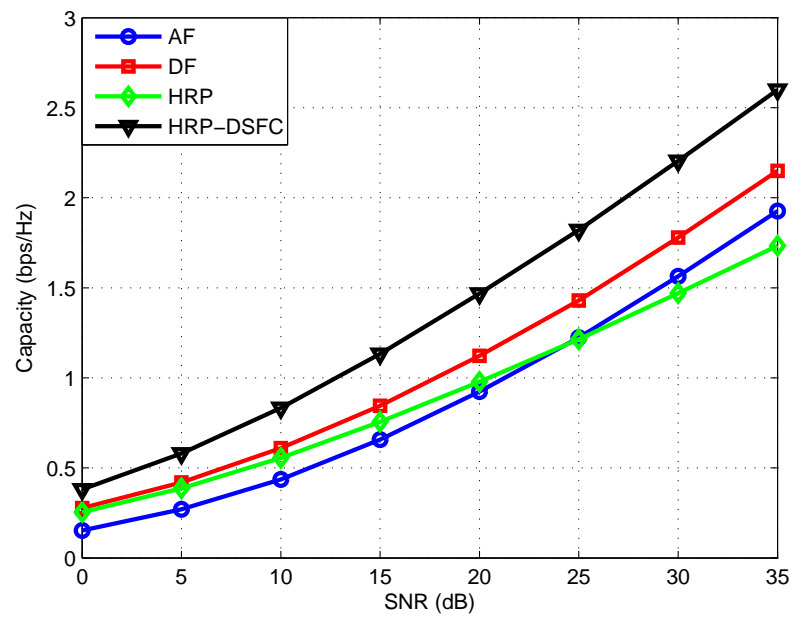


Figure 5.7: System capacity of the proposed versus SNR for two clusters with 4 relay nodes.

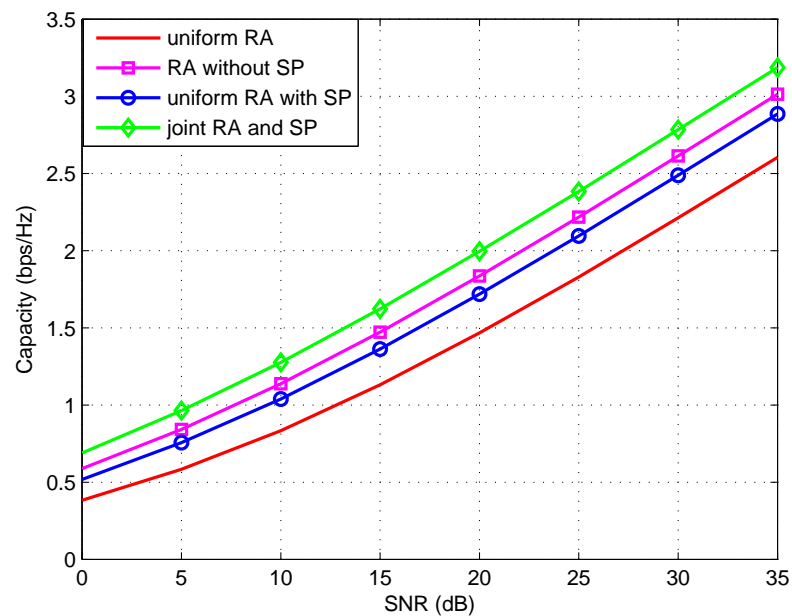


Figure 5.8: System capacity of the proposed versus SNR with and without adaptive techniques.

system capacity of the proposed scheme is illustrated in Figure 5.8. The power allocation can provide better performance than sub-carrier pairing while joint resource allocation and sub-carrier permutation provides the best throughput as expected.

## 5.6 Conclusion

In this chapter, a hybrid relay selection protocol based upon DSFC and OFDM has been proposed. The system performance can be enhanced by using adaptive power allocation and sub-carrier permutation. The DSFC is obtained at the destination with a very simple operation at the relay nodes. Previous work comprised: time reversal, circular shift, and encoding of the received symbols at the AF relay nodes whereas here the selected AF relay nodes simply amplify the received noisy signals. Moreover, very simple processes (complex conjugate) are implemented at the selected DF relay nodes. The computer simulations show that the proposed scheme achieves full spatial diversity and significant improvement in terms of BEP as the number of relay nodes increases. The additional gains of the spectral efficiency are not only due to usage of DSFC, power allocation and subcarrier permutation but also due to the use of hybrid relay selection. The proposed protocol also demonstrate that a full transmission rate is attainable.

# Chapter 6

## 3D Video Transmission Over Cooperative OFDM Relaying Systems

### 6.1 Introduction

Three dimensional video communication over wireless network is a significant challenge for current multimedia technology. As it is well known, wireless channels often suffer from multi-path fading, shadowing and inter-symbol interference. A digital video sequence is composed of many frames with a potentially large amount of data. The design issue of communication system is posed as follows: how to transmit 3D video sequences with high fidelity over drastically limited channel bandwidth?. In order to solve this problem a new field in signal processing has been applied to represent 3D scenes proposed with a minimal amount of data while maintaining an acceptable quality at the destination. Data compression is generally used to make the high data rate sequence more compatible for transmission over wireless channels.

Several standards for video data compression have been released in order to reduce the storage space and bandwidth to make them more appropriate with broadband channels. These included the H263, MPEG-2 and Advanced Video Coding (H.264/AVC) standard [212,213]. Recently (in April 2013) a new standard

for video compression has been released known as high-efficiency video coding (HEVC)/ H.265 [214].

H.264/AVC is still use due to it was created to provide better compression of video and error robustness compared to previous standards. However bit streams of the video compression standard are very sensitive to channel errors with some types of bits, in the bit stream, requiring higher levels of error protection than others. Therefore, unequal error protection (UEP) was proposed to cope with this problem by providing different levels of protection [40]. Numerous works have examined UEP performance based on forward error correction [167], hierarchical modulation [168, 215] and MIMO systems [41]. However these techniques may result in a reduction of throughput delivered at the destination, and increase in transmitter complexity and are often difficult to implement in small sized devices. Cooperative communications can provide different levels of robustness with convenient implementation by exploiting the relay nodes over error-prone channels.

In this chapter, UEP is implemented in the physical layer by exploiting the advantages of cooperative diversity introduced by cooperative system over frequency-selective channels. The most popular technique in cooperative communications that can provides full diversity gain is relay selection [14]. The proposed system combines relay selection with OFDM technique to further improve system performance. Two kinds of relay selection are considered, being hybrid relay selection and first-best second-best selection. In the relay selection schemes, the color sequence is transmitted through the relay that has the best channel gain in order to provide more protection than for the depth sequence.

The main contribution of this chapter can be summarized as follows:

- An improved relay selection scheme based on a dual relay selection protocol is investigated to assign more protection to the color sequence than depth sequence through DF and AF relays respectively.
- proposed two UEP based 3-D video transmission schemes using first-best second-best and hybrid relay selection over frequency-selective fading channels.

- The theoretical error and outage probabilities are analyzed and evaluated for both protocols.

The remainder of this chapter is organized as follows. In Section 6.2, Motivation and related works are discussed. Section 6.3 will describe 3D video coding and DIBR representation briefly. A system model is presented in Section 6.4. In Section 6.5, the probability density function of the proposed protocols is derived. The end-to-end performance analysis of the proposed protocols in terms of bit error probability and outage probability are investigated in Section 6.6. Numerical and simulation results are given and discussed in Section 6.7. Finally, concluding remarks are drawn in Section 6.8.

## 6.2 Motivation and Related Work

Recently, 3D video multimedia transmission has been gaining increasing attention in wireless systems over different types of channels. This requires efficient techniques in both application and physical layers to make 3D video transmission reliable in error-prone environments. Error-resilience is one of the most popular application-layer technologies to overcome the shortcoming of 3D video transmission. 3D scenes can be demonstrated using several methods, with video plus depth being a popular approach for representing 3D video transmission [216, 217]. It consists of a conventional 2D video with an associated per-pixel depth map represented with luma component. In order to represent 3D based on a stereoscope video, depth image-based rendering (DIBR) was proposed in [218]. In this technique, depth maps are required to generate good quality 3D video but they do not need to be of significantly high resolution to render 3D scenes, unlike the color sequence.

Color and depth images need to be transmitted over communication channels to the end user for display. However, the color sequence is directly viewed by the user. Therefore, if the color sequence is lost in transmission, it will result in more degradation of 3D video quality than the loss of the depth sequence. In [44] the authors proposed a joint source channel coding (JSCC) for 3D video

based DIBR to overcome the effect of source and channel distortion. In this method, different channel coding rates have been implemented to protect color and depth sequences. The results obtained show that the quality of depth image does not significantly affect the reconstructed quality. As a result, lower priority to protection can be used for depth sequence relative to color. The bit streams of the video compression standards are very sensitive to channel errors and each type of bits in the bit stream necessitates different error protection. Therefore, unequal error protection (UEP) was proposed to cope with this problem.

The underlying concept of UEP scheme is to splitting the source data according to its priority. In [23], a UEP-based 3D video transmission scheme is proposed which assigns more protection to the color sequence than the depth map. Different levels of protection are realized by allocating an unequal transmission power to various 3D video components. The most important data is assigned higher protection level than less important data. Several techniques to achieve UEP for multimedia data have been proposed in the literature [40, 216, 218]. In [40], 3D video transmission scheme based on UEP was proposed, where the UEP method assign more protection levels to the color sequence than the depth map sequence. Different levels of protection have been achieved by allocating unequal transmission power to 3D video components.

There has been a considerable research activity into multimedia transmission over MIMO systems due to the provision of high transmit or receive spatial diversity to mitigate channel fading [41–43, 169]. In [43], a joint design between application and physical layers to transmit multimedia data over a closed loop MIMO system has been proposed, where UEP can be achieved automatically for scalable video. Experimental results show that the proposed system achieved better performance relative to open-loop systems. Channel coding and spatial diversity can be combined together to achieve UEP as reported in [41]. In this scheme, more channel coding rates and spatial diversity have been allocated to the most important bits with less spatial diversity and less coding rates to least important bits. Robust channel code design may lead to a better performance, but at the expense of bandwidth efficiency.

The use of multiple antennas may be impractical in many instances due to limitations on the size and power of communications devices. However, cooperative communication, as a new technology to deal with the problems encountered by MIMO technology, has received much attention. In cooperative communication systems, several intermediate nodes located between the source and the destination attempt to help forward information leading to an improved link quality and provides high spectral efficiency [4, 17, 55]. Relay selection (RS) protocol [14, 18, 19] is an efficient technique to achieve high end-to-end throughput by choosing the best relay between source and destination and improving the diversity in a distributed mode. By utilizing cooperative communication with relay selection context, a new form of UEP has been developed to deliver a high data rate to the receiver. UEP combined with selective DF protocol were investigated in [89] over error-prone wireless channels. In this protocol, the most significant bits can be delivered through direct transmission. The less significant bit-streams are conveyed with high data rate via indirect links. The closed-form expression of symbol error probability was derived for single and multiple relay protocol. Although UEP based upon relay selection is proposed for single carrier systems in [50, 51]. Most of the existing studies on RS combined with 3D transmission have assumed the channel is flat-fading. As a result, 3D video transmission over OFDM-based relay system is an open issues.

Orthogonal frequency division multiplexing (OFDM) has become a dominant technique for multimedia transmission over wideband channels. OFDM technique can convert a high rate data stream into several low rate streams to be transmitted over independent frequency sub-carriers. There appears to have been limited work on considering the OFDM technique incorporated with 3D video transmission [6–8]. However all described techniques were obtained through the use of multiple antennae.

## 6.3 3D video coding and DIBR Representation

In the last decade, the techniques for video compression have developed toward reductions in system complexity, storage space for archived video information and transmission bandwidth to have little or no adverse effect on the visual quality perceived by the end user. Today, H.264/AVC is the video coding standard that is widely used for 3D video compression in communication systems.

### 6.3.1 H.264/AVC Coding

H.264/AVC is an industry standard for video compression which can provide high video quality with remarkably lower data rates and complexity compared to prior standards. It was developed by the ITU-T Video Coding Experts Group (VCEG) and the ISO/IEC Moving Picture Experts Group (MPEG). To date, it has been adopted by several application standards. In addition, there are several techniques to represent 3D content including, stereo video signals, multiview video coding and video-plus-depth. Previously it has been shown in [219] that the efficiency of a 3D video transmission system can be drastically improved by utilizing scene geometry information such as a depth map. As a consequence, video-plus-depth has become one of the most popular formats for representing 3D video scenes because the amount of data required for depth information is relatively small. It consists of a conventional 2D video with an associated per-pixel depth map which allows the decoder to synthesize the received sequences using depth image based rendering (DIBR) technique.

To transmit video-plus-depth format using H.264/AVC, the video and depth sequences are encoded independently at the transmitter. Figure 6.1 illustrates an overview diagram for color-plus-depth format using H.264/AVC encoder. The primary coded sequence can be represented by video sequence while the auxiliary coded sequence is the depth map. Both sequences are then transmitted through wireless channels to the destination separately. At the display side, these streams are decoded to obtain the distorted video and depth sequences. Finally, DIBR reconstructs the left and right views.

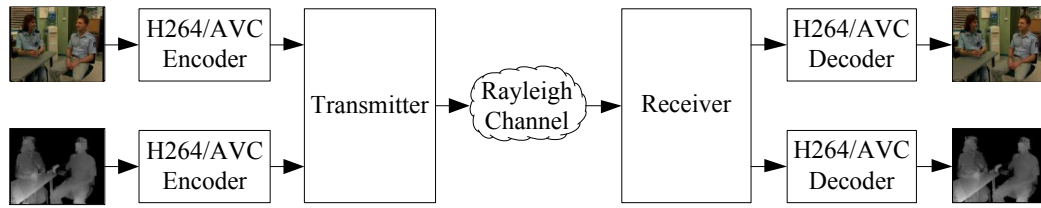


Figure 6.1: Block diagram of color-plus-depth video representation.

### 6.3.2 Depth Image Based Rendering (DIBR) Representation

In order to understand how 3D imaging works, it is important to understand the human visual system (HVS) [220]. The construction of the HVS consists of the brain and two eyes. The retina in each eye collects information and transfers it to the lateral geniculate body in the brain and then to the visual cortex through the optic nerve. Due to the distance of about 6-8 cm between the human eyes, human 3D depth perception is the product of two slightly different images projected to the left and right eye retinas. The brain fuses the two images to yield the depth perception. To deliver a 3D sequence to the eyes, autostereoscopic or shutter glasses can be used at the destination terminal to supply each eye with its corresponding video stream.

Depth image-based rendering (DIBR) is an efficient technique to overcome the drawback in the 3D depth perception realization proposed in [218] to represent 3D on a monoscopic video. It is based on the video plus depth (V+D) technique which is the dominant approach for 3D video representation [216]. In this technique, depth maps are required to generate good quality 3D video, but do not need to be of the same quality as the color sequence.

DIBR can provide high quality 3D video with a smaller bandwidth and reduced storage requirements for transmission compared to the traditional representation of 3D video using left-right views. Figure 6.2 illustrates the color and depth map sequences of the “Interview” at the input of the DIBR. The image warping process can be summarized as: Depth map can be used to generate two virtual views from the original view. The pixels of the original image are projected into



Figure 6.2: Color-plus-depth representation in DIBR for Newspaper test sequence  
a) color image b) depth map.

the 3D domain, utilizing their depth values specified by the depth stream. Then this 3D model is projected into the image plane of the virtual camera. The visual view generation process is shown in Figure 6.3 [44, 221]. The original pixels located at  $(x, y)$  are moved to the new locations  $(x_l, y)$  and  $(x_r, y)$  for left and right view respectively. The two virtual views  $x_l$  and  $x_r$  can be calculated as

$$x_r = x_c + \frac{f \cdot t_c}{2} \left( \frac{1}{Z} - \frac{1}{Z_c} \right) \quad (6.1)$$

$$x_l = x_c - \frac{f \cdot t_c}{2} \left( \frac{1}{Z} - \frac{1}{Z_c} \right) \quad (6.2)$$

where  $f$  is the focal length of the reference camera and  $t_c$  is the baseline distance between left and right camera positions.  $Z_c$  is the selected convergence distance located at the zero parallax setting (ZPS) plane and  $Z$  represents the depth value of each pixel in the reference view. The user can control the parameters  $f$ ,  $Z_c$  and  $t_c$  by setting the depth impression at the destination [221].

## 6.4 System Model

The proposed relay selection system is illustrated in Figure 6.4 and consists of one source denoted as S, one destination denoted as D, and  $M$  relays located



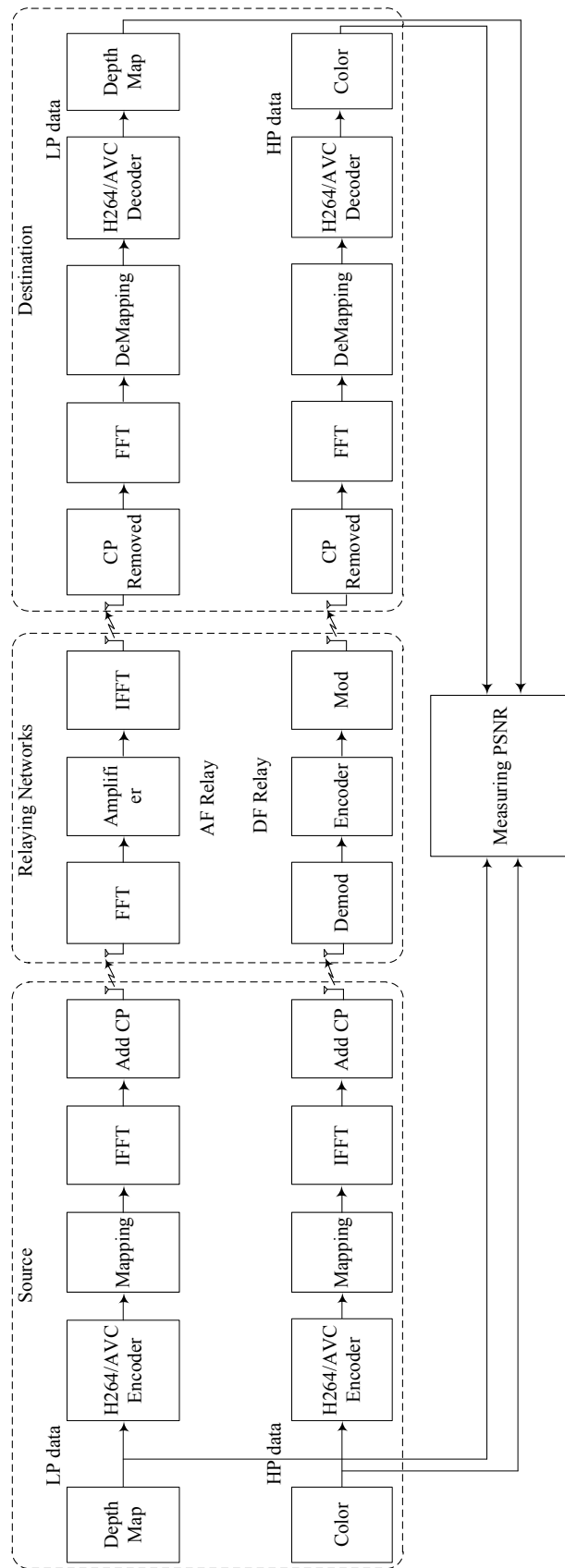


Figure 6.4: System Model.

### 6.4.1 UEP Based on HRP

In this scheme, it is assumed that the relays have the ability to perform perfect error-checking. Therefore any relay which can perform CRC checksum successfully will be included in the DF group, otherwise it is included in the AF group. In the AF group, the  $n$ th subcarrier in each relay simply amplifies the received signal by an amplification factor  $\beta_{i,n}$  and forwards it to the destination. The relays in the DF group decode the received signal from the source, re-encode and then forward it to the destination. After finding the optimal relay in each group, the destination informs the source which relay is selected with a corresponding forwarding scheme through a reverse broadcast channel. In the communication protocol, the source encodes each frame of multimedia data and classifies it into two sequences. The former one is the color sequence which is relayed in a highly reliable scheme using a DF relay and the latter is depth sequence which is transmitted through the AF relay. Figure 6.5 illustrates the system model where each group consists of several relays and only a single relay in each group is participating in the communication phase. The communication occurs through direct and indirect links with a two-phase protocol. During the first phase, the source node conveys the color and depth signals to the destination and the relays. The received signals at the destination and each relay for  $n$ th subcarrier can be expressed as

$$\begin{aligned} y_{s_j,r_i,n} &= \sqrt{P_{s,n}}h_{s_j,r_i,n}x(n) + w_{r_i,n} \\ y_{s_j,d,n} &= \sqrt{P_{s,n}}h_{s_j,d,n}x(n) + w_{d,n}, \end{aligned} \quad (6.3)$$

where  $x$  and  $P_{s,n}$  denote the transmitted signal (color or depth) and the signal power at the source, respectively.  $y_{s_j,r_i,n}$ , and  $y_{s_j,d,n}$  denote the signals received at the destination and the  $n$ th subcarrier of  $i$ th relay node, respectively.  $i = \{1, \dots, M\}$  and  $j = \{1, 2\}$  represent the numbers of the relays and transmitter antennas, respectively.  $h_{s_j,r_i,n}$  and  $h_{s_j,d,n}$  are the channel coefficients between S - D and S - R.  $w_{r_i,n}$  and  $w_{d,n}$  denote the additive white Gaussian noises (AWGN) in the corresponding channels at the relay and destination, respectively.

In the second time slot, the best relay in each group forwards the received information to the destination. The best AF relay node amplifies the depth se-

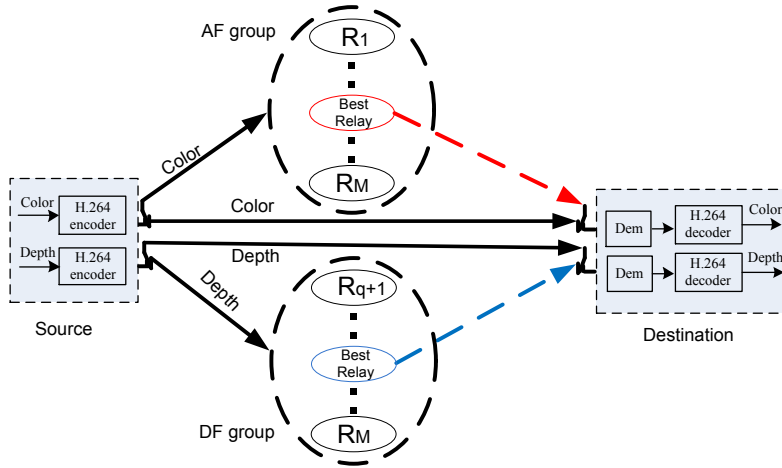


Figure 6.5: Hybrid relay selection system model.

quence map while the best DF relay decodes the color sequence and re-encodes with the same code as at the source. The color and depth signals received by the destination from AF and DF best relays are given by

$$\begin{aligned} y_{color} &= \sqrt{P_{r_i,n}^{DF}} h_{r_i,d,n}^{DF} x(n) + w_{d,n} \\ y_{depth} &= \beta_{r_i,n} h_{r_i,d,n}^{AF} y_{s,r_i,n} + w_{d,n}, \end{aligned} \quad (6.4)$$

where  $P_{r_i,n}^{DF}$  denote the signal power at the DF relay. The instantaneous end-to-end SNR for each relay at the destination is

$$\gamma_n = \begin{cases} \frac{\gamma_{s,r_i,n} \gamma_{r_i,d,n}}{\gamma_{s,r_i,n} + \gamma_{r_i,d,n} + 1}, & \text{for depth sequence} \\ \gamma_{r_i,d,n}, & \text{for color sequence} \end{cases} \quad (6.5)$$

where  $\gamma_{s,r_i,n}$  and  $\gamma_{r_i,d,n}$  are the instantaneous SNR of the first and second hop for best relays respectively. The overall received SNR at the destination after using maximum ratio combining (MRC) is given by

$$\begin{aligned} \gamma_{color} &= \gamma_{sd}^{color} + \arg \max_{i=1,\dots,\in \mathcal{G}^{DF}} \gamma_i \\ \gamma_{depth} &= \gamma_{sd}^{depth} + \arg \max_{i=1,\dots,\in \mathcal{G}^{AF}} \gamma_i, \end{aligned} \quad (6.6)$$

where  $\gamma_{sd}^{color}$  and  $\gamma_{sd}^{depth}$  are the end-to-end SNR for the direct link of both color and depth respectively.

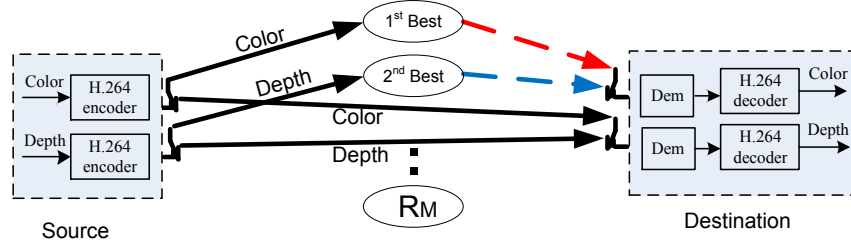


Figure 6.6: First and second best relay selection system model.

### 6.4.2 UEP Based on First and Second Best AF relays (FBSB)

In this protocol all the relays are assumed to use the AF scheme. The destination chooses the first and second best relay among available relays between the source and destination as shown in Figure 6.6. As in the previous protocol the communication process consists of two time slots. In the first time slot, the source broadcasts color and depth sequences to the relays and the destination independently. Therefore, the received signals at the relay and destination for the  $n$ th subcarrier are as shown in (6.3). In the second phase, the first best relay and the second best relay nodes simply amplify the received color and depth signals from the source and forward them to the destination through the  $h_{r_1,d,n}$  and  $h_{r_2,d,n}$  channels respectively. The color and depth signals received by the destination from first and second best relays are given by

$$\begin{aligned} y_{color} &= \beta_{r_1,n} h_{r_1,d,n} y_{s_j,r_1,n} + w_{d,n} \\ y_{depth} &= \beta_{r_2,n} h_{r_2,d,n} y_{s_j,r_2,n} + w_{d,n}, \end{aligned} \quad (6.7)$$

where  $\beta_{r_1,n}$  and  $\beta_{r_2,n}$  are the amplification factors for first and second best AF relays, respectively. The MRC can be employed at the destination to improve overall SNR. Therefore, the aggregate received SNR is given by

$$\begin{aligned} \gamma_{color} &= \gamma_{sd}^{color} + \arg \max_{i=1,\dots,M} \gamma_i \\ \gamma_{depth} &= \gamma_{sd}^{depth} + \arg \max_{i=1,\dots,M} 2^{nd} \gamma_i. \end{aligned} \quad (6.8)$$

## 6.5 PDF of proposed protocols

Since the relay retransmits the entire OFDM symbol from the source, it is in a state of outage if any subcarrier has an outage. Although the channel coefficient between any two nodes follows a Rayleigh fading distribution, the instantaneous SNR is exponentially distributed. Therefore, the cumulative distribution function (CDF) of the end-to-end link can be written as in [45, 176]

$$F_\gamma = 1 - \prod_{n=1}^N (1 - F_{\gamma_n}(\gamma)), \quad (6.9)$$

where  $F_{\gamma_n}$  is the CDF of the  $n$ th subcarrier at the destination and can be written for both AF and DF schemes as

$$F_{\gamma_n}(\gamma) = \begin{cases} 1 - e^{-\gamma(\frac{1}{\bar{\gamma}_{sr}} + \frac{1}{\bar{\gamma}_{rd}})} = 1 - e^{-\frac{\gamma}{\bar{\gamma}_{eq}}}, & \text{for AF scheme} \\ 1 - e^{-\frac{\gamma}{\bar{\gamma}_{rd}}}, & \text{for DF scheme.} \end{cases} \quad (6.10)$$

By substituting (6.10) into (6.9), the CDF can be expressed as

$$F_\gamma = \begin{cases} 1 - e^{-N\frac{\gamma}{\bar{\gamma}_{eq}}}, & \text{for AF scheme} \\ 1 - e^{-N\frac{\gamma}{\bar{\gamma}_{rd}}}, & \text{for DF scheme.} \end{cases} \quad (6.11)$$

The probability density function (PDF) can be evaluated by differentiation (6.11) with respect to  $\gamma$  as

$$f_\gamma = \begin{cases} \frac{N}{\bar{\gamma}_{eq}} e^{-N\frac{\gamma}{\bar{\gamma}_{eq}}}, & \text{for AF scheme} \\ \frac{N}{\bar{\gamma}_{rd}} e^{-N\frac{\gamma}{\bar{\gamma}_{rd}}}, & \text{for DF scheme.} \end{cases} \quad (6.12)$$

### 6.5.1 UEP Based on HRP

In this protocol, the relays are classified into two groups according to their ability to perform CRC checksums successfully. Assuming  $M$  relays are arbitrarily located between S and D and are classified into AF and DF groups. It is assumed that the AF and DF groups consist of  $Q$  and  $M - Q$  relays respectively. The destination chooses the best relay among the relays in each group which has the maximum end-to-end SNR independently. In the following analysis, the PDF and CDF for the end-to-end SNR of the best relay in both groups can be evaluated

by using the moment generating function (MGF) approach. Firstly, the MGF of the end-to-end SNR of color, depth and direct transmission are calculated and combined by utilizing MGF properties. Then, the corresponding PDF of each scheme can be evaluated by using the inverse Laplace transform. The end-to-end SNR of selected relay in each group can be written as

$$\begin{aligned}\gamma_{color,1} &= \arg \max_{i=1,..Q} \gamma_i \\ \gamma_{depth,1} &= \arg \max_{i=1,..M-Q} \gamma_i.\end{aligned}\tag{6.13}$$

The CDF of  $\gamma_{color}$  and  $\gamma_{depth}$  can be evaluated as

$$\begin{aligned}F_{\gamma,1}^{depth} &= \prod_{q=1}^Q F_{\gamma_q}^{depth} \\ F_{\gamma,1}^{color} &= \prod_{m=1}^{M-Q} F_{\gamma_m}^{color}.\end{aligned}\tag{6.14}$$

By differentiating the CDF in (6.14) with respect to  $\gamma$ , the PDF can be obtained as

$$\begin{aligned}f_{\gamma,1}^{depth} &= \sum_{q=1}^Q f_{\gamma_q}^{depth} \prod_{j=1}^Q F_{\gamma_j}^{depth} \\ f_{\gamma,1}^{color} &= \sum_{m=1}^{M-Q} f_{\gamma_m}^{color} \prod_{j=1}^{M-Q} F_{\gamma_j}^{color}.\end{aligned}\tag{6.15}$$

Substituting (6.11) and (6.12) into (6.15), the PDF of color and depth sequences can be rewritten as

$$\begin{aligned}f_{\gamma,1}^{depth} &= \sum_{q=1}^Q \frac{N}{\bar{\gamma}_{eq}} e^{-N \frac{\gamma}{\bar{\gamma}_{eq}}} \prod_{j=1}^Q 1 - e^{-N \frac{\gamma}{\bar{\gamma}_{eq}}} \\ f_{\gamma,1}^{color} &= \sum_{m=1}^{M-Q} \frac{N}{\bar{\gamma}_{rd}} e^{-N \frac{\gamma}{\bar{\gamma}_{rd}}} \prod_{j=1}^{M-Q} 1 - e^{-N \frac{\gamma}{\bar{\gamma}_{rd}}}.\end{aligned}\tag{6.16}$$

After some mathematical simplification and manipulation, (6.16) can be rewritten as

$$\begin{aligned}f_{\gamma,1}^{depth} &= \sum_{q=1}^Q C_Q^q (-1)^{q-1} \frac{Nq}{\bar{\gamma}_{eq}} e^{-Nq \frac{\gamma}{\bar{\gamma}_{eq}}} \\ f_{\gamma,1}^{color} &= \sum_{m=1}^{M-Q} C_{M-Q}^m (-1)^{m-1} \frac{Nm}{\bar{\gamma}_{rd}} e^{-Nm \frac{\gamma}{\bar{\gamma}_{rd}}}.\end{aligned}\tag{6.17}$$

where  $C_Q^q = \binom{Q}{q} = \frac{Q!}{(Q-q)!q!}$  is the binomial distribution. The PDF of the direct link  $\gamma_{s,d}$  for both color and depth is

$$f_{\gamma_{s,d}} = \frac{N}{\bar{\gamma}_{sd}} e^{-N \frac{\gamma}{\bar{\gamma}_{sd}}}, \quad (6.18)$$

By using the definition of the MGF generally given by

$$M_\gamma(s) = E\{e^{-s\gamma}\} = \int_0^\infty e^{-s\gamma} f_\gamma(\gamma) d\gamma, \quad (6.19)$$

the MGF of  $\gamma_{s,d}$  can be evaluated as

$$M_{\gamma_{s,d}}(s) = \frac{N}{N + \bar{\gamma}_{sd}s} \quad (6.20)$$

Similarly, the MGF of  $\gamma_{color,1}$  and  $\gamma_{depth,1}$  can be derived by substituting (6.17) into (6.19)

$$\begin{aligned} M_{\gamma_{depth,1}}(s) &= \sum_{q=1}^Q C_Q^q (-1)^{q-1} \frac{Nq}{Nq + \bar{\gamma}_{eq}s} \\ M_{\gamma_{color,1}}(s) &= \sum_{m=1}^{M-Q} C_{M-Q}^m (-1)^{m-1} \frac{Nm}{Nm + \bar{\gamma}_{rd}s}. \end{aligned} \quad (6.21)$$

Since the received SNR from direct and indirect links for both color and depth at the destination are independent, the MGF of  $\gamma_{color}$  and  $\gamma_{depth}$  can be expressed as

$$\begin{aligned} M_{\gamma_{depth}}(s) &= M_{\gamma_{s,d}}(s) M_{\gamma_{depth,1}}(s) \\ M_{\gamma_{color}}(s) &= M_{\gamma_{s,d}}(s) M_{\gamma_{color,1}}(s). \end{aligned} \quad (6.22)$$

By substituting (6.20) and (6.21) into (6.22), and applying partial fraction algorithm with several manipulations we arrive at

$$\begin{aligned} M_{\gamma_{depth}}(s) &= \sum_{q=1}^Q C_Q^q (-1)^{q-1} \left( \frac{A}{1 + \frac{\bar{\gamma}_{eq}}{Nq}s} + \frac{B}{1 + \frac{\bar{\gamma}_{SD}}{N}s} \right) \\ M_{\gamma_{color}}(s) &= \sum_{m=1}^{M-Q} C_{M-Q}^m (-1)^{m-1} \left( \frac{C}{1 + \frac{\bar{\gamma}_{rd}}{Nm}s} + \frac{D}{1 + \frac{\bar{\gamma}_{SD}}{N}s} \right). \end{aligned} \quad (6.23)$$

where  $A = -\frac{\bar{\gamma}_{eq}}{q\bar{\gamma}_{SD} - \bar{\gamma}_{eq}}$ ,  $B = \frac{q\bar{\gamma}_{SD}}{q\bar{\gamma}_{SD} - \bar{\gamma}_{eq}}$ ,  $C = -\frac{\bar{\gamma}_{rd}}{m\bar{\gamma}_{SD} - \bar{\gamma}_{rd}}$  and  $D = \frac{m\bar{\gamma}_{SD}}{m\bar{\gamma}_{SD} - \bar{\gamma}_{rd}}$ .

By applying the inverse Laplace transform to MGF in (6.23), the PDF can be

evaluated as

$$\begin{aligned}
f_{\gamma}^{depth} &= \mathcal{L}^{-1}\{M_{\gamma_{depth}}\} = \int_0^{\infty} e^{-s\gamma} M_{\gamma_{depth}}(s) ds \\
&= \sum_{q=1}^Q C_Q^q (-1)^{q-1} \frac{Nq}{q\bar{\gamma}_{SD} - \bar{\gamma}_{eq}} (e^{-N\frac{\gamma}{\bar{\gamma}_{SD}}} - e^{-qN\frac{\gamma}{\bar{\gamma}_{eq}}}) \\
f_{\gamma}^{color} &= \mathcal{L}^{-1}\{M_{\gamma_{color}}\} = \int_0^{\infty} e^{-s\gamma} M_{\gamma_{color}}(s) ds \\
&= \sum_{m=1}^{M-Q} C_{M-Q}^m (-1)^{m-1} \frac{Nm}{m\bar{\gamma}_{rd} - \bar{\gamma}_{rd}} (e^{-N\frac{\gamma}{\bar{\gamma}_{SD}}} - e^{-mN\frac{\gamma}{\bar{\gamma}_{rd}}}).
\end{aligned} \tag{6.24}$$

### 6.5.2 UEP Based on First and Second Best AF relays (FBSB)

The PDF and CDF of this protocol are evaluated by following the same procedure as in the previous subsection. The  $M$  relays are assumed to be located randomly between the source and the destination. The PDF of the best relay is similar to (6.17) being

$$f_{\gamma,2}^{color} = \sum_{m=1}^M C_M^m (-1)^{m-1} \frac{Nq}{\bar{\gamma}_{eq}} e^{-Nm\frac{\gamma}{\bar{\gamma}_{eq}}}. \tag{6.25}$$

and the PDF of the second best relay can be evaluated by considering a similar setup as in [222, 223] and substituting  $K = 2$  as

$$f_{\gamma,2}^{depth} = M(M-1) \sum_{m=1}^M C_{M-2}^m (-1)^{m-1} \frac{N}{\bar{\gamma}_{eq}} e^{-N(m+2)\frac{\gamma}{\bar{\gamma}_{eq}}}. \tag{6.26}$$

The MGF for both first and second best relays can be evaluated by substituting (6.25) and (6.26) in (6.19) as

$$\begin{aligned}
M_{\gamma_{depth,2}}(s) &= \sum_{m=1}^M C_M^m (-1)^m \frac{Nm}{Nm + \bar{\gamma}_{eq}s} \\
M_{\gamma_{color,2}}(s) &= M(M-1) \sum_{m=2}^{M-2} C_M^m (-1)^m \frac{N}{Nm + 2 + \bar{\gamma}_{eq}s}.
\end{aligned} \tag{6.27}$$

The MRC is employed at the receiver to combine the received signal from the direct and indirect links. The MGF of the combined signals can be calculated by substituting the PDF of direct transmission in (6.20) and for FBSB protocol in (6.27) with applying partial fraction expansion. The MGF of first and second

best after some mathematical manipulations can be written as

$$\begin{aligned}
 M_{\gamma_{color}}(s) &= \sum_{m=1}^M C_M^q (-1)^m \left( \frac{A}{1 + \frac{\bar{\gamma}_{eq}}{Nm} s} + \frac{B}{1 + \frac{\bar{\gamma}_{SD}}{N} s} \right) \\
 M_{\gamma_{depth}}(s) &= M(M-1) \sum_{m=1}^{M-2} C_{M-2}^m (-1)^m \times \left( \frac{C}{1 + \frac{\bar{\gamma}_{eq}}{N(m+2)} s} + \frac{D}{1 + \frac{\bar{\gamma}_{SD}}{N} s} \right).
 \end{aligned} \tag{6.28}$$

where  $A = -\frac{\bar{\gamma}_{eq}}{m\bar{\gamma}_{sd} - \bar{\gamma}_{eq}}$ ,  $B = \frac{m\bar{\gamma}_{sd}}{m\bar{\gamma}_{sd} - \bar{\gamma}_{eq}}$ ,  $C = -\frac{\bar{\gamma}_{rd}}{m\bar{\gamma}_{sd} - \bar{\gamma}_{rd}}$  and  $D = \frac{m\bar{\gamma}_{sd}}{m\bar{\gamma}_{sd} - \bar{\gamma}_{rd}}$ .

Finally, the PDF of color and depth signals at the destination can be derived as

$$\begin{aligned}
 f_{\gamma}^{color}(\gamma) &= \sum_{m=1}^M C_Q^m (-1)^{m-1} \frac{Nm}{m\bar{\gamma}_{SD} - \bar{\gamma}_{eq}} (e^{-N\frac{\gamma}{\bar{\gamma}_{SD}}} - e^{-mN\frac{\gamma}{\bar{\gamma}_{eq}}}) \\
 f_{\gamma}^{depth}(\gamma) &= M(M-1) \sum_{m=1}^{M-2} C_Q^m (-1)^m \frac{N}{(m+2)\bar{\gamma}_{SD} - \bar{\gamma}_{rd}} (e^{-N\frac{\gamma}{\bar{\gamma}_{SD}}} - e^{-(m+2)N\frac{\gamma}{\bar{\gamma}_{rd}}}).
 \end{aligned} \tag{6.29}$$

## 6.6 End-To-End Performance Analysis

In this section, the closed-form expression of BEP and outage probability system performances are derived over independent identical Rayleigh fading channels.

### 6.6.1 Bit Error Probability Performance

The average BEP can be found by averaging the conditional error probability in AWGN  $P(e/\gamma)$  over the PDF of  $\gamma$  as follows

$$P(e) = \int_0^{\infty} P(e/\gamma) f_{\gamma}(\gamma) d\gamma, \tag{6.30}$$

where  $P(e/\gamma)$  is represented by Gaussian Q-function for a wide range of modulation schemes. For binary phase shift key (BPSK), the conditional error probability is given by  $Q(\sqrt{\beta}\gamma)$ , where  $a = 2$  and  $Q(x) = (1/\sqrt{2\pi}) \int_x^{\infty} \exp(-\frac{t^2}{2}) dt$ . The conditional error probability for BPSK modulation can be expressed as

$$\begin{aligned}
 P(e/\gamma) &= \int_0^{\infty} \frac{1}{\pi} \int_0^{\frac{\pi}{2}} \exp\left(\frac{a^2\gamma}{2\sin^2\theta}\right) d\theta f_{\gamma_i}(\gamma) d\gamma \\
 &= \frac{1}{\pi} \int_0^{\frac{\pi}{2}} \left[ \int_0^{\infty} \exp\left(\frac{a^2\gamma}{2\sin^2\theta}\right) f_{\gamma_i}(\gamma) d\gamma \right] d\theta \\
 &= \frac{1}{\pi} \int_0^{\frac{\pi}{2}} M_{\gamma} \exp\left(\frac{a^2\gamma}{2\sin^2\theta}\right) f_{\gamma_i}(\gamma) d\theta.
 \end{aligned} \tag{6.31}$$

The closed-form expression for the average error probability of each scheme at the destination can be evaluated by substituting (6.24) and (6.29) into (6.31) and can be expressed as

$$\begin{aligned}
P_{HRP}^{depth} &= \frac{1}{2} \sum_{q=1}^Q C_Q^q (-1)^{q-1} \frac{q}{\bar{\gamma}_{eq} - q\bar{\gamma}} \left[ \bar{\gamma}_{eq} \left( 1 - \sqrt{\lambda_{eq,n}} \right) - qN\bar{\gamma}_{SD} \left( 1 - \sqrt{\lambda_{SD,n}} \right) \right] \\
P_{HRP}^{color} &= \frac{1}{2} \sum_{m=1}^{M-Q} C_{M-Q}^m (-1)^{m-1} \frac{m}{\bar{\gamma}_{rd} - m\bar{\gamma}} \\
&\quad \times \left[ \bar{\gamma}_{rd} \left( 1 - \sqrt{\lambda_{rd,n}} \right) - mN\bar{\gamma}_{SD} \left( 1 - \sqrt{\lambda_{SD,n}} \right) \right]
\end{aligned} \tag{6.32}$$

$$\begin{aligned}
P_{FBSB}^{depth} &= \frac{1}{2} \sum_{m=1}^M C_M^m (-1)^{m-1} \frac{m}{\bar{\gamma}_{eq} - m\bar{\gamma}} \\
&\quad \times \left[ \bar{\gamma}_{eq} \left( 1 - \sqrt{\lambda_{eq,n}} \right) - mN\bar{\gamma}_{SD} \left( 1 - \sqrt{\lambda_{SD,n}} \right) \right] \\
P_{HRP}^{color} &= \frac{1}{2} M(M-1) \sum_{m=1}^{M-2} C_{M-2}^m (-1)^m \frac{m}{\bar{\gamma}_{eq} - (m+2)\bar{\gamma}} \\
&\quad \times \left[ \frac{\bar{\gamma}_{eq}}{m+2} \left( 1 - \sqrt{\lambda_{eq,n}} \right) - \bar{\gamma}_{SD} \left( 1 - \sqrt{\lambda_{SD,n}} \right) \right]
\end{aligned} \tag{6.33}$$

where  $\lambda_{SD,n} = \frac{\bar{\gamma}_{SD,n}}{1+\bar{\gamma}_{SD,n}}$ ,  $\lambda_{eq,n} = \frac{\bar{\gamma}_{eq,n}}{1+\bar{\gamma}_{eq,n}}$  and  $\lambda_{rd,n} = \frac{\bar{\gamma}_{rd,n}}{1+\bar{\gamma}_{rd,n}}$

### 6.6.2 Outage Probability Performance

The outage probability is defined as the probability that the mutual information between the source and destination falls below a predefined threshold value  $\gamma_{th}$ . Mathematically can be written as

$$P_{out} = F_{\gamma}(\gamma_{out}) = P_r(\gamma < \gamma_{out}) = \int_0^{\gamma_{out}} f_{\gamma}(\gamma) d\gamma \tag{6.34}$$

where  $\gamma_{out} = 2^{2r} - 1$  and  $r$  is the number of bits in each subcarrier. The outage probability is corresponds with the CDF with respect to  $\gamma_{th}$ . Therefore the outage probability for both schemes can be evaluated by substituting (6.24) and (6.29)

into (6.34)

$$\begin{aligned}
 P_{HRP}^{depth} &= \sum_{q=1}^Q C_Q^q (-1)^{q-1} \frac{q}{\bar{\gamma}_{eq} - q\bar{\gamma}_{SD}} \left(1 + \frac{\bar{\gamma}_{SD}}{N} e^{-N \frac{\gamma}{\bar{\gamma}_{SD}}} - \frac{\bar{\gamma}_{eq}}{qN} e^{-qN \frac{\gamma}{\bar{\gamma}_{eq}}}\right) \\
 P_{HRP}^{color} &= \sum_{m=1}^{M-Q} C_{M-Q}^m (-1)^{m-1} \frac{m}{\bar{\gamma}_{SD} - m\bar{\gamma}_{rd}} \left(1 + \frac{\bar{\gamma}_{SD}}{N} e^{-N \frac{\gamma}{\bar{\gamma}_{SD}}} - \frac{\bar{\gamma}_{rd}}{mN} e^{-mN \frac{\gamma}{\bar{\gamma}_{rd}}}\right).
 \end{aligned} \tag{6.35}$$

$$\begin{aligned}
 P_{FBSB}^{color} &= \sum_{m=1}^M C_M^m (-1)^{m-1} \frac{m}{\bar{\gamma}_{eq} - m\bar{\gamma}_{SD}} \left(1 + \frac{\bar{\gamma}_{SD}}{N} e^{-N \frac{\gamma}{\bar{\gamma}_{SD}}} - \frac{\bar{\gamma}_{eq}}{mN} e^{-mN \frac{\gamma}{\bar{\gamma}_{eq}}}\right) \\
 P_{FBSB}^{depth} &= M(M-1) \sum_{m=1}^{M-2} C_{M-2}^m (-1)^m \frac{1}{(m+2)\bar{\gamma}_{SD} - \bar{\gamma}_{rd}} \\
 &\quad \times \left( \frac{\bar{\gamma}_{SD}}{N} (1 - e^{-N \frac{\gamma}{\bar{\gamma}_{SD}}}) - \frac{\bar{\gamma}_{rd}}{(m+2)N} e^{-(m+2)N \frac{\gamma}{\bar{\gamma}_{rd}}} \right).
 \end{aligned} \tag{6.36}$$

It can be seen from (6.35) and (6.36) that the outage probability depends on the number of relays in each group in HRP while based upon all relays in FBSB protocol.

## 6.7 Simulation and Numerical Results

In this section, the simulation and numerical results are presented to demonstrate the error probability and outage probability performances of the proposed protocols. The performance of the HRP and FBSB schemes are compared with the EEP scheme. BPSK modulation is performed for all simulations and the path-loss exponent was assumed to be equal to 4 and shadowing is not considered. The channels between any two nodes in the system are modeled as frequency-selective Rayleigh fading channels. The OFDM symbol is assumed to consist of  $N = 64$  sub-carriers with a cyclic prefix (CP) length of 16. It is also assumed that perfect CSI is available at the relay, and at the destination. The system is assumed to consist of 6 relays. The DF group in the HRP scheme has 4 relays while AF group is composed of 2 relays. The EEP scheme has 3 AF relays for each color and depth. All the relays are assumed to be located at the center of the source-to-destination path in which the SNR of each hop is equal (i.e.  $\gamma_{sr,n} = \gamma_{rd,n}$ ). The

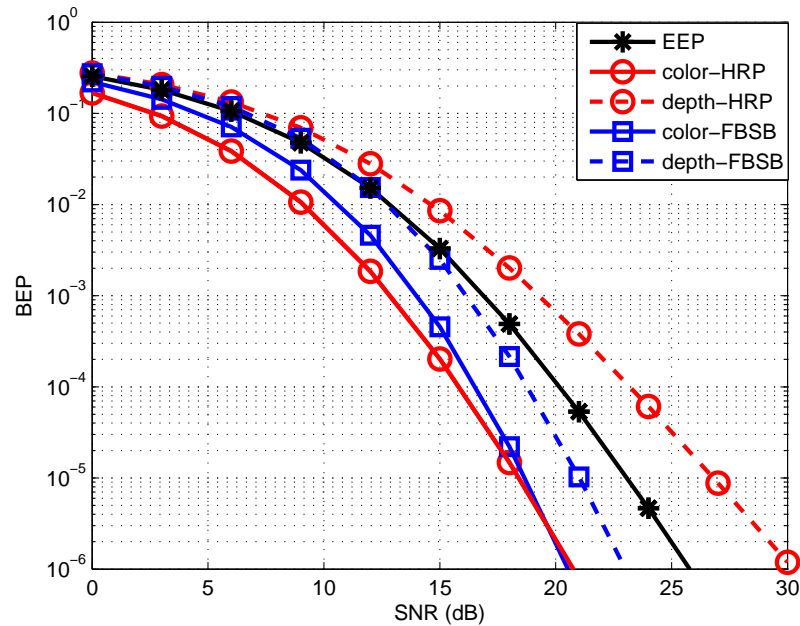


Figure 6.7: Bit error probability performance of the UEP-based HRP and EEP versus SNR

total transmission power is divided equally between the source and the relays and each sub-carrier transmits one bit ( $r = 1$ ).

Figure 6.7 plots the BEP performance of the analyzed proposed protocols as a function of the average SNR of the source-relay link. The closed-form expressions of the analytical BEP for color and depth and for HRP and FBSB are presented in (6.32) and (6.33) respectively. It can be seen that the color sequence of the HRP scheme provides better performance than FBSB at low and medium SNR values. This outcome is reasonable because the HRP is transmitted with perfect DF scheme. Whereas above the SNR of 20 dB, the FBSB outperforms the HRP scheme due to its provision of a higher diversity ordered  $(6 + 1)$ -fold. From the same figure, it is obvious that the EEP protocol exhibits lower performance than HRP and FBSB protocols. The depth sequence of the HRP scheme demonstrates worse performance than either EEP or FBSB schemes because it provides the lowest diversity gain. The performance of the depth sequence of the FBSB and EEP are approximately the same when the SNR is less than 15 dB. However

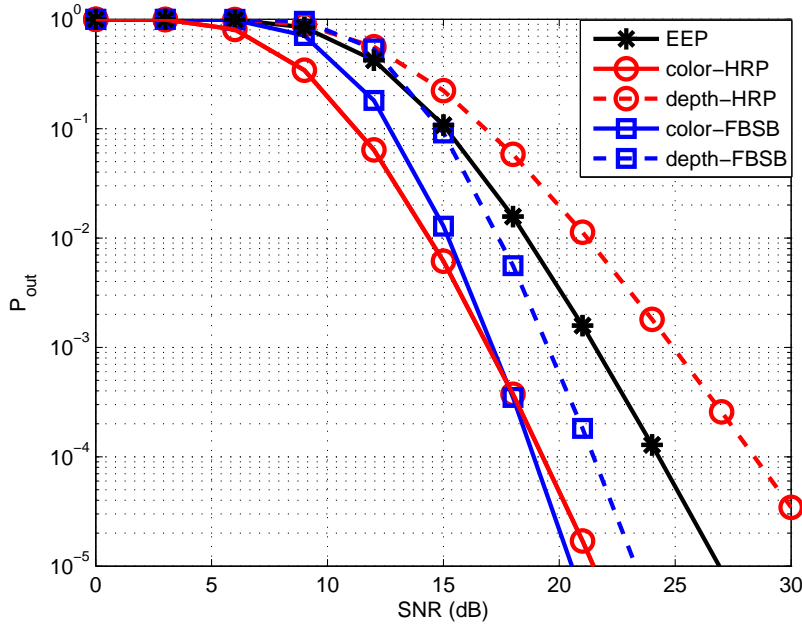


Figure 6.8: Outage probability performance of the UEP-based HRP and EEP versus SNR.

when the SNR is greater than 15dB the behavior of FBSB deviates significantly due to the exploitation of the advantages of diversity. It can be seen that the theoretical and simulation results are perfectly matched.

Figure 6.8 shows the outage probability for the analyzed protocols versus SNR with each sub-carrier assigned 1 bps/Hz. The analytical results of the outage probability are achieved using (6.34) and (6.35) for the HRP and FBSB protocols respectively. It shows that the color sequence of the HRP and FBSB performs much better than the EEP protocol. The performance depends directly on the number of participating relays in each group. When the SNR drops below 17 dB, the color sequence of the HRP exhibits better performance than FBSB. Without loss of generality, the performance of the HRP scheme only depends on the relay-destination channel ( $\gamma_{rd,n}$ ), while EEP and FBSB protocols depend upon the equivalent SNR of the first and second hop (i.e.,  $\frac{1}{\gamma_{eq,n}} = \frac{1}{\gamma_{sr,n}} + \frac{1}{\gamma_{rd,n}} = 0.5\gamma_{rd,n}$ ). Accordingly, the instantaneous SNR is double that of other protocols. On the other hand, after 19 dB of the SNR the performance of FBSB is greatly improved

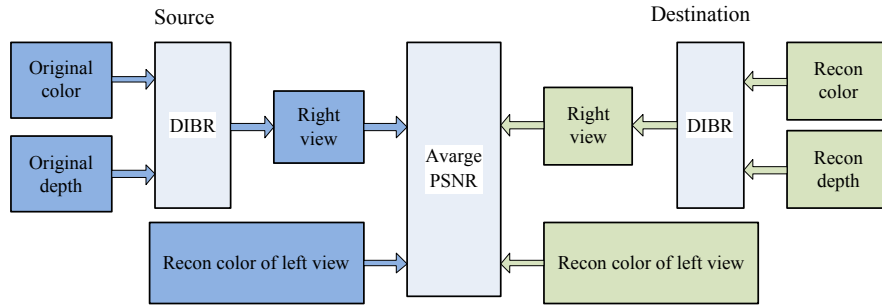


Figure 6.9: Average PSNR of video sequence.

against the HRP protocol.

In addition, it can be seen from Figure 6.8 that the outage probability of the depth sequence for the HRP showed a poorer performance than other protocols. Meanwhile, the FBSB outperforms the EEP when the SNR is greater than 17dB. Again, the theoretical results are in a good match with simulation results.

To evaluate the proposed UEP scheme, the 3D *interview* video sequence with 100 frames is tested. A resolution of  $720 \times 576$  and 4:2:0 color format with a frame rate of 15 frames/s, is considered. The H.264/AVC reference software JM version 16.1 is used to encode the video sequences. Simulations are repeated 20 times for each channel SNR condition and the average peak signal-to-noise ratio (PSNR) of the left and right views are adopted as the performance evaluation metric.

The quality of video can be measured at the destination by using either are objective quality metric or a subject quality metric [224]. Electrical measurements are used in the objective quality metric, while human observation is used in the subjective quality metric. Here, several parameters such as illumination and the distance between the user and the display affect the quality of the received signals. Most of existing research in the field of video quality measurement have adopted objective quality metric [225]. The PSNR is the most commonly used video quality metric [226].

The PSNR is measured at the destination by computing the mean square error (MSE) between a reconstructed and an original video frame as shown in Figure 6.9, mathematically represented as the ratio of the maximum value of the

pixel data (8 bits) and MSE in decibels and can be written as

$$PSNR = 10\log_{10}\left(\frac{255^2}{MSE}\right) \quad dB, \quad (6.37)$$

MSE depends on the original and compressed video and can be expressed as

$$MSE = \frac{1}{K} \sum_{k=1}^K (x_k - y_k)^2 \quad (6.38)$$

where  $K$  is the number of pixels and  $x_k$  and  $y_k$  denote the original and distorted video sequence of pixel  $k$ , respectively. When the MSE is lower value that mean the distorted video sequence (received video) is substantially high and leads to higher PSNR. As a result, the quality of the video sequence seen by end user is better. In 3D video transmission, the reconstructed left and right views are influenced more by the color sequence than depth sequence [221].

Table 6.1: Average PSNR of different UEP Protocols for the *Interview* sequence

Channel SNR (dB)	PSNR of EEP (dB)		PSNR of HRP (dB)		PSNR of FBSB (dB)	
	color	depth	color	depth	color	depth
5	5.22	5.12	9.27	4.95	7.38	4.98
7	5.52	5.45	13.05	5.25	8.61	5.32
9	6.16	6.02	16.87	5.75	11.43	5.94
11	7.03	6.87	20.3	6.44	15.48	6.75
13	9.24	8.74	22.95	7.26	19.82	8.84
15	11.31	10.91	25.3	8.52	23.95	11.37
17	15.20	14.83	27.08	10.17	26.79	15.97
19	18.65	18.13	28.55	15.31	28.92	19.5
21	21.42	20.93	29.74	17.13	30.15	23.05
23	23.58	22.81	30.84	19.79	31.56	25.14
25	25.29	24.63	31.58	21.42	32.38	26.85
27	27.0	26.42	32.15	24.38	33.23	29.14
29	28.17	27.36	32.60	25.51	33.87	30.48
31	29.2	28.31	33.04	26.28	34.51	31.27
33	29.53	28.78	33.35	26.95	35.02	32.18

Table 6.4 demonstrates the outcome of the investigated protocols of the *Interview* sequence versus different values of SNRs for color and depth maps. It can be seen

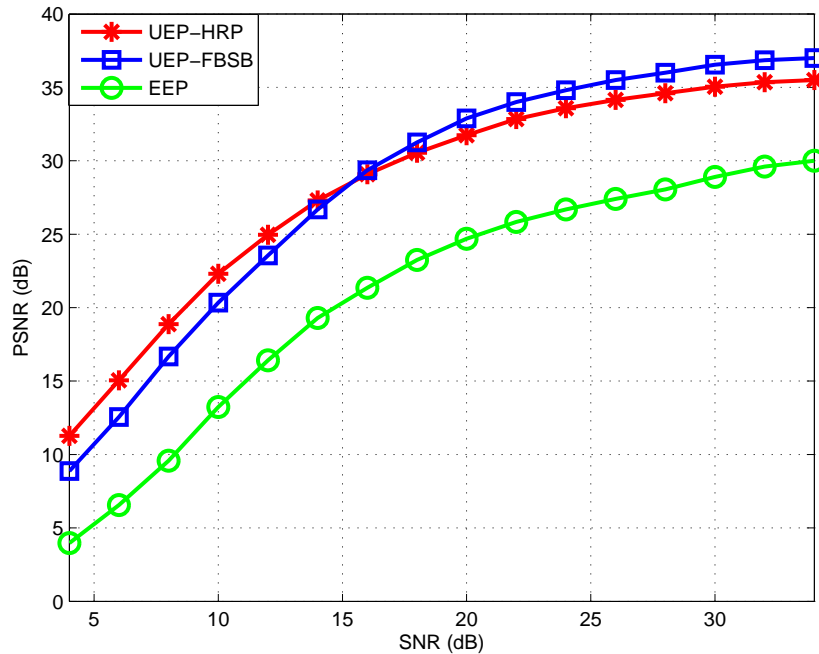


Figure 6.10: Average PSNR of the Interview sequence versus SNR for EEP and UEP based HRP.

that the PSNR of the reconstruction color for the EEP is less than the other UEP protocols for all the values of SNR. The reconstruction color sequence for the UEP based HRP exhibits higher PSNR than FBSB scheme where the SNR is below than 19dB. Otherwise the FBSB provides better PSNR than HRP. The response of the PSNR for the reconstruction depth sequence seems to be the same as in Figures. 6.7 and 6.8.

Figures 6.10 and 6.11 show the PSNR of the decoded left and right views of the schemes under consideration over a range of SNR for the *Interview* test sequence. HRP exhibits better performance at low SNRs while FBSB achieves remarkable gain over HRP and EEP for highest SNRs values.

Figures 6.12 shows the average PSNRs of the decoded left and right views with the proposed scheme over a range of SNR conditions. It can be seen that both proposed protocols consistently outperform EEP over the entire range of SNRs. For the UEP-based HRP, the performance gap is high at low SNRs (e.g, 5 dB gain at SNR of 8 dB) and decreases at high SNRs (e.g, 2 dB gain at SNR

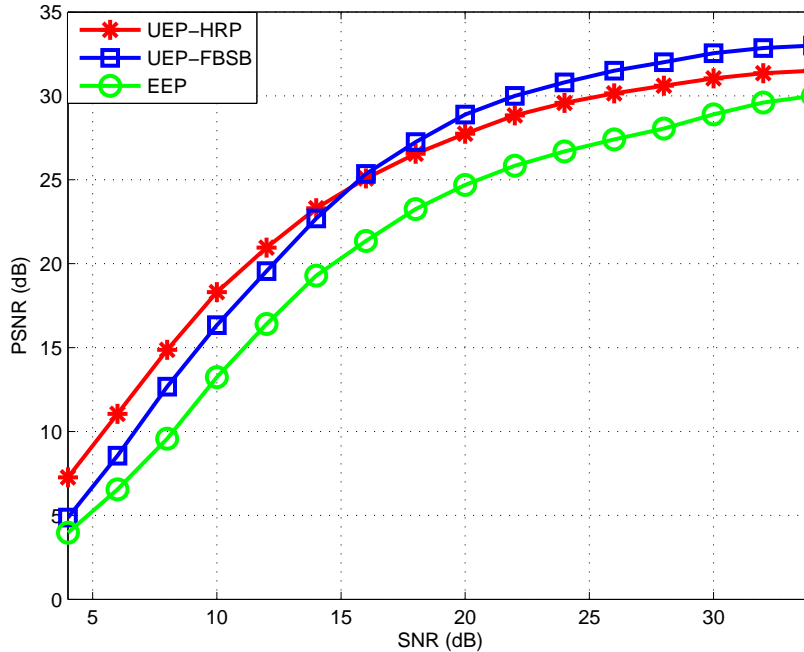


Figure 6.11: Average PSNR of the Interview sequence versus SNR for EEP and UEP based HRP.

of 30 dB). Also this figure shows that the FBSB protocol delivers an increase the PSNR of 3dB at SNR of 8 dB and an increase of 5 dB at high SNR compared to EEP. It is clear that HRP outperforms the FBSB when the SNR is less than 25dB, and vice versa.

Figures 6.13, 6.14, 6.15 and 6.16 demonstrate the subjective results of *Interview* test sequence in terms of subjective quality evaluation for different schemes of UEP based on relay selection. The frame under consideration is 81st of the color, depth map, left and right views as well as EEP. Frames are decoded at SNR = 12 dB. Figure 6.13 shows the original color and depth map sequences. It can be seen from Figure 6.14 that the color and depth sequences in EEP are provided the same protection quality. As a result the quality of the reconstructed left and right views is low due to its direct dependence on the quality of the color sequence, which is also low.

Figure 6.15 illustrates the subjective quality of the UEP based of first best second best protocol. It can be seen that the quality of the color is improved

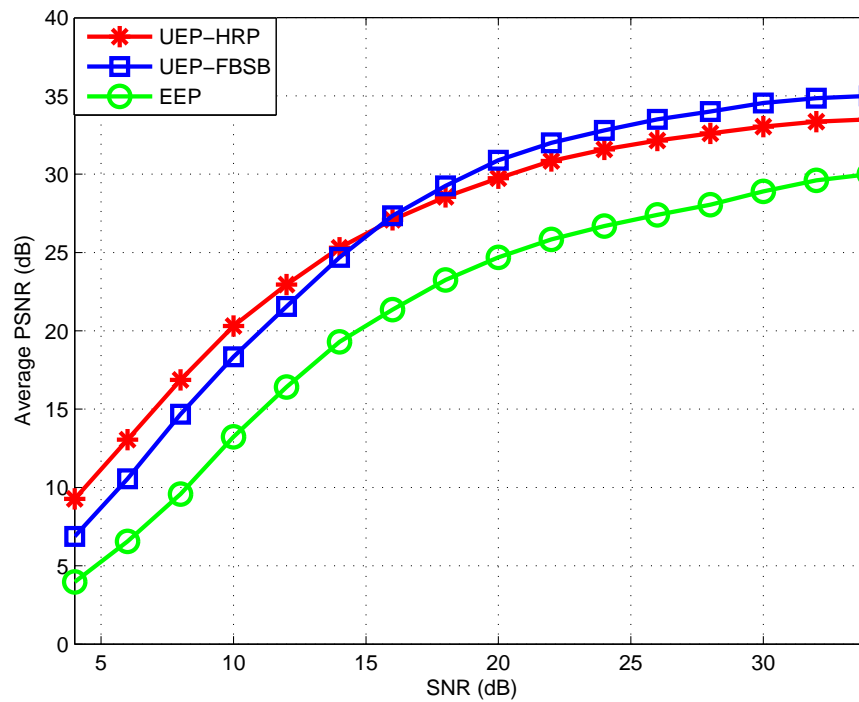


Figure 6.12: Average PSNR of the Interview sequence versus SNR for EEP and UEP based HRP.

relative to the EEP scheme and the depth exhibits the same quality. The visual quality of the left and right views is convenient at the end user. In the case of UEP based HRP at a SNR set to 12 dB, the color sequence can provide a substantial improvement at the expense of the depth quality as shown in Figure 6.16. As a result, even though the depth quality is decreased in UEP, the quality of the reconstructed left and right views at the display end are significantly improved compared with EEP and FBSB protocols.

The results presented above emphasize that the quality of the reconstructed left and right views build upon on the color sequence. By exploiting this outcome, the UEP should be designed to provide more protection to the color sequence rather than depth map. Furthermore, It is obvious from the results obtained that, the output quality in error-prone circumstance has been improved using diversity gain. As a result cooperative communication becomes an attractive technique to achieve this task efficiently.



(a) *Color*



(b) *Depth*



(c) *Left view*



(d) *Right view*

Figure 6.13: Original frames of *Interview* sequence.

(a) *Color*(b) *Depth*(c) *Left view*(d) *Right view*Figure 6.14: Reconstructed frames of EEP at  $SNR = 12$  dB for *Interview* sequence.



(a) *Color sequence*



(b) *Depth sequence*



(c) *Left view*



(d) *Right view*

Figure 6.15: Reconstructed frames of UEP based HRP at  $SNR = 12$  dB for *Interview* sequence.

(a) *Color sequence*(b) *Depth sequence*(c) *Left view*(d) *Right view*

Figure 6.16: Reconstructed frames of UEP based FBSB at  $SNR = 12$  dB for *Interview* sequence.

## 6.8 Conclusion

In this chapter, the advantages of diversity in the physical layer are exploited to provide UEP in 3D video transmission. In particular, the UEP scheme is proposed for color plus depth 3D video transmission in wireless relay networks based on two protocols of relay selection. The closed-form expressions of the BEP and outage probability is then derived for the proposed systems for frequency-selective Rayleigh fading channels. Theoretical and simulation results are provided to show the significant advantages of the proposed protocols over EEP.

From the simulation results, the quality of the color sequence is the dominant factor to the visual quality of the left and right views at the end user. The UEP based HRP, which exhibited higher gains, provides significant improvements at low SNR values. On the other hand, the UEP based FBSB protocol with higher diversity gain shows better results at the high SNR values. Even though the depth sequence of the UEP based HRP shows lower performance at SNR=12dB, the quality of the reconstructed left and right views are sufficiently good.

# Chapter 7

## Conclusions and Future Work

### 7.1 Introduction

In this dissertation, several types of diversity were investigated to increase the reliability of the wireless communication networks. Selective OFDM(A) relaying based on “all-subcarrier” and “per-subcarrier” were studied and Chapters 3 and 5 presented protocols to overcome the drawbacks in existing schemes. Power allocation with and without sub-carrier pairing was investigated in Chapter 4. When used with hybrid relay selection, this technique can enhance the diversity and combat multi-path fading over frequency-selective Rayleigh fading channels. DSFC has been shown to provide a full data rate as well as full diversity order and is easily implemented at the relay nodes to provide Alamouti code at the destination. In addition, cooperative communications can provide high reliability for data transmission by splitting the communication path into multiple paths with short distance has been discussed. These make the high data rate required for applications such as 3D video transmission are possible. Chapter 6 introduced unequal error protection as a component of the physical layer to further exploiting the advantages of the forwarding schemes in relaying systems over error-prone channels.

In this chapter, the contributions envisaged from the work presented in this thesis are summarized, and possible future research into cooperative communica-

tions and high data rate applications is discussed.

## 7.2 Conclusions

In this dissertation, two areas of research in wireless communication systems were investigated.

In Chapter 3, selective OFDM(A) relaying schemes with, and then without direct transmission were investigated over wireless broadband channels. A new scheme using unequal block OFDM relaying was proposed to tradeoff between the complexity and diversity gain as well as to overcome the challenge of load balancing of sub-carriers distribution. The outage probability of the selective OFDM, selective OFDMA, selective block-OFDM and proposed protocol (unequal block OFDM relaying) were addressed and compared. The selective OFDM protocol was less complex than selective OFDMA but it delivered lower performance compared the other protocols. The more complicated selective OFDMA relaying provided higher performance due to takes benefits of the full diversity order available in the system. The system with direct transmission outperformed the one without direct transmission for all protocols due to it exploiting the diversity of broadcast nature. The results also demonstrated that employing direct transmission can provide significant improvement in terms of diversity order and gain for all protocols examined except selective OFDMA.

A new strategy of hybrid relay selection called multicarrier-adaptive hybrid relay protocol (MC-AHRP) was proposed in Chapter 4 to avoid sub-carriers that experience deep fading. It does this by exploiting the advantages of the adaptive DF scheme. The relay selection in Chapter 3 was based on “all-subcarrier basis”. However it is difficult to find relays which can decode all sub-carriers correctly using frequency-selective channels. The “per-subcarrier basis” was considered in the single relay MC-AHRP system. The sub-carriers are divided into two groups depending on their SNR, which can reduce the system complexity and removes the need of a CRC code.

Adaptive bit and power allocation with and without sub-carrier permutation

was adopted to further improve the system performance in terms of bit error probability, outage probability and system capacity. The ABPA was optimized under individual power constraints. The number of bits assigned to each sub-carrier at the source based on the SNR of the first hop and a water-filling algorithm was employed to calculate the power allocated. Since the AF sub-carriers group retransmits the information with same data rates, the water-filling algorithm was used. The total power used by the AF group was easily calculated and the residual power was distributed optimally over sub-carriers in the DF group. This technique substantially improved the system performance, especially where the relay was close to the destination. The closed-form expressions of bit error probability and outage probability were investigated for both the proposed scheme and conventional HRP when the channel fading coefficients are independent and have identical distribution. Simulation and numerical results show that the MC-AHRP outperformed the conventional HRP for the entire range of SNR and at any location except when the relay is located close to the source and a low threshold value is specified. In addition, joint ABPA with sub-carrier pairing provides a slight enhancement to system capacity (about 0.5 bps/Hz) compared with uniform bit and power allocation.

In Chapter 5, a simple implementation of DSFC was added to hybrid relay selection to deliver an Alamouti code to the destination. The selected relay nodes of the proposed hybrid relay protocol were classified into clusters where each cluster consisted of a pair of AF and DF relay nodes. The Alamouti code was implemented at the source and the DF relay node by exploiting the fact that the DF scheme can undertake some processing of the received signal. The DF relay performed a very simple processing (complex conjugate) to the received signal whereas the AF relay simply forwards the received signals after scaling with amplification factor.

Optimization of power allocation with, and then without sub-carrier matching was investigated to reduce the detrimental effect of multi-path fading over frequency-selective channels. In order to reduce the system complexity, the aggregate transmit power for each sub-carrier was divided optimally between the

source and selected relay nodes. Then the assigned power to the selected relay nodes was split amongst them optimally depending on the power channel gains of the second time interval. The simulation results confirm that DSFC implemented with HRP provided full spatial diversity and full data rate. Furthermore, the results demonstrated that the performance of four selected relay nodes using two clusters was equal to two selected relay nodes utilizing a single cluster. The throughput of the joint power allocation with sub-carrier pairing outperformed conventional protocols and the HRP scheme utilizing orthogonal channel transmission (repetition based).

Finally, in Chapter 6 the advantages of cooperative communication in high data rate transmission were used to investigate unequal error protection (UEP) of 3D video transmission. This protocol was employed in the physical layer which does not require any extra information at the transmitter and leads to a decrease in system complexity. Two UEP schemes were proposed based on relay selection. The first was UEP-based on the hybrid relay protocol which was investigated in Chapter 4, while the second one was based on first-best second-best (FBSB) relay selection using the AF approach.

In color-plus-depth 3D video representation, color and depth sequences demonstrate different error sensitivities as color is the dominant contributor to the quality of the reconstruction video at the end user. The color sequence is broadcast over reliable channels and assigned high protection level. For UEP-based HRP, the color sequence is sent through the best relay in the DF group while the depth map sequence is sent via the best relay in AF group. In the first-best second-best AF protocol, the color sequence utilizes the best relay and the depth sequence uses second best. The closed-form expressions of the bit error probability and outage probability were investigated for both schemes. In addition, the PSNR was presented to illustrate the quality of the reconstructed 3D video transmission. The simulation results demonstrate that the color sequence in the UEP-based HRP exhibits better performance than other protocols at low and medium SNR values (less than 17dB) due to it exploiting the advantages of the DF scheme. The color sequence of the UEP-based first-best second-best scheme

provides higher improvement because it achieved higher diversity. The depth sequence of the HRP obtained worse performance compared with FBSB and equal error protection schemes. The proposed UEP-based HRP outperforms the FBSB and conventional EEP schemes in terms of reconstruction left and right views when the SNR is set to 12 dB. It was illustrated that the cooperative gains can be leveraged to improve the reconstruction views by providing high channel gain to the high priority information.

## 7.3 Future Work

While our cooperative protocols can be naturally extended to the kind of highly mobile scenarios in which time-selective fading is encountered, the potential impact of our protocols becomes less substantial when other forms of diversity can be exploited in the system. This section lists some future directions.

- **Selective OFDM relaying with Bit loading**

Most of the previous research of selective OFDM relaying systems assumed that the destination is unable to receive the source signal directly. In this dissertation, four schemes of selective OFDM were studied with, and then without direct transmission to demonstrate the benefits of broadcast nature. The system considered used equal bit loading where the bits were assigned to all sub-carriers uniformly distributed. However, this may not support the frequency diversity of multipath fading channels. A bit loading algorithm could be employed to overcome this problem where the total data rate is spread over all sub-carriers at the transmitter and selected relay(s) according to the end-to-end channel quality. The overall system would be in “outage” if an aggregate rate of all sub-carriers combined at the destination was smaller than the target rate. The performance analysis over frequency-selective channels is a challenging issue.

- **Hybrid Relay Selection for Multi-user Systems**

In multiuser systems, OFDMA has been identified as one of the most commonly used in practical applications. In this kind of system, the sub-carriers should be assigned to all users optimally to obtain higher multiuser diversity. The en-

agement of OFDMA relaying systems with multiuser could improve the system performance. Employing the conventional relays (AF or DF) may corrupt the received signal due to the noise amplification and error propagation caused by the AF and DF relays respectively. The hybrid relay protocol offers a viable solution to overcome these drawbacks, however this can increase the complexity of the seeking algorithm for the best sub-carrier with suitable forwarding scheme. The issue of computational complexity should be addressed for sub-carrier assignment over frequency-selective channels in multiuser OFDMA relaying system.

- **Rateless Code for Cooperative OFDM Networks**

Transmitting high data rates over broadband wireless channels can lead significant signal deterioration. Coding and cooperative OFDM systems have become a promising solution to combat the problem of channel fading. The fixed rate codes require full knowledge of channel parameters at the relay node. This can impose higher overhead signals and as a result induce high transmission latency. Raptor code, which consists of an outer high-rate low density parity check code combined with an inner Luby transform code, or known as “rateless” code can be used. The preliminary results in [227] demonstrated that the computational complexity and latency can be reduced without any loss of reliability by using fountain codes with cooperative communication in single carrier systems. However, it does exhibit a high error floor over error-prone channels. For practical applications, the OFDM-based cooperative network has been extensively studied to provide high data rates with reasonable reliability. The analysis of the performance of raptor code concatenated with OFDM relaying systems over noisy channels is an open issue.

- **Multi-views 3D video Transmission over Cooperative Networks**

Three-dimensional video transmission has received significant development in high data rate systems. Several techniques have exploited the advantages of the physical layer concept to achieve unequal error protection for multimedia transmission. These protocols considered a single view of 3D where only a single image was transmitted for each scene. In order to deliver a good quality scene at the destination, multiview video technique is adopted where a high number of views

have to be provided of the same scene. This can generate a huge amount of data and it becomes a major challenge in bandwidth limited channel problem environments. This is worthy of future investigation.

## 7.4 Final Remarks

Diversity is a potential technique to combat the detrimental effect of multipath fading in broadband wireless networks. It has been extensively studied in recent years and are still an active area of research. Diverse techniques have been investigated in this dissertation including; relay selection, distributed space frequency coding, power allocation and adaptive bit and power allocation.

The demand for high data rate applications is increasing rapidly due to evolution in communication consumption. 3D video applications over wireless networks become more promising and attractive which require re-design of existing systems to counter the inherently high error probability and bandwidth constraints. It is hoped that the proposed algorithms will find their applications in the next generation of wireless networks.



# References

- [1] S. M. Alamouti, “A simple transmit diversity technique for wireless communications,” *IEEE J. Sel. Areas Commun.*, vol. 16, no. 8, pp. 1451–1458, Aug. 1998.
- [2] V. Tarokh, H. Jafarkhani, and A. Robert Calderbank, “Space-time block coding for wireless communications: performance results,” *IEEE J. Sel. Areas Commun.*, vol. 17, no. 3, pp. 451–460, Mar. 1999.
- [3] W. Zhang, X.-G. Xia, and P. C. Ching, “High-rate full-diversity space-time-frequency codes for broadband MIMO block-fading channels,” *IEEE Trans. Commun.*, vol. 55, no. 1, pp. 25–34, Jan 2007.
- [4] J. N. Laneman, D. N. C. Tse, and G. W. Wornell, “Cooperative diversity in wireless networks: Efficient protocols and outage behavior,” *IEEE Trans. Inf. Theory*, vol. 50, no. 12, pp. 3062–3080, 2004.
- [5] P. S. Chow, J. M. Cioffi, and J. A. C. Bingham, “A practical discrete multitone transceiver loading algorithm for data transmission over spectrally shaped channels,” *IEEE Journal on Communications*, vol. 43, no. 2/3/4, pp. 773–775, 1995.
- [6] Y. Noh, H. Lee, W. Lee, and I. Lee, “Design of unequal error protection for MIMO-OFDM systems with hierarchical signal constellations,” *Journal of Communication and Networks*, vol. 9, no. 2, pp. 167–176, 2007.
- [7] S. Zhao, Mingle You, Yan Meng, and L. Gui, “Scalable video transmission over MIMO-OFDM wireless systems with antenna selection,” in *Proc.*

- IEEE 21st International Symposium on Personal Indoor and Mobile Radio Communications (PIMRC)*, Istanbul, Turkey, Sept. 2010, pp. 2563–2568.
- [8] Z. Yang and X. Wang, “Scalable video broadcast over downlink MIMO OFDM systems,” *IEEE Transactions on Circuits and Systems for Video Technology*, vol. 32, no. 2, pp. 212–223, Feb. 2013.
- [9] D. S. Michalopoulos, H. A. Suraweera, G. K. Karagiannidis, and R. Schober, “Amplify-and-forward relay selection with outdated channel estimates,” *IEEE Trans. Commun.*, vol. 60, no. 5, pp. 1278–1290, May. 2012.
- [10] B. V. Nguyen, R. O. Afolabi, and K. Kim, “Dependence of outage probability of cooperative systems with single relay selection on channel correlation,” *IEEE Commun. Lett.*, vol. 17, no. 11, pp. 2060–2063, Nov. 2013.
- [11] B. Can, H. Yomo, and E. D. Carvalho, “Hybrid forwarding scheme for cooperative relaying in OFDM based networks,” in *Proc. IEEE International Conference on Communications, ICC '06.*, Istanbul, Turkey, June 2006, pp. 4520–4525.
- [12] T. T. Duy and H.-Y. Kong, “Performance analysis of hybrid decode-amplify-forward incremental relaying cooperative diversity protocol using snr-based relay selection,” *Journal of Communications and Networks*, vol. 14, no. 6, pp. 703–709, Dec. 2012.
- [13] K. K. Gurrula and S. Das, “Performance study of hybrid decode-amplify-forward (HDAF) scheme in distributed Alamouti coded cooperative network,” in *Proc. IEEE International Conference on Advances in Computing, Communications and Informatics (ICACCI)*, Mysore, India, Aug. 2013, pp. 271–276.
- [14] J. N. Laneman and G. W. Wornell, “Distributed space-time coded protocols for exploiting cooperative diversity in wireless networks,” *IEEE Trans. Inf. Theory*, vol. 49, pp. 2415–2425, Oct. 2003.

- [15] Y. Zhao, R. Adve, and T. J. Lim, "Outage probability at arbitrary SNR with cooperative diversity," *IEEE Comm. Litter*, vol. 9, no. 8, pp. 700–702, 2005.
- [16] N. C. Beaulieu and J. Hu, "A closed-form expression for the outage probability of decode-and-forward relaying in dissimilar Rayleigh fading channel," *IEEE Comm. Litter*, vol. 10, pp. 813–815, Dec. 2006.
- [17] S. S. Ikki and M. H. Ahmed, "Performance analysis incremental relaying cooperative diversity networks over Rayleigh fading channels," in *Proc. IEEE Wireless Communications and Networking Conference, WCNC '08.*, Las Vegas, USA, Mar. 2008, pp. 1311–1315.
- [18] Y. Li, B. Vucetic, Z. Chen, and J. Yuan, "An improved relay selection scheme with hybrid relaying protocols," in *Proc. IEEE Conference Global Telecommunications Conference, GLOBECOM '07.*, Washington, DC, Nov. 2007, pp. 3704–3708.
- [19] A. Bletsas, H. Shin, and M. Z. Win, "Cooperative communications with outage-optimal opportunistic relaying," *IEEE Trans. Wireless Commun.*, vol. 6, no. 9, pp. 3450–3460, Sep. 2007.
- [20] M.A.Manna, G.Chen, and J.A.Chambers, "Outage probability for four relay selection in wireless relay networks," in *Proc. IEEE 20th International Conference on Software, Telecommunications and Computer Networks (SoftCOM)*, Split, Croatia, Sept. 2012, pp. 1–4.
- [21] M. Abouelseoud and A. Nosratinia, "Heterogeneous relay selection," *IEEE Trans. Wireless Commun.*, vol. 12, no. 4, pp. 1735–1743, Apr. 2013.
- [22] IEEE802.11-1999, "Wireless LAN medium access control (MAC) and physical layer (PHY) specifications," August 1999.
- [23] IEEE802.16-2004, "IEEE standard for local and metropolitan area networkspart 16: Air Interface for Broadband Wireless Access Systems," May 2004.

- [24] Y. Lin, W. Wang, B. Fan, L. Huang, and K. Zheng, "Resource allocation optimization for OFDM-based amplify-and-forward multi-relay system," in *Proc. IEEE International Conference on Wireless Communications and Networking WCNC*, Budapest, Hungary, Apr. 2009, pp. 1–6.
- [25] Y. Ma, N. Yi, and R. Tafazolli, "Bit and power loading for OFDM-based three-node relaying communications," *IEEE Trans. Signal Process.*, vol. 56, no. 7, pp. 3236–3247, 2008.
- [26] D. Hughes-Hartogs, "Ensemble modulated structure for imperfect transmission media," U. S. Patent Nos. 4,679,227 (July 1978), 4,731,816 (March 1988), and 4,833,796 (May 1989).
- [27] J. A. C. Bingham, "Multicarrier modulation for data transmission: an idea whose time has come," *IEEE Journal on Communications Magazine*, vol. 28, no. 5, pp. 5–14, May 1990.
- [28] R. F. H. Fisher and J. B. Huber, "A new algorithm for discrete multi-tone transmission," in *Proc. IEEE Conference Global Telecommunications Conference, GLOBECOM '96.*, London, UK, Nov. 1996, pp. 724–728.
- [29] J. Campello, "Optimal discrete bit loading for multicarrier modulation systems," in *Proc. International Symposium on Information Theory (ISIT)*, Cambridge, MA, USA, Aug. 1998, p. 193.
- [30] Y. Li and G. SU, "An adaptive modulation and power-allocation algorithm in OFDM system," in *Proc. IEEE International Conference on Communications, Circuits and Systems, ICCAS*, June 2004, pp. 339–343.
- [31] G. Lai, J. Yin, and fan Lin Huawen Yu, "Performance of adaptive bit and power allocation MIMO-OFDM system based on greedy algorithm," in *Proc. IEEE International Conference on Wireless Communications, Networking and Mobile Computing*, Maui, HI, Sept. 2005, pp. 24–29.
- [32] K. Liu, F. Yin, W. Wang, and Y. Liu, "An efficient greedy loading algorithm for adaptive modulation in OFDM systems," in *Proc. IEEE 16th Interna-*

- tional Symposium on Personal, Indoor and Mobile Radio Communications, PIMRC*, Berlin, Germany, Sept. 2005, pp. 1130–1134.
- [33] Y. Wu, J. Tan, and Y. Fu, “Adaptive bit and power loading for OFDM systems,” in *Proc. IEEE IET International Conference on Wireless, Mobile and Multimedia Networks*, Hangzhou, China, Nov. 2006, pp. 1–4.
- [34] Z. Xiaoguang, T. Zhijian, Z. Hongdang, Z. Liping, and M. Xiao, “Performance of adaptive OFDM transceiver in wireless channels with loading algorithm,” in *Proc. IEEE International Conference on Intelligent Computing and Intelligent Systems, ICIS*, Shanghai, China, Nov. 2009, pp. 13–16.
- [35] I. Hammerstrom and A. Wittneben, “On the optimal power allocation for nonregenerative OFDM relay links,” in *Proc. ICC*, Istanbul, Turkey, Jun. 2006, pp. 4463–4468.
- [36] M. Herdin, “A chunk based OFDM amplify-and-forward relaying scheme for 4G mobile radio systems,” in *proc. IEEE international Conference on Communications, ICC’06*, June 2006, pp. 4507–4512.
- [37] R. Ayadi, I. Kammoun, and M. Siala, “An efficient space-frequency coding scheme over unknown frequency-selective fading channels,” in *Proc. IEEE 24th International Symposium on Personal, Indoor and Mobile Radio Communications*, London, United Kingdom, Sep. 2013, pp. 1163–1167.
- [38] S. Yiu, D. Calin, O. Kaya, and K. Yang, “Distributed STBC-OFDM and distributed SFBC-OFDM for frequency-selective and time-varying channels,” in *Proc. IEEE Wireless Communications and Networking Conference (WCNC)*, Paris, France, Apr. 2012, pp. 251–255.
- [39] G. J. Sullivan and T. Wiegand, “Video compression—from concept to the H.264/AVC standard,” *Proceedings of the IEEE*, vol. 93, no. 1, pp. 18–31, 2005.
- [40] C. T. Hewage, Z. Ahmad, S. T. Worrall, S. Dogan, W. Fernando, and A. Kondo, “Unequal error protection for backward compatible 3-D video

- transmission over WiMAX,” in *Proc.in IEEE International Symposium on Circuits and Systems, ISCAS 2009*, Taipei, Taiwan, May 2009, pp. 125–128.
- [41] M. F. Sabir, R. W. Heath, and A. C. Bovik, “An unequal error protection scheme for multiple input multiple output systems,” in *Proc.in Thirty-Sixth Asilomar Conference on Signals, Systems and Computers*, Pacific Grove, California, USA, Nov. 2002, pp. 575–579.
- [42] Y. Qian, L. Ping, and M. Ronghong, “Unequal error protection scheme for multiple-input and multiple-output wireless systems,” in *Proc.in IEEE 64th Vehicular Technology Conference*, Montreal, Canada, Sep. 2006, pp. 1–5.
- [43] D. Song and C. W. Chen, “Scalable H.264/AVC video transmission over standard MIMO wireless systems with adaptive channel selection based on partial channel information,” *IEEE Transactions on Circuits and Systems for Video Technology*, vol. 17, no. 9, pp. 1218–1226, 2007.
- [44] M. M. B. Kamolrat, W. Fernando and A. Kondo, “Joint source and channel coding for 3D video with depth image-based rendering,” *Transactions on Consumer Electronics*, vol. 54, no. 2, pp. 887–894, May 2008.
- [45] I. K. Sileh, W. Xiang, and K. M. Alajel, “Outage probability of unequal block-based OFDM amplify-and-forward relay protocol over wideband channels,” in *Proc.International Symposium on Communications and Information Technologies (ISCIT)*, Gold Coast, Australia, Oct. 2012, pp. 604–608.
- [46] I. K. Sileh, W. Xiang, and A. Maxwell, “Error probability of OFDM-based hybrid relay protocols over wideband fading channels,” in *Proc. IEEE International Conference on Ultra-Wideband (ICUWB)*, Sydney, Australia, Sep. 2013, pp. 255–260.
- [47] ———, “Joint subcarrier pairing and resource allocation for adaptive hybrid relay protocol in OFDM systems,” in *Proc. IEEE 24th International Sympo-*

- sium on Personal, Indoor and Mobile Radio Communications (PIMRC13)*, London, UK, Sep. 2013, pp. 2011–2015.
- [48] I. K. Sileh and W. Xiang, “Distributed space-frequency coding for OFDM-based hybrid relay selection,” in *Proc. IEEE International Symposium on Communications and Information Technologies (ISCIT)*, Gold Coast, Australia, Oct. 2012, pp. 599–603.
- [49] I. K. Sileh, W. Xiang, and A. Maxwell, “Power allocation of distributed space-frequency coding for OFDM-based hybrid relay selection,” in *Proc. IEEE 7th International Conference on Signal Processing and Communication Systems, ICSPCS2013*, Gold Coast, Australia, Dec. 2013.
- [50] I. K. Sileh, K. M. Alajel, and W. Xiang, “Cooperative relay selection based UEP scheme for 3D video transmission over Rayleigh fading channel,” in *Proc. IEEE International Conference on Digital Image Computing Techniques and Applications (DICTA 2011)*, Noosa, Australia, Dec. 2011, pp. 689–693.
- [51] K. M. Alajel, W. Xiang, and I. K. Sileh, “Best relays selection method for error-resilient 3-D video transmission,” in *Proc. 12th International Symposium on Communications and Information Technologies (ISCIT 2012)*, Gold Coast, Australia, Oct. 2012, pp. 1–5.
- [52] E. C. V. D. Meulen, *Transmission of Information in a T-Terminal Discrete Memoryless Channel*, Berkeley, CA: Dept. Statistics, Univ. California, 1968.
- [53] —, “Three-terminal communication channels,” in *Proc. International Symposium on Information Theory*, Noordwijk, The Netherlands, June 1970, pp. 15–19.
- [54] T. Cover and A. E. Gamal, “Capacity theorems for the relay channel,” vol. 25, no. 5, p. 572584, Sept. 1979.
- [55] A. Sendonaris, E. Erkip, and B. Aazhang, “User cooperation diversity. part

- I: System description,” *IEEE Trans. Commun.*, vol. 51, no. 11, pp. 1927–1938, Nov. 2003.
- [56] Y. Zhao, R. Adve, and T. J. Lim, “Improving amplify-and-forward relay networks: optimal power allocation versus selection,” *IEEE Trans. Wireless Commun.*, vol. 6, no. 8, pp. 3114–3123, Aug. 2007.
- [57] A. Sendonaris, E. Erkip, and B. Aazhang, “User cooperation diversity—part II: Implementation aspects and performance analysis,” *IEEE Trans. Commun.*, vol. 51, no. 11, pp. 1939–1948, Nov. 2003.
- [58] T. E. Hunter and A. Nosratinia, “Cooperation diversity through coding,” in *Proc. IEEE Int. Symp. Inf. Theory*, Lausanna, Switzerland, Jul. 2002, p. 220.
- [59] J. Boyer, D. D. Falconer, and H. Yanikomeroglu, “Multihop diversity in wireless relaying channels,” *IEEE Trans. Commun.*, vol. 52, no. 10, pp. 1820–1830, 2004.
- [60] Y. Li, W. Wang, J. Kong, W. Hong, X. Zhang, and M. Peng, “Power allocation and subcarrier pairing in OFDM-based relaying networks,” in *Proc. IEEE International Conference on Communications, ICC '08.*, Beijing, China, May. 2008, pp. 2602–2606.
- [61] H. Mheidat and M. Uysal, “Impact of receive diversity on the performance of amplify-and-forward relaying under APS and IPS power constraints,” vol. 10, no. 6, pp. 468–470, June 2006.
- [62] M. Kaneko, K. Hayashi, P. Popovski, K. Ikeda, H. Sakai, and R. Prasad, “Amplif-and-forward cooperative diversity schemes for multi-carrier systems,” *IEEE Trans. Wireless Commun.*, vol. 7, no. 5, pp. 1845–1850, May 2008.
- [63] Y. Ding and M. Uysal, “Amplify-and-forward cooperative OFDM with multiple-relays: Performance analysis and relay selection methods,” *IEEE Trans. Wireless Commun.*, vol. 8, no. 10, pp. 4963–4968, Oct. 2009.

- [64] T. Islam, R. Schober, R. K. Mallik, and V. K. Bhargava, "Amplify-and-forward cooperative diversity for BICM-OFDM systems," in *proc. IEEE Global Telecommunications Conference (GLOBECOM 10)*, Miami, Florida, USA, Dec. 2010, pp. 1–6.
- [65] R.-L. Chung and S.-H. Chang, "Cooperative MMSE OFDM receiver for half-duplex and multiple-relays system," in *proc. IEEE International Symposium on Information Theory and its Applications (ISITA)*, Taichung, Taiwan, Oct. 2010, pp. 17–20.
- [66] W. Su, A. K. Sadek, and K. J. R. Liu, "SER performance analysis and optimum power allocation for decode-and-forward cooperation protocol in wireless networks," in *Proc. IEEE Global Telecommunications Conference, WCNC*, New Orleans, USA, Mar. 2005, pp. 984–989.
- [67] X. Liu and W. Su, "Optimum selection relaying protocols in cooperative wireless networks," in *Proc. IEEE Global Telecommunications Conference, WCNC 06*, San Francisco, California, USA, Dec.. 2006, pp. 984–989.
- [68] J. Hu and N. C. Beaulieu, "Performance analysis of decode-and-forward relaying with," *IEEE Comm. Litter*, vol. 11, no. 6, pp. 489–491, 2007.
- [69] L. Dai, B. Gui, and J. Leonard J. Cimini, "Selective relaying in OFDM multihop cooperative networks," in *Proc. IEEE Wireless Communications and Networking Conference, WCNC 2007*, Hong Kong, China, Mar. 2007, pp. 964–969.
- [70] B. Gui, L. Dai, and J. Leonard J. Cimini, "Selective relaying in cooperative OFDM systems: Two-hop random network," in *Proc. IEEE Wireless Communications and Networking Conference, WCNC 2008*, Las Vegas, USA, Apr. 2008, pp. 996–1001.
- [71] W. Yang, W. Yang, N. Li, and Y. Cai, "Outage probability of selective relaying in cooperative OFDM network over Nakagami-m fading channels,"

- in *Proc. IEEE International Communication Conference on Wireless mobile and Computing*, Marrakech, Morocco, Oct. 2009, pp. 148–151.
- [72] W. Yang, Y. Cai, and W. Yang, “Closed-form error analysis of OFDM-based selective decode-and forward cooperative networks over Nakagami-m fading channels,” in *Proc. IEEE 6th International Conference on Wireless Communications Networking and Mobile Computing (WiCOM)*, Chengdu, China, Sep. 2010, pp. 1–5.
- [73] W. Yang, W. Yang, and Y. Cai, “Outage probability of OFDM-based selective decode-and forward cooperative networks over Nakagami-m fading channels,” *Wireless Pers Commun*, vol. 56, pp. 503–515, 2011.
- [74] H. Boostanimehr and V. K. Bhargava, “Outage capacity analysis for OFDM decode-and-forward systems in frequency selective Rayleigh fading channels,” *IEEE Commun. Lett.*, vol. 16, no. 6, pp. 937–940, June. 2012.
- [75] S. S. Ikki and M. H. Ahmed, “On the performance of adaptive decode-and-forward cooperative diversity with the Nth best-relay selection scheme,” in *Proc. IEEE Global Telecommunications Conference, GLOBECOM '09.*, Honolulu, USA, Dec. 2009, pp. 1–6.
- [76] J. Proakis, *Digital Communications, 4th ed.* New York: McGraw-Hill, 2000.
- [77] R. Madan, N. B. Mehta, A. F. Molisch, and J. Zhang, “Energy-efficient cooperative relaying over fading channels with simple relay selection,” in *Proc. IEEE Conference Global Telecommunications Conference, GLOBECOM '06.*, San Francisco, California, USA, Dec. 2006, pp. 1–6.
- [78] S. S. Ikki and M. H. Ahmed, “Performance analysis of decode-and-forward incremental relaying cooperative-diversity networks over Rayleigh fading channels,” in *Proc. IEEE Vehicular Technology Conference, VTC Spring*, Barcelona, Spain, Apr. 2009, pp. 1–6.

- [79] Y. Li and V. B., "On the performance of a simple adaptive relaying protocol for wireless relay network," in *Proc. IEEE Vehicular Technology Conference, VTC Spring 2008*, May. 2008, pp. 2400–2405.
- [80] H. Lu, H. Nikookar, and X. Lian, "Performance evaluation of hybrid DF-AF OFDM cooperative in Rayleigh channel," in *Proc. of the 3rd European Wireless Technology Conference*, Paris, France, Sep. 2010, pp. 85–88.
- [81] Q. Huo, T. Liu, L. Song, and B. Jiao, "All-participate hybrid forward cooperative communications with multiple relays," in *Proc. IEEE International Conference on Wireless Communications and Signal Processing (WCSP), 2010.*, Oct. 2010, pp. 1–6.
- [82] T. Liu, L. Song, and B. Jiao, "Threshold-based frame error rate analysis of incremental hybrid relay selection scheme," in *Proc. IEEE International Globecom, 2010.*, Oct. 2010, pp. 1–5.
- [83] T. Liu, L. Song, B. Jiao, and Y. Zhao, "A threshold-based hybrid relay selection scheme," in *Proc. IEEE International Globecom, 2010.*, Oct. 2010, pp. 1–5.
- [84] T. Liu, L. Song, Y. Li, Q. Huo, and B. Jiao, "Performance analysis of hybrid relay selection in cooperative wireless system," *IEEE Trans. Wireless Commun.*, vol. 60, no. 3, pp. 779–788, Mar. 2012.
- [85] T. Liu, L. Song, and B. Jiao, "Optimum power allocation for hybrid relay selection schemes," in *Proc. IEEE International Conference on Wireless Communications Signal Processing, WCSP '09.*, Nov. 2009, pp. 1–5.
- [86] G. Chuai, L. Gao, and B. Zhang, "Outage probability performance of hybrid forwarding for wireless relaying," in *Proc. of IC-NIDC*, Nov. 2009, pp. 847–850.
- [87] L. Yubo, Y. Qinye, and W. Junsong, "Outage optimal relaying through opportunistic hybrid forward cooperation," *SCIENCE CHINA Information Sciences*, vol. 54, no. 6, pp. 1264–1273, Aug. 2011.

- [88] H. Boujemaa, "Static hybrid amplify and forward AF and decode and forward DF relaying for cooperative systems," *Physical Communication*, vol. 4, pp. 196–205, 2011.
- [89] T. Q. Duong and H.-J. Zepernick, "On the performance gain of hybrid decode-and-forward (DAF) cooperative communication," *EURASIP Journal on Wireless Communications and Networking*, vol. 2009, article ID 479463, 10 pages, 2009. doi:10.1155/2009/479463.
- [90] H. Chen, J. Liu, C. Zhai, and L. Zheng, "Performance analysis of SNR-based hybrid decode-amplify-forward cooperative diversity over Rayleigh fading channels," in *Proc. of IEEE WCNC*, Nov. 2010, pp. 1318–1322.
- [91] S. Bouanen, H. Boujemaa, and W. Ajib, "Threshold-based adaptive decode-amplify-forward relaying protocol for cooperative systems," in *Proc. of International Wireless Communications and Mobile Computing*, Nov. 2011, pp. 725–730.
- [92] S. M. Mishkat-Ul-Masabih, M. S. Alam, and M. R. Hasan, "Adaptive relay selection scheme using hybrid forwarding protocol," in *Proc. International Conference on ICT Convergence (ICTC)*., Seb 2011, pp. 46–51.
- [93] A. Heo and D.-J. Park, "Adaptive relay selection on individual power constraint for hybrid relay systems," in *Proc. of IEEE International Symposium Communication and Information Technology*, Nov. 2009, pp. 1496–1497.
- [94] A. Heo, J.-H. Park, S.-R. Jin, and D.-J. Park, "Adaptive relay selection for hybrid relay systems," in *Proc. of IEEE International Conference on Computer and Automation Engineering*, Nov. 2010, pp. 432–435.
- [95] X. Li, J. Zhang, Y. Zhang, and J. Huang, "Power allocation for OFDM based links in hybrid forward relay," in *Proc. IEEE International Conference on Vehicular Technology Conference, VTC Spring '09.*, April 2009, pp. 1–5.

- [96] M. O. Hasna and M.-S. Alouini, "Optimal power allocation for relayed transmission over Rayleigh-fading channels," *IEEE Trans. Wireless Commun.*, vol. 3, no. 6, pp. 1999–2004, Nov. 2004.
- [97] Z. Qi, Z. Jingmei, S. Chunju, W. Ying, Z. Ping, and H. Rong, "Power allocation for regenerative relay channel with Rayleigh fading," in *Proc. Vehicular Technology Conference, VTC Spring*, Milan, Italy, May. 2004, pp. 1167–1171.
- [98] Z. Jingmei, Z. Qi, S. Chunju, W. Ying, Z. Ping, and Z. Zhang, "Adaptive optimal transmit power allocation for non-regenerative wireless relaying system," in *Proc. Vehicular Technology Conference, VTC Spring*, Milan, Italy, May. 2004, pp. 1213–1217.
- [99] C. Y. Wong, R. S. Cheng, K. B. Letaief, and R. D. Murch, "Multiuser OFDM with adaptive sub-carrier, bit, and power allocation," *IEEE J. Sel. Areas Commun.*, vol. 17, no. 10, pp. 1747–1758, Oct. 1999.
- [100] D. Kivanc, L. Guo-Qing, and L. Hui, "Computationally efficient bandwidth allocation and power control for OFDMA," *IEEE Trans. Wireless Commun.*, vol. 2, pp. 1150–1158, 2003.
- [101] A. M. Wyglinski, F. Labeau, and P. Kabal, "Bit loading with BER-constraint for multicarrier systems," *IEEE Trans. Wireless Commun.*, vol. 4, no. 4, pp. 1383–1387, July. 2005.
- [102] J. Jang, K. B. Lee, and Y.-H. Lee, "Transmit power adaption for multiuser OFDM systems," *IEEE J. Sel. Areas Commun.*, vol. 21, pp. 171–178, 2003.
- [103] T. Wang and L. Vandendorpe, "Sum rate maximized resource allocation in multiple DF relays aided OFDMA transmission," *IEEE J. Sel. Areas Commun.*, vol. 29, no. 8, pp. 1559–1571, 2011.
- [104] E. Pazouki and K. Navaie, "Resource allocation in decode-and-forward relaying systems based on OFDM," in *Proc. 20th Iranian Conference on Electrical Engineering (ICEE)*, Tehran, Iran, May. 2012, pp. 1066–1071.

- [105] J. Wang, X. Chai, X. Zhang, Z. Zhang, and K. Long, "Adaptive power allocation in cooperative OFDM transmission with three-hop df relaying," in *Proc. IET International Conference on Information and Communications Technologies (IETICT 2013)*, Beijing, China, Apr. 2013, pp. 387–393.
- [106] N. Yi, Y. Ma, and R. Tafazolli, "Bit and power loading for OFDM with an amplify-and-forward cooperative relay," in *Proc. IEEE 19th International Symposium on Personal, Indoor and Mobile Radio Communications PIMRC 2008*, Sep. 2008, pp. 1–5.
- [107] —, "Rate-adaptive bit and power loading for OFDM based DF relaying," in *Proc. IEEE 65th Vehicular Technology Conference, VTC2008-Spring*, Marina Bay, Singapore, May. 2008, pp. 1340–1344.
- [108] W. Ying, Q. Xin-Chun, W. Tong, and L. Bao-Ling, "Power allocation and subcarrier pairing algorithm for regenerative OFDM relay system," in *Proc. IEEE 65th Vehicular Technology Conference, VTC2007-Spring*, Tokyo, Japan, Apr. 2007, pp. 2727–2731.
- [109] Y. Pan, A. Nix, and M. Beach, "Resource allocation technique for OFDMA decode-and-forward relaying networks," in *Proc. IEEE 65th Vehicular Technology Conference, VTC2008-Spring*, Marina Bay, Singapore, May. 2008, pp. 1717–1721.
- [110] L. Vandendorpe, R. T. Duran, J. Louveaux, and A. Zaidi, "Power allocation for OFDM transmission with DF relaying," in *Proc. IEEE International Conference on Communications, ICC '08.*, Beijing, China, May. 2008, pp. 3795 – 3800.
- [111] L. Vandendorpe, J. Louveaux, O. Oguz, and A. Zaidi, "Improved OFDM transmission with DF relaying and power allocation for a sum power constraint," in *Proc. 3rd International Symposium on Wireless Pervasive Computing, ISWPC 2008*, Santorini, Greece, May. 2008, pp. 665–669.

- [112] ———, “Rate-optimized power allocation for OFDM transmission with multiple DF/regenerative relays and an improved protocol,” in *Proc. IEEE International Conference on Wireless Communications and Networking WCNC*, Budapest, Hungary, Apr. 2009, pp. 1–6.
- [113] L. Wang, H. Zhao, and J. W. Yong Xi and, “Optimal power allocation and relay selection in OFDM-based cooperative systems,” in *Proc. 6th International Conference on Wireless Communications Networking and Mobile Computing (WiCOM)*, Chengdu, China, Sept. 2010, pp. 1–5.
- [114] J. Shi and W. Wu, “Adaptive power allocation for multi-hop OFDM system with non-regenerative relaying,” in *Proc. IEEE International Conference on Computer Science and Software Engineering*, Wuhan, Hubei, China, Dec. 2008, pp. 1077–1080.
- [115] M. Saito, C. R. Athaudage, and J. Evans, “On power allocation for dual-hop amplify-and-forward OFDM relay systems,” in *Proc. IEEE Global Telecommunications Conference, GLOBECOM 2008*, New Orleans, Louisiana, USA, Nov. 2008, pp. 1–6.
- [116] W. Zhang, U. Mitra, and M. Chiang, “Optimization of amplify-and-forward multicarrier two-hop transmission,” *IEEE Trans. Commun.*, vol. 59, no. 5, pp. 1434–1445, 2011.
- [117] Y. Guan-Ding, Z. Zhao-yang, C. Yan, C. Shi, and Q. Pei-Liang, “Power allocation for non-regenerative OFDM relaying channels,” in *Proc. International Conference on Wireless Communications, Networking and Mobile Computing*, May. 2005, pp. 185–188.
- [118] T. Liu, L. Song, and B. Jiao, “Optimum power allocation for hybrid relay selection schemes,” in *Proc. IEEE International Conference on Wireless Communication and Signal Processing WCSP*, Nanjing, China, Nov. 2009, pp. 1–6.

- [119] M. Ibrahim and B. Liang, "Efficient power allocation in cooperative OFDM system with channel variation," in *Proc. IEEE International Conference on Communications, ICC '08.*, Beijing, China, May. 2008, pp. 3022–3028.
- [120] J. Lu, K. B. Letaief, J. C.-I. Chuang, and M. L. Liou, "M-PSK and M-QAM BER computation using single-space concept," *IEEE Trans. Commun.*, vol. 47, no. 2, pp. 181–184, Feb. 1998.
- [121] E. Kocan, M. Pejanovic-Djurisic, D. S. Michalopoulos, and G. K. Karagiannis, "BER performance of OFDM amplify-and-forward relaying system with subcarrier permutation," in *Proc. IEEE 1st International Conference on Wireless Communication, Vehicular Technology, Information Theory and Aerospace and Electronic Systems Technology, Wireless VITAE 2009*, Aalborg, Denmark, May 2009, pp. 252–256.
- [122] S. Zhenhui, W. Xiaoxiang, and Z. Hongtao, "Power allocation and subcarrier pairing for OFDM based AF cooperative diversity systems," in *Proc. IEEE 69th Vehicular Technology Conference, VTC2009-Spring.*, Barcelona, Spain, Apr. 2009, pp. 1–5.
- [123] Z. Mingyu, L. Lihua, W. Haifeng, Z. Ping, and T. Xiaofeng, "Sub-carrier coupling for OFDM based AF multi-relay systems," in *Proc. 18th Annual IEEE International Symposium on Personal, Indoor and Mobile Radio Communications (PIMRC'07)*, Athens, Greece, Sep. 2007, pp. 1–5.
- [124] E. Jeon, J. Yang, and D. K. Kim, "A low complexity subcarrier pairing scheme for OFDM based multiple AF relay systems," in *Proc. Third International Conference on Convergence and Hybrid Information Technology ICCIT '08.*, Busan, Korea, Nov. 2008, pp. 675–678.
- [125] F. Li, X. Ke, and L. Wang, "A relay selection scheme with limit feedback in OFDM relay networks based on subcarrier mapping," in *Proc. IEEE Youth Conference on Information Computing and Telecommunications (YC-ICT)*, Beijing, China, Nov. 2010, pp. 93–96.

- [126] S. Chen, F. Liu, X. Zhang, C. Xiong, and D. Yang, "Symbol error performance analysis of OFDM relaying system with subcarrier mapping scheme," *IEEE Commun. Lett.*, vol. 14, no. 7, pp. 638–640, 2010.
- [127] T. Riihonen, R. Wichman, J. Hamalainen, and A. Hottinen, "Analysis of subcarrier pairing in a cellular OFDM relay link," in *Proc. International ITG Workshop on Smart Antennas*, Feb. 2008, pp. 104–111.
- [128] K. Feng, F. Suili, and Z. Hongcheng, "Capacity analysis of subcarrier pairing for OFDMA based DF relay link over Rayleigh channel," in *Proc. 11th IEEE Singapore International Conference on Communication Systems ICCS*, Guangzhou, China, Nov. 2008, pp. 1635–1639.
- [129] C. K. Ho and A. Pandharipande, "BER minimization in relay-assisted OFDM systems by subcarrier permutation," in *Proc. IEEE 65th Vehicular Technology Conference, VTC2008-Spring*, Marina Bay, Singapore, May 2008, pp. 1489–1493.
- [130] W. Wang, S. Yan, and S. Yang, "Optimally joint subcarrier matching and power allocation in OFDM multihop system," *EURASIP Journal on Advances in Signal Processing*, vol. 2008, no. 146, pp. 1–8, Jan. 2008.
- [131] X. Li, G. Zhang, and J. Qin, "Joint power allocation and subcarrier pairing for cooperative OFDM AF multi-relay networks," *IEEE Commun. Lett.*, vol. 17, no. 5, pp. 872–875, May 2013.
- [132] W. Wang, S. Yan, and S. Yang, "Capacity maximization for OFDM two-hop relay system with separate power constraints," *IEEE Trans. Veh. Technol.*, vol. 58, no. 9, pp. 4943–4953, 2009.
- [133] C.-N. Hsu, H.-J. Su, and P.-H. Lin, "Joint subcarrier pairing and power allocation for OFDM transmission with decode-and-forward relaying," *IEEE Trans. Signal Process.*, vol. 59, no. 1, pp. 399–414, Jan. 2011.
- [134] L. Lihua, Z. Mingyu, Z. Xiaoxia, W. Haifeng, and Z. Ping, "Adaptive bit, power allocation and sub-carrier coupling for AF-OFDM relaying systems,"

- in *Proc. IEEE 65th Vehicular Technology Conference, VTC2008-Spring*, Marina Bay, Singapore, May 2008, pp. 1494–1498.
- [135] B. Gui and L. J. C. Jr, “Bit loading algorithm for cooperative OFDM systems,” *EURASIP J. Wireless Commun. and Networking*, pp. 1–9, July 2007.
- [136] H. Li, H. Yu, H. Luo, J. Guo, and C. Li, “Dynamic subchannel and power allocation in OFDMA-based DF cooperative relay networks,” in *Proc. IEEE Global Telecommunications Conference, GLOBECOM 2008*, New Orleans, Louisiana, USA, Nov. 2008, pp. 1–5.
- [137] D. Wang, Z. Li, and X. Wang, “Joint optimal subcarrier and power allocation for wireless cooperative networks over OFDM fading channels,” *IEEE Trans. on Vehicular Tech.*, vol. 61, no. 1, pp. 249–257, Jan. 2012.
- [138] Y. Liu and W. Chen, “Limited-feedback-based adaptive power allocation and subcarrier pairing for OFDM DF relay networks with diversity,” *IEEE Trans. on Vehicular Tech.*, vol. 61, no. 6, pp. 2559–2570, July 2012.
- [139] E. Koyuncu, Y. Jing, and H. Jafarkhani, “Distributed beamforming in wireless relay networks with quantized feedback,” *IEEE J. Sel. Areas Commun.*, vol. 26, no. 8, pp. 1429–1493, Oct. 2008.
- [140] R. U. Nabar and H. Blcskei, “Fading relay channels: Performance limits and space-time signal design,” *IEEE J. Sel. Areas Commun.*, vol. 22, no. 6, pp. 1099–1109, Aug. 2004.
- [141] M. Uysal and O. Canpolat, “On the distributed space-time signal design for a large number of relay terminals,” in *Proc. IEEE Wireless Communications and Networking Conference (WCNC)*, New Orleans, U.S.A., Mar. 2005, pp. 13–17.
- [142] S. Barbarossa and G. Scutari, “Distributed space-time coding for multihop networks,” in *Proc. IEEE International Conference on Communications (ICC)*, Paris, France, Feb. 2004, pp. 916–920.

- [143] T. Miyanoand, H. Murata, and K. Araki, "Cooperative relaying scheme with space time code for multihop communications among single antenna terminals," in *Proc. IEEE Conference Global Telecommunications Conference, GLOBECOM 04.*, Dallas, Texas, Nov. 2004, pp. 3763–3767.
- [144] Y. Jing and B. Hassibi, "Diversity analysis of distributed space time codes in relay networks with multiple transmit/receive antennas," *EURASIP J. Advances in Signal Process.*, vol. 5, no. 12, pp. 3524–3536, Dec. 2006.
- [145] W. Zhang and khaled Ben Lataief, "Full-rate distributed space-time codes for cooperative communications," *IEEE Trans. Wireless Commun.*, vol. 7, no. 7, pp. 2446–2451, July. 2008.
- [146] Y. Zou, Y.-D. Yao, and B. Zheng, "Opportunistic distributed space-time coding for decode-and-forward cooperation systems," *IEEE Trans. Signal Process.*, vol. 60, no. 4, pp. 1766–1781, Apr. 2012.
- [147] O. Mabrouk and H. Boujemaa, "Incremental decode and forward relaying using distributed space time coding," in *Proc. 5th International Symposium on Communications, Control and Signal Processing, ISCCSP 2012*, Rome, Italy, May 2012, pp. 1–5.
- [148] D. Agrawal, V. Tarokh, A. Naguib, and N. Seshadri, "Space-time coded OFDM for high data-rate wireless communication over wideband channels," in *Proc. 48th IEEE Vehicular Technology Conference VCT.*, Ottawa, Canada, May 1998, pp. 2232–2236.
- [149] Y. Gong and K. B. Letaief, "An efficient space-frequency coded OFDM system for broadband wireless communications," *IEEE Trans. Commun.*, vol. 51, no. 11, pp. 2019–2029, Nov. 2003.
- [150] K. F. Lee and D. B. Williams, "A space-time coded transmitter diversity technique for frequency selective fading channel," in *Proc. IEEE Sensor Array and Multichannel Signal Processing Workshop*, Mar. 2000, pp. 149–152.

- [151] B. Lu and X. Wang, "Space-time code design in OFDM systems," in *Proc. IEEE Global Telecommunications Conference GLOBECOM00*, Nov. 2000, pp. 1000–1004.
- [152] R. S. Blum, Y. G. Li, J. H. Winters, and Q. Yan, "Improved space-time coding for MIMO-OFDM wireless communications," *IEEE Trans. Commun.*, vol. 49, no. 11, pp. 1873–1878, Nov. 2001.
- [153] M. Uysal, N. Al-Dhahir, and C. N. Georghiades, "A space-time block-coded OFDM scheme for unknown frequency-selective fading channels," *IEEE Commun. Lett.*, vol. 5, no. 10, pp. 393–395, oct. 2001.
- [154] H. Blcskei and A. J. Paulraj, "Space-frequency coded broadband OFDM systems," in *Proc. IEEE WCNC00*, Chicago, USA, Sept. 2000, pp. 1–6.
- [155] K. F. Lee and D. B. Williams, "A space-frequency transmitter diversity technique for OFDM systems," in *Proc. IEEE Global Telecommunications Conference GLOBECOM00*, Nov. 2000, pp. 1473–1477.
- [156] L. Lihua, T. Xiaofeng, Z. Ping, and H. Haas, "A practical space frequency block coded OFDM scheme for fast fading broadband channels," in *Proc. 13th IEEE International Symposium on Personal, Indoor and Mobile Radio Communications*, Lisboa, Portugal, Sept. 2000, pp. 212–216.
- [157] B. Tao and L. Yongling, "Improved space-time-frequency block code for MIMO-OFDM wireless communications," in *Proc. IEEE International Conference on Signal Processing, Communication and Computing (IC-SPCC)*, Aug. 2012, pp. 538–541.
- [158] W. Zhang, X.-G. Xia, and K. B. Lataief, "Space-time/frequency coding for MIMO-OFDM in next generation broadband wireless systems," *IEEE Wireless Commun. Mag.*, vol. 14, no. 3, pp. 32–43, June 2007.
- [159] H. Mheidat, M. Uysal, and N. Al-Dhahir, "Distributed space-time block coded OFDM for relay-assisted transmission," in *Proc. IEEE International*

- Conference on Communications ICC06*, Turkey,Istanbul, June 2006, pp. 4513–4519.
- [160] Y. Li, W. Zhang, and X.-G. Xia, “Distributive high-rate full-diversity space-frequency codes for asynchronous cooperative communications,” in *Proc. IEEE International Symposium on Information Theory*, Seattle, USA, July 2006, pp. 2612–2616.
- [161] Z. Li and X.-G. Xia, “An Alamouti coded OFDM transmission for cooperative systems robust to both timing errors and frequency offsets,” *IEEE Trans. Wireless Commun.*, vol. 7, no. 5, pp. 1839–1844, Aug. 2008.
- [162] —, “A simple Alamouti space-time transmission scheme for asynchronous cooperative systems,” *IEEE Signal Process. Lett.*, vol. 14, no. 11, pp. 804–807, Nov. 2007.
- [163] K. G. Seddik and K. J. R. Liu, “Distributed space-frequency coding over broadband relay channels,” *IEEE Trans. Wireless Commun.*, vol. 7, no. 11, pp. 4748–4759, Nov. 2008.
- [164] W. Zhang, Y. Li, and X.-G. Xia, “Distributed space-frequency coding for cooperative diversity in broadband wireless Ad Hoc networks,” *IEEE Trans. Wireless Commun.*, vol. 7, no. 3, pp. 995–1003, 2008.
- [165] A. Y. Al-nahari, K. G. Seddik, M. I. Dessouky, and F. E. A. El-Samiel, “Cooperative space-frequency coding for broadband relay channels,” *IEEE Trans. Commun.*, vol. 58, pp. 567–572, 2009.
- [166] —, “Distributed space-frequency coding for cooperative diversity over broadband relay channels with DF relaying,” *IEEE Trans. Veh. Technol.*, vol. 61, no. 7, pp. 3266–3272, 2012.
- [167] D. B. A. T. A. G. Anil Aksay, M. Oguz Bici and G. B. Aksar, “A study on the effect of MPE-FEC for 3D video broadcasting over BVB-H,” in *Proc. International Mobile Multimedia Communications Conference.*, London, UK, Dec. 2009, pp. 1–8.

- [168] S. Shah and U. D. Dalal, "Characteristic analysis of hierarchical and non hierarchical modulation for DVB-H," *International Journal of Computer Applications*, vol. 59, no. 1, pp. 20–23, 2012.
- [169] G.-H. Yang, D. Shen, and V. O. K. Li, "Unequal error protection for MIMO systems with a hybrid structure," in *Proc. in IEEE International Symposium on Circuits and Systems, ISCAS 2006*, Island of Kos, Greece, May 2006, pp. 682–685.
- [170] T. Q. Duong, U. Engelke, and H.-J. Zepernick, "Unequal error protection for wireless multimedia transmission in decode-and-forward relay networks," in *Proc. IEEE Radio and Wireless Symposium*, San Diego, CA, USA, Jan. 2009, pp. 703–706.
- [171] H. X. Nguyen, H. H. Nguyen, and T. Le-Ngoc, "Signal transmission with unequal error protection in relay selection networks," in *Proc. IEEE International Conference on Communications (ICC)*., Guangzhou, China, May 2008, pp. 1–6.
- [172] —, "Signal transmission with unequal error protection in wireless relay networks," *IEEE Transactions on Vehicular Technology*, vol. 59, no. 5, pp. 2166–2178, 2010.
- [173] —, "Signal transmission with unequal error protection in relay selection networks," *IET Communications*, vol. 4, no. 23, pp. 1624–1635, 2010.
- [174] M. Eddaghel, U. Mannai, and J. Chambers, "Outage probability analysis of an AF cooperative multi-relay network with best relay selection and clipped OFDM transmission," in *Proc. IEEE Tenth International Symposium on Wireless Communication Systems*, Ilmenau, Germany, Aug. 2013, pp. 532–536.
- [175] L. Wang, H. Zhao, Y. Xi, and J. Wei, "Optimal power allocation and relay selection in OFDM-based cooperative systems," in *Proc. of 6th Inter-*

- national Conference on Wireless Communications Networking and Mobile Computing (WiCOM )*, Sep. 2010, pp. 1–5.
- [176] W. Yang and Y. Cai, “A block-based OFDM decode-and-forward relaying scheme for cooperative wireless networks,” in *Proc. IEEE International Symposium on Communication and Information Technology*, Incheon, Korea (South), Sep. 2009, pp. 938–942.
- [177] —, “On the performance of the block-based selective OFDM decode-and-forward relaying scheme for 4G mobile communication systems,” *Journal of Communications and Networks*, vol. 13, no. 1, pp. 56–62, 2011.
- [178] Z. Yi and L. Kim, “Decode-and-forward cooperative network with relay selection,” in *Proc. IEEE International Conference on Vehicular Technology Conference, VTC-fall 07*, Baltimore, Maryland, USA, Oct. 2007, pp. 1167–1171.
- [179] M. Torabi, W. Ajib, and D. Haccoun, “Performance analysis of amplify-and-forward cooperative networks with relay selection over Rayleigh fading channels,” in *Proc. IEEE 69th VTC Spring*, Apr. 2009, pp. 1–5.
- [180] D. B. D. Costa and S. Assa, “End-to-end performance of dual-hop semi-blind relaying systems with partial relay selection,” *IEEE Trans. Wireless Commun.*, vol. 8, no. 8, pp. 4306–4315, 2009.
- [181] M. Abramowitz and I. Stegun, *Handbook of Mathematical Functions with Formulas, Graphs, and Mathematical Tables.*, New York, 1972.
- [182] T. Liu, L. Song, and B. Jiao, “A threshold-based hybrid relay selection scheme,” in *Proc. of IEEE Wireless Communications and Networking Conference Workshop (WCNCW)*, Apr. 2010, pp. 1–5.
- [183] M. Kanekoi and P. Popovski, “Radio resource allocation algorithm for relay-aided cellular OFDMA system,” in *proc. IEEE international Conference on Communications, ICC’07*, June 2007, pp. 4831–4836.

- [184] M. Torabi, "Adaptive modulation for space-frequency block coded OFDM system," *International Journal of Electronics and Communications*, vol. 62, no. 7, pp. 521–533, Aug. 2008.
- [185] Y. Li, W. Wang, J. Kong, and M. Peng, "Subcarrier pairing for amplify-and-forward and decode-and-forward OFDM relay links," *IEEE Commun. Lett.*, vol. 13, no. 4, pp. 209–211, 2009.
- [186] O. Amin and M. Uysal, "Optimal bit and power loading for amplify-and-forward cooperative OFDM systems," *IEEE Trans. Wireless Commun.*, vol. 10, no. 3, pp. 772–781, Mar. 2011.
- [187] X. Li, J. Zhang, Y. Zhang, and J. Huang, "Power allocation for OFDM based links in hybrid forward relay," in *Proc. IEEE 69th Vehicular Technology Conference, VTC2009-Spring.*, Barcelona, Spain, Apr. 2009, pp. 1–5.
- [188] P. A. Anghel and M. Kaveh, "Exact symbol error probability of acooperative network in a Rayleigh-fading environment," *IEEE Trans. Wireless Commun.*, vol. 3, no. 5, pp. 1416–1421, Sep. 2004.
- [189] S. S. Ikki and M. H. Ahmed, "Performance analysis of cooperative diversity with incremental-best-relay technique over Rayleigh fading channels," *IEEE Trans. Commun.*, vol. 59, no. 8, pp. 2152–2161, Aug. 2011.
- [190] A. Papoulis and S. U. Pillai, *Probability, Random Variables and Stochastic Process, 4th ed.* McGraw-Hill, 2002.
- [191] S. S. Ikki, M. Uysal, and M. H. Ahmed, "Performance analysis of incremental-relay-selection decode-and-forward technique," in *Proc. IEEE Global Telecommunications Conference, GLOBECOM '09.*, Honolulu, USA, Dec. 2009, pp. 1–6.
- [192] S. S. Ikki and M. H. Ahmed, "On the performance of cooperative-diversity networks with the  $N^{\text{th}}$  best-relay selection scheme," *IEEE Trans. Commun.*, vol. 58, no. 11, pp. 3062–3069, Nov. 2010.

- [193] Z. Xiaoguang, T. Zhijian, Z. Hongdang, Z. Liping, and M. Xiao, "Performance of adaptive OFDM transceiver in wireless channels with loading algorithm," in *Proc. International Conference on Intelligent Computing and Intelligent Systems (ICIS)*., Shanghai, China, Nov. 2009, pp. 13–16.
- [194] P. G. Gallager, *Information Theory and Reliable Communication*. New York: Wiley, 1968.
- [195] H. A. Suraweera and J. Armstrong, "Performance of OFDM-based dual-hop amplify-and-forward relaying," *IEEE Commun. Lett.*, vol. 11, no. 9, pp. 726–728, sept. 2007.
- [196] M. K. Simon and M.-S. Alouini, *Digital Communications over Fading Channels: A United Approach to Performance Analysis, 1st ed.* New York: John Wiley and Sons, 2000.
- [197] S. Ikki and M. H. Ahmed, "Performance of decode-and-forward cooperative diversity networks over Nakagami-m fading channels," in *Proc. IEEE Global Telecommunications Conference, GLOBECOM '07*, Washington, DC, USA, Nov. 2007, pp. 4328–4333.
- [198] Y. Li, W. Zhang, and X.-G. Xia, "Distributive high-rate full-diversity space-frequency codes for asynchronous cooperative communications," in *Proc. IEEE International Symposium on Information Theory*, Seattle, WA, July 2006, pp. 2612–2616.
- [199] G. Scutari and S. Barbarossa, "Distributed space-time coding for regenerative relay networks," *IEEE Trans. Commun.*, vol. 4, no. 5, pp. 2387–2399, Sep. 2005.
- [200] W. Zhang, Y. Li, and X.-G. Xia, "Distributed space-frequency coding for cooperative diversity in broadband wireless Ad Hoc networks," *IEEE Trans. Wireless Commun.*, vol. 3, no. 7, pp. 995–1003, 2008.
- [201] J. Jang, K. B. Lee, and Y.-H. Lee, "Transmit power and bit allocations for OFDM systems in a fading channel," in *Proc. IEEE Conference Global*

- Telecommunications Conference, GLOBECOM '03.*, San Francisco, USA, Dec. 2003, pp. 858–862.
- [202] T. Wang and L. Vandendorpe, “WSR maximized resource allocation in multiple DF relays aided OFDMA downlink transmission,” *IEEE Trans. Signal Process.*, vol. 59, no. 8, pp. 3964–3976, 2011.
- [203] M. Herdin, “A chunk based OFDM amplify-and-forward relaying scheme for 4G mobile radio system,” in *Proc. IEEE International Conference on Communications, ICC '06.*, Istanbul, Turkey, June 2006, pp. 4507–4512.
- [204] W. Wang, S. Yang, and L. Gao, “Comparison of schemes for joint sub-carrier matching and power allocation in OFDM decode-and-forward relay system,” in *Proc. IEEE International Conference on Communications, ICC '08.*, Beijing, China, May. 2008, pp. 4983–4987.
- [205] S. Chen, F. Liu, XinZhang, C. Xiong, and D. Yang, “Symbol error probability analysis of OFDM relaying system with subcarrier mapping scheme,” *IEEE Commun. Lett.*, vol. 14, no. 7, pp. 638–640, July 2010.
- [206] Y. Chin, D. Jayalath, and B. Senadji, “Distributed orthogonal space-time block codes with adaptive diversity gain,” in *Proc. 4th International Conference on signal processing and communication systems (ICSPCS).*, Gold Coast, Australia, Sep. 2010, pp. 46–51.
- [207] V. L. Nir and M. Helard, “Reduced-complexity space-time block coding schemes with block linear precoding,” *Electronics Letters*, vol. 39, no. 14, pp. 1066–1068, July. 2003.
- [208] R. Jachoon, H. Liu, and E. K. Hong, “Transmission pattern selection for relay communication with distribution space-time codes,” in *Proc. IEEE International Conference on Communications (ICC).*, Guangzhou, China, May 2008, pp. 666–670.
- [209] G. Qiang and W. Shengnan, “Power allocation for OFDM relaying systems

- with bit error ratio formula,” in *Proc. IEEE Global Mobile Congress (GMC)*, Shanghai, China, Oct. 2010, pp. 1–6.
- [210] C. Yueyun, H. Xining, and T. Zhenhui, “Power allocation for OFDM-DF cooperative communication,” in *Proc. Third International Conference on Communications and Mobile Computing*, Qingdao, China, Apr. 2011, pp. 319–322.
- [211] S. Boyd and L. Vandenberghe, *Convex Optimization*, Cambridge University press, 2004.
- [212] T. Wiegand and G. J. Sullivan, “Draft ITU-T recommendation H.264 and final draft international standard of joint video specification (ITU-T Recommendation H.264 | ISO/IEC 14496-10 AVC), Joint Video Team of ISO/IEC JTC1/SC29/WG11 and ITU-T SG16/Q.6 Doc. JVT-G050,” Pattaya, Thailand, Mar. 2003.
- [213] T. Wiegand, G. J. Sullivan, G. Bjntegaard, and A. Luthra, “Overview of the H.264/AVC video coding standard,” *IEEE Trans. Circuits Syst. Video Technol.*, vol. 13, no. 7, pp. 560–576, Jul. 2003.
- [214] K. Mller, H. Schwarz, D. Marpe, C. Bartnik, S. Bosse, H. Brust, T. Hinz, H. Lakshman, P. Merkle, F. H. Rhee, G. Tech, M. Winken, and T. Wiegand, “3D high-efficiency video coding for multi-view video and depth data,” *IEEE Trans. on Image Process.*, vol. 22, no. 9, pp. 3366–3378, Sep. 2013.
- [215] K. M. Alajel, W. Xiang, and Y. Wang, “Unequal error protection scheme based hierarchical 16-QAM for 3-D video transmission,” *IEEE Transactions on Consumer Electronics*, vol. 58, no. 3, pp. 731–738, Aug. 2012.
- [216] P. Merkle, Y. Wang, K. Muller, A. Smolic, and T. Wiegand, “Video plus depth compression for mobile 3D services,” in *Proc. in 3DTV Conference: The True Vision - Capture, Transmission and Display of 3D Video*, May 2009, pp. 1–4.

- [217] G.-M. Su, Y. chi Lai, A. Kwasinski, and H. Wang, *3D Visual Communications*,. United Kingdom: John Wiley and Sons Ltd, 2013.
- [218] F. C., “A 3D-TV system based on video plus depth information,” in *Signals, System and Computers, 2003. Conference Record of the Thirty-Seven Asilomar Conference on*, vol. 2, Nov. 2003, pp. 1529–1533.
- [219] P. Ndjiki-Nya, D. Doshkov, H. Lakshman, P. Merkle, K. Mller, and T. Wiegand, “Depth image-based rendering with advanced texture synthesis for 3-D video,” *IEEE Transactions on Multimedia*, vol. 13, pp. 453–465, 2011.
- [220] B. Wandel, *Foundations of Vision*, *Sinauer Associates*,. Sunderland, MA: Wiley, 1995.
- [221] Y. K. Park, K. Jung, Y. Oha, S. Lee, J. K. Kim, G. Lee, H. Lee, K. Yun, N. Hur, and J. Kim, “Depth-image-based rendering for 3DTV service over T-DMB,” *Signal Processing: Image Communication*, vol. 24, no. 8, pp. 122–136, Jan. 2009.
- [222] S. S. Ikki and M. H. Ahmed, “On the performance of amplify-and-forward cooperative diversity with the Nth best-relay selection scheme,” in *Proc.IEEE International Communications Conference, ICC '09.*, Dresden, Germany, Aug. 2009, pp. 1–6.
- [223] R. J. Vaughan and W. N. Venables, “Permanent expressions for order statistics densities,” *J. Roy. Statist. Soc. Ser. B*, vol. 34, no. 2, pp. 308–310, 1972.
- [224] VQEG, “Final report from the video quality experts group on the validation of objective models of video quality measurment, phase II video quality experts group (VQEG),” no. [Online]. Available: <http://vqeg.org>, Aug. 2003, [Viewed: May. 2011].
- [225] S. Chikkerur, V. Sundaram, M. Reisslein, and L. J. Karam, “Objective video quality assesment methods: a classification, review, and performance comparison,” *IEEE Trans. Broadcast.*, vol. 57, no. 2, pp. 165–282, 2011.

- 
- [226] Z. Wang, A. C. Bovik, H. R. Sheikh, and E. P. Simoncelli, "Image quality assesment: from error visibility to structural similiraty," *IEEE Trans. Image Process.*, vol. 13, no. 4, pp. 600–612, 2004.
- [227] Y. Cao and L. Yang, "Decomposed LT codes for cooperative relay communications," *IEEE J. Sel. Areas Commun.*, vol. 30, no. 2, pp. 407–414, Feb. 2012.